Analysis and modelling of the flood pulse and vegetation productivity response in floodplain wetlands.

by

Susan Jennifer Powell

Submitted in fulfilment of the requirements for the degree of
Doctor of Philosophy
of the Australian National University
February 2011

THE AUSTRALIAN NATIONAL UNIVERSITY

Candidate's Declaration

This thesis contains no material which has been accepted for the award of any other degree or diploma in any university. To the best of the author's knowledge, it contains no material previously published or written by another person, except where due reference is made in the text.

24th October, 2011

Susan Jennifer Powell

Date:

Acknowledgements

I would like to thank Dr Rebecca Letcher and Professor Tony Jakeman for their support and encouragement throughout my time at the ANU. This support continued with Dr Carmel Pollino joining my supervisory team, providing a crucial sounding board and mentor. Professor Brendan Mackey was critical in early formulation of my research topic and writing while Dr Damian Barrett, CSIRO, greatly assisted in understanding the remotely sensed data.

I would also like to acknowledge Dr Barry Croke, Dr Sandy Berry, Susan Cuddy and all the staff and students of iCAM and the Fenner School, ANU, for many fruitful discussions and ideas. Dr Berry also provided many useful comments on the remote sensing approach and analysis. Dr Edward King, CSIRO, was invaluable in extracting data from the AVHRR database and assisting in the technical manipulation and analysis of the remote sensing. Dr Emma Knight and Dr Hwan-Jin Yoon, ANU, provided assistance with statistical analysis ideas and methods. Thanks also to Nicola Glendining who helped edit the final draft of this thesis and to the examiners whose comments and advice are appreciated.

The impetus for this research came from many years of fieldwork in river and wetland ecology and management in the Barwon Region of the (then) NSW Department of Land and Water Conservation. I am deeply indebted to Neal Foster, Warwick Mawhinney and Tracey Fulford from the Department for the many enjoyable years of working in and around the Gwydir wetlands, and their continued support of this research through the provision of data, photographs and personal communications. To Bruce and Jen Southern, previous owners of the property ‘Old Dromana’, their deep understanding of the Gwydir wetlands and the changes they have seen since river regulation have also contributed to my interest and understanding of Australian wetlands. More recently the NSW Department of Environment, Climate Change and Water have become involved in research and management of the Gwydir wetlands and I thank Rachel Thomas and Dr Neil Saintilan for some interesting and enlightening discussions. Support and advice often comes from unexpected quarters and I would like to thank Daren Barma, Paul Wettin, Sian Mulholland, Glenn Doney, Dr Lyndsey Vivian, Simon Dwyer, Dr Ben Long, Dr Sue Holzknecht and Dr Jane Roberts for their help and support along the way.

Financial support for this work was obtained through an ANU scholarship with top-up and operational support from the CSIRO Water for a Healthy Country and the Cotton Catchment Communities Cooperative Research Centre. This thesis was a little longer in the making than originally planned and I would like to thank everyone for their continued patience. From working on the development of the wetlands decision support tool, Ibis, to competing for Australia in the sporting arena, I have had some amazing opportunities and have been very fortunate to have this level of support to complete this research along the way.

Abstract

This thesis aims to develop a conceptual understanding of the flooding patterns and vegetation response of large floodplain wetlands, and to apply this knowledge to develop an inundation and vegetation response model for water management. Applicable to a range of floodplain wetland systems, the conceptual node-network approach was developed in relation to the Gwydir wetlands, NSW, Australia. The Gwydir floodplains and wetlands occur in a dryland setting and are reliant on flows from the upstream catchment that has substantial water resource development. The Gwydir wetlands include a range of ecological values and are listed under international agreements for the protection of wetlands and migratory waterbirds.

The challenge of understanding flooding patterns in the Gwydir wetlands are common to other floodplain systems where shallow inundation, rapid vegetation growth and canopy cover may preclude the assessment of open water flooding from conventional remote sensing techniques. To characterise the flooding patterns a multi-temporal decision tree approach was developed. Based on classification of flooding as open water or from the subsequent high vigour vegetation response, the method uses remotely sensed vegetation indices to map a range of flood events. The results are summarised into homogenous patches with respect to flood frequency and connectivity. Over 250 discrete patches were identified in the study area of which 17 patches could be used to describe over 92% of the floodplains. Using the patch analysis and assessment of connectivity between the patches and channels, the floodplain wetlands were conceptualised using a node-network model of the 17 patches.

Patches were categorised according to vegetation associations and the resulting landscape units used to develop models of vegetation productivity response measured as the fraction of photosynthetically active radiation (fPAR). Phenological attributes such as greenup, maturity, senescence and dormancy were extracted from the time series fPAR to characterise landscape units, and the fPAR response to inflow and soil moisture was modelled. Peak fPAR in the Gwydir is associated with macrophyte communities in the most frequently flooded areas, with fPAR exceeding 0.9 in summer months following inundation. Multiple linear regression models show significant relationship with inflows for many of the wetland landscape units.

The node-network and fPAR models are combined to develop the Inundation and Vegetation Response Model (IVRM) that provides a means of distributing river inflow and climate variables across the landscape and linking these to vegetation productivity response. Sensitivity testing is undertaken for uncertain parameters and further research needs identified. The model is applied to predicting inundation and vegetation response outcomes from predevelopment, current development and future climate change (2030) scenarios. Results suggested that in the most frequently flooded patch, inundation could have occurred over 99%

of the time under the predevelopment scenario, compared to less than 63% of the time under a ‘dry’ prediction of future climate change. This change could see a reduction in peak fPAR from 47% of the time in the predevelopment scenario, to less than 8% of time under the ‘dry’ climate change scenario.

This thesis integrates hydrological and ecological understanding, remote sensing analysis, statistical methods, and good modelling practice to develop the IVRM. The assessment framework takes a holistic view of an ecosystem, and explores how a wetting regime influences structure and function. The landscape scale approach uses the lateral, temporal and vertical connectivity, critical to the floodplain wetland functioning, to inform the development the model. The spatial and temporal scales are specific to the geomorphology, hydrology and ecology of the case study catchment, but the principles and methods can be applied to floodplain wetland systems in general.

Table of Contents

List of Figures

List of Tables

List of acronyms and abbreviations

AIRSAR	Airborne Synthetic Aperture Radar
ASTER	Advanced Spaceborne Thermal Emission and Reflection
AVHRR	Advanced Very High Resolution Radiometer
AVIRIS	Airborne Visible/Infrared Imaging Spectrometer
DSS	Decision Support System
ECA	Environmental Contingency Allowance
EFDSS	Environmental Flows DSS
ERS	European Remote Sensing Satellite
fPAR	Fraction of Photosynthetically Active Radiation
FPC	Flood Pulse Concept
IMEF	Integrated Monitoring of Environmental Flows
IRS	Infrared Optical Sensor
IVRM	Inundation and Vegetation Response Model
JERS	Japanese Earth Resources Satellite
Landsat	Land Satellite
LiDAR	Light Detection And Ranging
MIR	Mid infrared
MLR	Multiple Linear Regression
MODIS	Moderate Resolution Imaging Spectroradiometer
NDVI	Normalised Difference Vegetation Index
NIR	Near infrared
NOAA	National Oceanic and Atmospheric Administration
NPP	Net Primary Productivity
PP	Primary Productivity
RCC	River Continuum Concept
RPM	Riverine Productivity Model
SDC	Serial Discontinuity Concept
SeaWiFS	Sea-viewing Wide Field –of-view Sensor
SMMR	Scanning Multi-channel Microwave Radiometer
SRTM	Shuttle Radar Topography Mission
SY	Sustainable Yields
TIR	Thermal infrared

Chapter 1: Introduction

The primary aim of this thesis is to develop a conceptual understanding of the flooding patterns and vegetation productivity response of a large floodplain wetland system at the landscape scale. Furthermore, the thesis applies this understanding to build an inundation and vegetation productivity response model for water management. The methods developed are applicable to a range of floodplain wetland systems, particularly those in dryland settings.

In Australia, as in other parts of the world, there is a concerted effort to minimise human impacts on the environment, maintaining and restoring threatened and unique ecological systems (Finlayson *et al.* 1998; Finlayson and Rea 1999; Kingsford 2000; Mawhinney 2003). In riverine and wetland ecosystems, particularly those with significant water resource development, protecting the ecology requires an understanding of the system processes, and the impacts of different water management practices on them (Bunn and Arthington 2002; Chessman and Jones 2001; Kingsford 2000; Poff *et al.* 1997). Floodplain wetlands are particularly challenging as the flood assessment itself is not always straightforward. Challenges in examining flood history include: a lack of existing information on past flood events, shallow water depths and rapid vegetation growth, canopy cover over inundation and complex and changing landscapes, with land use development, water management and catchment processes influencing water flows and distribution (Benger 1997; Jain *et al.* 2005; Thomas *et al.* in press). The larger and more distributary the floodplain system becomes, the more difficult it is to build the links back to measured stream flow. Remote sensing provides a source of data to assess past flood events and provide the links to inflows (Costelloe *et al.* 2003; Jain *et al.* 2006; Jain *et al.* 2005; Kingsford and Thomas 2002; McCarthy 2002; McCarthy *et al.* 2003; Thomas *et al.* in press).

The study described in this thesis focuses on the Gwydir wetlands, a large terminal floodplain wetland complex of the Gwydir catchment, NSW, Australia. The challenges in modelling the inundation in the Gwydir wetlands are not unlike those found in other floodplain systems, where mapping open water distribution may not capture the whole flood event. Instead, the understanding of both the inundation and the vegetation response can improve the rigour and robustness in modelling total and changing flood extents. To do this in the Gwydir wetlands, a landscape scale approach is used that integrates remotely sensed spatial attributes of a range of flood events to develop a conceptual node-network model of the channels, wetlands and floodplains and the linkages between them. Using an iterative process, the thesis also characterises the vegetation productivity response to flooding using vegetation indices based on time series and combines the information to develop an inundation and vegetation response model (IVRM) of the Gwydir wetlands. Sensitivity testing of the IVRM is used to identify uncertain parameters, and further research needs are identified. The model is subsequently applied to predicting inundation and vegetation response outcomes from predevelopment, current development and future climate change (2030) scenarios.

This thesis contains a review of floodplain wetland systems with respect to their form and ecology (Chapter 2) (Figure 1.1). Methods of monitoring and assessment as well as the use of remote sensing for flood and vegetation response area also reviewed. Chapter 3 introduces the case study catchment including the physical and ecological attributes, as well as current land use and water management issues.

Chapter 4 provides an overview of the analysis approach that links the flood assessment, vegetation response and the inundation and vegetation response model developed in Chapters 5, 6 and 7, respectively. Each analysis chapter also includes a more detailed flowchart of the chapter methods, and the linkages with other chapters.

Chapter 5 is concerned with understanding the flood behaviour at a landscape scale in the Gwydir wetlands. Using a multi-temporal decision tree approach, the normalised difference vegetation index (NDVI) extracted from Landsat, Modis and AVHRR imagery is applied to map flood extent for a range of flood events. The information is synthesised into a spatial estimate of flood frequency and connectivity to provide relatively homogenous patches with respect to their flood behaviour and vegetation response. These patches form the basis of a conceptual node-network of the Gwydir wetlands. The patches are also characterised according to vegetation associations to provide landscape units for further analysis of vegetation response in Chapter 6.

Converting the NDVI used in Chapter 5 to the fraction of photosynthetically active radiation (fPAR), Chapter 6 then explores the vegetation productivity of landscape units in response to inflows and climate variables. Multiple linear regression models are developed which can be used in further modelling of vegetation response.

Taking the outcomes from Chapter 5 and 6, Chapter 7 fully develops a node-network model of inundation and vegetation response (IVRM) in the Gwydir wetlands. The model is verified using available data and a sensitivity analysis of uncertain parameters provided direction for further research. Finally, the model is applied to a range of water management scenarios: these are predevelopment, current development and three climate change scenarios representing the range of current climate change models.

In Chapter 8, the major outcomes and finding of the thesis are briefly reviewed and future directions for model development are discussed.

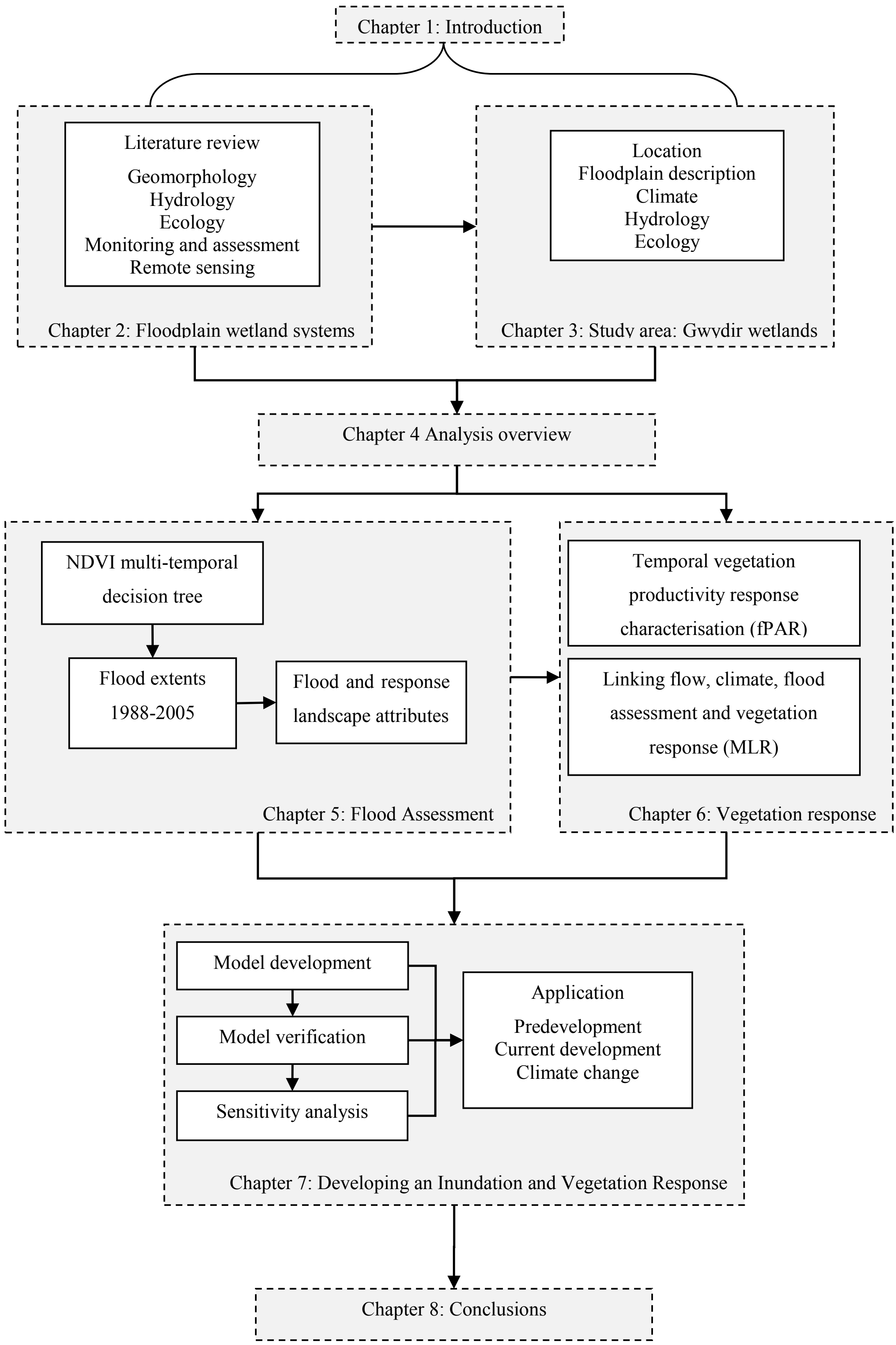

Figure 1.1: Thesis outline

Chapter 2: Floodplain wetland systems

2.1 Overview

In this chapter, the structure and function of floodplain wetland systems is reviewed, focusing on the relationship between vegetation response and flood regimes. To manage these wetland systems effectively, the flooding and response patterns must be considered temporally and at a landscape scale so that their unique combination of structure and function can be characterised. This review introduces the range of floodplain wetland structure and functions (including geomorphology, flow, climate and ecology) required to understand the temporal and spatial complexity of these systems, and in particular the case study presented in Chapter 3. The review focussing on floodplain wetlands found in dryland settings. The review also overviews the assessment, monitoring and management tools applied to floodplain wetland systems, relevant to the understanding of vegetation response to flood regime.

Floodplains can be characterised by their geomorphology, water regime, or ecological communities (Environment Australia, 2001; Ramsar Convention Secretariat, 2004; Roberts and Marston, 2000). Regardless of size or type, all floodplains rely on inundation from high flows of adjoining waterways (Junk *et al.*, 1989; Walker *et al.*, 1995; Ward, 1998) and have spatial and temporal complexity that makes them amongst the most dynamic ecosystems on earth (Kingsford, 2000). Junk *et al.* (1989) p. 112 defined floodplains as *"areas that are periodically inundated by the lateral overflow of rivers or lakes, and/or by direct precipitation or groundwater; the resulting physicochemical environment causes the biota to respond by morphological, anatomical, physiological, phenological and/or ethological adaptations, and produce characteristic community structures*". This definition sums up the important characteristics of floodplains that separate them from purely terrestrial or aquatic ecosystems.

2.2 Floodplain wetland form and function

2.2.1 Floodplain form

Fluvial geomorphology describes and analyses the landforms created by flowing waters and seeks to understand how surface processes control the development of these landforms (Gordon *et al.*, 2004). Within the physical context, a floodplain can be defined simply as a relatively flat valley floor formed by floods, with a flood being commonly defined as overbank flows (Gordon *et al.*, 2004). Nanson and Croke (1992) p. 460 provide a more detailed definition of the floodplain that considers the geomorphic history being "*the largely horizontally-bedded alluvial landform adjacent to a channel, separated from the channel by banks, and built of sediment transported by the present flow-regime*". These definitions are limited to the physical form of the floodplain and are perhaps more pertinent to the floodplains adjacent to major river channels rather than distributory, terminal and deltaic floodplains. They also neglect the functional attributes of the system compared to the definition proposed by Junk (1989) which considers all the components and processes, both biotic and abiotic.

There is a diverse range of floodplain types, with every case study requiring consideration of a new model of floodplain formation (Nanson and Croke, 1992; Tooth and McCarthy, 2007). Floodplain formation and type is a combination of a range of factors including, but not limited to: stream power, resistance to erosion, amount and texture of sediment loads, riparian vegetation, antecedent conditions and human interference (Nanson and Croke, 1992). A logical extension of this diversity of floodplain types is the diversity of functions and connections that must also be considered for each case study.

Dryland systems exist only where there is a locally positive water balance at some points in time. As, by definition, a dryland is a region in moisture deficit, it follows that dryland wetlands can only be found where a combination of factors such as exogenous river inflows along with a local geomorphology that impedes drainage or infiltration exist (Mitsch and Gosselink, 2000; Tooth and McCarthy, 2007). Knowledge of the geomorphic setting of floodplain wetlands in a dryland setting is critical to understanding the water balance of these regions. The range of terms for these types of floodplain wetlands can be confusing, but for this thesis, the term floodplain wetland refers to large sedimentary floodplains in lowland (dryland) river settings that support ephemeral, seasonal or permanent wetlands. These wetlands are commonly referred to in Australia and in Southern Africa as water meadows, marshes or swamps (McCosker, 1994b; Mitsch and Gosselink, 2000; Tooth and McCarthy, 2007).

In southern Africa, dryland wetlands have been characterised by the main river inflow type and by the factors that impede drainage or reduce infiltration such as faulting, rock outcrops, soils that swell and seal upon wetting and ponding by tributary or aeolian deposits (Tooth and McCarthy, 2007). Combined with variations in sediment supply, vegetation community structure and levels of animal activity, a range of wetlands are created that have different inundation characteristics.

Many dryland wetlands are characterised by channels that decrease in size downstream and may disappear altogether. As the channel size and stream power decreases, aggradation occurs in distal channel reaches or across floodouts influencing patterns of flow and sediment movement (Thoms and Sheldon, 2000; Tooth and McCarthy, 2007). The hydrochemical budgets of dryland wetlands can also influence geomorphology. Lower ratios between precipitation and potential evapotranspiration along with frequent desiccation and lack of flow-through channels results in the accumulation of high levels of ions in dryland wetlands. Pans and playas are characterised by high salt concentrations in surface sediments, however other wetlands rely on biological interactions to concentrate ions locally as in the salinised or sodic islands of the Okavango, Botswana (Ramberg and Wolski, 2008; Tooth and McCarthy, 2007). Frequent drying periods in dryland wetlands limit the formation of organic deposits and even when conditions are more perennial, sedimentation often leads to shifts in water distribution patterns and therefore to gradual drying. As the wetlands become more ephemeral, increasing decomposition rates and fires prevent or slow the accumulation of organic matter. Desiccation and loss of vegetative cover promote aeolian processes with some dryland wetlands dominated by dune formations, which may influence patterns of inundation and channel processes (Tooth and McCarthy, 2007). Another distinctive feature of many dryland wetlands is their long timescale of development with locally thick sedimentary successions and a mosaic of features developed over time such as abandoned channels, palaeochannels, scroll bars, inactive aeolian dunes and fossil shorelines (Ramberg and Wolski, 2008).

2.2.2 Rivers and floodplain function

Within the geomorphic setting a river-floodplain system can be considered to be highly connected in relation to energy and biotic function in four dimensions; longitudinal, lateral, vertical and temporal (Ward, 1989).

Longitudinal connectivity has been described by the River Continuum Concept (RCC) and its iterations (Vannote *et al.*, 1980; Ward and Stanford, 1983). In these conceptual models, the physical variables within a river system are a continuous gradient of physical conditions that drive biotic response. The processes are largely energy driven in relation to the loading, transport, utilization and storage of organic matter. The concept proposes that the structure and function of stream communities in natural rivers systems are adapted to the physical system, thereby providing a framework for predictable biological features of lotic systems. The RCC is based on the energy equilibrium theory, such that biological communities within a given reach of the river continuum should approach energy equilibrium with downstream communities taking advantage of processing inefficiencies from upstream (Vannote *et al.*, 1980). Discontinuity that may arise from river regulation breaks this continuum and is described in the Serial Discontinuity Concept (SDC) (Ward and Stanford, 1983). Discontinuity distance (that is, the longitudinal change of a parameter by stream regulation) may be positive (i.e. a downstream change) or negative (upriver) or near zero. The RCC and SDC assume that rivers are single-thread channels and primarily consider the longitudinal connectivity. Junk (1989) suggests that the RCC was developed on small temperate streams and cannot necessarily be extrapolated to other types of river systems.

Lateral and temporal connectivity is considered in the Flood Pulse Concept (FPC) (Junk *et al.*, 1989) particularly in relation to the river-floodplain system. In the FPC (Junk *et al.*, 1989) the flood pulse is the main driver of productivity and interactions of tropical river-floodplain systems. Flood pulse is dependent on geomorphologic and hydrological conditions and may range in predictability and duration. The FPC focuses on the energy dynamics of floodplains that are largely independent of upstream processing of organic matter and position within the river network, whereby nutrient recycling within the floodplain is a more important driver in energy budgets when compared to the RCC theory of downstream transport. The SDC has also been extended to floodplain rivers (Ward and Stanford, 1995) in an attempt to address the lateral connectivity missing in the RCC and SDC, but it is still limited to forested floodplains and explicitly excludes deltaic distributaries. The extended SDC postulates that regulation results in a reduction in biodiversity due to isolation of channels from floodplains and poses the question of whether temperate zone rivers have the same high levels of habitat heterogeneity and biodiversity pre-regulation as observed in unregulated tropical river floodplains. Tockner *et al.* (2000) extends the FPC to temperate rivers, the role of water level changes below bankfull, and inundation in river-floodplain systems other than the flood-pulse. The riverine productivity model (RPM) (Thorp and Delong, 1994) argues that the RCC and FPC models underestimate the importance of the organic carbon derived from both local autochthonous production (phytoplankton, benthic algae, aquatic vascular plants and mosses) and direct inputs from the riparian zone in certain river types. This hypothesis is directed at rivers characterised by constrained channels and appropriate substrate within the photic zone.

Temporal scales in river processes can vary from timescales required for behavioural response to time required for evolutionary change. The time scales of interest will therefore depend on the organism or process being investigated (Ward, 1989). Although some short-term temporal recovery to perturbations has been measured (Minchell *et al.* 1983 in Ward 1989), our understanding of ecosystem-level response to cyclic phenomena with periodicities greater than a few years is limited (Ward, 1989).

The vertical dimension considers the role of connected groundwater systems in river function. Although this dimension is often overlooked, Ward (1989) suggested that nutrients in aquifer discharge might be important to riverine productivity in generally nutrient poor river systems. The flood pulse may be influenced not only by river water inundating adjacent floodplains, but also by groundwater, hyporheic water, local flooding, direct precipitation and antecedent water from prior floods (Mertes, 1997; Tockner *et al.*, 2000). Flooding may therefore occur prior to the crest of the flood wave and the characteristics of the floodwaters and productivity will depend on the source. For example, hyporheic water may inundate an area of floodplain and provide nutrients to stimulate primary productivity but offer no opportunity for fish passage. In contrast an active flood pulse may favour fish migration whilst the strong current will depress primary productivity (Tockner *et al.*, 2000).

If the variety of different river and floodplain functional models is considered, it is clear that the application of the various hypotheses (RCC, FPC and RPM) varies with river size and geomorphology. A landscape scale approach is not only important to consider the unique river-floodplain form, it is also required to document and integrate the spatial patterns (longitudinal, lateral and vertical) and processes of flooding, to quantify the relationship between fluvial dynamics and landscape heterogeneity and to identify the flow characteristics that are required to maintain habitat and biological diversity (Poole, 2002; Tockner *et al.*, 2000; Wiens, 2002).

2.2.3 Hydrological regime

From the previous sections, it can be seen that the form and functioning of floodplain systems relies on the hydrological regime, both past and present. The contemporary hydrological regime of floodplain rivers is determined by the climate of its upstream catchment, valley slope, floodplain size and vegetation (Junk *et al.*, 1989).

'Hydrological regime' refers to the set of physical conditions related to the hydrological cycle whist the term 'flow regime' refers more specifically to a set of physical conditions relating to flow for a river system. Local climate influences are also important but may or may not be linked to the flow regime at a particularly location. The flow regime can vary spatially and temporally and as such must be defined in both dimensions. The flow regime metrics of interest may also differ depending on the purpose for which they are calculated. For example defining a 1 in 20 or 1 in 100 year flood size may be useful in engineering floodplain or river structures or in defining flood connectivity over the floodplain system, but it is largely irrelevant to fish spawning triggers. Poff *et al.* (1997) identifies five key measures of flow critical to ecosystem processes including the size of the flow, frequency for a given flow range, duration of a specific flow condition, the timing of the flow components and the rate of change.

The velocity of the flow is dependent on the channel shape and can vary across the channel and longitudinally. The term 'bankfull', often used in relation to the relationship between flow, inundation and the flood-pulse, must be considered at a specific location (Tockner *et al.*, 2000). Bankfull flows at one location may be overbank flows at another as channel capacity changes. Many texts describe increasing channel size and flow trends downstream, however this is often not true for floodplain wetlands located in dryland settings as channel size tends to decrease downstream and distributary channels form.

Junk (1989) suggests that large catchment areas result in a rather smooth and predictable flood curve. Although many Australian river systems are unpredictable in relation to the timing and size of the flood-pulse (Kingsford, 2000; Thoms and Sheldon, 2000), the flood curve in constrained lower reaches of these large catchments is relatively predictable in relation to the catchment rainfall characteristics. The distinct wet summer and dry winter seasons of Northern Australia transition though a uniform distribution to the winter dominated rainfall pattern in the southern part of the continent. Large areas of central Australia are arid while rainfall tends to be higher near the coast (Beeton et al. 2006; Smith 1998). The flood-pulse characteristics can be quite different across the continent and should be characterised for each floodplain system. Kennard *et al.* (2010) provides a framework for classification of the natural flow regimes in Australia which incorporates a range of metrics such as: zero flow; base flow; predictability; seasonality; variability; skewness; rate of rise and fall, and high flow analysis. However, as Kennard *et al.* (2010) discuss, caution needs to be used in extrapolating the flow-regime characteristics from a gauged site to an ungauged site.

The relationship between flow rate and water level can also be quite different where there are large floodplains. As flow rates increase, the rate of water level rise slows as the floodplains fill. The larger the floodplain, the slower the rate of water level rise and the more lentic habitats develop (Junk *et al.*, 1989). As the discharge rates fall, the floodplains become disconnected from the river channel and the flood dynamics become more reliant on local climate. Productivity on the floodplain can therefore be linked to the flood-pulse from the river catchment as well as in response to the local rainfall events during low flow periods.

Conserving and restoring river systems relies on the maintenance of the natural flow regime (Poff *et al.*, 1997) or meeting ecological requirements of biota. Flow is the major determinant of the range of habitats found in river and floodplain systems, which in turn dictates the range of species found (Poff *et al.*, 2010). A range of species have adapted to the variable habitats and have often developed specific life-history traits in response to the flow regime and habitats (Bunn and Arthington, 2002; Lytle and Poff, 2004; Poff *et al.*, 1997). As discussed in the previous section, longitudinal and lateral connectivity is critical in river and floodplain function and is a product of the flow regime coupled with structural attributes.

2.3 Floodplain wetland ecology

Floodplain wetlands encompass a broad range of habitats, from permanent lakes and waterholes to ephemerally flooded wetlands. Adaptation of biota may be through life history traits such as diverse offspring types in systems with unpredictable timing of floods and droughts, behaviour such as movement to protected areas during floods or the use of flood cues for reproduction, or morphology such as changing shape or allocation of biomass (Boulton and Brock, 1999; Boulton and Lloyd, 1991; Boulton and Lloyd, 1992; Brock and Casanova, 1997; Capon and Brock, 2006; Capon, 2003; Casanova and Brock, 2000; Froend and McComb, 1994; Kingsford and Johnson, 1998; Lytle and Poff, 2004; Pezeshki, 2001).

The basis of most aquatic food webs is the producers, those organisms that can fix carbon into organic material through the process of photosynthesis (Boulton and Brock, 1999; Winemiller, 2005). In floodplain systems, organic matter can enter the wetland system from terrestrial sources or insitu from producers that have adapted to flooding. Producers include terrestrial plants, aquatic macrophytes, periphyton and phytoplankton. The exact makeup of the producer community in a floodplain wetland system depends on a range of factors including the water depth, turbidity, flow and nutrient status. Vegetation of floodplains is discussed in more detail in Section 2.3.1.

Nutrient cycling in aquatic systems is dependent on oxygen status, inorganic minerals present and the microbial community including the diverse organisms found within aquatic biofilms (Baldwin and Mitchell, 2000; Scholz and Boon, 1993). Most of the primary production in floodplains is consumed by microbes that ultimately return nutrients to the inorganic pool (Winemiller, 2005). In floodplains and ephemeral or episodic wetlands, sediments undergo wetting and drying phases. The microbial community in floodplain systems that experience repeated wetting and drying cycles will include organisms that can produce drought resistant resting stages and facultative anaerobic bacteria that can survive oxic and anoxic conditions (Baldwin and Mitchell, 2000). As sediments dry out bacterial activity declines and once the soil is completely desiccated, nitrogen and phosphorus are released from dead bacterial cells. This results in a flush of N and P upon re-wetting of the sediments and soils, with macrophytes competing with bacteria for the readily available nutrients. Increased plant productivity and nutrient uptake has been shown for emergent macrophytes following the re-wetting of desiccated soils (Baldwin and Mitchell, 2000). Not all detritus is contained within the microbial loop, with some consumed directly by a variety of detrivorous invertebrates and fish, while omnivorous and piscivorous invertebrates and fish are also present (Boulton and Brock, 1999; Bunn and Arthington, 2002; James *et al.*, 2008; Winemiller, 2005).

Waterbirds are also a feature of many floodplain systems. In contrast to the northern hemisphere where the movements, reproductive ecology and moulting are often centred on marked seasonal factors, Australian waterbirds reflect the unpredictable climate and flood cycles where movements, feeding and reproductive ecology, moulting and habitat use are all highly adaptable to climatic patterns (Kingsford and Norman, 2002). Waterbirds may be herbivores, invertebrate feeders, piscivores or omnivores and the composition and abundance of waterbirds in a wetland often reflect the availability of food. Breeding habitat may also be specialised and require specific nest sites or suitable dense vegetation (Kingsford and Norman, 2002). The conceptual understanding of flood patterns and vegetation response is vital to understanding the waterbird ecology in these unpredictable floodplain systems. Other notable vertebrates in the floodplain ecosystems include amphibians (frogs) and reptiles such as turtles.

2.3.1 Vegetation

Vegetation found in floodplain wetlands can vary from submerged macrophytes adapted to permanent inundation to terrestrial species with high drought tolerance. Inundation and soil saturation are challenging environments for plant species and there are a range of survival strategies that plants may have developed (Blom and Voesenek, 1996). The ability to respond to a wide range of conditions is a feature of floodplain wetland vegetation in dryland settings. Considering the Junk *et al.* (1989) definition of floodplains introduced in Section 2.1, a range of adaptations can be considered in relation to vegetation. Vegetation response to inundation has been characterised by vegetation community structure and functional attributes (which may reflect the morphological and/or physiological adaptations) (Brock and Casanova, 1997; Capon, 2003; Capon, 2005; Casanova and Brock, 2000; Chauhan and Gopal, 2005; Mawhinney, 2003; Warwick and Brock, 2003). Vegetation response can also be measured through changes in gross primary productivity (PP) (Robertson *et al.*, 2001). Research on the relationship between precipitation and vegetation PP has been conducted in a variety of landscapes (Al-Bakri and Suleiman, 2004; Lupo *et al.*, 2007; Posse *et al.*, 2005), but is limited in relation to the temporal dynamics of the vegetation PP in response to inundation specifically.

Soil saturation and flooding in wetlands creates a range of reactions that lead to reduced soil conditions (low soil Eh or redox potential), where the rate of oxygen diffusion can be reduced, up to 10 000 times slower than in air, leading rapidly to anaerobiosis (Maltby 1989). Important oxygen-dependent microbial processes no longer take place and toxic substances accumulate from the anaerobic metabolism of plants or bacteria (Blom and Voesenek, 1996; Pezeshki, 2001). Flooding and water logging can also alter the physical structure of the soil, with the breakdown of large aggregates resulting in smaller pore diameters. This creates higher resistance to root penetration and low oxygen conditions (Blom and Voesenek, 1996). Plants can adapt to these conditions though life history adaptations, short term metabolic adaptation, long-term root or shoot responses and hormonal regulation of adaptive responses (Blom and Voesenek, 1996).

Over large floodplain wetlands, the frequency, depth and duration of flooding can vary dramatically. This results in a gradient of vegetation communities depending on the individual species' ability to tolerate the range of conditions experienced at a particular location (Brock and Casanova, 1997; Capon and Brock, 2006; Casanova and Brock, 2000; Nielsen and Chick, 1997; Reid and Quinn, 2004; Warwick and Brock, 2003). A classification system based on plant response to different water regimes has been developed which considers the germination, growth and reproductive attributes of the species (Brock and Casanova, 1997). The classification was developed using field and germination trials with plants grouped into terrestrial, amphibious or submerged functional groups. Although this approach does not identify the specific mechanisms for adaptation to the water regime (Roberts and Marston, 2000), it is a more practical approach to managing the vegetation communities at a wetland scale.

Submerged functional groups include those species that cannot tolerate drying and require continuous inundation for growth and reproduction. This group shows mechanisms to recolonise after drying events through long-lived seedbanks (Brock and Casanova, 1997). Similarly the terrestrial group cannot tolerate extended periods of inundation, although two subgroups were identified by Brock and Casanova (1997), those species that preferred dry conditions and those that required damp conditions. Of particular interest for floodplain wetland systems are the so-called amphibious groups. These groups can be further subdivided into those species which tolerate fluctuations (the fluctuation-tolerators) in water presence or absence without major changes in morphology or growth patterns, and those which respond (fluctuation-responders) through changes in growth pattern or morphology. These groups can be further subdivided by growth form such as the emergent or low-growing tolerators, or those species that respond to inundation by floating or by morphological plasticity (Brock and Casanova, 1997).

The range of vegetation species that have adapted to be able to utilise floodplain systems over a range of terrestrial and aquatic cycles results in higher primary productivity (PP) than in comparable purely terrestrial or aquatic systems alone (Junk *et al.*, 1989). A comparison of the annual aboveground PP for different ecosystem types has demonstrated that swamps and marshes are the most productive ecosystems with a mean net primary productivity (NPP) of 2500 g m-2 yr-1 compared to tropical rainforests of 2000 g m-2 yr-1 and average land NPP of 720 g m-2 yr-1 (Cronk and Fennessy, 2001). In the Amazon, ecosystem net primary production estimates of up to 2900 g m-2 yr-1, and individual species of over 5000 g m-2 yr-1 have been reported (Silva *et al.*, 2009) with around one-third emergent plant material while two-thirds were submerged. The timing of peak biomass varied between species which contributes to higher overall productivity (Junk *et al.*, 1989; Silva *et al.*, 2009). Local biotic and abiotic conditions including sediment quality, topography, water chemistry, turbulence, nutrient input and competition can result in significant differences in productivity (Silva *et al.*, 2009). In dryland floodplains, moisture is the main factor limiting plant growth and flooding is the main reason why productivity is higher in floodplains than surrounding areas. There is a substantial body of research on vegetation diversity, structure and function in Australian floodplains and wetlands which clearly demonstrate that standing biomass and cover increase after flooding (Brock, 1991; Brock and Casanova, 1997; Capon and Brock, 2006; Capon, 2003; Capon *et al.*, 2009; Casanova and Brock, 2000; Mawhinney, 2003; Warwick and Brock, 2003). Quantitative information on the overall productivity in the Australian context is generally lacking.

2.4 Monitoring and assessment

2.4.1 Flow

Flow is generally measured by recording water level (stage) at a set location. Over a variety of different stages, cross-sectional velocity is measured and the total flow is calculated. This forms a stage-flow relationship called a rating curve from which stage can be converted to flow. In Australia, automated gauging stations are common on most large river systems and can provide a good record of stage height at high temporal resolution. The converted flow data are readily available, although some understanding of the rating curve and channel characteristics are necessary to define the limitations of the data. Although the SI unit for discharge is m^3/s, ML/day is commonly used in Australia both in reporting of streamflow data and in management context and will be used in this thesis.

There are numerous papers that discuss the general limitations and errors in flow gauging data (Harmel *et al.*, 2006; Harmel *et al.*, 2008; Harmel and Smith, 2007). This thesis however is concerned primarily with the limitations of flow data associated with inflow to, and the flows within, large floodplain wetland systems. One of the major limitations in flow data for these systems is the issue of overbank or out-of-channel floodplain flows. These flows may bypass gauging stations and the ability to directly measure overbank flows for use in constructing reliable rating curves is hampered by practical considerations such as accessibility, width and depth of overbank flows (can be kilometres wide but only millimetres deep) and slow velocities. Multiple channels and crossover flows between channels can further complicate the task of accurately measuring an overbank flow. Large floods can potentially alter the stream cross-sections and flowpaths due to erosion or deposition, changing the flow to stage relationship. Another consideration is length of record as in highly variable dryland settings, a sufficient length of reliable record is required to characterise the flow regime.

2.4.2 Flooding and inundation patterns

Several approaches have been used to map or model flood and inundation of floodplains. Simple daily mass-balance water budget models including inflow, outflows, precipitation, evapotranspiration and groundwater seepage have been used to model a range of wetlands and dryland rivers (Costelloe *et al.*, 2003; Costelloe *et al.*, 2005; Zhang and Mitsch, 2005). Complex hydraulic models in 1, 2 and 3 dimensions have also been used to represent flood flows over floodplains (Caddy, 2004; Department of Infrastructure Planning and Natural Resources, 2004a; Thompson *et al.*, 2004; Whigham and Young, 2001). These models require large amounts of data, especially with respect to the spatial representation of the terrain, and are often used to assess floodplain development impacts. Another approach has been spatial modelling using remote sensing to map and classify wetlands and to estimate flood extent (Costelloe *et al.*, 2003;

Jain *et al.*, 2006; Jain *et al.*, 2005; Johnston and Barson, 1993; Kingsford and Thomas, 2002; McCarthy *et al.*, 2003; Ordoyne and Friedl, 2008; Sakamoto *et al.*, 2007; Shaikh *et al.*, 2001; Sheng *et al.*, 2001). Remote sensing has also been applied to determine the spatial variability of evaporation and moisture storages for use in hydrological water balance models (Mohamed *et al.*, 2004).

Inundation and flood patterns are highly dependent on local micro-topography in large floodplain wetlands. Often surface water flow paths are not immediately apparent, but can be conceptualised as "*a collection of depressions rather like an egg carton, but where the depressions are irregularly shaped, have varying depths and are separated by divides of varying height*" (Jones *et al.*, 2008). Mapping these features can be challenging as small-scale changes in vertical height can dramatically change the flow and inundation patterns, while the connectivity between depressions is dependent on inundation levels. Existing topographic information such as mapped contours and digital elevation models based on these maps or derived from Spot imagery have insufficient resolution in many floodplain systems (Rayburg *et al.*, 2009). Airborne lasers such as LIDAR (laser induced direction and ranging) provide a vertical resolution of 8-15 cm (Jones *et al.*, 2008; Rayburg *et al.*, 2009; Roberts *et al.*, 2000) enabling more accurate representation of topography and high resolution digital elevation models. Sedimentation processes may alter this micro-topography in relatively short time-frames and the growth of vegetation may be sufficient to alter flow paths (Pietsch, 2006).

The recent advances in computing power and remote sensing technology provide high-quality quantitative data allowing the development of high-resolution hydrodynamic modelling of floodplain inundation (Hunter *et al.*, 2007). However, the spatial and temporal scales of representation of any inundation mapping or modelling should be carefully considered in relation to the purpose of the assessment and the geomorphic complexity of the system (Rayburg *et al.*, 2009). Although LIDAR digital elevation models and high resolution hydrodynamic modelling would greatly enhance the knowledge base of inundation processes in the case study of this thesis (the Gwydir wetlands) this information is not readily available yet. In addition, the application of models of this complexity to simpler node-network models capable of running long-term inflow and climate scenarios, or to linkages with vegetation response to flooding, has not yet been demonstrated.

2.4.3 Wetland functional classification

Assessing the functional capacity of wetlands is another approach that have been used in the United States and in Europe (Brinson 2009; Maltby et al. 2009) which incorporates aspects of both the form and function and can be applied to floodplain wetlands like those in this thesis. The hydrogeomorphic (HGM) approach was designed to determine how changes to wetlands influences their condition and ability to perform functions related to hydrology, biogeochemistry and habitat in the United States (Brinson 2009). The approach uses classification of wetlands based on hydrogeomophology and the selection of reference wetlands within each classification. This provides a benchmark that establishes the range of conditions for each subclass of wetlands and may consider the temporal variability from natural disturbances such as fire or floods. The HGM approach is limited to a single classification for entire wetlands due to both limited extent of scientific information of within wetland variation and the scale of application (Maltby et al. 2009).

In Europe, a functional wetland assessment method is used that takes into consideration some distinct attributes such as spatial size and diversity, management practices and policy frameworks (Maltby et al. 2009). The functioning in a wetland will vary for three main reasons (Maltby et al. 2009) as outlined below.

- The hydrology will vary spatially due to elevation and/or differences in groundwater and surface water interactions.
- Wetland may form 'ecotones' between terrestrial and aquatic ecosystems and exhibit variations in functions through these transitional areas.
- Natural process can be altered or distrupted by land management and other human impacts at local scales

A wetland can therefore be broken down into smaller identifiable units that show funtional homogeneity with respect to the hydrogeomorphology, hydrology and soils. Vegetation is not used in defining these hydrogeomorphic units (HGMU) due to its dependence on land use and management (Maltby et al. 2009). Relationships between individual HGMUs and specific wetland functions have been established in European case studies (Maltby et al. 2009).

2.4.4 Vegetation response

The dynamic nature of floodplain wetlands requires an understanding of the vegetation response to the floodpulse. Vegetation response can be considered in relation to individual species response and adaptations and the impact on community structure, or as overall measures of productivity.

To measure response at the species or community structure level, field surveys based on pre- and post-flood assessment of vegetation assemblages, cover and/or biomass can be made at site scales across floodplain systems (Capon, 2003; Capon, 2005; Mawhinney, 2003). Conducted over a range of floods and at varying timescales, these studies can provide insights into the plant community dynamics and flood pulse characteristics. Seedbank studies can provide more detailed knowledge of specific species requirements for germination and growth (Brock and Casanova, 1997; Capon, 2005; Casanova and Brock, 2000; Warwick and Brock, 2003). In addition, seed banks contain the complete range of species that are available at a location rather than just the extant plant community at the time of field sampling. In highly variable systems this shows the potential of a site to respond to the floodpulse and the range of species that may occur given any set of conditions (James *et al.*, 2007). These studies are essential in understanding the vegetation ecology of a system; however, they may be limiting in their spatial extent. Moreover, in systems that have highly irregular flood cycling, they may not provide sufficient power of analysis to analyse longer term trends in response or to identify changes in response through time.

Phenological dynamics of wetland and floodplain plant communities reflect the response to seasonal and interannual variation in climate. At the landscape scale phenology dynamics can be measured using indicators of primary productivity from remotely sensed data to determine the timing and relative productivity of vegetation greenup, maturity and senescence (Sakamoto *et al.*, 2007; Zhang *et al.*, 2003), adding temporal and spatial scales not available through field studies alone. The inclusion of primary productivity of wetland vegetation in the understanding of flood response is also relevant to the nutrient and carbon dynamics and the functioning of the ecosystem as a whole.

2.4.5 Knowledge Gaps

The objective of this thesis is to develop a conceptual understanding of the flooding patterns and vegetation response of a large floodplain wetland system at the landscape scale. In reviewing the literature a number of knowledge gaps have been identified which include:

1. A lack of robust flood assessment methods in floodplain wetland systems with highly variable flood regimes.
2. The flood assessments often focus on the extent of flooding. In order to deliver water for ecological benefit, an understanding of the ecological response to flooding is needed.
3. Ecological functioning in floodplain wetlands is dependent on the flood pulse and the connectivity (whether that be longitudinal, lateral, vertical and/or temporal). This requires a landscape scale approach whereas much of the work in the Australian context has been at the site or species scale.
4. There is little information on the role of soil moisture and antecedent conditions in vegetation response of floodplain wetlands, particularly those in dryland settings.

2.5 Remote sensing of floodplain wetlands

2.5.1 Overview

As reviewed in previous sections, floodplain wetlands operate at landscape scales, with ecological functioning reliant on connectivity over different dimensions (lateral, longitudinal, vertical and temporal). Remote sensing is increasingly being used for assessing, monitoring and analysing these systems over some of these scales and dimensions. This thesis seeks to explore the flood regime and vegetation response of a large floodplain wetland system using remote sensing to address some of the knowledge gaps identified in 2.4.5. This section provides an overview of what remote sensing is, what types of information and data are available and how it can be applied specifically for flood and vegetation analysis.

Remotely sensed images can be taken from satellites or aircraft and can be of reflected solar light (ultraviolet, visible and mid-infrared wavelengths), energy emitted from the earth surface (thermal) or from a return of energy emitted from the platform itself (microwave) (Richards and Jia, 1999). The key characteristics of a remotely sensed image are the wavelengths measured (spectral bands), radiometric resolution (wavelengths of each band), spatial resolution (pixel size) of the image and the temporal resolution.

Visible, near and middle infrared wavelengths (reflected solar energy) are particularly useful in distinguishing landscape attributes. As solar energy is reflected off the earth's surface, different wavelengths of energy are absorbed or reflected depending on the properties of the vegetation, soil or water components of the landscape. Deep, clear water reflects little in the blue/green wavelengths, less in the red wavelengths and nil in the infrared while shallow or turbid water increases the reflectance in all bands. Vegetation reflectance in the visible wavelengths is controlled by the leaf pigmentation, with strong chlorophyll absorption in the blue and red regions resulting in higher green reflectance (Richards and Jia, 1999). Soil reflectance generally increases with wavelength with some variation due to moisture content or soil type. Figure 2.1 shows the theoretical spectral reflectance for vegetation, soil and water (clear and turbid) in relation to common remote sensing platforms. Emitted thermal energy is useful in measuring surface temperature (infrared) and soil moisture (microwave) (Schmugge *et al.*, 2002). Reflected microwave radiation, such as imaging radars, can show differences in surface roughness and geometry, as well as soil moisture content.

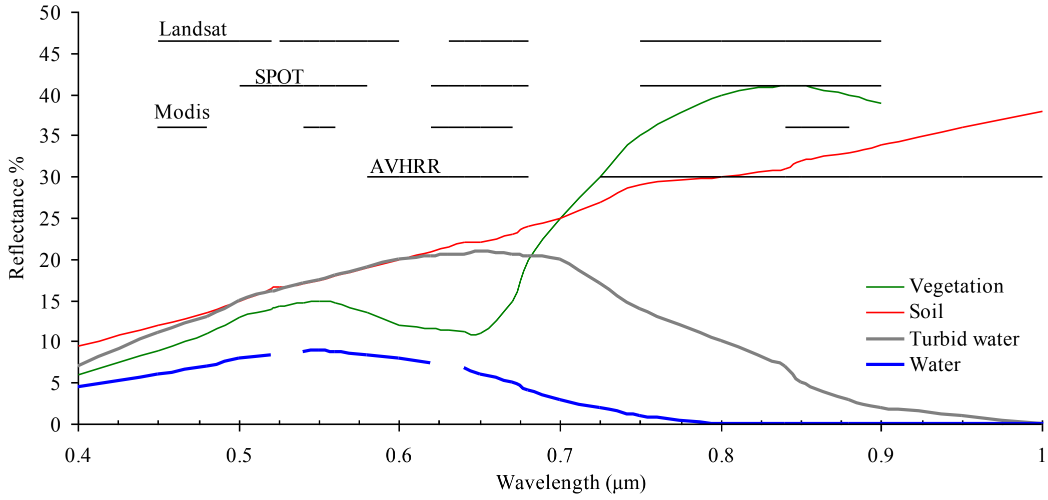

Figure 2.1: Spectral reflectance characteristics of water, soil and vegetation. Position of the visible, near infrared and middle infrared bands of various satellite platforms are also shown. Adapted from Richards and Jia (1999).

Spatial resolution of remotely sensed imagery is expressed as the size of the pixels at nadir (where the satellite is directly overhead). Depending on the swath width (width of the instantaneous field of view) of the instrument, the actual resolution may vary considerably as the edge of the view may be some distance from nadir resulting in larger pixels. Temporal resolution is also important in understanding the temporal dynamics and phenology of floodplain systems. Some instruments may provide irregular or on-demand data, while others will have a regular repeat cycle of anything from daily to monthly, depending on the satellite. Considering these scales of interest, Mertes (2002) provides an overview of available remote sensing instruments in relation to flood assessment (Figure 2.2). Instruments such as LIDAR provide high detail in the spatial dimension and may represent the flood process at a point in time (hours). However, the downside of such high resolution is the size of the area that is captured and the ability to repeat the measurements over time (not reflected in the figure). In contrast AVHRR and Modis provide a much lower spatial resolution but can capture this data much more frequently (daily overpass), while Landsat provides a spatial resolution between LIDAR and Modis, but at fortnightly to monthly repeat intervals. The specific application of remote sensing to flooding and vegetation response is covered in Sections 2.5.2 and 2.5.3 respectively, while a review of the different sensors is in Section 2.5.4.

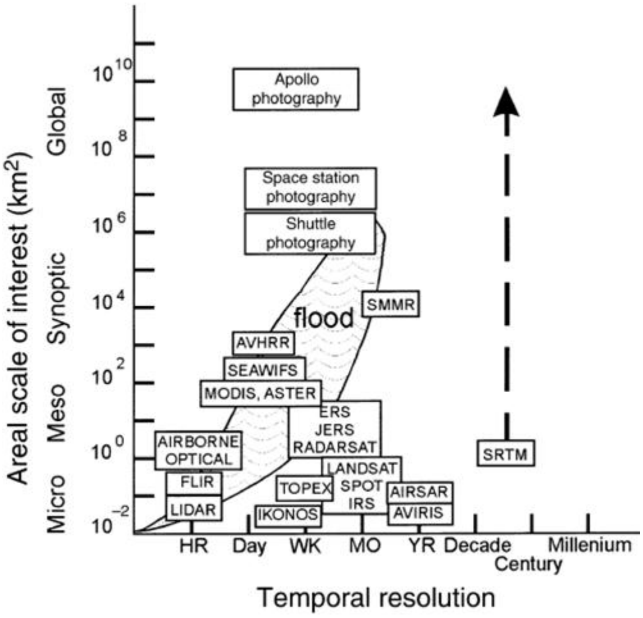

Figure 2.2: The spatial and temporal resolution of various remote sensing instruments in relation to flood assessment (Mertes, 2002). (see list of Acronyms, pg. xvi)

2.5.2 Remote sensing of flooding

Detecting flood extent from remotely sensed data can be quite straightforward where there are large expanses of open water. The simplest approach to mapping open water is density slicing of near infrared reflectance which is largely absorbed by water bodies (Frazier and Page, 2000; Johnston and Barson, 1993; Shaikh *et al.*, 2001; Sheng *et al.*, 2001). Density slicing is a simple process whereby the reflectance values are sliced at various values to classify the image. As the flood characteristics become more mixed across the landscape, factors such as shallow and turbid floodwaters, canopy cover, emergent vegetation, canopy shadow and soil saturation limit the effectiveness of density slicing (Jain *et al.*, 2005; Thomas *et al.*, in press).

Unsupervised and supervised classification of multi-spectral images are also used for identifying flood extent (McCarthy, 2002; Thomas *et al.*, in press). Unsupervised classification assigns pixels to a spectral class most often by using clustering methods (Richards and Jia, 1999). By reference to available reference data, these classes can then be assigned to landscape components. Supervised classification assumes that each spectral class can be described by a probability distribution in multi-spectral space (Richards and Jia, 1999). Using training data sets, an image is then classified based on the probability of each pixel belonging to one of the training sets (McCarthy *et al.*, 2003).

Simple ratio or difference models using two or more bands can be used to help distinguish landscape attributes. Jain *et al.* (2006) found that when there was less water in the landscape simple ratio methods produced better results, while during the monsoon period, single band thresholds were better. Normalised ratio's such as the wetness index (NDWI) have been developed to better differentiate areas of open water from other landscape components (Jain *et al.*, 2006; Jain *et al.*, 2005; McFeeters, 1996). The NDWI uses reflectance properties in the green wavelength and NIR wavelengths to provide an index in which water features are positive while vegetation and soil are negative. The range of NDWI values for water is from zero to one, providing more information about the specific properties of the areas of open water.

The more widely used index of vegetation greenness, the normalised difference vegetation index, NDVI, was developed primarily as an index of primary productivity, but it does separate landscape components due to the use of Red/NIR band ratios. Open water generally has very low or negative index values, bare soil has low values and vegetation has high values in the negative one to one index range. The other advantage of NDVI is that the index has been very well developed and researched (Barrett *et al.*, 2005; Di Bella *et al.*, 2004; Gallo *et al.*, 2004; Goetz, 1997; Huete *et al.*, 2002; King, 2003; Myneni and Williams, 1994; Pettorelli *et al.*, 2005; Scanlon *et al.*, 2002; Trishchenko *et al.*, 2002), and composite products well developed and readily accessible to develop time series of NDVI. NDVI is discussed further in Section 2.5.3 in relation to vegetation response.

In landscapes that have significant flood or open water areas, it is generally possible to determine appropriate thresholds to define these areas using the various indices or single bands as the histograms will often be bi-modal (Jain *et al.*, 2006). In smaller floods this may not be apparent and more detailed examination of the image, ground data and other information may be required to determine the thresholds.

2.5.3 Remote sensing of vegetation response

Vegetation response and growth is a product of plant photosynthesis, but is also controlled by a number of factors such as water availability, competition, disturbance, nutrient availability and loss through herbivory (Field *et al.*, 1995). Through the process of photosynthesis, plants use light energy to produce carbohydrates from CO_2 and water and release O_2. This light energy, or photosynthetically active radiation (PAR), is in the wavelengths 0.4-0.7 μm. These wavelengths are strongly absorbed by the plant pigments (chlorophyll a, chlorophyll b, carotenoids), with maximum absorption around 0.69μm and the reflectance in these wavelengths is therefore low (Boresjo Bronge and SwedPower, 2004; Glenn *et al.*, 2008). The structures within the leaves cause scattering and high reflectance of the near-infrared wavelengths (0.7-1.3 μm) while water content within the leaves results in higher absorption in the 1.3-2.5 μm range (Boresjo Bronge and SwedPower, 2004). Combined, these features of light energy absorption and reflectance have been used to develop a range of vegetation indices from the reflectance data captured by remote sensing sensors. The measurement of primary productivity in-situ using spectral data derived vegetation indices is complicated by the mix of landscape components. Soil backgrounds, or in the case of inundated floodplains water backgrounds, can influence the light reflectance. Using specific wavelengths and ratios can optimise the signal from vegetation and provide a spectral contrast from background materials (Boresjo Bronge and SwedPower, 2004).

Vegetation indices such as the normalised difference vegetation index (NDVI) combine the reflected red and near infrared radiation in a normalised ratio as shown in Equation 2.1.

$$NDVI = \frac{(NIR - \mathrm{Re}\,d)}{(NIR + \mathrm{Re}\,d)} \qquad \text{Equation 2.1}$$

The use of such a ratio allows comparison between different images through time and space by reducing the impact of illumination differences, cloud shadows, atmospheric attenuation and some topographic variation (Huete *et al.*, 2002). NDVI is strongly correlated with above ground net primary productivity and absorbed PAR (Boresjo Bronge and SwedPower, 2004; Glenn *et al.*, 2008; Huete *et al.*, 2002; Johnston and Barson, 1993; Kerr and Ostrovsky, 2003; Pettorelli *et al.*, 2005).

2.5.4 Sensor comparisons

Evaluating the flood or vegetation behaviour over a period of time using a variety of satellite sensors requires an understanding of the differences between the sensors. Sensor differences may impact on the relationship between vegetation indices, energy balance components, surface moisture status and landcover classification (Goetz, 1997). Some of the sensors that may be useful to flood or vegetation analyses include Advanced Very High Resolution Radiometer (AVHRR), Moderate Resolution Imaging Spectroradiometer (Modis) and Landsat, as shown in Figure 2.2.

The NOAA (National Oceanic and Atmospheric Administration) AVHRR High Resolution Picture Transmission (HRPT) dataset has a nominal 1km^2 pixel size and daily overpass. In reality, the pixel size at nadir is 1.1km^2, while at the edge of the swath pixels might exceed 5km^2. The first of the NOAA satellites (TIROS-N) which carry the AVHRR sensor was launched in 1978 and there has been almost uninterrupted temporal coverage since that time. The HRPT dataset is archived for Australia from 1992 to present (King, 2003) and includes visible, near and mid infrared and thermal channels depending on the satellite (Table 2.1). The Common AVHRR Processing Software (CAPS) is used by CSIRO Marine and Atmospheric Research to provide a best-practice AVHRR processing algorithm with includes radiometric calibration, geolocation and cloud detection (King, 2003). One of the significant problems with the AVHRR datasets for use in multi-temporal studies is the relatively large variation in view zenith angle and illumination direction due to large geographical coverage by the sensor and significant orbital drift (Chopping, 1998; King, 2003). These problems can be reduced by applying a Bidirectional Reflectance Distribution Function (BRDF) correction (Chopping, 1998) and using temporal composites (Pettorelli *et al.*, 2005). Another potential problem in the use of pre-processed datasets is aggressive cloud masking algorithms. The CAPS used for the AVHRR dataset utilizes the CLAVR (Clouds from AVHRR) algorithm (Stowe *et al.*, 1999) for cloud masking which can potentially mask areas of temporary flooding.

Table 2.1: Spectral bands of the AVHRR sensors of various NOAA satellites.

Channel	Bandwidth (um)	Description	NOAA satellites
1	0.58-0.68	Visible	All
2	0.725-1.00	Vis: NIR	Al
3a	1.58-1.64	Vis: MIR	15-17
3b	3.55-3.93	TIR	All
4	10.3-11.3	TIR	All
5	11.5-12.5	TIR	7,9, 11-17

The MODIS instrument is carried on the Terra (launched December 1999) and Aqua (launched May 2002) satellites and includes 36 different spectral bands. It acquires data at 250m, 500m and 1km resolution and has a daily temporal resolution, although many products derived from this data are produced at 8 or 16-day intervals (Paget and King, 2008). Vegetation indices (MOD13Q1) are produced at 250m spatial resolution and 16-day temporal resolution and include NDVI.

The Landsat earth resources satellite system commenced operation in 1972 with the first 3 satellites carrying the Return Beam Vidicon (RBV) and Multispectral Scanner (MSS) with coverage from 1972 through to 1983 with an 18-day cycle covering the earth's surface. From 1982 the Landsat satellites started carrying the Thematic Mapper (TM) instrument and the enhanced TM (ETM+) from 1999, with a repeat cycle of 16 days (Richards and Jia, 1999). The spectral and spatial characteristics of the various instruments found on Landsat satellites are shown in Table 2.2.

Table 2.2: Landsat instruments, spectral bandwidths and spatial resolution (adapted from Richards and Jia, 1999)

Instrument	Band	Spectral bandwidths (µm)	Spatial resolution (m)
RBV Landsat 1-3	1	0.475-0.575 (blue)	79x79
	2	0.580-0.680 (red)	79x79
	3	0.689-0.830 (near IR)	79x79
	P	0.505-0.750 (panchromatic)	40x40
MSS Landsat 1-5	4	0.5-0.6 (green)	79x79 (81.5, 82.5 for Landsat 4,5)
	5	0.6-0.7 (red)	79x79 (81.5, 82.5 for Landsat 4,5)
	6	0.7-0.8 (near IR)	79x79 (81.5, 82.5 for Landsat 4,5)
	7	0.8-1.1 (near IR)	79x79 (81.5, 82.5 for Landsat 4,5)
	8 (Landsat 3 only)	10.4-12.6 (thermal)	237x237
TM/ETM+ Landsat 4-7	1	0.45-0.52 (blue)	30x30
	2	0.52-0.60 (green)	30x30
	3	0.63-0.69 (red)	30x30
	4	0.76-0.90 (near IR)	30x30
	5	1.55-1.75 (mid IR)	30x30
	7	2.08-2.35 (mid IR)	30x30
	6	10.4-12.5 (thermal)	120x120 (60x60 on ETM+)
ETM+ only Landsat 7	p	0.52-0.90 (panchromatic)	15x15

A comparison of the 16-composite NDVI products of the AVHRR and MODIS sensors indicates that results are similar and that a linear relationship exists between the NDVI values for the two sensors (Barrett *et al.*, 2005; Gallo *et al.*, 2004; Gallo *et al.*, 2005). Gallo *et al.* (2004) concluded that given the differences in composite techniques, observation timing and wavelengths of the sensors, the composite NDVI values are generally similar when sampled over similar time intervals, spatial areas and land cover types. In a comparison of the NDVI data between many commonly used sensors, results showed that the index could be corrected for the spectral band effects to a precision of about ±0.02 and the values were strongly linearly related, allowing intercalibration between the instruments (Steven *et al.*, 2003). Data from different sensors can be used to augment the spatial and temporal characteristics of datasets providing appropriate calibration or corrections are performed (Barrett *et al.*, 2005; Gallo *et al.*, 2004; Gallo *et al.*, 2005; Goetz, 1997; Steven *et al.*, 2003).

2.5.5 Case studies applicable to the remote sensing of wetlands and floodplains

In the Okavango Delta, Botswana, there has been a concerted effort to understand the flood and inundation patterns (Andersson *et al.*, 2003; Gumbricht *et al.*, 2004a; Gumbricht *et al.*, 2005; Gumbricht *et al.*, 2004b; McCarthy, 2002; McCarthy *et al.*, 2005; McCarthy *et al.*, 2003; Wolski and Murray-Hudson, 2005). This floodplain wetland system is best described as an extremely flat alluvial fan that is fed by seasonal flows and rainwater originating in the highlands of central Angola (Gumbricht *et al.*, 2005; McCarthy, 2002). Up to 98% of the inflowing water is lost to evapotranspiration over the 40 000km^2 of the semi-arid inland delta

(Gumbricht *et al.*, 2005). The seasonal and interannual flood patterns were described using satellite time series data (McCarthy, 2002; McCarthy *et al.*, 2003). Flood waters were identified in almost 3000 images from the AVHRR satellites using unsupervised classification and the spatial duration of inundation for each year determined (McCarthy *et al.*, 2003).

AVHRR was also used to track a flood of the Darling River in Australia (Barton and Bathols, 1989). Using channels 1 and 2 (visible and near infra-red), NDVI and night-time temperature data it was found that the temperature difference between floodwaters and adjacent landscape provided the best discrimination based on the histogram distribution. In southern Tunisia and north-eastern Algeria, AVHRR time series data were applied to the inundation regimes of large, climatically sensitive playas (arid, ephemeral lakes without surface outflows) in the Zone of Chotts region (Bryant, 1999). Key analytical methods included the use of reflectance profiles to infer inundation processes and the extraction of lake areas from sequential image data to determine the extent of inundation. Density thresholding of channel 2 AVHRR data was used to identify lake pixels. In order to maintain a 50:50 balance of lake and land pixels a variable area of interest was used for each image and manual clipping based on curve fitting to separate the histogram peaks. Validation was conducted using Landsat MSS data. The results were used to extract data relating to the individual inundation events, their timing and residence periods. The use of simple hydrological models allowed relationships between the magnitude of events with monthly precipitation and evaporation data.

In the Macquarie Marshes, Australia, flooding analysis of Landsat TM and SAR imagery was undertaken to determine how accurately flood waters could be mapped and whether different techniques were more efficient than conventional image interpretations and boundary digitisation (Benger, 1997). Incorporating digital elevation models (DEM) to model flood surface gradient, the Macquarie Marshes was used to test the methods. The wetlands contain large sections which are either sparsely vegetated or contain forested stands of minimal canopy density. Problems encountered in the Macquarie Marshes included shallow water depths, effects of turbidity and organic matter and emergent vegetation. Benger (1997) found that using MIR/Blue ratios to detect water produced very poor results and radar could not be used to directly map floodwaters. He suggested that application of remote sensing models over large areas in predicting the spatial distribution of flood water for given flow releases are likely to be affected by variable surface roughness and soil porosity. Temporal patterns would only be achieved through a time series analysis of images taken across flood events and would be limited due to the time of satellite overpass (for Landsat). Some of these limitations have been addressed with the application of AVHRR and, more recently, MODIS time series imagery, to the analysis of inundation. Using multi-temporal Landsat imagery (both MSS and TS), these limitations were addressed in a more recent study in the Macquarie Marshes. By selecting 28 spring images from 1979 to 2006, the inundation frequency could be assessed (Thomas *et al.*, in press). Rather than relying on a single method of open water detection, Thomas *et al.* (in press) used a combination of open water and high vigour vegetation response to define the inundated area regardless of whether open water flooding was still apparent at the time of Landsat overpass. The study defined the inundated area at the same time of year (spring) over the 28 years period. An overview of some relevant case-studies examining wetland and floodplain inundation using remotely sensed data are shown in Table 2.3.

Table 2.3: An overview of some case-studies examining wetland and floodplain inundation and response using a variety of remote sensed data and methods.

Research aims	Methods	Data sources	Location	References
Inundation mapping, ecosystem classification, landscape function prediction modelling (Integrative project)	NDVI, Wetness and brightness indices, unsupervised and rule-based classification, regression models	AVHRR, Landsat, Modis, ATSR Flow, rainfall data DEM, field surveys	Okavango Delta, Botswana	(Andersson *et al.*, 2003; Gumbricht *et al.*, 2004a; Gumbricht *et al.*, 2005; Gumbricht *et al.*, 2004b; McCarthy, 2002; McCarthy *et al.*, 2005; McCarthy *et al.*, 2003; Wolski and Murray-Hudson, 2005)
Identification of commence-to-flow levels of wetlands, map inundation extent	Thresholding of night-time thermal brightness, density slicing Landsat TM5	AVHRR, Landsat	Darling River, Australia	(Barton and Bathols, 1989), (Shaikh *et al.*, 2001)
Inundation processes and extent	Density thresholding of channel 2	AVHRR, Landsat	Zone of Chotts, Tunisia, Algeria	(Bryant, 1999)
Flood mapping, modelling of flood surface gradients	Generic algorithms using MIR/Blue ratios, radar	Landsat, SAR, DEM	Macquarie Marshes, Australia	(Benger, 1997)
Wetland function and role of hydrology and climate	NDVI temporal patterns, Spearman rank correlations	AVHRR NDVI time series, water level and climate variables	Parana Delta, South America	(Zoffoli *et al.*, 2008)
Detecting temporal changes in annual flood extent	Decision tree based on thresholds of time series indices (EVI, LSWI), wavelet-based filters,	MODIS time series, inundation maps, Landsat, water level	Mekong Delta, Cambodia/Vietnam	(Sakamoto *et al.*, 2007)
Inundation extent, detecting changes in inundation frequency and extent	Unsupervised classification, open water and vegetation response	Landsat, flow, vegetation, landuse	Murrumbidgee and Macquarie, Australia	(Kingsford and Thomas, 2002; Thomas *et al.*, in press)

In relation to the knowledge gaps identified in 2.4.5., these case-studies provide methods that might be applicable to the objectives of this thesis. The combination of open water and high vigour response determined from Landsat imagery (Thomas *et al.* in press) may overcome the issues of short duration of flooding and coverage of floodwaters by vegetation growth. Unlike the Macquarie Marshes, where the maximum inundated area was determined at a single point in time, this thesis is interested in the dynamic of the flood and response to highly variable flood regime. The overpass frequency of Landsat may not be frequent enough in some floodplain systems, while the cost of acquisition is prohibitive (this was the case during the thesis research, at the time of writing Landsat archives are now freely available through the USGS). To overcome these issues, Modis and AVHRR imagery provide daily coverage free of charge but the spatial resolution is reduced.

The classification methods used in the Macquarie Marshes (Thomas *et al*. in press) and the Okavango (McCarthy, 2002) were not as effective in the Gwydir case-study catchment due to the highly variable landscape and the temporal nature of the analysis. Temperature differentials used by Barton and Bathols (1989) was also ineffective due to climate and similarity between landscape and water temperature in the large floodplain wetlands. A method that could define open water and/or high response of vegetation in time-series data is needed. Density slicing approach is used to define a NDVI indicative of open water (Barton and Bathols 1989; Bryant 1999) and of high vegetation response (Box et al. 1989; Gallo *et al*. 2004; Huete *et al*. 2002; Myneni and Williams 1994; Pettorelli *et al*. 2005). A temporal decision tree is then applied to the time-series data to classify the landscape. The resultant landscape scale classification of the floodplain wetland system is similar in principle to the assessment and classification of wetland function (Brinson 2009; Maltby *et al*. 2009). The advantage of using NDVI in assessing inundation is that it also provides a direct measure of the productivity functioning of the landscape in response to flooding. In producing a time-series of productivity response at a landscape scale not only is an understanding of the ecological response possible, information on the longitudinal, lateral and temporal connectivity can be extracted.

Chapter 3: The Gwydir floodplains and wetlands

3.1 Location

The Gwydir catchment is located in north-eastern NSW, Australia (Figure 3.2). The Gwydir River flows from the New England Plateau in the east to the Barwon River at Collarenebri in the west. The major tributaries join the Gwydir upstream of the largest town in the catchment, Moree, while downstream the river forms an inland delta of floodplains and wetlands. It is these floodplains and wetlands that are the focus of this thesis. The Gwydir River has a large headwater storage, Copeton Dam, which regulates over 55% of the total catchment inflows. Downstream of Copeton several mid-catchment tributaries join the Gwydir River to provide some unregulated flows into the lower parts of the catchment.

The Gwydir wetlands and floodplains were chosen as the case study to address the knowledge gaps in section 2.4.5. The system is located in a dryland setting and is reliant on catchment inflows. The wetlands and floodplains also form a distributary system with variable landuse, vegetation types and flood. There is increasing efforts to supply environmental flows to protect internationally recognised areas of the wetlands; however the understanding of the ecological response to the flood pulse is still relatively poor.

The catchment as a whole covers an area of around 25 000km^2 (CSIRO, 2007; Department of Environment and Conservation, 2003) and the Gwydir floodplain and wetland complex is located within the Darling Riverine Plains Bioregion. The area is dominated by privately owned land tenure, with less than 5% under crown ownership in 2001 (Cox *et al.*, 2001), although plans are underway to purchase and protect some of the key wetland areas. In 2010 the property 'Old Dromana', which includes 2000ha of core wetlands, was purchased by the NSW and Australian Governments and will be managed by the National Parks and Wildlife service (NSW Department of Environment Climate Change and Water, 2010). The wetland areas produce rich cattle grazing country (Keyte, 1994) while in surrounding drier areas sheep are also grazed and dryland cereal cropping is undertaken on the western plains. Irrigated and broadacre agriculture has continued to increase with substantial development surrounding the wetlands as shown in Figure 3.10, with over 35 000ha of land developed for irrigation (including on-farm storages) and over 130 000ha cleared and cultivated (Table 3.2).

Flooding regimes are irregular in size and timing and in all but the largest flood, the inflows are retained within the wetlands and do not contribute to flows in the Barwon River. It is difficult to establish the exact extent of the system due to its variable nature and the impact of landuse. However in 1993 102 000ha of the Gwydir wetlands were listed in the Directory of Important Wetlands (Environment Australia, 2001). In 1999, 823ha of privately owned farming properties were designated as Wetlands of International Importance under the Ramsar Convention (Environment Australia, 2001). The listings were in recognition of the ecological significance of the wetlands as waterbird habitat (Environment Australia, 2001) and their large populations of water couch and marsh club-rush (Allan and Lovett, 1997), but there are many equally important habitat areas within the lower Gwydir wetlands (Mawhinney, 2003; McCosker, 1994b; Spencer, 2010).

3.2 Floodplain description

The Lower Gwydir floodplains and wetlands occur on a large sedimentary floodplain that fans out over an alluvial plain to the west of Moree (Figure 3.3). Although the floodplains are fan-shaped in the upper reaches, the slope is considered too low to be a true alluvial fan (Pietsch, 2006). The Gwydir is close to a low sinuosity/meandering fluvial fan of a type to which the Okavango in Botswana belongs. However the Gwydir tends towards a planar surface in the lower reaches and hence fan-plain is a more appropriate term (Pietsch, 2006). Although this is a more technically correct term for the study area, the term floodplain is used for simplicity throughout the thesis.

The Gwydir River diverts upstream of Moree into the Mehi River and Gwydir Rivers with a constrained ‘pan-handle’ river channel from the start of the plains at Pallamallawa to Moree (Mehi) and Yarraman (Gwydir). From here, a number of channels diverge across the floodplain with some becoming poorly defined ‘floodrunners’ or ‘watercourses’. These terms are used locally for lower lying depressions that route floodwaters across the floodplain. The floodplains of the lower Gwydir (including the Lower Gwydir or ‘Big Leather’ and the Gingham Watercourses) tend to merge with the floodplains of Carole Creek, Gil Gil Creek and the Macintyre River to the north. The Mehi and its anabranches flood out to join the Thalaba Creek and Namoi River floodplains to the south. In large floods, the entire Gwydir floodplain and the Barwon River floodplain to the west converge, but for the most part, the Gwydir floodplains of the Gingham and Big Leather watercourses can be considered as terminal floodplains.

The alluvium of the Gwydir floodplains has been accumulating since the mid-Miocene (Martin 1994 in Pietsch, 2006) with depths of relatively unconsolidated alluvium of 40-60m over sandstone, siltstone and claystone. The floodplain surface contains numerous paleochannels which have been dissected and heavily obscured by the younger floodplain accretions while the paleochannel remnants suggest that the past fluvial activity was much higher than the present hydrological regime (Pietsch, 2006). The soils overlying the alluvium and paleochannels are heavy textured brown and grey soils and black earths and feature surface micro relief or ‘gilgai’ formation (Cox *et al.*, 2001).

The Gwydir floodplains originate at around 230m above sea level (ASL) at the start of the pan-handle at Pallamallawa and drop to around 150m near Collarenebri (Pietsch, 2006). Figure 3.3 shows the longitudinal profile for the Gwydir catchment with relatively gentle slopes in the upper catchment. Copeton dam is located around 125km from the Gwydir River source and is immediately upstream of a steep drop in elevation through the mid-catchment. The slope gradually flattens out across the Gwydir floodplains to less than 0.05%. Almost the entire runoff for the catchment is generated upstream of Pallamallawa with local rainfall on the floodplain contributing little to stream flows due to a combination of very low slope, absorbent soil conditions and high moisture deficits (Pietsch, 2006). The Gwydir wetlands are therefore reliant on exogenous river inflows.

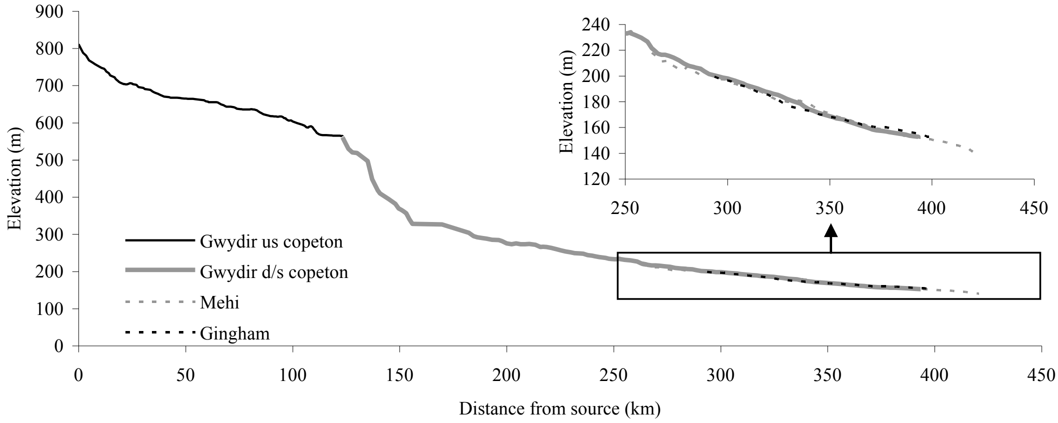

Figure 3.1: Longitudinal profile of the Gwydir River developed from the 250m DEM. Inset shows the Lower Gwydir, Mehi and Gingham channels in more detail.

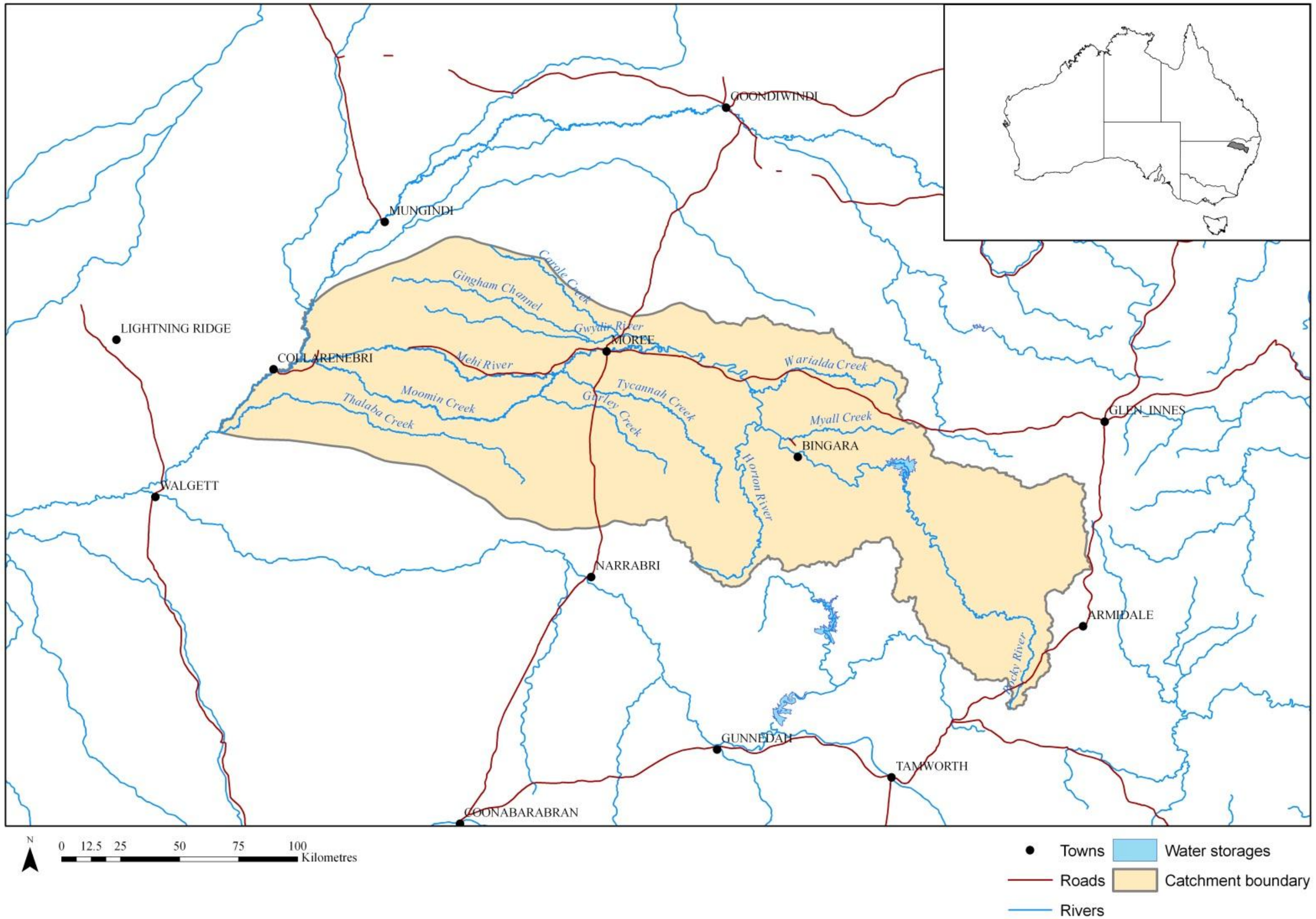

Figure 3.2: Gwydir catchment: location, towns, roads

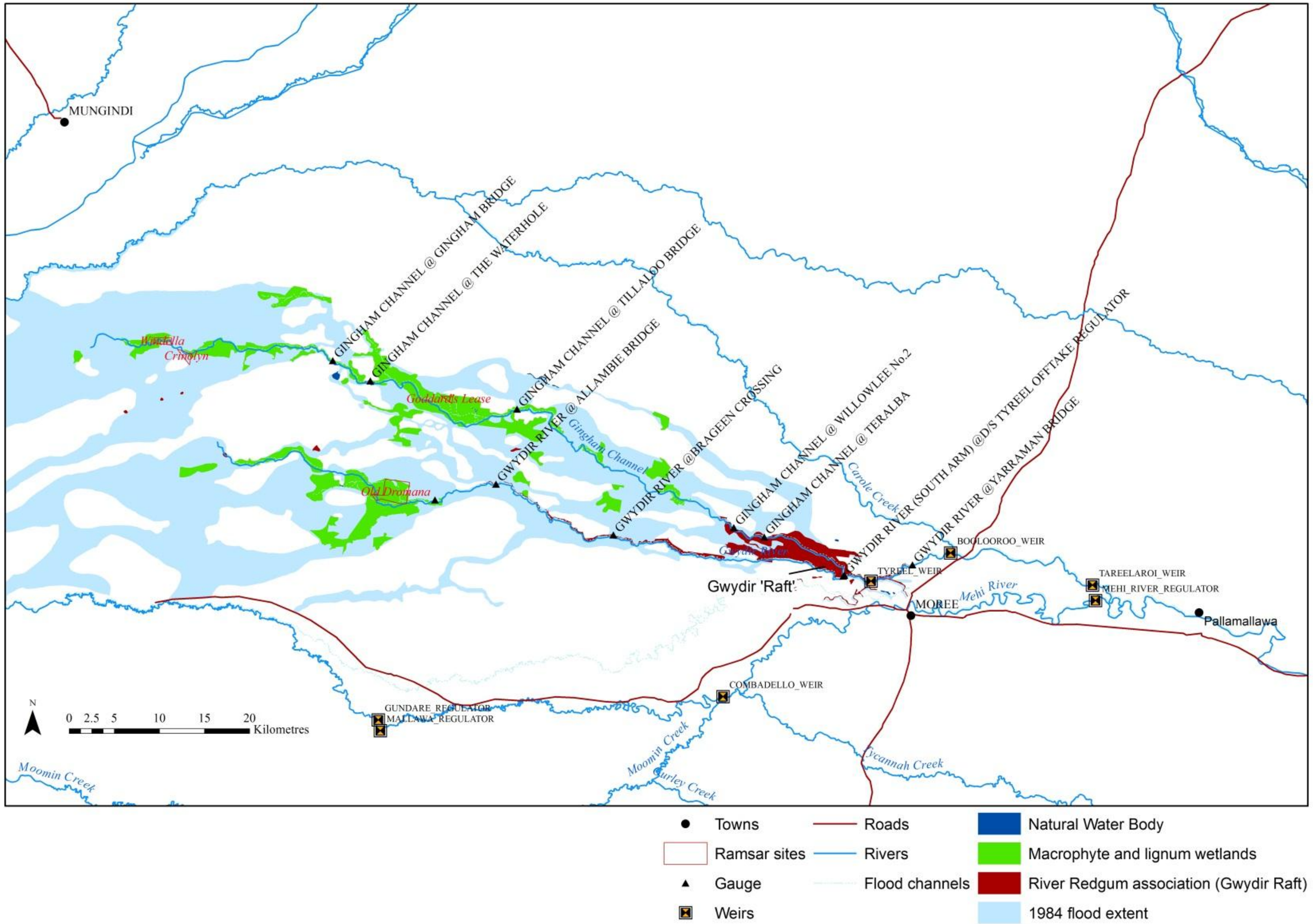

Figure 3.3: Gwydir floodplain and wetlands (vegetation mapping undertaken by McCosker (1994) and updated using 2004 Spot5 imagery based on visual estimation of areas cleared and cultivated, 1984 flood extent from NSW DLWC Gwydir data)

3.3 Climate

Moree is located on the eastern fringe of the floodplains and has a mean annual rainfall of 582mm (Bureau of Meteorology, 2004; Bureau of Meteorology, 2010). The rainfall decreases from the headwaters of the Gwydir catchment in the east with rainfall around 850mm/yr to the junction of the Mehi and Barwon Rivers to the west where rainfall is less than 500mm/yr (Bureau of Meteorology, 2004; CSIRO, 2007; Keyte, 1994; Pietsch, 2006). Rainfall in the region has not shown any long-term trends over the past 50 years (CSIRO, 2007) but is highly variable from year to year as shown in Figure 3.4.

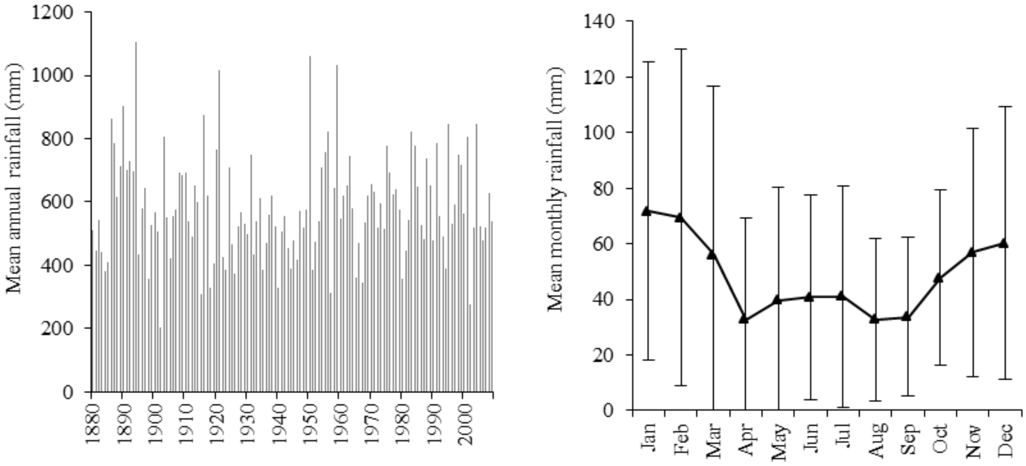

Figure 3.4: Mean annual and monthly rainfall at Moree 1890-2009 (Moree Post Office 1880-1965, Moree Comparison 1966-1995, Moree Aero 1996-2009) (Bureau of Meteorology, 2010).

The Gwydir floodplain and wetlands are located on the cusp of two main climatic systems with summer storms historically producing the largest floods. These summer storms are dominated by tropical low pressure systems and monsoonal troughs approaching from the northwest that then decay into inland rain depressions. Winter storms occur when cold fronts from the south or southwest pass over warmer, moisture laden low pressure systems from the northwest that can trigger substantial rainfall events. During the summer months, the region can also experience high intensity, short duration convectional thunderstorms generating heavy localised rainfall and local flooding and runoff (Keyte, 1994). The mean monthly rainfall peaks in January and February with the lowest rainfall in April, August and September (Figure 3.4). With mean daily temperatures exceeding 33°C at Moree and 35°C at Collarenebri in January, the daily evaporation averages in this month exceed 9mm (Bureau of Meteorology, 2004). Long-term average pan evaporation in the study area is in excess of 2200mm/yr, with a mean daily pan evaporation at Moree of 5.9mm. The mean annual (modelled) runoff over the catchment for a 112 year period is 41mm, ranging from over 200mm in some areas of the upper catchment to less than 20mm across most of the floodplain (CSIRO, 2007) (Figure 3.5).

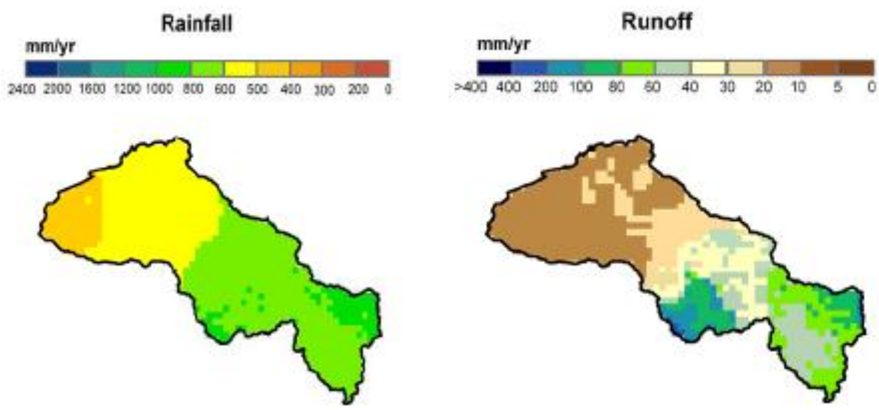

Figure 3.5: Average annual rainfall and modelled runoff over the Gwydir catchment 1895-2006. Reproduced with permission (CSIRO, 2007).

Rainfall-runoff modelling with climate change projections indicates that future runoff in the Gwydir catchment is more likely to decrease than increase, with two-thirds of results indicating a decrease and one-third an increase in runoff. The median estimate is a 9% reduction in mean annual runoff in around 2030 compared to 1990 (CSIRO, 2007). In comparison the estimated increase in farm dam water storage volume is projected to decrease annual runoff by about 1.5% (CSIRO, 2007).

3.4 Hydrology

3.4.1 Overview

The Gwydir wetlands receive inflows from the Gwydir River. Upstream of the wetlands, flow is diverted south to the Mehi River and north into Carole Creek for irrigation (discussed further in Section 3.5.4). Figure 3.3 shows the location of flow and height recording gauges in the study area. The Gwydir River then flows through Yarraman Gauge (418004), before entering the Gwydir Raft accumulation. The Tyreel regulator controls some flow distribution over the wetlands to the north via Gingham Channel and to the south via the Gwydir or 'Big Leather' system. The Tyreel regulator can only control lower (within channel) flows, with higher (flooding) flows largely uncontrolled.

There is no doubt that significant channel alteration and catchment development since European settlement in the 1860's has changed the flow and flood characteristics of the Gwydir floodplain and wetlands (Arthington, 1995; Pietsch, 2006). Early modifications included cuttings (creation of artificial waterways or deepening of existing channels) to promote flow (Figure 3.6) and the development of a network of open bore drains which distributed water across the floodplain from artesian wells. The "Cap and pipe the bore" scheme (NSW Department of Land and Water Conservation, 2000) has replaced some of these open bore drains with piped water distribution systems from capped artesian bores as a means for providing stock water but the drains remain a feature of the landscape and still influence flood flows.

The Gwydir Raft (Figure 3.2) is an accumulation of timber and debris on the Gingham Channel which has resulted in sedimentation. The Raft has built up along the former channel blocking and altering flows for more than 30 km. It is assumed that the Raft formed during early European settlement due to tree clearance and subsequent erosion (Arthington, 1995) and, even in the early 1900's, the Raft was significant enough to be clearly marked on maps of the Gwydir catchment and floodplains (Figure 3.6).

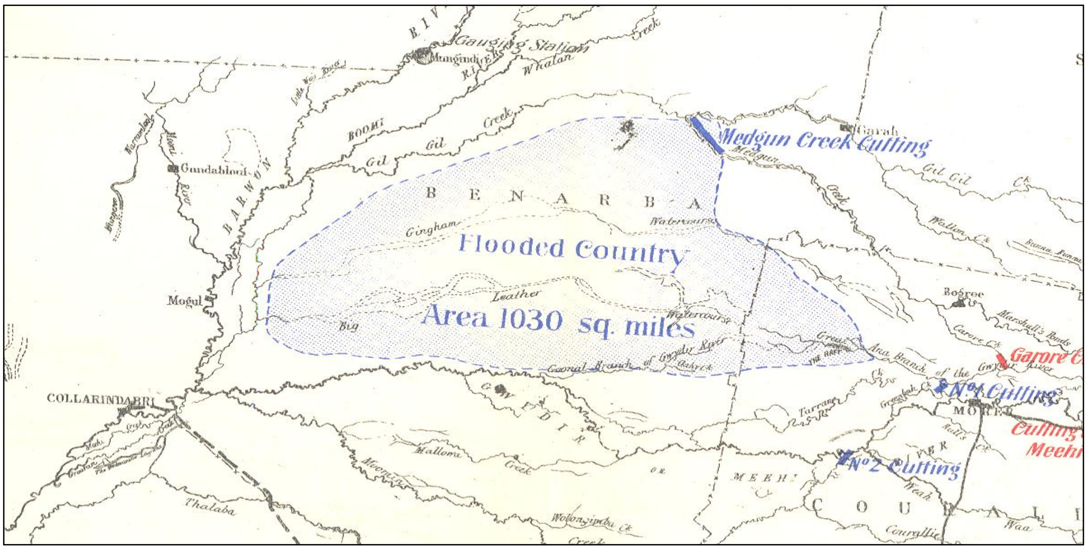

Figure 3.6: Map of the Gwydir Floodplains c1902. Note the disconnection of the Gingham Channel to the east and also the Raft on the eastern most extent of the flooded country on the junction of the Big Leather Watercourse and Goonal Branch of the Gwydir River. (The Gwydir flooded country map was a part of the evidence presented to the Interstate Royal Commission on the River Murray in 1902. It was *Exhibit 24: Plan Showing Dumaresq, Macintyre and Gwydir River districts*.)

The Gingham and Lower Gwydir watercourses have been defined by stock and domestic channels. These channels are typically a few metres wide and deep and were constructed to distribute regulated water supplies to landowners across the floodplain for stock and domestic use. This provision was to replace some of the natural flows that would have occurred prior to the completion of Copeton Dam and water extractions upstream. These channels have altered the natural flood patterns over some previously naturally irrigated pastures and wetlands (Pietsch, 2006).

The construction of Copeton Dam in the 1970's, regulation of the Gwydir River and the development of irrigation infrastructure have further changed the nature of the system (Keyte, 1994). Copeton Dam regulates 55% of the total inflows to the Gwydir River and has a capacity of over 1,360GL. The Horton River is the major unregulated tributary and is responsible for many of the flooding flows to the floodplains and wetlands. The irrigation industry also relies on off-river storages to divert and store unregulated flows, with over 300GL of off-river storage capacity developed by 1996 (Kingsford, 2000). A number of regulating weirs control flows in the lower catchment with Tareelaroi and Combadello controlling flows to the southern effluents of the system through the Mehi River. Boolooroo weir forces water down Carole Creek to Gil Gil Creek. Prior to regulation, the Mehi River, the largest effluent of the system, only flowed 15% of the time, when the Gwydir River height exceeded six metres (Water Conservation and Irrigation Commission, 1972). Similarly, Carole Creek and Gil Gil Creek only carried water for around 7% of time prior to regulation.

As the name suggests, the Gwydir floodplains are highly prone to flooding, however there are areas of high ground associated with sand dunes and paleochannel remnants that never flood. Most of the floodplain contains floodways and watercourses that distribute overland flows, with lower lying floodways forming wetlands that may remain flooded for months at a time following large floods. The wetlands contain interconnecting flowpaths and scattered waterholes and billabongs. The total capacity of the watercourses and channels that flow through the Gwydir floodplains is much less than the capacity of the upstream 'pan-handle' of the Gwydir River between Pallamallawa and Yarraman. Flows greater than the combined capacity occur around 1 in 2 years (Pietsch, 2006). Flooding occurs more frequently however, and core wetlands form where channels gradually reduce in size and eventually distribute even relatively small flows to floodouts.

The behaviour of the Gwydir floodplains cannot be explained by paleochannel remnant alone (Pietsch, 2006). Rather it is a result of declining stream power due to declining slope and vegetation accumulation. It has also been suggested that movement of water into aquifers may also contribute to declining stream power (Pietsch, 2006). Underlying the western floodplains are alluvial aquifers that form a three-layered system comprised of the Cubbaroo Formation, overlain by the Gunnedah Formation and then the Narrabri Formation (CSIRO, 2007). Most of the watertable in the western parts of the floodplain is well below the streams, and surface water may leak to the underlying aquifer whilst streamflow persist. There may also be direct hydraulic contact with the watertable at the eastern margin of the floodplain (CSIRO, 2007). The largest attenuation of flow is most likely due to floodplain storage created by natural geomorphic elements. The storage capacity is difficult to calculate but estimates of volumes required to flood the wetlands suggest storage capacities of around 3-6ML/ha (McCosker, 1996; Roberts, 1993). The natural capacity has been reduced in many areas due to simplification of the geomorphic character through agricultural development on the floodplain, but this has been offset by the building of large on-farm storages (OFS) on the floodplain as shown in Figure

3.10. These storages had an estimated capacity of over 300GL by 1996 (Kingsford, 2000) and this has increased substantially. Although flooding is a relatively normal state for this system, it is unpredictable as shown in figure 3.7. Daily inflows at Gwydir River at Yarraman gauge show high inflows to the wetland system can occur in most months while periods between high flows are unpredictable. Predicting flood response to system changes such as ongoing changes to 'the Raft', channel manipulation and river regulation is not straightforward. Vegetation in watercourses and channels can change flood behaviour, and flow can be greatly affected by minor geomorphic and hydrologic disturbance (Pietsch, 2006).

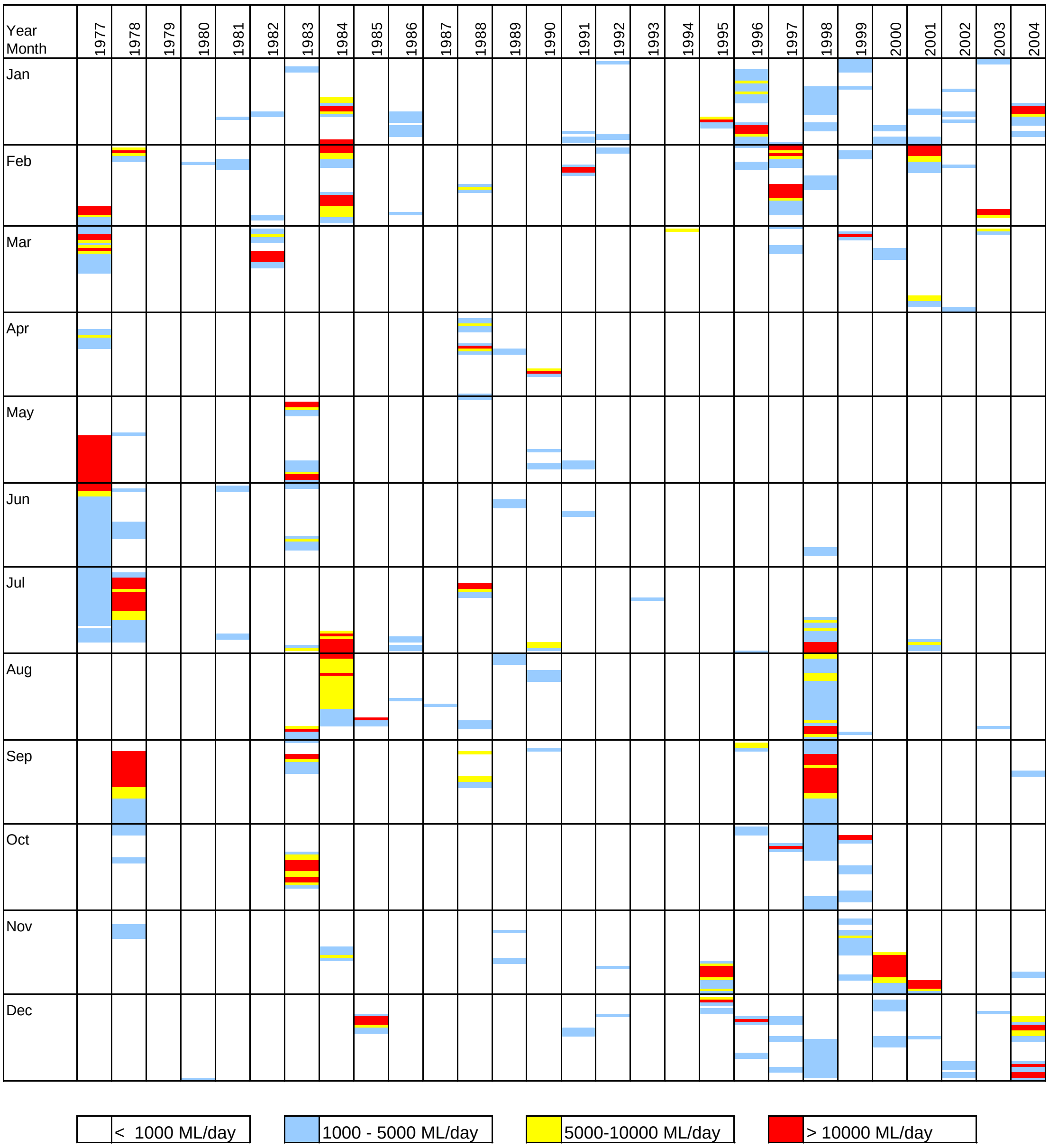

Figure 3.7: High flow periods through Gwydir River at Yarraman (418004) from 1977 to 2004 (Powell, 2005)

3.4.2 Flow measurement

Understanding that the system has changed significantly from its 'natural' state, this thesis is concerned primarily with the contemporary flow and flood behaviour of the floodplain wetlands. The network of gauging stations shown in Figure 3.3 provides a range of data that can be used to assess the flow through the study area in more detail. Most of these gauges can only effectively measure low flows as channel capacity is relatively low. Table 3.1 provides a comparison of the channel depth, bank-full width and estimated bank-full discharge for selected gauging stations.

Table 3.1: Gauging station characteristics. Depth, width and bankfull discharge for selected inflow and wetland gauging stations (NSW Water Information database, waterinfo.nsw.gov.au, accessed 2010)

Station No.	**Name**	**Channel depth m**	**Bankfull width m**	**Estimated bankfull discharge ML/day**
418004	Gwydir R @ Yarraman	25	200	>50 000
418078	Gwydir R @ Allambie Bridge	3.3	25	4 500
418075	Gingham @ Willowlee 2	3.5	22	2 500
418074	Gingham @ Teralba	3.5	30	5 000
418076	Gingham @ Tillaloo	1.0	10	500
418079	Gingham @ Gingham Bridge	1.0	17	1 000

The rating tables for Gwydir River at Yarraman and Gingham Channel at Tillaloo are shown in Figure 3.8 a and b while the cross-sections for a range of gauging stations are compared in Figure 3.9. The Gwydir River at Yarraman has seen a distinct change in the rating curve (that is, the relationship between water depth and flow) which occurred as a result of lowering of the gauge zero level in 1994 (NSW Water Information database, waterinfo.nsw.gov.au, accessed 2010). In contrast, the channel at Tillaloo Bridge has seen a more gradual change in ratings which is not associated with a distinct event and may represent changes to the river cross-section over time. As the table and figures demonstrate, other than the Gwydir River at Yarraman (418004), the wetland gauging stations can only provide flow or discharge information for flows of less than 5000ML/day. With small floods recording over 10 000ML/day entering the system, and large floods recording peak inflows in excess of 50 000ML/day, the distribution of flows through the study area is difficult to determine using this gauge information. Changes to river and channel cross-sections and therefore the relationship between gauged water height and flow can also complicate the gauged flow records used in model development and testing.

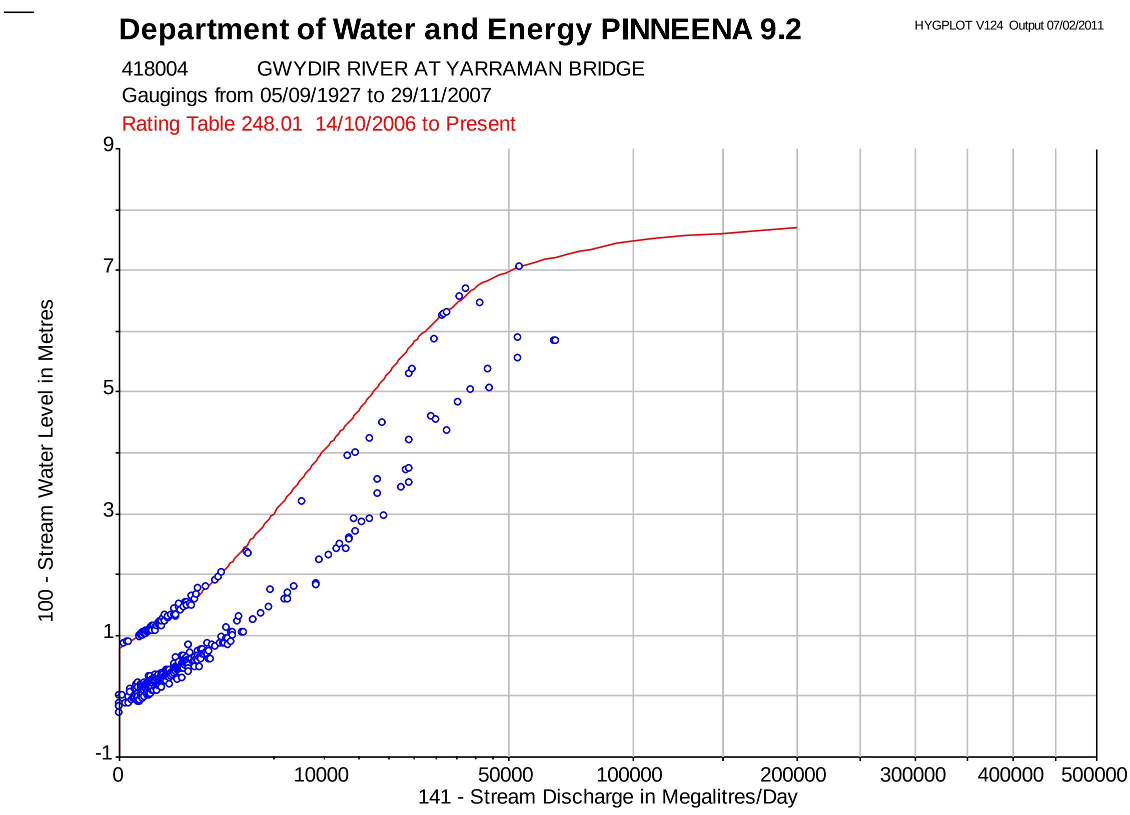

a

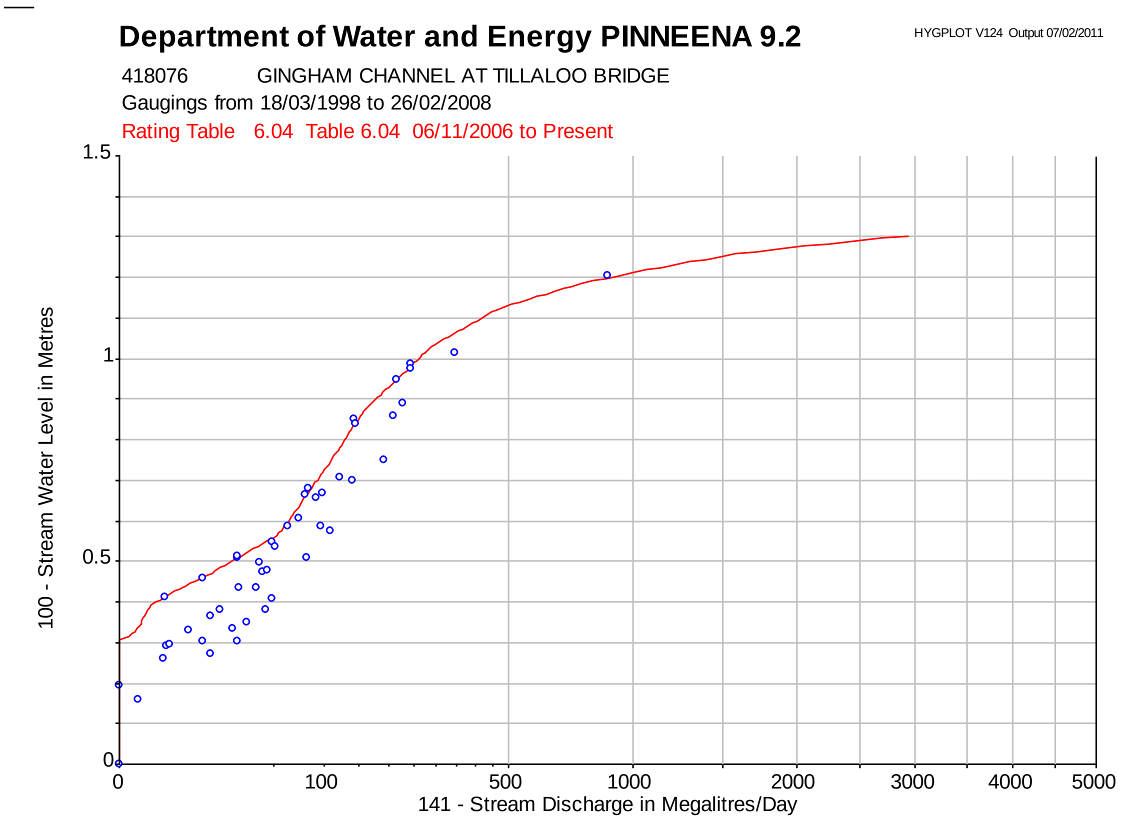

b

Figure 3.8: Rating curve for a) Gwydir River at Yarraman and b) Gingham Channel at Tillaloo. (Department of Water and Energy, 2007)

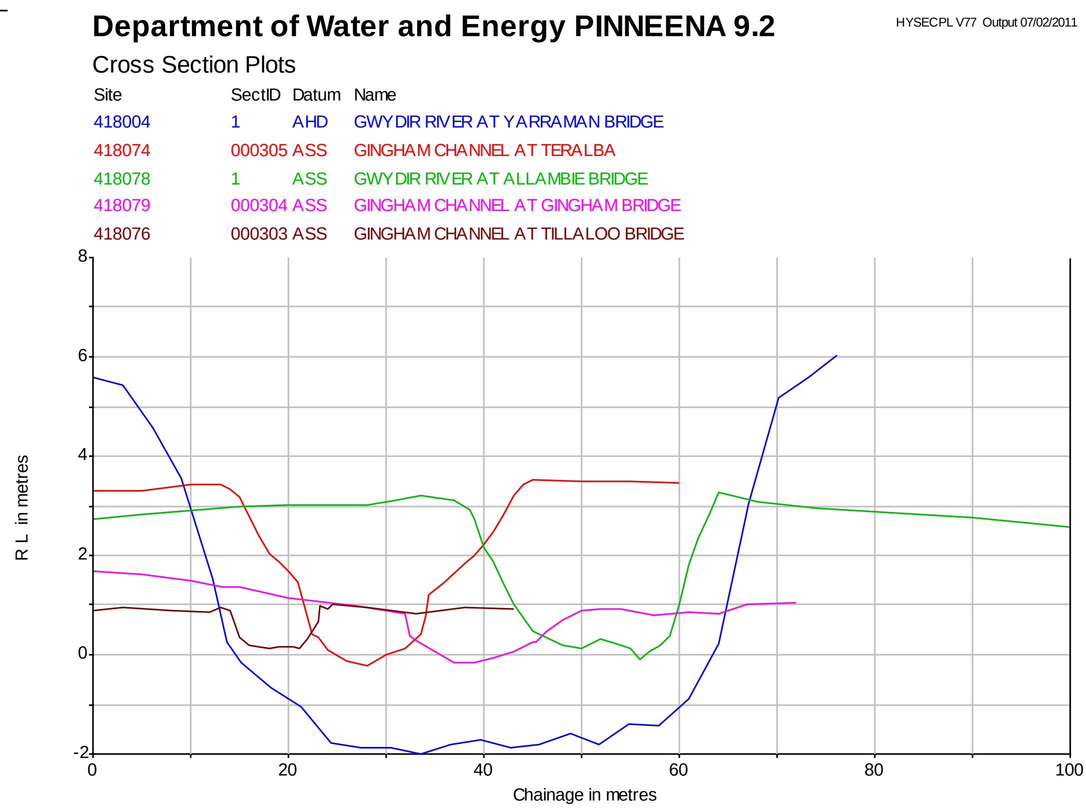

Figure 3.9: Cross-section for Gwydir River at Yarraman (418004) and downstream gauges of Gingham Channel and Gwydir River. (Department of Water and Energy, 2007).

3.4.3 Water management and environmental flows

River regulation has resulted in a significant reduction in the frequency and magnitude of flooding in the Gwydir wetlands with modelling in the early 1990's suggesting a 70% reduction in the occurrence of flows large enough to flood the Gingham and Lower Gwydir wetlands (Bennett and Green, 1993; Keyte, 1994). These reductions have come about due to a reduction in catchment area, diversion of flows and harvesting of unregulated flows. Copeton Dam captures 55% of the total catchment flows and regulates 42% of the catchment area. Uncontrolled spill from the dam has occurred only twice between 1976 and 1993 (Keyte, 1994). Prior to water resource development, much of the catchment flow entered the Lower Gwydir wetlands and floodplains, and only in the largest floods did water flow through to the Barwon River. Diversion of waters to the Mehi River and Carole Creek have turned these naturally ephemeral floodrunners into regulated streams and take much of the unregulated low flows away from the wetlands (Keyte, 1994). In the planning for Copeton Dam, it was considered that the dam could supply water to irrigate about 56 000ha with good reliability and minimal impact on the wetlands but by 1979 irrigation licences had been issued for a total of 86 000ha (Keyte, 1994). Since the early 1980's the volume of surface water diverted has varied depending on supply and climatic conditions from less than 100GL during the early 1990's drought to over 500GL in 1997 (Figure 3.). Due to the low reliability of Copeton Dam from the over-issue of licences, on-farm storages developed to capture extra water during flooding became economically feasible, with 300GL of such storage developed by 1993 and as much as 520GL by 2007 (CSIRO, 2007; Keyte, 1994). Groundwater is also used in the Gwydir catchment for irrigation with up to 50GL/yr extracted from the Lower Gwydir Alluvium (CSIRO, 2007). Increased groundwater use has often been associated with lower surface water availability (Figure 3.b).

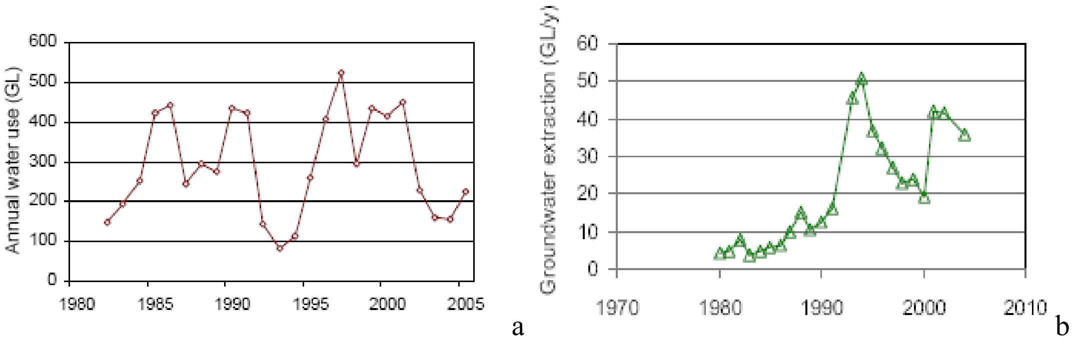

Figure 3.10: Historical water diversions of a) surface water of the Gwydir region and b) groundwater extractions within the Lower Gwydir Alluvium. Reproduced with permission (CSIRO, 2007).

In response to the declining condition of many rivers in NSW and the over-allocation of water, the Water Management Act 2000 required the implementation of plans to share water between the environment and water users and to clarify water rights. However environmental flow rules were introduced in the Gwydir in the 1990's, with the 1994-1997 plan of management just one example (Keyte, 1994). In 2003, the Water Sharing Plan for the Gwydir Regulated River Water Source was gazetted (Department of Infrastructure Planning and Natural Resources, 2004b). The plan includes almost 530 000 shares of general (bulk of regulated water supplied to irrigators) and high security (has a higher priority of supply compared to general category) entitlements. A further 178 000 shares are allocated to supplementary (i.e. the extraction of water during periods of high unregulated flows) licensed entitlement. In any given year, the available water is determined (AWD), and allocations announced as a volume per unit share (i.e. 1 megalitre per unit share). In addition, a long-term average annual extraction limit in the order of 400GL has been set for the catchment and is based on water use development that existed in 1999/2000 and recognises climatic variability.

The Water Sharing Plan also specifies environmental flow provisions which aim to ensure water remains available to the environment, that a portion of natural tributary inflows reach the Gwydir wetlands and to provide for water to be released from Copeton Dam when required for environmental purposes such as flooding of wetlands or to support water bird breeding

(Department of Infrastructure Planning and Natural Resources, 2004b). A minimum flow is to be passed through to the wetlands, and is the lesser of 500ML/day or the sum of flows in nominated upstream tributaries, plus any water spill or pre-release for flood mitigation purposes from Copeton Dam. Environmental flows can be suspended if this would be to the environmental benefit of the wetland (for example to assist in the control of water hyacinth). If suspended, these flows must be used elsewhere to support ecosystem health. In addition, no more than 50% of uncontrolled flows can be extracted (supplementary flow access). An Environmental Contingency Allowance (ECA) is also specified in the plan as a volume held in Copeton Dam for environmental purposes and is the lesser of 45GL multiplied by the number of megalitres per unit share specified in the AWD, or 90GL minus the volume currently in the account.

The ECA can be used to support a range of ecological purposes including colonial bird breeding events that have been initiated by natural flood inundation and additional inundation during extended dry climatic conditions. The ECA Operations Advisory Committee has been established to provide advice regarding the releases and to date this has been based on expert opinion. To assist in the development of environmental flow rules and the management of water resources for environmental benefit in the Gwydir, a decision support system (DSS), Ibis, is currently under development and applied to the Gwydir wetlands (Merritt *et al.*, 2010). Ibis is linked to a daily water balance model developed by NSW government agencies. The model outputs are used to extract key event information such as timing, duration, depth and frequency of flooding. This information is linked to likely ecological response models for specific species of fish, birds and vegetation using Bayesian Decision Networks (Merritt *et al.*, 2010). In contrast this thesis develops an alternative daily water balance of water depth across the landscape including both surface water and sub-surface soil moisture. Time-series vegetation productivity models are also developed and the outcomes may help inform future development of Ibis with respect to water balance modelling and landscape scale vegetation productivity response.

3.5 Ecology

This thesis is largely focussed on flood and inundation patterns of the lower Gwydir and on the vegetation response to that flooding. This section reviews the current state of native vegetation communities found in the Lower Gwydir as well as some specific information on invasive species relevant to inundation and water management.

A brief overview of current research on waterbirds and fish found in the Lower Gwydir, as well as other biota and trophic structure, is included. Although this thesis does not focus on these elements, they are all reliant to some extent on the flooding patterns and the habitat value of the vegetation structure and productivity.

3.5.1 Vegetation

The Gwydir wetlands are one of few terminal wetlands found within inland NSW and contain one of the largest stands of Paspalum distichum (water couch) and Bulboschoenus fluviatilis (marsh clubrush) remaining in NSW (Green and Bennett, 1991; McCosker, 1994b; Ramsar Convention Secretariat, 2004). Other wetland flora of note in the core wetland areas include Eleocharis plana (ribbed spike-rush), E. sphacelata (tall spike-rush), Juncus aridicola (tussock rush) and Typha domingensis (cumbungi), in association with various other aquatic plants including Ranunculus undosus (swamp buttercup), Ludwigia peploides (water primrose), Ottelia ovalifolia (swamp lily), Cyperus sp. (sedges) and Myriophyllum sp. (water milfoil) (Mawhinney, 2003; McCosker, 1994b). Together these associations are referred to as water meadows in this thesis with a distinction made where spatial scale allows between the water couch/spike rush meadows and the small stand of marsh clubrush as shown in Figure 3.11.

Surrounding these core wetland areas are a range of vegetation communities that are closely related to the elevation, soil types and frequency and duration of flooding. Of significance to this research are the Muehlenbeckia florulenta (lignum) and Acacia stenophylla (river cooba) associations on frequently flooded, low lying clay soils, Eucalyptus coolabah (coolibah) associations on less frequently flooded clay soils (Keyte, 1994) and Eucalyptus camaldulensis (river red gum) in association with larger channels and the Gwydir Raft. Other mapped vegetation associations include Alectryon forsythia (rosewood), Acacia pendula (myall), Eucalyptus populnea (poplar box), Casuarina cristata (belah) and native grasslands. These occur on less frequently flooded areas as well as small sand ridges known colloquially as sand monkeys.

Detailed information on water regime requirements of some of the core wetland species is available. One of the most significant stands of Marsh clubrush in the Murray-Darling Basin occurs in the Gwydir wetlands where is grows in shallow waters of wetlands associated with the Lower Gwydir River. Using flow-inundation area relationships Bennett and McCosker (1994) estimated that Marsh Clubrush in the Gwydir flooded in about 85% of years under natural conditions with river inflows of at least four weeks. Duration of flooding is likely to be much longer with field observations indicating several months to seed set (McCosker 1999; Roberts and Marston 2011). Marsh clubrush does not grow in the absence of flooding and rainfall alone will not sustain vigorous growth (Roberts and Marston 2011).

Water couch is widespread in the Gwydir wetlands and its vigour is controlled by depth, duration, timing and frequency of flooding (Mawhinney 2003; Roberts and Marston 2011). The most favourable growing conditions are shallow water with water couch grown in depths from 5cm to 20cm had similar weight whereas plants grown in 60cm weighed less (Roberts and Marston 2011). Flood duration should continue for several months and water couch is frost sensitive, so in the Gwydir spring-summer flooding in preferred and winter floods are not effective unless inundation persists into spring (McCosker 1999; McCosker 2001; Wilson *et al.* 2009). Flood frequency is also important with estimated frequency of one in two years to 85% of years in the Gwydir wetlands (Bennett and Green 1993; Wilson *et al.* 2009)

Cumbungi occur in wetlands that have permanent, near-permanent or seasonal water regimes and can tolerate slightly brackish water and high water temperatures. Although native, Cumbungi can be invasive in habitats with suitable water regimes and can form dense stands potentially reducing wetland plant diversity (Roberts and Marston 2011). Cumbungi can be found over a wide range of water depths and generally occur in deeper areas and on the margins of billabongs and channels in the Gwydir (NSW DLWC, unpublished data). Peak mid-summer biomass of Cumbungi stands can be very high, with some species exceeding 2000 g m-2 (Froend and McComb 1994).

Lippia (Phyla canescens) invasion is a continuing problem in the Gwydir wetlands. This invasive perennial forb originated in South America and has become widespread throughout the Murray Darling Basin (Julien *et al*., 2004; Mawhinney, 2003; Price *et al*., 2010). Due to the deep tap-root and growth form, Lippia is drought resistant and when favourable conditions occur it forms a dense matt that excludes other plant species. It invades areas that are not cultivated and is a lowland and wetland plant in its native range, thriving on floodplains with frequent flooding of short duration (Julien *et al*., 2004; McCosker, 1994a). Prolonged flooding of depths greater than 20cm allows native vegetation to outcompete Lippia (Mawhinney, 2003; Price *et al*., 2010), however Lippia is likely to return during dryer periods or flood regimes unfavourable to native vegetation. The other invasive that is a particular issue in the Gwydir wetlands is water hyacinth (Eichhornia crassipes), a floating aquatic weed originating in Brazil with the highest growth rate of any saltwater, freshwater or terrestrial vascular macrophyte (Toft *et al*., 2003). The plants form a dense floating matt excluding other plant species and create hypoxic conditions in underlying floodwaters. Water hyacinth reproduces vegetatively and by seed and was first reported in the Gingham Watercourse in the 1950s. In the 1970s the weed was a major concern and underwent some control measures. In 1999 the plant had re-emerged as a serious weed problem with an aerial survey in April 2001 finding about 4000 hectares of wetland affected by hyacinth (McCosker, 2001b). Fortunately the invasion has been limited to the Gingham system and has not been detected in the lower Gwydir (Mawhinney, 2003).

The Gwydir floodplains have been extensively cleared over the last three decades as the value of cotton and wheat has increased compared to grazing (Cox *et al*., 2001). The total area cleared and the area and patch size of remnants were analysed in 2001 (Cox *et al*., 2001) using remote sensing from Landsat and aerial photography. In an area of northern NSW bounded by the NSW border to the north, the 300m contour interval to the east, the Barwon river to the west and Walgett to the south, over 110 000ha of native woody vegetation were cleared between 1985 and 2000. This is 16% of the extant vegetation in 1985. Not only has the area of native woody vegetation declined, there has been increased fragmentation of the remaining vegetation. Large areas were cleared to the east of Collarenebri and Mungindi that is near the Gwydir wetlands and floodplains.

In relation to different vegetation communities, the most extensive clearing occurred in the lignum shrublands, floodplain mosaics (including open forests to low woodlands, sedgelands and grasslands associated with grey cracking clays soils of floodplains), open coolibah, poplar box and belah woodlands, all recording more than 15% of the 1985 area being cleared (Cox *et al.*, 2001). Increased fragmentation, smaller patch sizes and increasing edge effects have also been observed (Bowen and Simpson, 2009). The loss of coolibah woodlands across the Gwydir floodplain, and continued high rates of decline in the area, are significant, with a 25% decline found during remote sensing analysis of spot imagery in this thesis from 2004 compared to the mapping undertaken in the mid 1990's by McCosker (1994b). Add to this the definition of 'clearing' being total removal of the canopy, the thinning and cultivation under coolibah woodlands that is occurring as a response to lippia invasion may further undermine the quality of the vegetation patches that are left.

Table 3.2: Estimated change in vegetation community extent of the Lower Gwydir floodplains and wetlands. Areas estimated for this thesis using vegetation mapping undertaken by McCosker (1994) and updated using 2004 Spot5 imagery based on visual estimation of areas cleared and cultivated.

Vegetation community	1994 (ha)	2004 (ha)	% change
belah	1224	1216	-0.7
black box/ coolibah association	18748	15580	-16.9
cleared cultivated land	90066	131201	45.7
coolibah woodlands	119308	89327	-25.1
coolibah/river redgum association	3416	3371	-1.3
land developed for cotton irrigation	29687	33569	13.1
marsh clubrush	317	317	0.0
myall/rosewood association	12386	8841	-28.6
native grasslands	10545	6872	-34.8
natural water body	126	139	10.6
on farm water storage	3498	4120	17.8
poplar box association	10411	10345	-0.6
river redgum association	433	433	0.0
river cooba/lignum association	5527	4225	-23.6
river redgum	254	311	22.4
spikerush	13648	9873	-27.7

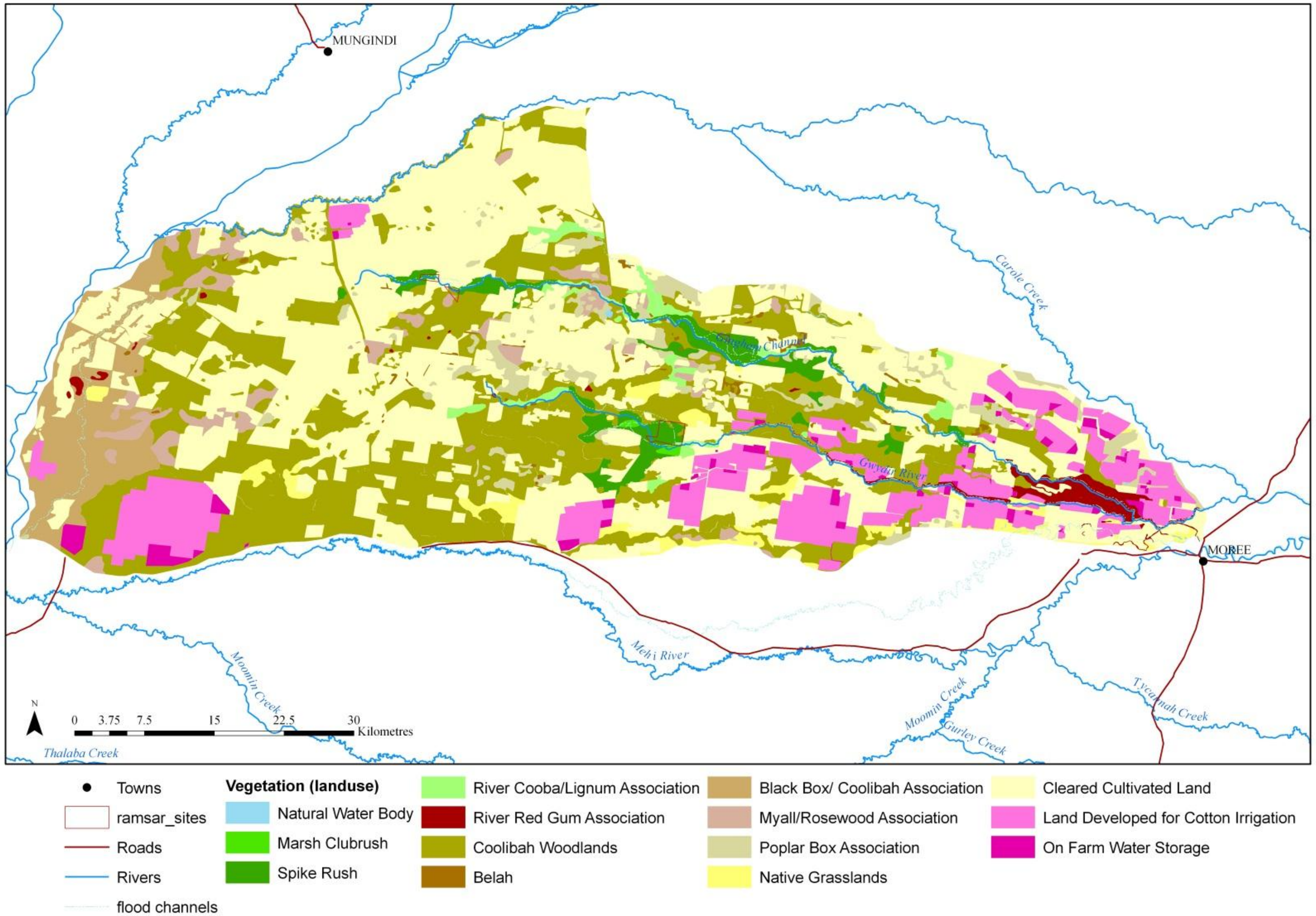

Figure 3.11: Vegetation and landuse of the Gwydir floodplain and wetlands (vegetation mapping undertaken by McCosker (1994) and updated using 2004 Spot5 imagery based on visual estimation of areas cleared and cultivated).

3.5.2 Waterbirds

The Gwydir wetlands provide breeding and feeding grounds for large numbers of colonial water bird species (over 500 000 breeding pairs in 1998) and habitat for many threatened species. Over 255 bird species in total and at least 75 species of waterbirds have been recorded in the Gwydir Wetlands (Spencer, 2010). Colonial waterbirds that breed in the Gwydir wetlands include: *Threskiornis spinicollis* (straw-necked ibis), *T. aethiopica* (sacred ibis), *Plegadis falcinellus* (glossy ibis); *Ardea ibis* (cattle egret), *A. garzetta* (little egret), *A. alba* (great egret), *A. intermedia* (intermediate egret); *Nycticorax caledonicus* (nankeen night heron); *Phalacrocorax sulcirostris* (little black cormorant), *P. melanoleucos* (little pied cormorant); *Platalea regia* (royal spoonbill) and *P. flavipes* (yellow-billed spoonbill) (McCosker, 1996). Six species listed as vulnerable and rare have been recorded in the Gwydir wetlands including *Anseranas semipalmata* (magpie geese), *Oxyura australia* (blue-billed duck), *Stictonetta naevosa* (freckled duck), *Grus rubicundus* (brolga), *Rostratula benghalensis* (painted snipe) and *Calyptorhynchus lathami* (glossy-black cockatoo) (Keyte, 1994). The wetlands are utilised by eight species listed under the China Australia Migratory Birds Agreement (CAMBA) and seven species listed under the Japan Australia Migratory Birds Agreement (JAMBA).

Flooding is the major breeding stimulus for many of the species that breed in the Gwydir wetlands (Scott, 1997) with floods in the late winter, spring or early summer generally providing the most successful breeding events. Food sources such as invertebrates, tadpoles, frogs and fish are also important to build fat supplies and feed young, and expansive areas of water couch, spike rush and marsh club-rush form valuable feeding areas on the Gwydir floodplains (Keyte, 1994; McCosker, 1996; McCosker, 1999; McCosker, 2001a; Spencer, 2010). Water level is critically important for species such as ibis and egrets which build nests surrounded by water and if water levels drop the adult birds may abandon nests before the young are fully fledged (Scott, 1997). Nesting sites vary depending on species. The ibis species in the Gwydir use predominantly lignum bushes but also form platform nests by trampling down emergent macrophytes such as Typha. Other species such as egrets, cormorants and night herons nest in trees including belah and river cooba (Spencer, 2010).

Using historical records of breeding events and modelling of flow data (Johnson, 2004; Spencer, 2010) it was estimated that colonial waterbirds bred on average seven out of every 10 years prior to river regulation, but after regulation this declined to four in 10 years. Johnson (2004) in (Spencer, 2010) assumed that breeding events required two months of inflows of 100 000ML with a minimum of 250 000ML distributed over four months of breeding and a further 10 000-15 000ML over the final month to complete the breeding event. An analysis of flows and breeding events between 1988 and 2007 indicated that over 200 000ML was needed for straw-necked ibis to breed in the Gwydir (Spencer, 2010) but flow only explained a small proportion of the total variance of breeding events. Other factors such as water depth at the nesting sites, rate of water level change and food availability were also considered important.

3.5.3 Fish

Fish surveys of the main channels and waterholes of the Gwydir Wetlands have recorded 12 native and three alien (i.e. those species introduced from overseas and now established in the wild) fish species (Siebentritt, 1999; Spencer, 2010). In a recent study the Lower Gwydir fish community was dominated by three native fish species: bony bream (50% of the fish caught), carp gudgeon and spangled perch (Wilson *et al.*, 2009). Carp and goldfish were widely dispersed, with carp making up more than 50% of the total fish biomass (Wilson *et al.*, 2009).

Limited studies linking flow and fish recruitment have been undertaken but results from a flow event in 2007/8 suggest that high flows do trigger spawning and movement of spangled perch and bony bream in the lower Gwydir. Larger scale flooding triggers may be required for other native fish species such as golden perch and Murray cod which were less abundant (Spencer, 2010; Wilson *et al.*, 2009). In suitable habitat, spawning cues include increases in water temperature, day length and flow, which normally correlates to spring and summer months in unregulated systems (Wilson *et al.*, 2009). Alien species are thought to have less specific flow requirements and high reproductive rates. Carp, for example, can withstand very low dissolved oxygen. The invasive water hyacinth can reduce dissolved oxygen levels (discussed in Section 3.5.1) and may therefore create conditions that would favour alien species such as carp, while altered flow regimes may also influence fish assemblages. The Gingham Watercourse has a low diversity of fish species, with carp making up about 80% of the total biomass during recent surveys, and was thought to be related to the degraded channel structure (Wilson *et al.*, 2009).

Table 3.3: Fish species recorded in the Lower Gwydir (Spencer, 2010)

Common name	**Scientific Name**
Australian smelt	*Retropinna semoni*
Bony bream	*Nematalosa erebi*
Eastern gambusia*	*Gambusia holbrooki**
European carp*	*Cyprinus carpio**
Freshwater catfish	*Tandanus tandanus*
Golden perch	*Macquaria ambigua*
Goldfish*	*Carassius auratus**
Lake’s carp gudgeon	*Hypseleotris* sp. 2
Midgeley’s carp gudgeon	*Hypseleotris* sp. 1
Murray cod	*Maccullochella peelii peelii*
Murray-Darling rainbowfish	*Melanotaenia fluviatilis*
Olive perchlet**	*Ambassis agassizii*
Silver perch	*Bidyanus bidyanus*
Spangled perch	*Leiopotherapon unicolour*
Unspecked hardyhead	*Craterocephalus stercusmascarum fulvus*
Western carp gudgeon	*Hypseleotris klunzingeri*

* alien species, ** assumed to be present

3.5.4 Other biota and trophic structure

Other biotic components of the Gwydir wetlands include zooplankton, micro-invertebrates, macro-invertebrates, bacterial assemblages, reptiles such as frogs, snakes and turtles, kangaroos and other native wildlife, and introduced mammals such as pigs, rabbits, foxes and cats (Keyte, 1994; McCosker, 1999; McCosker, 2001a; McCosker, 2001b). Over 500 species of macro-invertebrates have been recorded from the Gwydir wetlands (Wilson *et al.*, 2009). Benthic micro-invertebrates include over 70 taxa with rotifers comprising over half the taxa, and microcrustaceans and insect larvae the other major groups found (Wilson *et al.*, 2009). Nevertheless, studies have been limited and information on the habitat use and flow responses of invertebrates in the Gwydir is not available. Investigations into the effects of rising salinity have indicated that changes in zooplankton structure are likely above 1000 mg L^{-1} (Brock *et al.*, 2005), however water quality in the Gwydir wetlands rarely exceeds 500 mg L^{-1} (approx. 900 µS cm^{-1}) (Brock *et al.*, 2005; Wilson *et al.*, 2009).

In a study of trophic structure in the main channels of the lower Gwydir (Mehi River, Lower Gwydir River and Gingham Channel) the aquatic food webs were found to be supported by multiple primary carbon sources including sediment organic matter, riparian trees and groundcover, and to a lesser extent aquatic plant species such as water couch (Kelleway *et al.*, 2010a). The sediment organic matter comprises a range of sources including benthic algae, bacteria, fungi, micro-crustaceans, and animal and plant detritus (Kelleway *et al.*, 2010b).

3.6 Summary

The Gwydir floodplains and wetlands are located on a large terminal fan-plain formation that is characterised by multiple channels and watercourses that diminish in capacity and tend towards floodouts. These channels and watercourses contain valuable areas of wetland vegetation and associated water birds that are recognised nationally and internationally.

With local evaporation far in excess of local rainfall, the wetlands rely on flows that originate from the upstream catchment and are highly variable in magnitude and timing. These flows and the floods they create have also been substantially altered from the natural state through landuse changes and river regulation. Flows diminish downstream naturally due to the storage capacity of the geomorphic character of the watercourses, channels, waterholes and floodplains that make up the wetlands as well as to groundwater recharge. Water extraction, on-farm storage and stock and domestic use also contribute to diminishing downstream flows.

Chapter 4: Analysis overview

This chapter provides a brief overview of the analysis approach taken in this thesis. Over Chapters 5, 6 and 7, the floodplain landscape of the Lower Gwydir is characterised according to flood frequency and connectivity. This provides a basis for creating a network of linked patches, which are used to develop a node-network water balance model. Combining the patches and dominant vegetation communities provides a classification of relatively homogenous landscape units with respect to flood and vegetation response behaviour. These landscape units provide the scale at which the vegetation productivity response to inflows and climate variables is modelled. The Inundation and Vegetation Response Model (IVRM) is described and applied in Chapter 7. A flow chart describing the steps in the analysis is shown in Figure 4.1.

The use of satellite imagery to detect flood extent and duration has been used in large wetlands systems and major river channels (Barton and Bathols, 1989; McCarthy, 2002; McCarthy *et al.*, 2003; Quan *et al.*, 2003; Shaikh *et al.*, 2001; Sheng *et al.*, 2001; Thomas *et al.*, in press; Wolski and Murray-Hudson, 2005,). These studies are all characterised by large spatial extents of open flood waters, often persisting in time. In the floodplain wetlands of inland Australia, and some areas of systems such as the Parana River Delta in South America, flooding is characterised by periods of shallow flooding with rapid growth of emergent macrophytes. Detection of flood extent in these systems or areas is more difficult. Rather than mapping the open water flooding alone, the vegetation response to flooding can also be used to estimate the flood extent (Thomas *et al.*, in press; Zoffoli *et al.*, 2008).

Using the conceptual model of normalised difference vegetation index (NDVI) to characterise phenology response (Zhang *et al.*, 2001) (Figure 4.2), analysis of patterns are evident in the NDVI data for the Lower Gwydir. The vegetation response could be differentiated on the basis of peak NDVI (maximum greenness) between flooded and non-flooded pixels (Powell *et al.*, 2007) (Appendix 3). These response patterns are used in Chapter 5 to estimate inundated area as described below, and were confirmed in the analysis in Chapter 6 of this thesis.

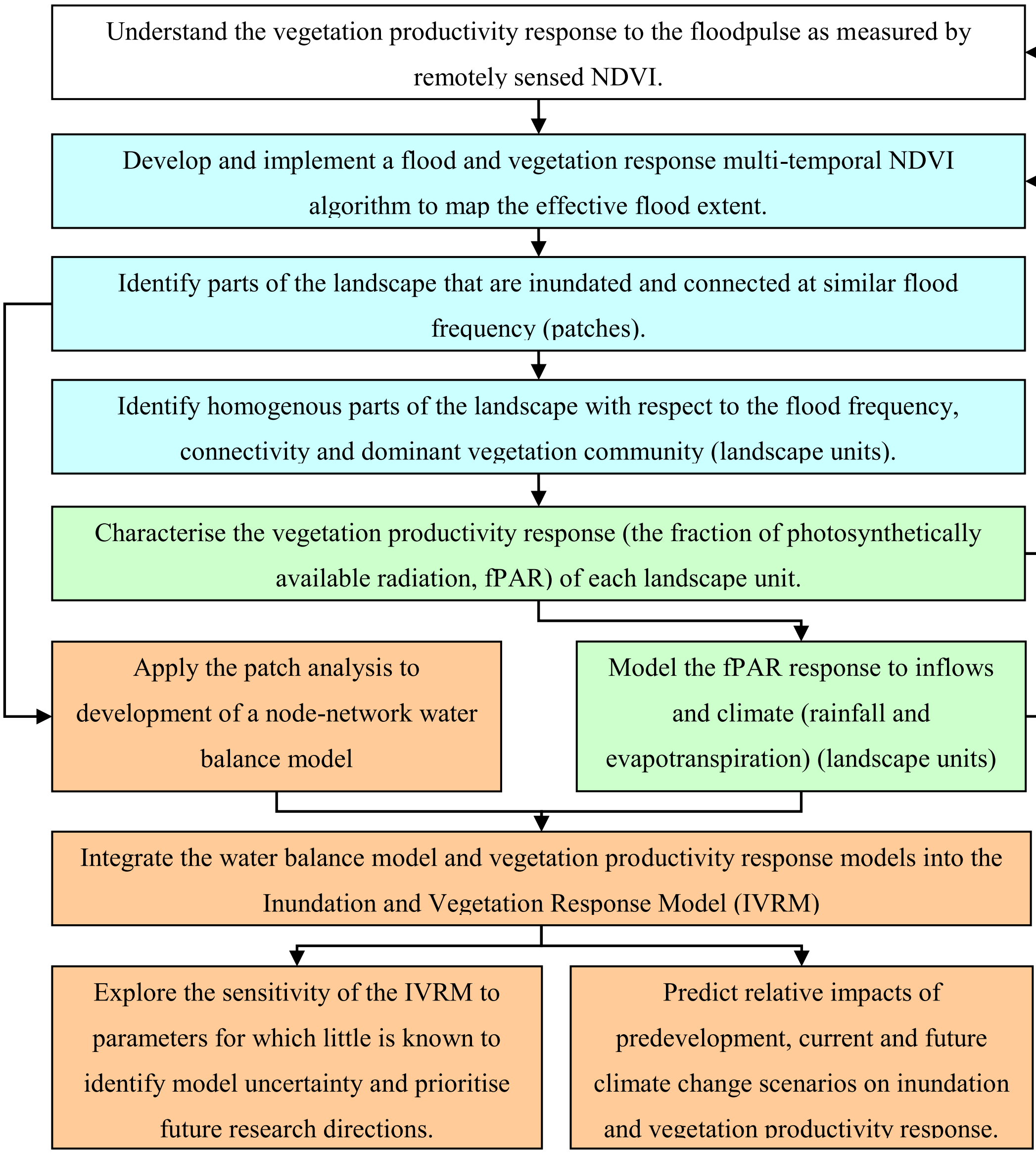

Figure 4.1: Analysis overview (white) of the flood assessment (blue, Chapter 5), vegetation response (green, Chapter 6) and development of the Inundation and Vegetation Response Model (orange, Chapter 7).

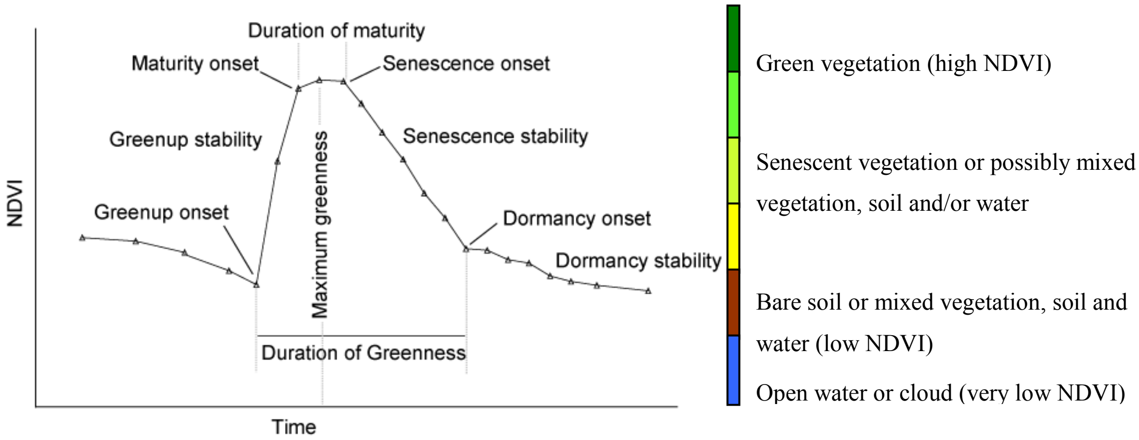

Figure 4.2: Phenological cycle showing key indicators such as green-up, maturity, senescence and dormancy at a 16-day time step. (adapted from Zhang *et al.*, 2001).

In Chapter 5 temporal NDVI data are used as the basis for estimating the inundated area. By combining both the open water flood extent where apparent, and the high NDVI response in weeks following the flood peak, an estimate of the total inundated area following a range of flood events is mapped. Using Landsat, Modis and AVHRR sensors a wide range of events could be mapped. An analysis of inflow and rainfall data are undertaken to determine the appropriate metrics that can be applied to describe and model the events. Integrating the information across sensors and flood events, each pixel was then identified by flood frequency and connectivity to its neighbours during flooding (patch analysis). This then forms the basis for a conceptual model of the system and provides a framework for the node-network water balance model developed in Chapter 7. Although each patch may be relatively homogenous in relation to its flood frequency and connectivity, it may still contain a range of vegetation communities. Using vegetation mapping (McCosker, 1994b), each patch is divided into discrete landscape units of similar flood frequency, connectivity and dominant vegetation community.

Landscape units are used to characterise and model the vegetation productivity response to inflows and climate, as measured by the fraction of photosynthetically available radiation, (fPAR), in Chapter 6. In a somewhat iterative approach the understanding developed in Chapter 6 is necessary to develop the algorithms to map the inundation area in Chapter 5, conversely it is necessary to map and classify the landscape into the relatively homogenous landscape units to undertake the analysis in Chapter 6. The results presented in this thesis are the culmination of that iterative approach.

Chapter 7 extends the knowledge and results from Chapters 5 and 6 into an Inundation and Vegetation Response Model (IVRM) of the Gwydir wetlands. The node-network water balance component of the IVRM builds on earlier work that developed a simple semi-distributed water balance model of the Gwydir Wetlands (Powell *et al.*, 2008) (Appendix 4). The vegetation response component of the IVRM incorporates the fPAR response models developed in Chapter 6, linked to the patches and landscape units that characterise the system. The patch analysis and conceptual model of the Lower Gwydir greatly enhances the information and parameterisation of the node-network water balance component, but there is still much uncertainty over some of the parameters in the IVRM. Sensitivity analysis of these parameters is undertaken in Chapter 7 and identifies the areas where further research is required. The IVRM is used to predict the relative impact of different inflow and climate inputs in Chapter 7. Using pre-development conditions, current conditions and three climate change scenarios that were modelled by CSIRO in the Gwydir Sustainable Yields (SY) project (CSIRO, 2007), the model outputs including inundation depth for specific patches and the fPAR response for some landscape units are reported and compared.

Chapter 5: Flood assessment

5.1 Introduction

The first step in understanding inundation and vegetation productivity response in the Gwydir wetlands is to characterise the historical flood extent at a landscape scale. As discussed in section 2.4.5. the knowledge gaps include lack of robust flood assessment methods and the need for methods to encompass the response to flooding, particularly at landscape scales. Mapping flood extent in the Gwydir can be especially problematic with much of the floodplain during flood events a heterogeneous mix of water (of varying depth and turbidity), vegetation canopy structure, and unflooded areas of both native vegetation and cropping (Powell, 2005). In addition the flood pulse is somewhat unpredictable in timing and frequency as discussed in Section 3.4. To link event based metrics such as inflow and rainfall to spatial and temporal inundation extent and vegetation (productivity) response, multiple sensors have been used in this thesis to provide higher temporal resolution using readily available NDVI from AVHRR, Modis and Landsat imagery.

The objective of this chapter is to assess the spatial and temporal characteristics of flood behaviour at the landscape scale in the Gwydir wetlands and to identify relatively homogenous landscape units in relation to their flood frequency, connectivity (during flooding) and vegetation associations. These landscape units form the basis for more detailed analysis in Chapter 6 of the vegetation response as measured by productivity. The combination of flood frequency and connectivity provides a template for further development of a node-network water balance model to further explore flow and vegetation response in Chapter 7.

5.2 Methods

This section describes the data used and methods applied in this chapter (Figure 5.1). Section 5.3 goes on to present the results of these analyses. The analyses rely on flow and rainfall data, satellite imagery and flood and vegetation maps. A range of event metrics were calculated from the observed daily flow and rainfall data. The metrics were analysed to remove redundant measures using correlation analysis, leaving the most appropriate metrics to describe a flood pulse in the Lower Gwydir. The normalised difference vegetation index (NDVI) from AVHRR, Modis and Landsat imagery were used to determine inundated area following the analysis methods described below.

A multi-temporal analysis of both open water flooding and vegetation response was used to estimate and spatially map the inundated area for each flood event. The analysis relies on not only the use of multi-temporal imagery, but also the application of geographical and statistical techniques to provide a robust estimate of inundated area consistent with existing mapping and inflows.

Using the spatial estimates of inundated area over a range of flood events, the flood frequency across the landscape was determined. Coupled with a geographical analysis of neighbourhood connectivity, this provides a **patch** analysis that was used to construct a conceptual node-network model of the Lower Gwydir applied in Chapter 7. Combining this information with vegetation maps gives relatively homogenous **landscape units** with respect to flood and vegetation response behaviour, used in Chapter 6 to characterise and model the vegetation productivity response.

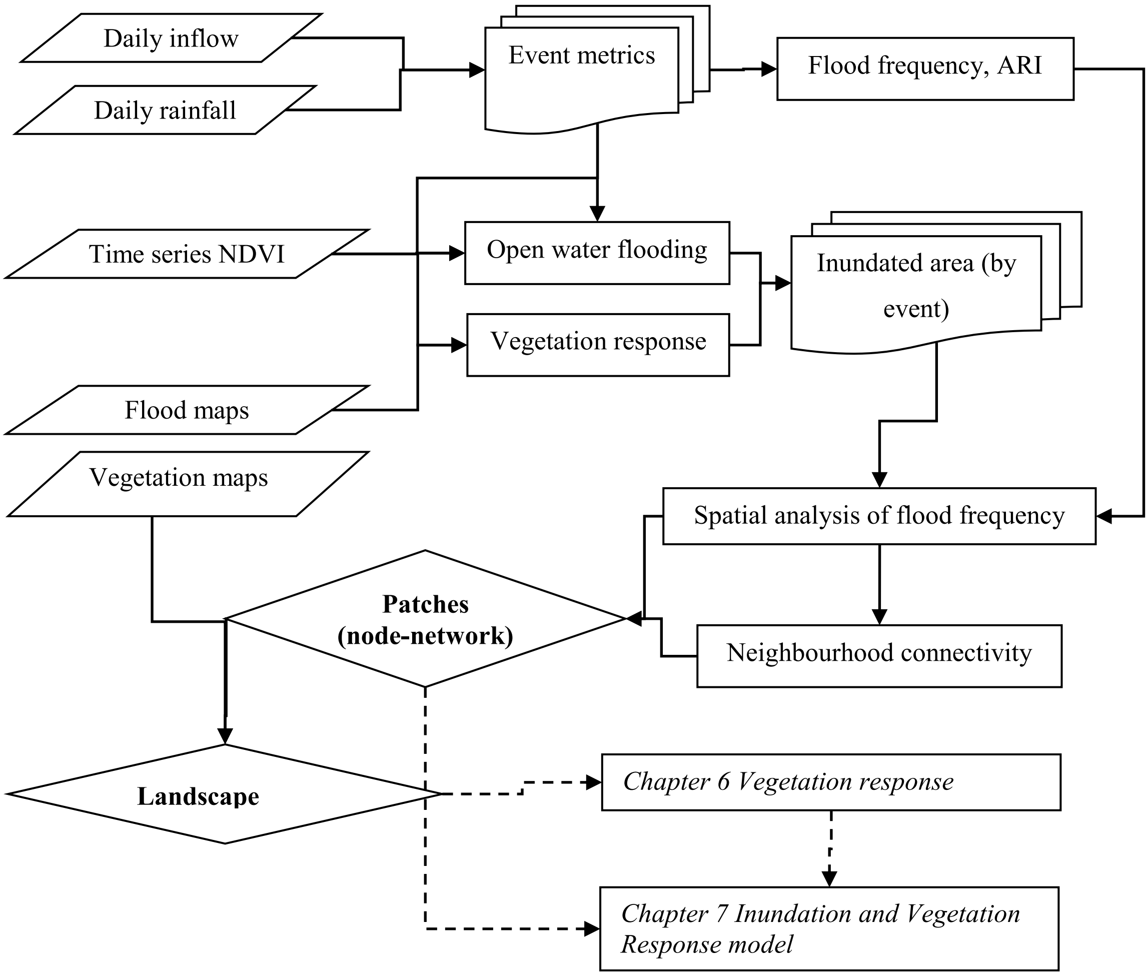

Figure 5.1: Flow chart of flood assessment analysis in this Chapter and linkages (dotted lines) with Chapters 6 and 7.

5.2.1 Study area

The study area was defined using flood mapping from 1995, 1996, 1997 and 1998/9 for the Lower Gwydir and Gingham wetlands (McCosker, 1996; McCosker, 1999; McCosker, 2001a). The 1998/9 event was the second largest event since Copeton Dam was completed in the 1970's and approximates a 1 in 33 year event. These maps were buffered by 500m to remove edge effects associated with the larger pixel sizes of the AVHRR data and to ensure the entire floodplain is included for a larger event (Figure 5.2). The study area was bounded to the west to align with available Landsat data and to reduce the influence of flooding from the Barwon and Boomi Rivers to the west, constraining the analysis to flooding from the Gwydir River inflows. The total study area covers 217 236ha.

The major vegetation associations within the study area are shown in Figure 5.3. Over 45% of the study area is cleared cultivated land while a further 8.6% is developed for irrigation (laser-levelled cleared fields surrounded by levee banks and associated on-farm water storages and infrastructure). For the purpose of estimating inundated extent, irrigation development was excluded from the analysis. Of the remaining 45.7% of native vegetation, the majority (29.9%) is coolibah associations of variable density. Associations generally regarded as 'wetland' communities, which are assemblages of plant species reliant on soil saturated by water or on inundation, such as marsh clubrush, spikerush, river red gum and lignum comprise 7.7% of the area (Table 5.1).

Table 5.1: Area and percent of major vegetation associations within the study area. (vegetation mapping undertaken by McCosker (1994) and updated using 2004 Spot5 imagery based on visual estimation of areas cleared and cultivated).

Vegetation association	Area (ha)	% of total
Cleared cultivated land	107 787	45.7
poplar box association	8 552	3.6
belah	1 157	0.5
Native grasslands	4 421	1.9
coolibah associations	70 486	29.9
river redgum associations	3 775	1.6
Irrigation development (excluded from analysis)	20 182	8.6
March clubrush	317	0.1
Myall/rosewood association	4 769	2.0
Natural water bodies	122	0.1
river cooba/lignum associations	4 212	1.8
spikerush	9 869	4.2
Total	***237 418***	

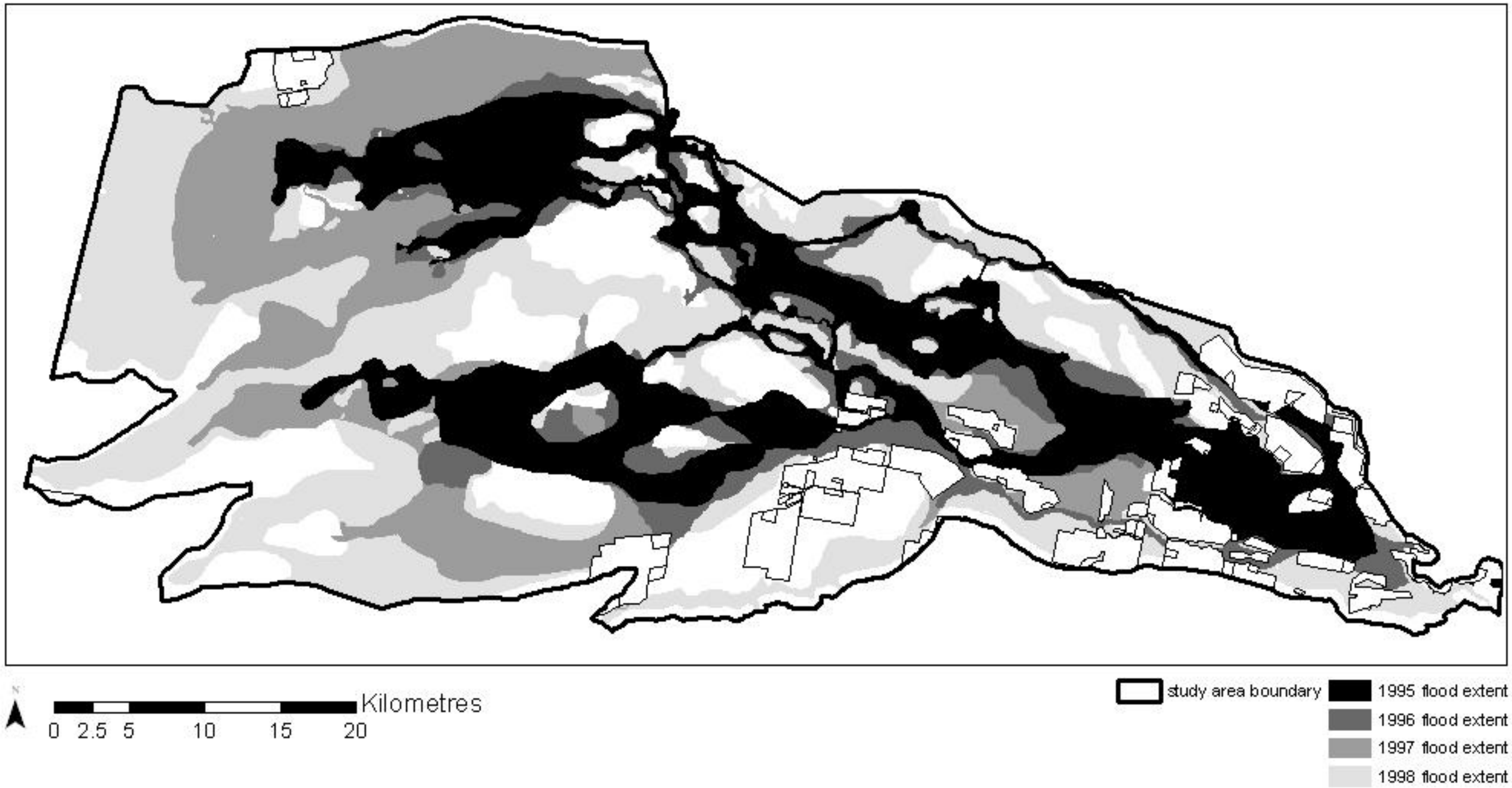

Figure 5.2: Mapped flood extents (1995-1998 shape-files) and study area boundary used for the remote sensing analysis and modelling. (source: Unpublished shape files, NSW Department of Land and Water Conservation, 2004).

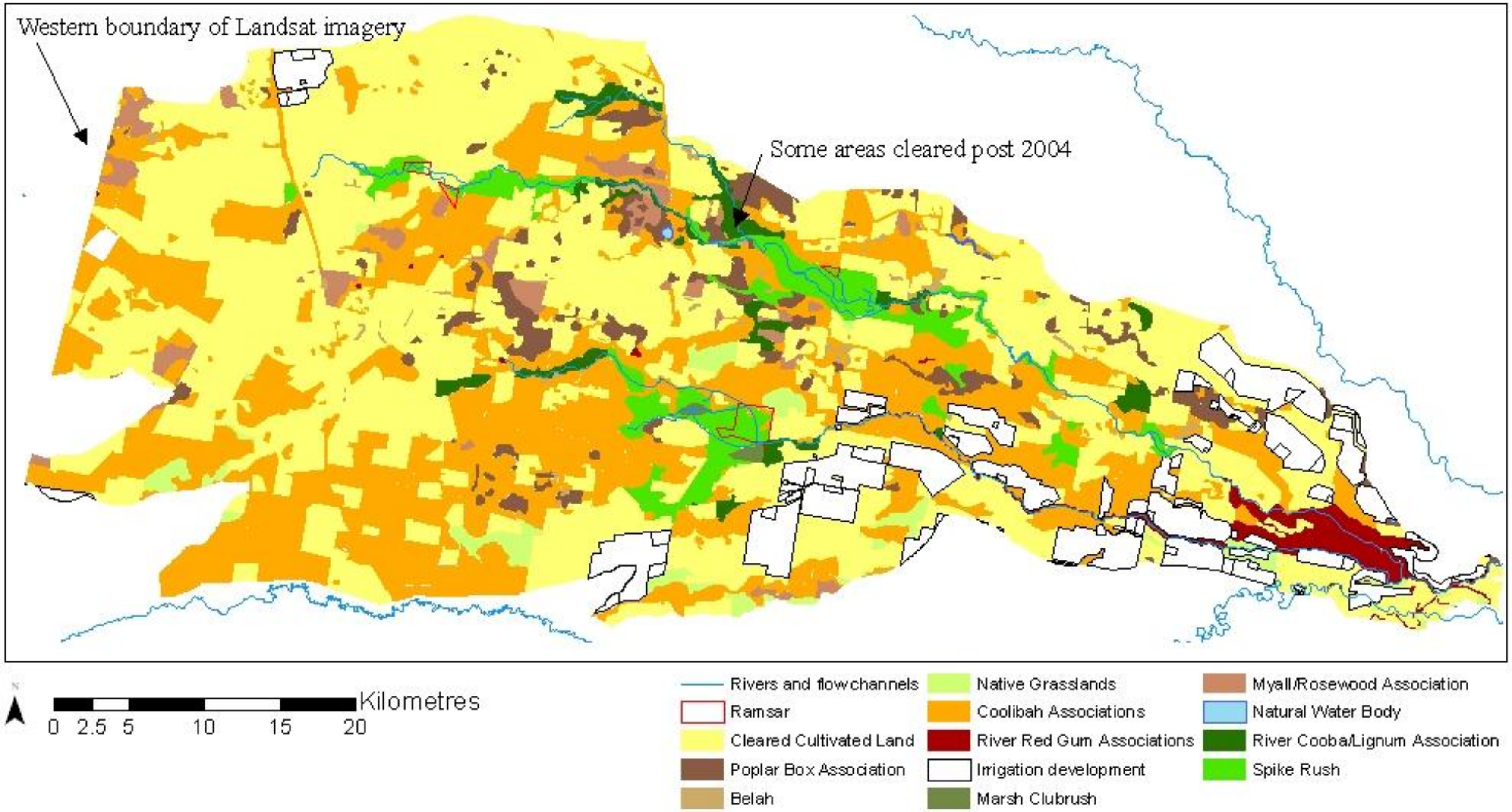

Figure 5.3: Spatial distribution of vegetation associations within the flood assessment study area. Updated from existing vegetation and irrigation development mapping using 2004 Spot5 imagery (McCosker, 1994; NSW Department of Land and Water Conservation, 1996).

5.2.2 Flow and rainfall metrics

Daily flow data for the Gwydir River at Yarraman gauge (418004) was extracted from the Pineena database (Department of Water and Energy, 2007) and the NSW Water Information website (http://waterinfo.nsw.gov.au/) for the period of record (1977 – 2009) (Figure 5.4). This location is the closest inflow gauge to the wetlands that can reliably measure relatively large flows. The flow duration curve for flows since 1977 (post-Copeton Dam) is shown in Figure 5.5. Flows on over 90% of days have been less than 1GL while flows greater than 10GL/day have occurred on less than 1.5% of days. Daily rainfall data was extracted from the BoM website (http://www.bom.gov.au/) for the three Moree stations for the period 1977-2009 (refer Section 3.3, Figure 3.4).

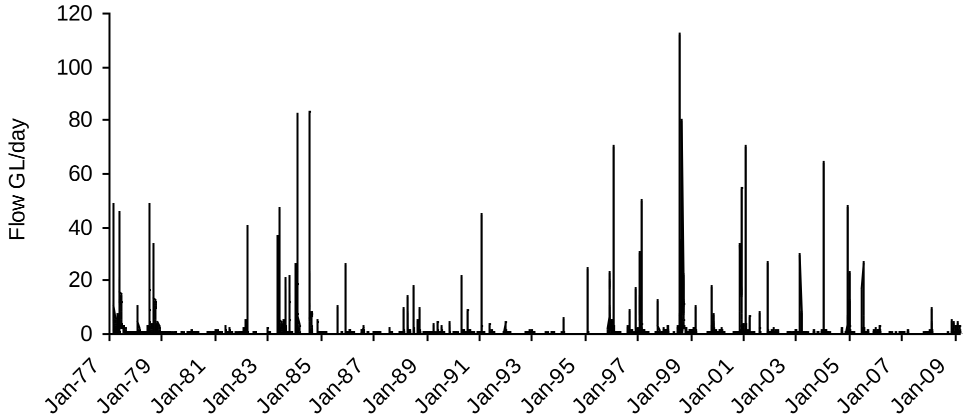

Figure 5.4: Daily flow into the Gwydir wetlands, Gwydir River at Yarraman (418004) 1977-2009.

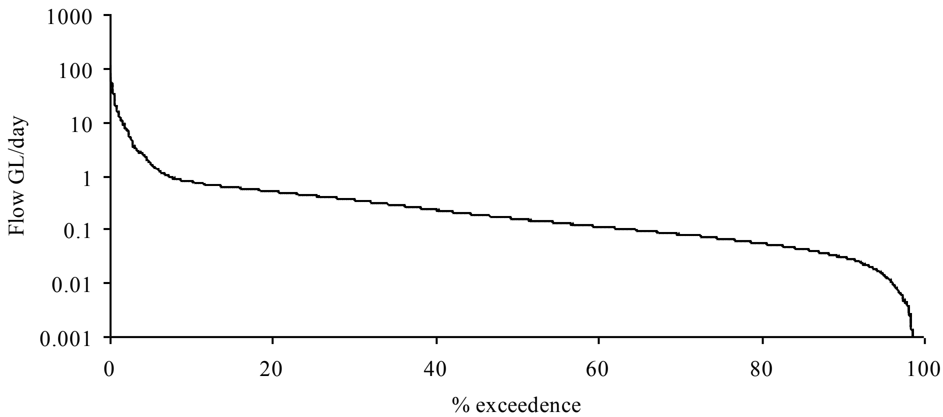

Figure 5.5: Flow duration curve for Gwydir River at Yarraman (418004) 1977-2009.

When flows exceed the bankfull capacity of a channel the water will spill over the banks causing flooding to some area of the landscape. At what point this becomes a 'flood event' is largely subjective and depends on the purpose for defining the flood event. In this chapter the focus is on the inundation of wetlands over the floodplain of sufficient size and duration to result in open water flooding and associated vegetation response. Flow greater than 10GL/day have the potential to cause overbank flooding to both the Gingham Channel and Lower Gwydir core wetlands based on the estimated bankfull discharge in mid-wetland gauges (i.e. Gwydir River at Allambie Bridge and Gingham Channel at Teralba (Table 3.1). To test whether a smaller threshold may result in flooding a smaller event with a clearly defined peak (4.2GL) was included for analysis.

Each event was characterised by a range of inflow and rainfall metrics as shown in Table 5.2 A variety of inflows, antecedent and rainfall summations (including weekly and monthly) were initially evaluated (not shown) but reduced after initial exploratory analysis to those metrics likely to best describe flooding events. Using the 40-day event inflow, the annual exceedance probability (post Copeton Dam completion) was determined for each flood event and all events were then ranked by size. Pearsons correlation (r) and the significance of the correlation ($p<0.05$) is calculated in Statistica (StatSoft Inc, 2009) for all metrics. The results were used to determine the metrics that are redundant (those metrics that were highly correlated to other metrics) in characterising event flow and rainfall.

Table 5.2: Flow and rainfall metrics extracted from the time series record

Metric	**Symbol**	**Description**
Peak inflow	Q_{peak}	The largest single day inflow of the event
Total inflow	Q_{total}	The total inflow for the event from the start of an event (where Q > 1GL/day) to the end of the event (Q < 1GL/day). A separation of 10 days is used to determine that an event has 'finished' for this metric
40-day inflow	Q_{40}	The total inflow from the start of the event for a period of 40-days (Note: a range of periods were initially trialled however 40 days was found to best describe most flood events)
Antecedent inflows	AQ_{60} AQ_{90} AQ_{180}	Sum of 60, 90 and 180 -day antecedent inflows.
Days since last event	D	Number of days since the last event
Peak rainfall	R_{peak}	The highest single day rainfall in association with the event
Antecedent rainfall	AR_{30}	The sum of the 30 days rainfall leading up to the event

5.2.3 Satellite imagery

AVHRR NDVI datasets for this thesis were extracted from the CSIRO Marine and Atmospheric Research archive by Dr Edward King at nominal 1km^2 resolution. The datasets are maximum value 16-day BRDF corrected composites (MVC) with no cloud masking for 305 composite periods from 21 March 1992 to 26 June 2005. As discussed in section 2.5.4., BRDF (Bidirectional Reflectance Distribution Function) is a correction used to minimise problems associated with large variations in view zenith angles and illumination directions due to large geographical coverage and orbital drift (Chopping, 1998. Following testing of a range of functions, Dr Edward King applied the BRDF correction to the AVHRR dataset for use in this Thesis. The MVC periods were aligned with the Modis dataset. Cloud masking was omitted to reduce the risk of flooded pixels being removed through the cloud masking algorithm. Instead low or negative values were examined manually to determine whether they were likely to be flooded pixels or as a result of cloud contamination or other sensor errors. The MVC periods were converted to a common map projection (UTM, GDA94, zone 55S) and stacked to produce a continuous time series dataset cut to the study area. A summary of the AVHRR data extracted and processed for use in this thesis is shown in Table 5.3.

The Level 3, MODIS 16-day, 250m NDVI MOD13Q1 product was extracted from the CSIRO Water Resource Observation Network (Paget and King, 2008). The NDVI product was stacked for 187 composite periods from the 29 September 2000 to 23 May 2008, converted to common map projection (UTM, GDA94, zone 55S) and clipped to the study area. The MODIS data processing stream for this product includes a cloud mask and a maximum value composite (MVC) to create a 16-day product (Barrett *et al.*, 2005; Huete *et al.*, 1999) and is not available without this cloud mask. Cloud masking provided a more reliable data product, but it may inadvertently detect flooded pixels due to their low NDVI values. Hence this product may not be sensitive to the expected decrease in NDVI values associated with flooding. Similarly the 16-day period will only detect flooding that persists for this period. A summary of the Modis data extracted and processed for use in this thesis is shown in Table 5.3.

Landsat data was sourced through Geoscience Australia and NSW Department of Environment and Climate Change as georeferenced and calibrated reflectance band data, and was processed by Neil Sims, CSIRO (Sims, 2007). Landsat data included MSS, TM and ETM sensors on a range of Landsat missions. Georeferenced, calibrated reflectance band data at 25m resolution was imported into ENVI (ENVI version 4.3, ITT Industries Inc, USA) as UTM, GDA94, zone 55S and cut to the study area. Only images that were predominantly cloud free over the study area were used in subsequent analysis. Using the visible and near infrared bands, NDVI was calculated for each viable image. A summary of the Landsat data extracted and processed for use in this thesis is shown in Table 5.3.

Pre-processing, georeferencing and manipulation of the satellite imagery were performed using ENVI (ENVI version 4.3, ITT Industries Inc, USA). Subsequent analysis and mapping was carried out using ArcMAP (ESRI ArcMap 9.2, ESRI Inc.) as identified in the methods.

Table 5.3: Satellite imagery extracted and used in this thesis

Date range	Satellite	Sensor	Temporal resolution	Spatial resolution	Systematic corrections and processing	Number of images
21 May 1992 to 26 June 2005	NOAA	AVHRR	daily	1km	BRDF MVC 16-day NDVI	305
29 Sept 2000 to 23 May 2008	Terra	MODIS	daily	250 m	MVC 16-day Cloud masked NDVI	187
7 Jun 1988 to 26 Sep 2005	Landsat	MSS, TM, ETM+	16 days to > 1 month	30-80m (resampled to 25 – 60m)	NDVI	54

5.2.4 Inundation and response mapping

This flood assessment focuses on extracting the likely area of inundation based on wetted area and vegetation response. The assessment uses higher resolution Landsat imagery over a range of inflow events and the maximum value NDVI composites from AVHRR and Modis imagery at $1km^2$ and $250m^2$ respectively. A range of classification methods were also tested in the initial stages of research including supervised and unsupervised classification of multi-spectral imagery, (McCarthy, 2002; Thomas *et al.*, in press) as discussed in Section 2.5, but were less effective in distinguishing flood and response areas than a simple decision tree using a range of NDVI thresholds post flooding.

For each flood event identified from the flow record, the area inundated and/or showing high vigour vegetation response was estimated from the NDVI composites using a decision tree approach (Figure 5.6) in ENVI (ENVI version 4.3, ITT Industries Inc, USA). The Modis and AVHRR MVC datasets for the first period after the start of the event and subsequent five 16-day periods were used where possible to account for full vegetation response. All available images were used for Landsat analysis up to 6 months post flooding in some instances. Significant correlations between rainfall, inflows and NDVI of up to 80 days have been shown (Eklundh, 1998; Powell *et al.*, 2007). Vegetation analysis in Chapter 6 also showed that the peak in vegetation vigour occurs within this period (for example see Figure 6.18b). Extending this period to six 16-day MVC periods (96 days), or the equivalent for Landsat imagery, provides a temporal buffer to ensure the peak response is captured. Where a second 'event' occurs within 96 days a lesser number of MVC periods was used to separate the events, but this may not always capture the full NDVI response and may underestimate the area of high vegetation response.

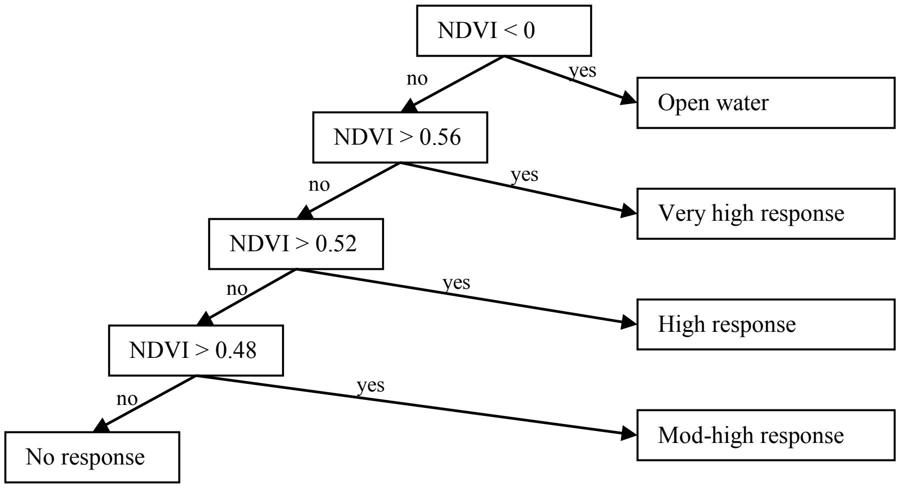

Figure 5.6: Example of a decision tree classification of landscape flood and high vigour vegetation response for an AVHRR NDVI scene. The NDVI thresholds used to define response are determined using geographical and statistical techniques to ensure they represent flood related response.

At each time-step and for each pixel, NDVI was classified in ENVI (ENVI version 4.3, ITT Industries Inc, USA) as most likely to be open water or as a level of vegetation response. As shown conceptually in Figure 5.7, multi-temporal NDVI in a pixel following a flood pulse follows a predictable curve. The NDVI value will dip as the soil and/or vegetation component of the pixel is flooded, giving a very low or negative NDVI. In areas adapted to the flood pulse, vegetation response to inundation is rapid (greenup phase) with NDVI increasing to a high peak approximating saturation of NDVI (maturity phase) before vegetation vigour is lost (senescence) and finally reaches dormancy. The low NDVI values of open water flooding may not be apparent in the NDVI data due to timing, canopy cover or incomplete flooding of the entire pixel. The increase and peak in NDVI can still be seen in most of the NDVI data available. Figure 5.7 also shows the hypothetical application of the decision tree discussed above to the NDVI response curve. At each available time-step, the pixel was classified as either wet or vegetation response. All time-steps post event were combined to determine the final status of each pixel as flooded (wet or vegetation response) or not flooded.

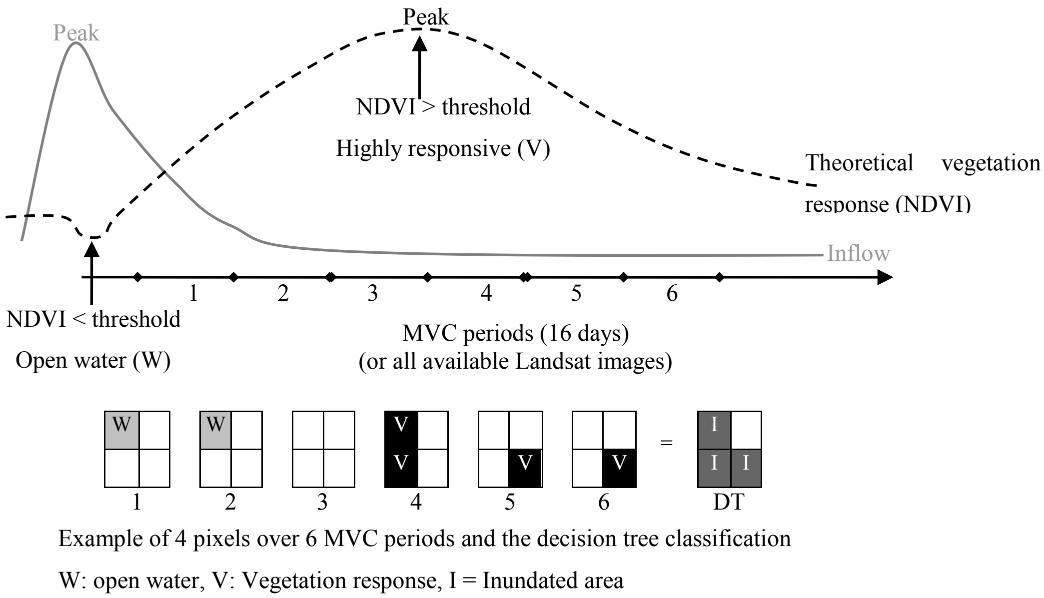

Figure 5.7: Using multi-temporal NDVI to estimate inundated area (open water and vegetation response to flooding as an indicator of inundated area). The top graph is a hypothetical time-series of inflow and NDVI following a flood event. The bottom boxes represent pixels at each time step and the decision tree classification result. The final summation of each time step classifies each pixel as inundated or not inundated.

Setting the appropriate NDVI value to classify likely post-flooding vegetation response is not straight forward and can vary depending on the sensor used and the vegetation community type. Barrett *et al.* (2005) and Gallo *et al.* (2005) showed significant linear relationships between AVHRR and Modis NDVI and that the relationship was dependent on land cover types (Section 2.5.4). This was also found in preliminary data analysis for the Gwydir (Powell *et al.*, 2007) (Appendix 3). A comparison of Landsat, Modis and AVHRR NDVI for a wetland site in the Lower Gwydir following the 2004 flood event indicated similar values for Modis and Landsat and lower values for the AVHRR NDVI (Figure 5.8). For this reason, the NDVI thresholds were set separately for each sensor as described below.

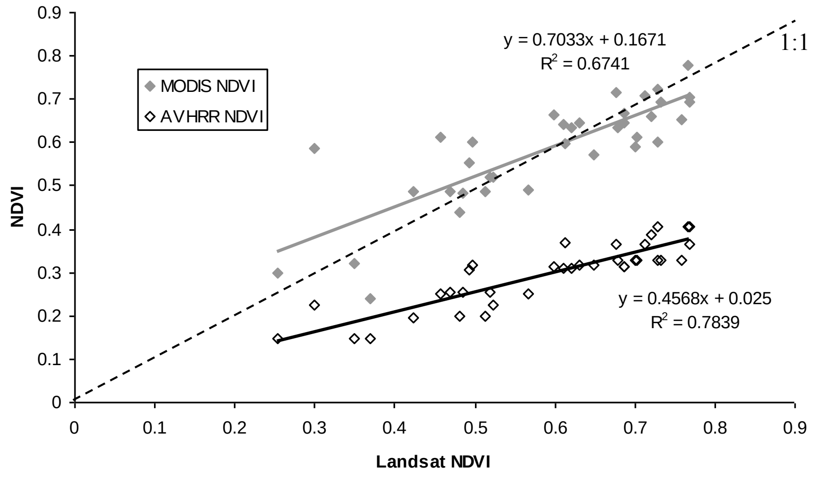

Figure 5.8: Comparison of NDVI values from Landsat, Modis and AVHRR during a flood event in 2004 at Old Dromana on the Lower Gwydir.

The approach taken in this thesis was to use a range of NDVI values to estimate the total flood and vegetation response area (hereafter referred to simply as the inundated area) and compare the results with the event metrics and mapped flood extent where available. In an iterative process, the correlation and regression analysis to both inflows and rainfall, and the accuracy in reference to mapped flood extent, were both used to determine the NDVI value that provides the most robust estimate of inundated area for all flood events.

The inundated area for each of the NDVI thresholds of high response used was compared to the flow and rainfall metrics individually and the Pearson correlation (r) and significance of the correlation co-efficient calculated in Statistica (StatSoft Inc, 2009). Inundation extent in the Gwydir is correlated with inflow volumes (Bennett and Green, 1993; McCosker, 1994b) so significant correlations between the flood response NDVI should be expected for Q_{40}. Rainfall is more likely to be a key driver in seasonal, non-flood response, so significant correlations with R_{peak} or AR_{30} would suggest that the NDVI threshold for vegetation response is too low and is detecting normal seasonal response. To further explore the relationship between the inundated areas estimated from each of the NDVI thresholds a backwise-stepwise multiple linear regression (MLR) analysis was undertaken in Statistica (StatSoft Inc, 2009) to determine the significant explanatory variables for the inundated area. As for correlation analysis a highly significant relationship between inundated area and Q_{40} is sought. As the number of observations are relatively small, outliers can greatly influence the final estimates. Outliers were identified in the residual analysis as a residual greater than plus or minus two times the standard deviation. The MLR analysis was repeated with outliers excluded.

Accuracy of the inundated area was calculated using a confusion matrix (Richards and Jia, 1999). Inundated area of the flood map layers and the results of the NDVI classification were overlaid to produce the confusion matrix (Table 5.4). Using this matrix, accuracy is determined as the overall probability of a correct prediction. ‘Producer’ accuracy is the probability that a wet area is classified wet whilst ‘user’ accuracy is the probability that an area classified as wet is actually wet (Richards and Jia, 1999). For the purpose of estimating the inundated area, the overall accuracy should be maximised and in particular the producer and user accuracy for wet areas.

Table 5.4: Confusion matrix for evaluation of NDVI DT classification.

		NDVI classification results		**Accuracy**	**wet**		**dry**	
		wet	**dry**		**producer**	**user**	**producer**	**user**
Flood mapping	**wet**	a	b	(a+d)/(a+b+c+d)	a/(a+b)	a/(a+c)	d/(c+d)	d/(b+d)
	dry	c	d					

The correlations and accuracy for each of the NDVI thresholds of vegetation response tested were compared graphically to determine the most appropriate NDVI threshold for each sensor (Landsat, Modis and AVHRR). This is a somewhat subjective assessment to try to find the balance between over-estimating the inundated area by adopting too low a NDVI threshold of response and underestimating the area by adopting too high a threshold. Final estimates of inundated area for each event were therefore presented with error bands representing the level of uncertainty inherent in the choice of appropriate NDVI values. This provides a clear understanding of the level of uncertainty compared to many existing flood maps which have little or no metadata or uncertainty bounds included.

5.2.5 Defining landscape units

The results of the inundation and response mapping for each flood were combined to characterise the frequency of flood response across the landscape for each sensor (AVHRR, Modis and Landsat). Using the information from all three sensors provides an overview of the most likely areas of inundation and response. The spatial resolution of the Modis imagery (250m^2) was chosen as the most appropriate resolution. AVHRR had to be subdivided to this resolution. This does not add any new information or enhance the scale of the AVHRR analysis but does provide a common scale for analysis. Landsat was initially filtered using a maximum 3x3 filter then aggregated to the final resolution. The period of analysis for flood events is 1988 to 2005 due to data availability, however the flood event frequency (Table 5.5) corresponds to the period post-Copeton Dam 1977-2008, as discussed in Section 5.2.2. The available imagery covers a wide range of flood events and was representative of the total post-Copeton flood history.

Connectivity of areas was determined by assessing each 250m^2 pixel for its connection to its eight neighbours (including diagonal connectivity) in relation to flood frequency in ESRI ArcMap 9.2 using the ‘Regions’ tool (Spatial Analysis). All pixels that are connected to each other at the same flood frequency were defined as a single patch and given a unique identifier. Visual assessment of the patches and their relationship with mapped channels was carried out to assess if the patch is in direct connection to the channel, or if they are remote from the channel and rely on overland flow of water for flooding. In combination with the vegetation layers (Figure 3.11), the landscape was remapped into homogeneous landscape units (in relation to vegetation community, inundation behaviour and connectivity), using the ‘union’ analysis tool in ArcMap. The landscape units were used in Chapter 6 as the base units for modelling of vegetation response behaviour. Note that a single landscape unit may include elements that are not necessarily contiguous. For example a large connected patch may contain two separate areas of spikerush vegetation. These would form a single landscape unit. (Figure 5.9).

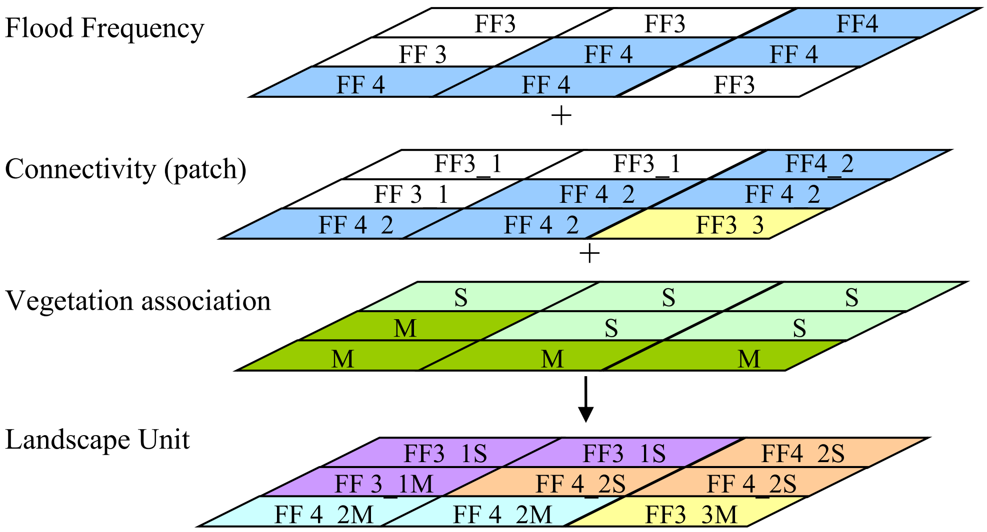

Figure 5.9: Combining flood frequency (FF1-4), connectivity (unique number for each connected patch) and vegetation associations defines homogenous landscape units (unique identifier made up of patch + vegetation association).

5.3 Results

As discussed in section 5.2 (Figure 5.1), the analysis includes assessment of flow and rainfall metrics, inundated area, flood frequency and connectivity. The results of the analysis include landscape scale assessment of connected patches and landscape units used in subsequent chapters of this thesis. The results of these analysis are presented below.

5.3.1 Flow and rainfall metrics

Analysis of the daily flow record from Gwydir River at Yarraman gauge over a 32 year period provided an indication of the contemporary recurrence interval of event sizes based on 40-day inflows as shown in Figure 5.10. A total of 17 events coincided with available Landsat, AVHRR or Modis imagery for analysis. These events were subjectively classified into sizes based on the probability of exceedance (Figure 5.10 and Table 5.5). Of these 17 events, two were defined as small events (with one being under the 10GL threshold for comparison purposes), three were moderately small events, four were moderate events, three were moderately large events and five were large events where event size is defined by the 40-day total inflows (Table 5.5). Most of the events analysed occurred post the 1992-1995 drought during which time there were no significant inflows to the system. Since 1995, events have occurred relatively regularly (Figure 5.11).

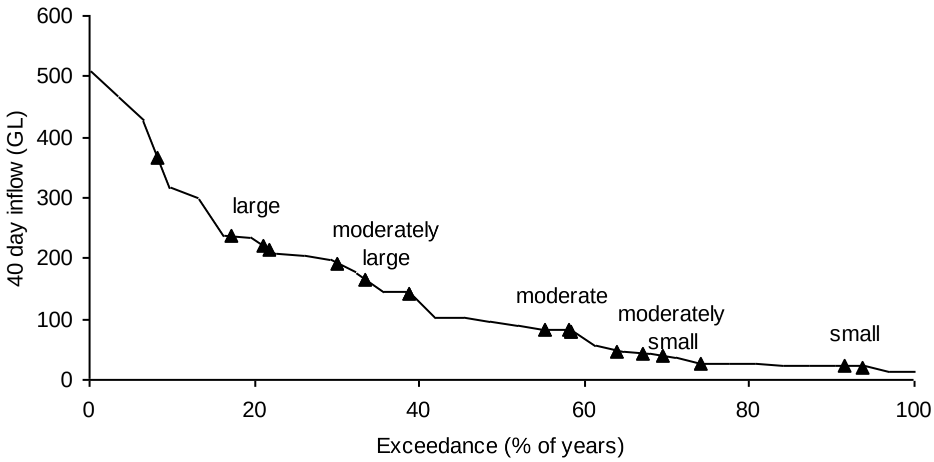

Figure 5.10: Annual exceedance probability of 40-day inflow, Gwydir River at Yarraman Gauge. Observed daily data 1977-2009 Events analysed ▲

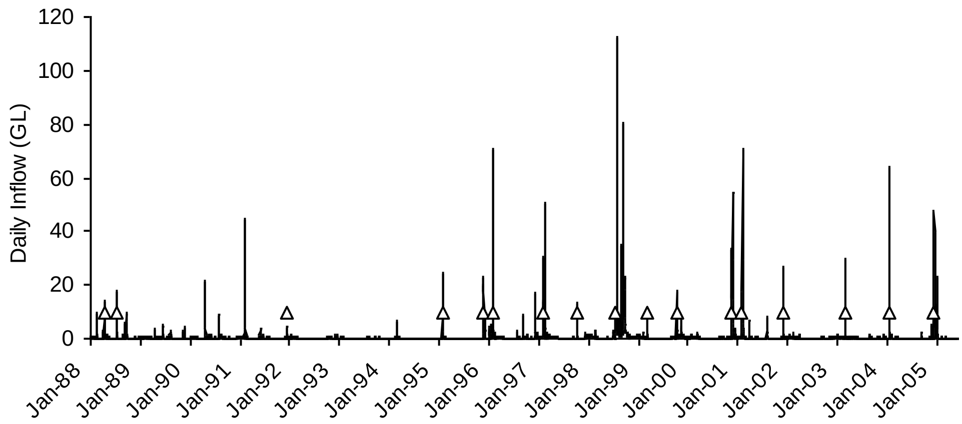

Figure 5.11: Temporal flood analysis dates. Daily inflow for Gwydir River at Yarraman gauge (GL) and events for which satellite imagery was available for analysis (Δ)

Table 5.5: Summary of events analysed. Event size according to 40-day inflow volumes and estimated number of events per 10 years (post Copeton Dam). Codes reflect the flood frequency (FF) such that FF4 is more than six events per 10 years.

Event size (number)	40-day inflow	number of events per 10 years	Code
Small (2)	< 25GL	> 9	FF4
Moderately small (3)	25 - 50GL	> 6	
Moderate (4)	50 - 100GL	> 5	FF3
Moderately large (3)	100 - 200GL	> 3	FF2
Large (5)	> 200GL	< 3	FF1

The metrics for each event are shown in Table 5.6. Peak inflow (Figure 5.12) ranged from 4.2GL from July 1988 to over 112GL from July 1998. These events also recorded the lowest and highest 40-day cumulative inflows at 22.3GL and 366GL respectively. Peak rainfall of over 100mm in a single day fell in association with the January 2001 and December 2004 events. The longest period between events was 1440 days following the 1992-1995 drought, while several events occurred in quick succession between 1995 and 2001.

Table 5.6: Event metrics extracted for all events analysed including peak (Qpeak), 40-day (Q40) and total event (Qtotal) inflows, antecedent inflows (60, 90 and 180-day cumulative, AQ60, AQ90 and AQ180 respectively), peak (Rpeak) and antecedent (30-day cumulative, AR30) rainfall and the number of days since last event (D).

Start date	Q_{peak}	Q_{40}	Q_{total}	AQ_{60}	AQ_{90}	AQ_{180}	D	R_{peak}	AR_{30}
03-Apr-88	14.2	54.4	50	27.4	41.1	57.9	839	40	182
07-Jul-88	18.1	43.1	85.2	5.5	44.2	97.7	82	64	77
14-Dec-91	4.2	22.3	9	14.0	19.7	34.6	305	75	136
22-Jan-95	24.6	46.8	37.4	5.2	5.7	6.8	1440	65	119
20-Nov-95	23.3	144.6	141.8	1.7	3.2	6.2	298	57	169
26-Jan-96	70.8	167	157.5	114.9	185.7	189.4	28	26	104
31-Jan-97	50.4	237.7	237.7	60.2	65.1	110.3	50	53	34
10-Oct-97	13.1	27.4	19.9	11.3	12.7	36.9	211	21	34
30-Jul-98	112.4	366.6	823.2	18.5	21.0	61.2	281	69	139
04-Mar-99	10.2	21.4	13	39.0	69.6	497.9	140	45	38
06-Oct-99	18.1	81.8	93	19.7	23.5	32.0	213	73	45
16-Nov-00	54.7	300.1	298.4	18.2	29.3	40.2	356	40	146
29-Jan-01	70.6	223.2	214.5	46.7	330.3	355.1	40	129	177
27-Nov-01	26.8	83.5	69.1	8.9	13.3	43.4	289	36	52
24-Feb-03	29.8	81.1	73.6	34.9	51.7	73.0	449	36	42
17-Jan-04	64.2	170.4	159.1	12.3	20.6	32.4	325	96	76
09-Dec-04	47.8	204.9	198.7	13.5	22.2	26.2	315	120	158
Means	*38.4*	*133.9*	*157.7*	*26.6*	*56.4*	*100.1*	*333.0*	*61.5*	*101.6*
Std. Dev.	*28.9*	*104.5*	*191.5*	*27.8*	*82.3*	*132.9*	*343.8*	*30.6*	*55.0*

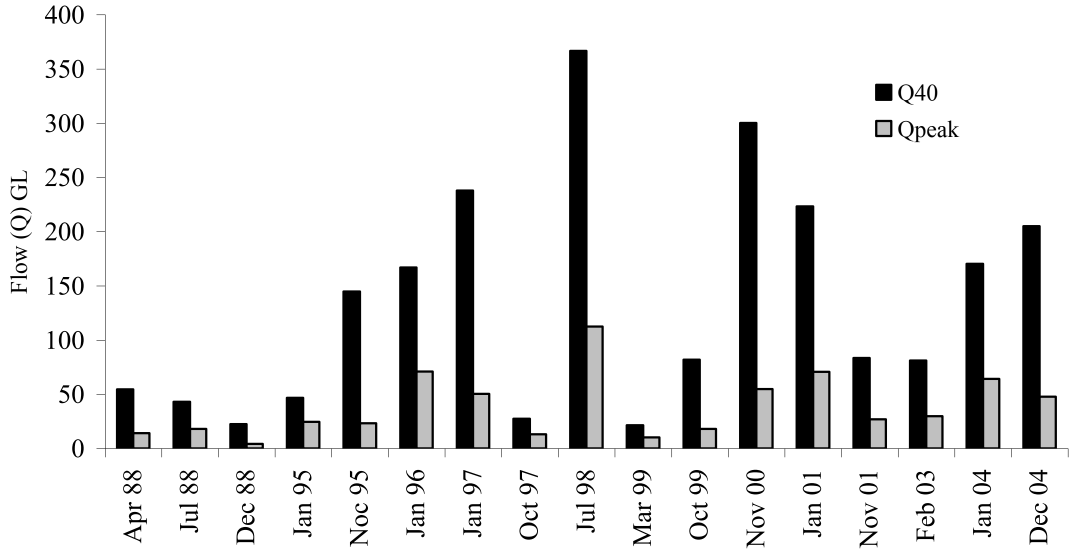

Figure 5.12: Comparison of 40-day and peak inflow for events analysed.

Table 5.7 shows the correlation matrix for all metrics with significant correlations shown in bold. The 40-day cumulative inflow is significantly correlated with both the peak inflow and total event inflow (Figure 5.13). Antecedent inflow is best described by the 90-day antecedent inflow, which is significantly correlated with both 60-day, and 180-day antecedent inflows (Figure 5.14). Days since last event, peak rainfall and antecedent rainfall are not significantly correlated to other variables (Figure 5.15).

Table 5.7: Correlation matrix for flow and rainfall summary data for all events. Significant correlations ($p<0.05$) are shown in bold.

	Q_{40}	Q_{total}	AQ_{60}	AQ_{90}	AQ_{180}	D	R_{peak}	AR_{30}
Q_{peak}	**.8963 p=.000**	**.8631 p=.000**	.3507 p=.168	.3711 p=.143	.0585 p=.824	-.2329 p=.368	.3062 p=.232	.2710 p=.293
Q_{40}		**.8740 p=.000**	.2018 p=.437	.2233 p=.389	-.0546 p=.835	-.2601 p=.313	.2971 p=.247	.3593 p=.157
Q_{total}			.0540 p=.837	.0508 p=.847	-.0789 p=.763	-.1799 p=.490	.1994 p=.443	.2883 p=.262
AQ_{60}				**.6447 p=.005**	.4814 p=.050	-.3695 p=.144	-.2081 p=.423	-.1017 p=.698
AQ_{90}					**.6571 p=.004**	-.3750 p=.138	.3266 p=.201	.2288 p=.377
AQ_{180}						-.3867 p=.125	.0898 p=.732	-.1203 p=.645
D							-.0714 p=.785	.2643 p=.305
R_{peak}								.4320 p=.083

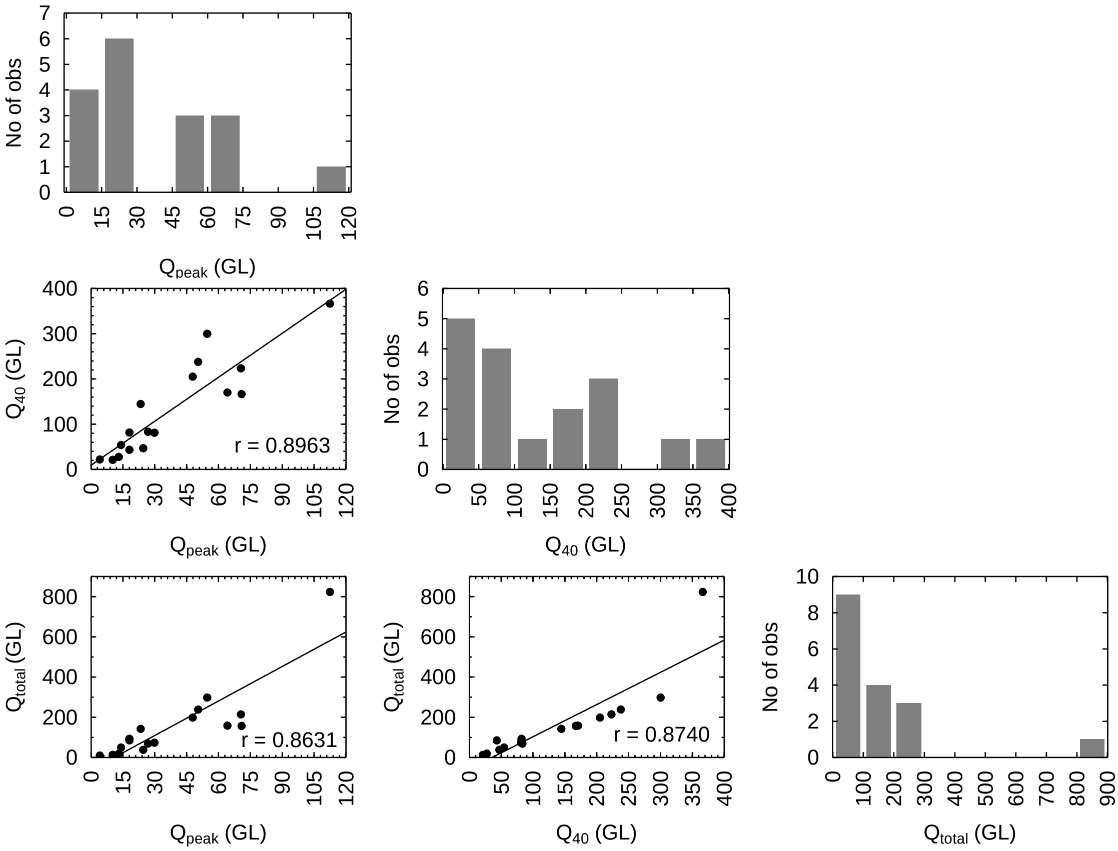

Figure 5.13: Scatterplots and histograms for inflow measures of all events.

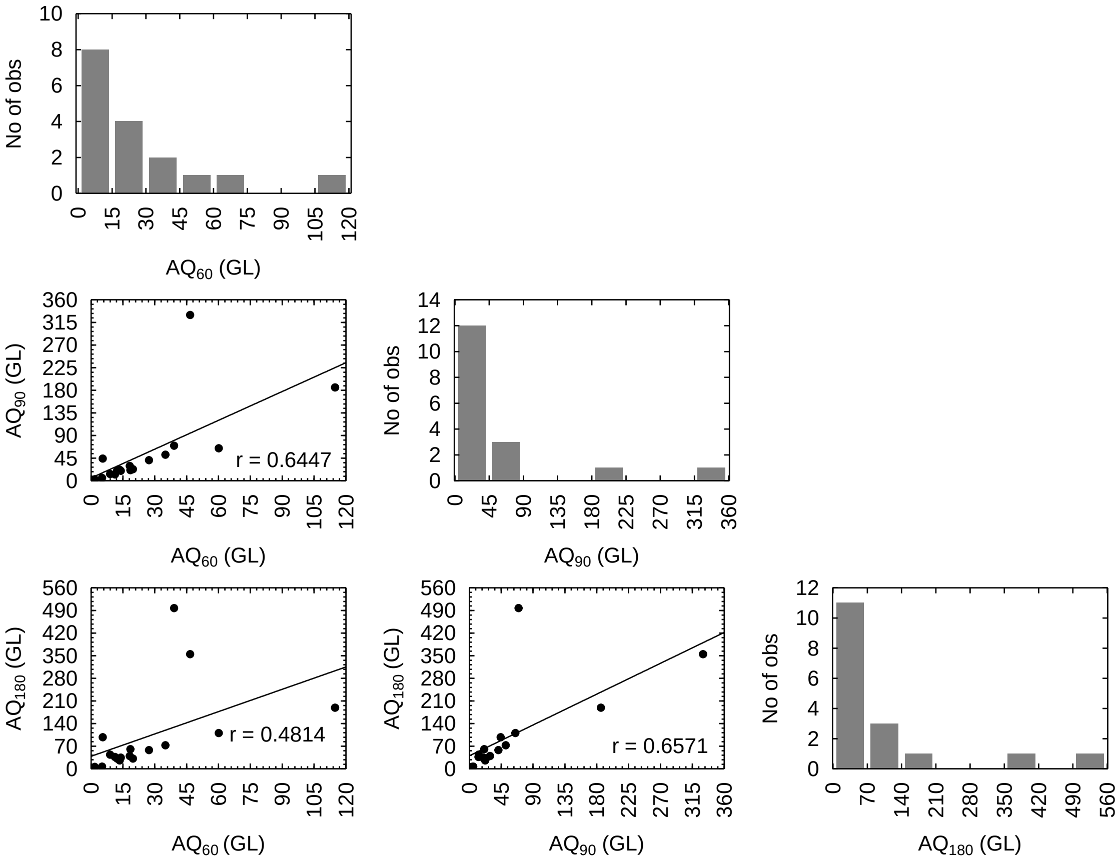

Figure 5.14: Scatterplots and histograms for antecedent inflow measures of all events.

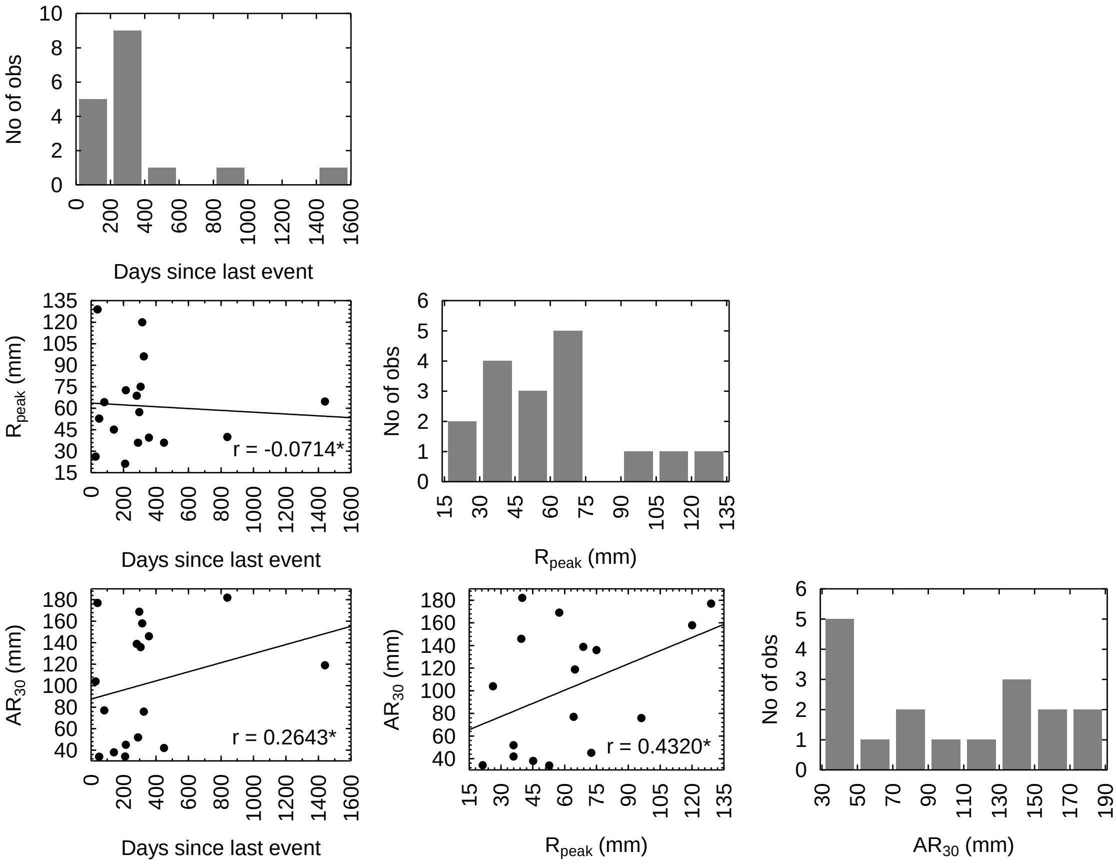

Figure 5.15: Days since last event, peak rainfall and 30-day antecedent rainfall are not correlated with other event variables.

The analysis of the event metrics showed that peak event inflow and total event inflow are significantly correlated ($p<0.001$) with the 40-day cumulative event inflow. Similarly cumulative antecedent flows of 60 and 90, and 90 and 180 days are significantly correlated ($p=0.005$ and 0.004 respectively) and the 90-day antecedent inflow has been chosen to represent antecedent inflow conditions prior to each event. The days since last event, peak rainfall and 30-day antecedent rainfall were not significantly correlated with any of the event metrics and are included as event descriptors.

5.3.2 Inundation and response mapping

The results and classification maps for each flood event are present in detail in Appendix 2: Flood assessment 1988-2005. The following is a summary of the assessments for Landsat, Modis and AVHRR imagery.

5.3.2.1 Landsat

Landsat was available for 15 flood events with varying number and timing of images as shown in Appendix 1.

Correlation and regression analysis

The area of inundation from the decision tree analyses (Section 5.2.4) was significantly correlated with 40-day inflow volumes for NDVI values of 0.7 and greater. Peak rainfall was also significantly correlated for NDVI of 0.7 through 0.9 (Table 5.8). The scatter plot (Figure 5.16) of the areas classified by different NDVI values and the correlated event variables show that the correlations are influenced by outliers (for peak rainfall).

Two outliers (peak rainfall > 100mm/day) were removed from the statistical analysis that removed the correlation with rainfall for the remaining events (Table 5.9). Significant correlations still occurred for 40-day inflow volumes at NDVI values of 0.75 and greater. The scatter plot was redrawn without the rainfall outliers and shows that the inundated and responsive areas for the remaining 13 events (Figure 5.17) have a linear relationship with 40-day inflows. The analysis dates for the rainfall outliers in both cases included an image soon after the initial flood peak and heavy rainfall. This heavy rainfall resulted in surface flooding which was quickly transferred into the soil profile and did not result in persistent flooding. Therefore, although the area was detected as open water by the initial image, subsequent images did not show the expected vegetation response as measured by NDVI. These events do not appear as outliers in either the Modis or AVHRR analysis.

Table 5.8: Correlations for all events analysed using Landsat NDVI decision tree. Thresholds from 0.65 to 0.9 for responsive vegetation and event inflow and climate measures. Significant correlation ($p<0.05$) shown in bold.

	Lwet	Lwet0.9	Lwet0.85	Lwet0.8	Lwet0.75	Lwet0.7	Lwet0.65
Q_{40}	**.6034**	**.7147**	**.7288**	**.7328**	**.6950**	**.6240**	.4862
	p=.022	**p=.004**	**p=.003**	**p=.003**	**p=.006**	**p=.017**	p=.083
AQ_{90}	-.1321	.2825	.3669	.4200	.4313	.3950	.2219
	p=.652	p=.328	p=.197	p=.135	p=.124	p=.162	p=.446
D	-.0603	-.1764	-.2010	-.2199	-.2303	-.1795	-.0657
	p=.838	p=.546	p=.491	p=.450	p=.428	p=.539	p=.824
Rpeak	.4613	**.7073**	**.7326**	**.7496**	**.7476**	**.6867**	.3798
	p=.097	**p=.005**	**p=.003**	**p=.002**	**p=.002**	**p=.007**	p=.180
AR_{30}	.2854	.3949	.3682	.3148	.2457	.2013	.2728
	p=.323	p=.162	p=.195	p=.273	p=.397	p=.490	p=.345

Table 5.9: Correlations for events analysed using Landsat NDVI decision tree excluding high rainfall events (peak rainfall > 100mm). Thresholds from 0.65 to 0.9 for responsive vegetation and event inflow and climate measures. Significant correlation (p<0.05) shown in bold.

	Lwet	Lwet0.9	Lwet0.85	Lwet0.8	Lwet0.75	Lwet0.7	Lwet0.65
Q_{40}	**.7994**	**.8070**	**.7976**	**.7595**	**.6329**	.5005	.4898
	p=.002	**p=.002**	**p=.002**	**p=.004**	**p=.027**	p=.097	p=.103
AQ_{90}	-.0760	-.0632	-.0502	-.0441	-.0440	-.0413	-.0824
	p=.814	p=.845	p=.877	p=.892	p=.892	p=.899	p=.799
D	-.0766	-.1019	-.1130	-.1227	-.1266	-.0592	.0186
	p=.813	p=.753	p=.727	p=.704	p=.695	p=.855	p=.954
R_{peak}	-.0535	-.0643	-.0372	.0628	.2184	.3025	.1292
	p=.869	p=.843	p=.909	p=.846	p=.495	p=.339	p=.689
AR_{30}	.1209	.0452	-.0464	-.1515	-.2104	-.1626	.1203
	p=.708	p=.889	p=.886	p=.638	p=.512	p=.614	p=.710

Multiple regression analysis (backward stepwise) of the Landsat area of inundation and response (using the NDVI values of 0.75) for all analysis dates shows that the 40-day inflow volume and peak rainfall were highly significant explanatory variables using all available flood events (adjusted R^2 0.83, $p <0.007$) (Table 5.10). The results appear skewed by the high rainfall events. However using the MLR for all results indicated that both inflow and rainfall were significant explanatory variables and no outliers were identified in the MLR analysis.

Table 5.10: Summary of regression results for Landsat classification

	b*	Std. Err of b*	b	Std. Err of b	t(11)	p-value
Intercept			-42706	12905	-3.31	0.0070
Q_{40}	0.5566	0.1184	286	61	4.70	0.0006
R_{peak}	0.6242	0.1184	946	179	5.27	0.0003
Area = 286 Q_{40} + 946 R_{peak} – 42706 + e						
Multiple R = 0.9238, R^2 = 0.8535, adj. R^2=0.8535, F=32.04 (df 2,11), p=0.00003						

* regression coefficient for standardised variables (mean = 0, st. dev. = 1)

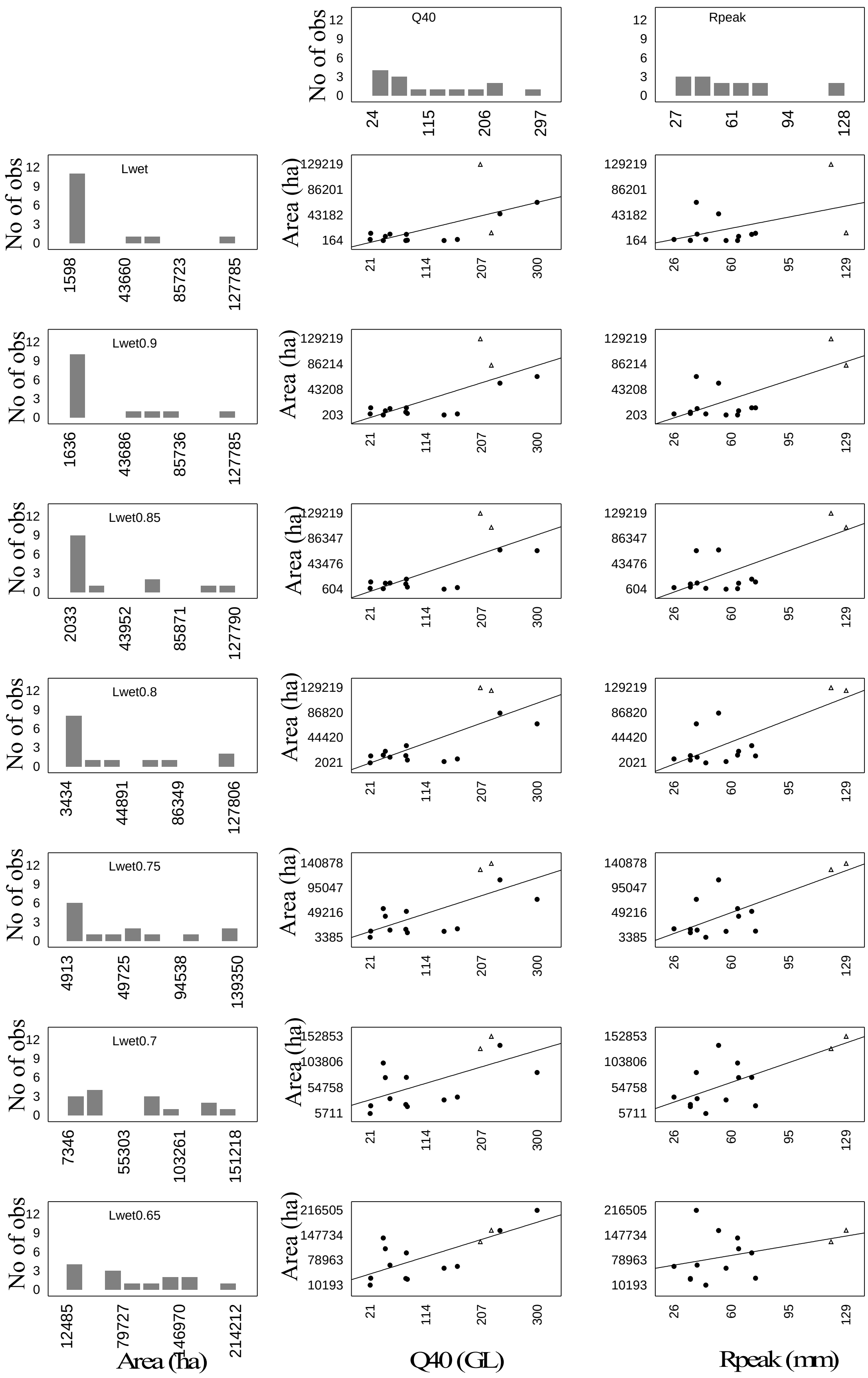

Figure 5.16: Scatter plot for all Landsat NDVI thresholds, 40-day inflow and peak rainfall. Marked (Δ) points are outliers.

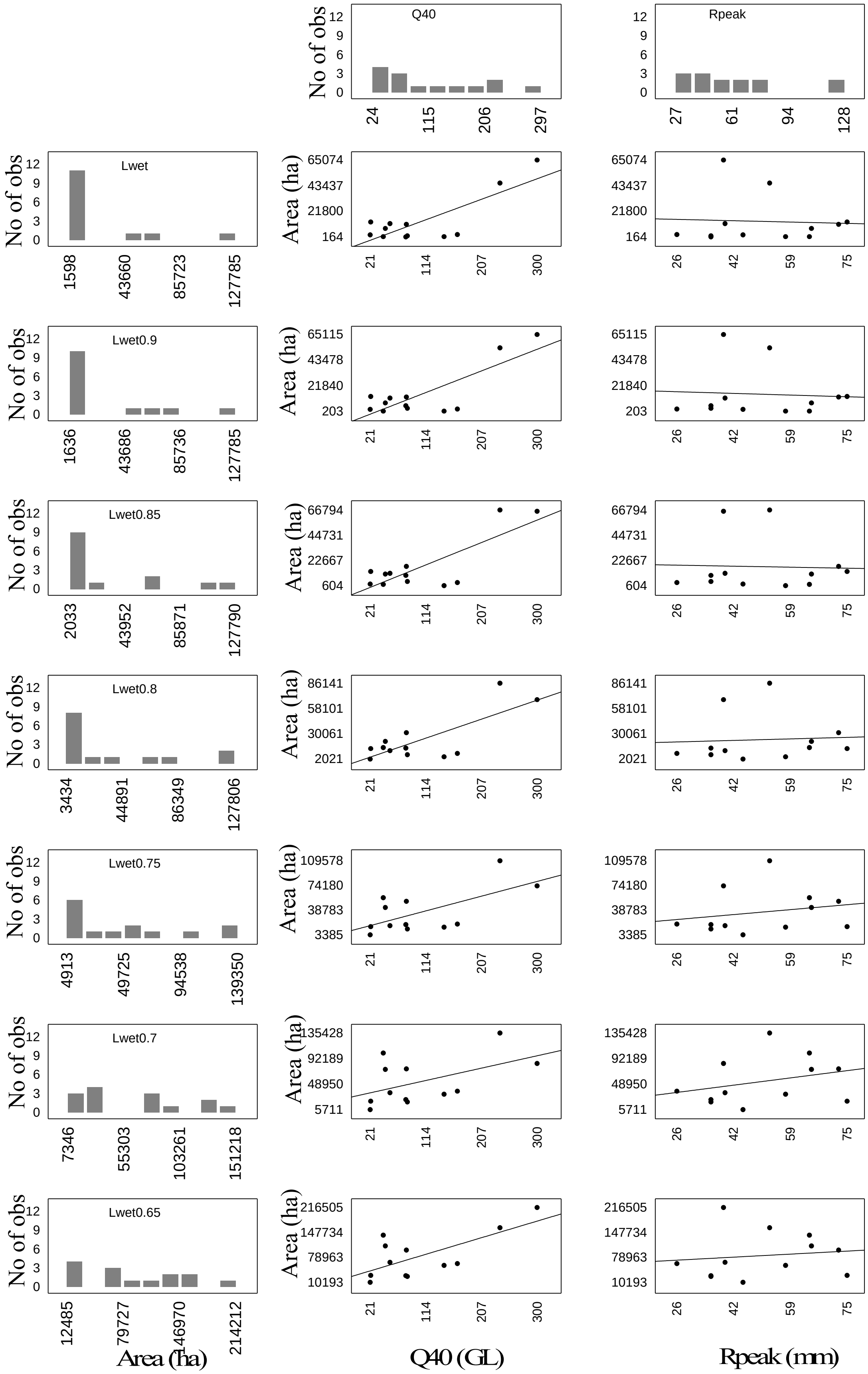

Figure 5.17: Scatter plot for Landsat NDVI thresholds excluding cases where peak rainfall > 100.

Mapped flood events

The November 1995 event was a moderately large event with 40-day inflow of 144.6GL. The event peaked on the 24th November at 23.3GL/day and the existing extent map showed almost 54 000ha flooded in the lower Gwydir and Gingham. Only a single Landsat image (20 December, 1995) was available post event, prior to the next large inflow. The areas classified as wet, using the NDVI decision tree method for Landsat (that is both open water and responsive vegetation), and dry are shown in Table 5.11 and in Figure 5.20a. Overall accuracy was highest for the NDVI > 0.8 vegetation response threshold. However both user and producer accuracy for classification of wet pixels were well under 50% for all cases. The area classified as wet or responsive was less than the area mapped. Using an NDVI of < 0 or > 0.8 resulted in an estimated total area of wet or responsive vegetation of only 4 420ha compared to the mapped flood area of almost 54 000ha. This is most likely due to only the single image being available for this event. The decision tree method relies on multiple images over a sufficient period of time for vegetation to respond to the flood event. This was not available for this event.

Table 5.11: November 1995 flood event with mapping undertaken in November and Landsat NDVI analysis from December 1995. Error matrix showing area mapped and predicted and associated errors.

Mapped	NDVI Decision tree				wet		dry	
	Wet (ha)	Dry (ha)	*Total*	Accuracy	producer	users	producer	users
NDVI < 0				75	0	23	100	75
Wet (ha)	47	53951	*53999*					
Dry (ha)	155	162351	*162506*					
Total	*203*	*216302*						
NDVI < 0 or > 0.9				75	0	23	100	75
Wet (ha)	47	53951	*53999*					
Dry (ha)	155	162351	*162506*					
Total	*203*	*216302*						
NDVI < 0 or > 0.85				75	1	54	100	75
Wet (ha)	328	53671	*53999*					
Dry (ha)	276	162230	*162506*					
Total	604	215901						
NDVI < 0 or > 0.8				75	4	49	99	76
Wet (ha)	2160	51838	*53999*					
Dry (ha)	2259	160247	*162506*					
Total	4420	212086						
NDVI < 0 or > 0.75				74	12	44	95	76
Wet (ha)	6431	47567	*53999*					
Dry (ha)	8175	154331	*162506*					
Total	14607	201898						
NDVI < 0 or > 0.7				72	23	40	88	78
Wet (ha)	12589	41410	*53999*					
Dry (ha)	18983	143523	*162506*					
Total	31572	184933						
NDVI < 0 or > 0.65				67	38	36	77	79
Wet (ha)	20294	33705	*53999*					
Dry (ha)	36669	125837	*162506*					
Total	56963	159542						

The January 1996 flood event had a similar 40-day inflow volume to the previous event, but the peak was almost three times the size with over 70GL passing the Yarraman gauge on the 26th January, 1996. The event came only two months after the previous flood in November 1995. Despite the much larger flood peak and wet antecedent conditions, the mapped extent was very similar to the November 1995 event, with a total area of 59 990ha. Four Landsat images were available for analysis covering a period of almost four months (6 February, 9 March, 10 April and 12 May) which is greater than the 96 days required to ensure vegetation response. Overall accuracy was highest for an NDVI threshold of >0.7 (Table 5.12), with an overall area classified as wet/response of almost 37 000ha compared to the mapped area of close to 60 000ha (Figure 5.20b).

Table 5.12: January 1996 flood event with mapping undertaken in January and Landsat NDVI analysis from February to May 1996. Error matrix showing area mapped and predicted and associated errors.

Mapped	NDVI Decision tree				wet		dry	
	Wet (ha)	Dry (ha)	*Total*	Accuracy	producer	users	producer	users
NDVI < 0				72	2	57	99	73
Wet (ha)	1114	58876	*59990*					
Dry (ha)	849	155707	*156556*					
Total	*1962*	*214584*						
NDVI < 0 or > 0.9				72	2	56	99	73
Wet (ha)	1187	58803	*59990*					
Dry (ha)	922	155635	*156556*					
Total	*2109*	*214438*						
NDVI < 0 or > 0.85				73	4	66	99	73
Wet (ha)	2200	57791	*59990*					
Dry (ha)	1138	155418	*156556*					
Total	*3338*	*213208*						
NDVI < 0 or > 0.8				74	11	79	99	74
Wet (ha)	6518	53472	*59990*					
Dry (ha)	1769	154787	*156556*					
Total	*8287*	*208259*						
NDVI < 0 or > 0.75				78	26	80	98	77
Wet (ha)	15384	44606	*59990*					
Dry (ha)	3786	152770	*156556*					
Total	*19170*	*197376*						
NDVI < 0 or > 0.70				80	44	72	93	81
Wet (ha)	26692	33298	*59990*					
Dry (ha)	10225	146331	*156556*					
Total	*36918*	*179628*						
NDVI < 0 or > 0.65				78	62	60	84	85
Wet (ha)	37083	22907	*59990*					
Dry (ha)	24978	131578	*156556*					
Total	*62061*	*154485*						

A peak inflow 30 854GL occurred on the 2nd February, 1997 closely followed by a larger peak of 50.4GL on the 18th February, 1997. Over a 40-day period, over 237GL flowed through Yarraman gauge resulting in a large event with mapped inundation area of over 100 000ha. Landsat imagery was available for 8 February, 9 March, 10 April and 12 May and all images were used for the classification of open water and vegetation response. The Landsat NDVI classification had the highest accuracy at NDVI threshold of 0.7 and 0.75 (65%), with the 0.75 threshold having the highest wet user accuracy and the closest agreement to the total area flooded (109 583ha classified compared to 101 915ha mapped) (Table 5.13 and Figure 5.20c).

Table 5.13: February 1997 flood event with mapping undertaken in May and Landsat NDVI analysis from February to May 1997. Error matrix showing area mapped and predicted and associated errors.

Mapped	NDVI Decision tree				wet		dry	
	Wet (ha)	Dry (ha)	*Total*	Accuracy	producer	users	producer	users
NDVI < 0				56	26	58	83	56
Wet (ha)	26312	75603	101915					
Dry (ha)	19341	95259	114600					
Total	45653	170862						
NDVI < 0 or > 0.9				58	31	59	81	57
Wet (ha)	31953	69963	101915					
Dry (ha)	21942	92658	114600					
Total	53895	162620						
NDVI < 0 or > 0.85				60	40	61	77	59
Wet (ha)	40787	61129	101915					
Dry (ha)	26010	88590	114600					
Total	66797	149719						
NDVI < 0 or > 0.8				63	53	62	72	63
Wet (ha)	53679	48236	101915					
Dry (ha)	32466	82134	114600					
Total	86145	130370						
NDVI < 0 or > 0.75				65	67	62	64	68
Wet (ha)	68040	33875	101915					
Dry (ha)	41543	73057	114600					
Total	109583	106932						
NDVI < 0 or > 0.70				65	79	60	52	74
Wet (ha)	80616	21299	101915					
Dry (ha)	54818	59781	114600					
Total	135435	81080						
NDVI < 0 or > 0.65				61	88	56	38	78
Wet (ha)	89240	12676	101915					
Dry (ha)	70899	43700	114600					
Total	160139	56376						

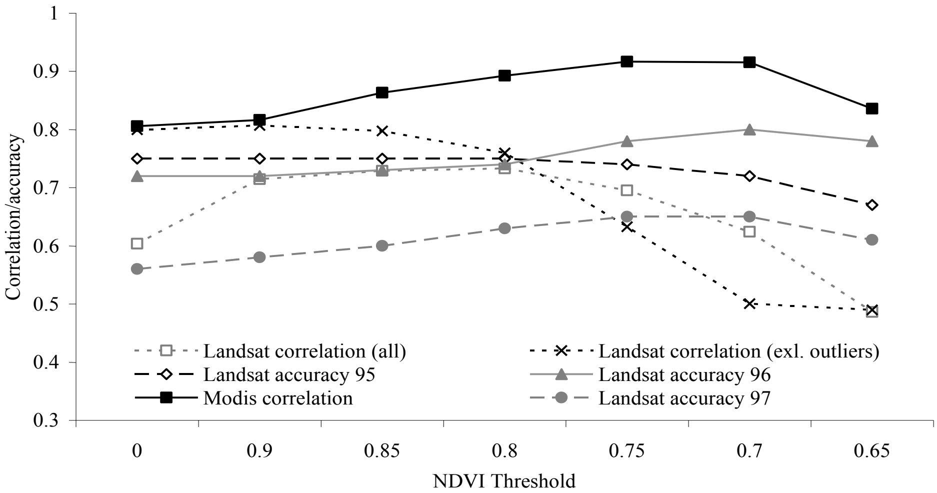

Figure 5.18: Comparison of Landsat and Modis NDVI values with 40-day inflow correlations and validation accuracy (area).

Summary

Using the NDVI values greater than 0.75 to indicate high vegetation vigour resulted in total estimated flood areas of up to 141 000ha (2001). Figure 5.19 shows the classified area of inundation and response at the time of the last image analysed for each flood event against the rolling 40-day inflow volumes and the mapped flood extent that was used for validation.

There is still a degree of uncertainty regarding the NDVI values used. The areas of response for NDVI values greater than 0.7 and 0.8 are also shown as upper and lower bounds to give an indication of the level of uncertainty associated with the choice of NDVI threshold. The 1995 and 1996 validation indicated the decision tree method may underestimate area inundated when there are a limited number of images available for analysis (in this case due to subsequent flood events). Where the full six MVC periods were available for analysis in 1997 there was good agreement between the mapped flood extent and the decision tree results.

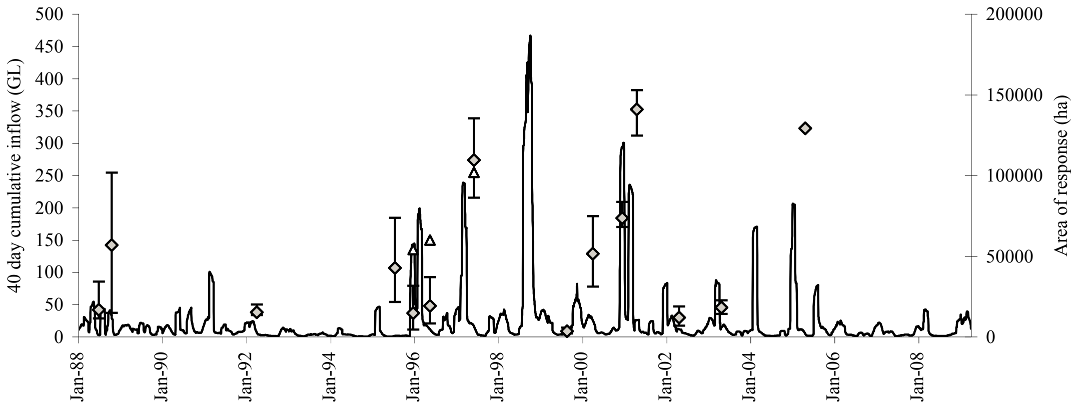

Figure 5.19: Classified area of inundation and response at a threshold of NDVI>0.75(◇) to indicate highly responsive vegetation. Error bands are NDVI values greater than 0.7 and 0.8 and represent uncertainty in the choice of threshold. The plotted date of response is aligned with the last image analysed for each flood and is the cumulative or total area classified since commencement of the event. Flood extent from mapped floods (Δ).

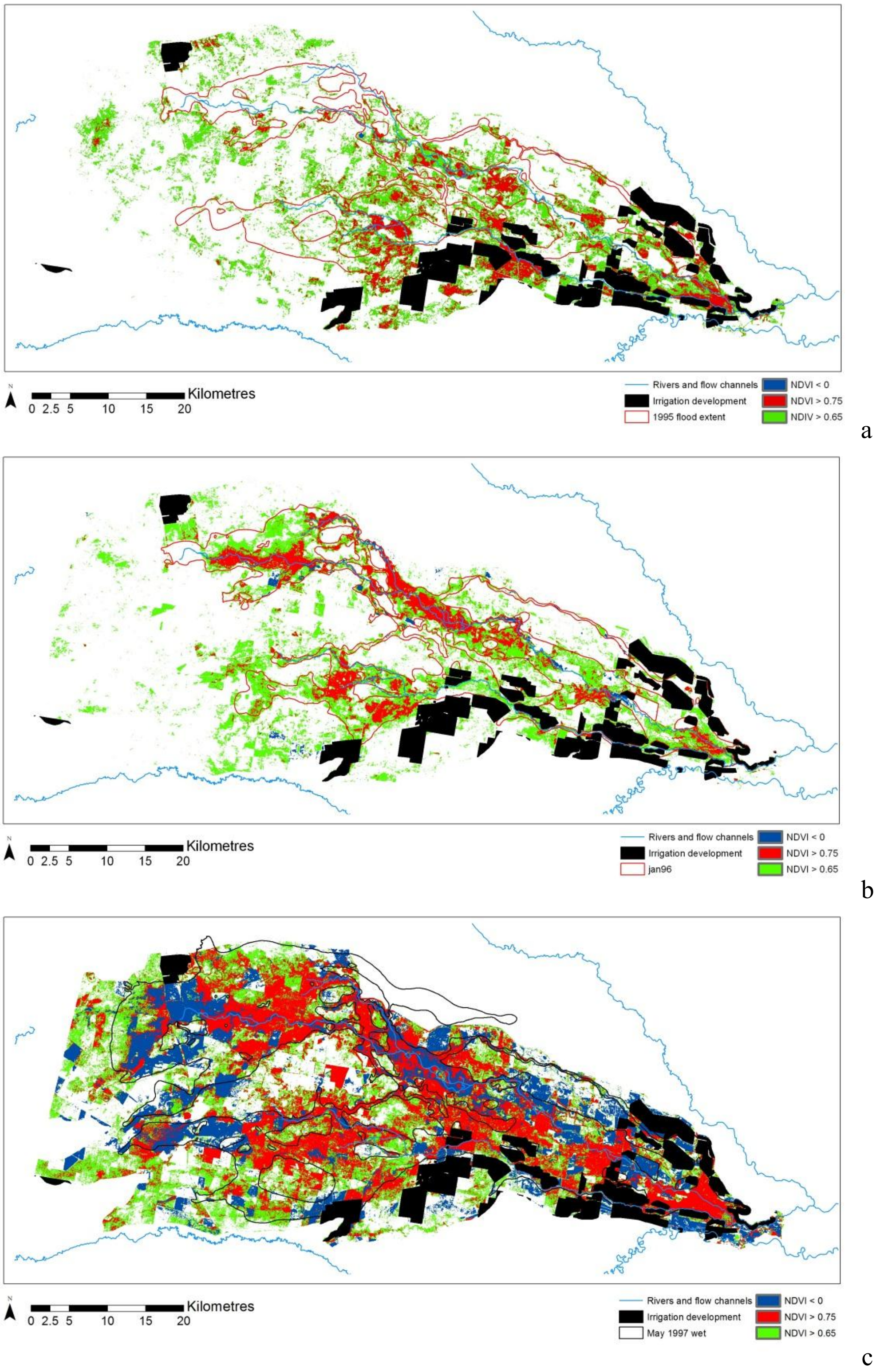

Figure 5.20: Landsat decision tree classification and mapped flood boundary for a) November 1995, b) January 1996 and c) February 1997 events

5.3.2.2 Modis

Modis data were only available for six flood events since the satellite commenced operations in 2000.

Correlation and regression analysis

The area of inundation and response estimated from the decision tree method was significantly correlated with 40-day inflow volumes but not with peak rainfall (Table 5.14). The highest correlation was at thresholds of NDVI > 0.65 (p <0.05). Comparison however, with Landsat, AVHRR and existing flood mapping (Figure 5.18 and Figure 5.24) indicated that a NDVI threshold of 0.75 provides the best estimate of flood and response extent. At NDVI > 0.75 the correlation between area and the 40-day inflow volume was still highly significant considering the small sample size (n=6), with correlation of 0.92 (p<0.01). The scatter plot shown in Figure 5.22 demonstrates that a linear fit is appropriate for the regression analysis. Regression analysis (backwards stepwise) confirmed the significance of the 40-day inflow volume with removal of all other variables (Table 5.15).

Table 5.14: Correlations for events analysed using Modis NDVI decision tree. Thresholds from 0.65 to 0.9 for responsive vegetation and event inflow and climate measures. Significant correlation (p<0.05) shown in bold.

	Mwet	Mwet0.9	Mwet0.85	Mwet0.8	Mwet0.75	Mwet0.7	Mwet0.65
Q_{40}	.8058	**.8164**	**.8634**	**.8923**	**.9167**	**.9155**	**.8355**
	p=.053	**p=.047**	**p=.027**	**p=.017**	**p=.010**	**p=.011**	**p=.036**
AQ_{90}	.0632	.1724	.2975	.4192	.4586	.4633	.4555
	p=.905	p=.744	p=.567	p=.408	p=.360	p=.355	p=.364
D	-.0240	-.1150	-.2404	-.3810	-.4478	-.4826	-.4980
	p=.964	p=.828	p=.646	p=.456	p=.373	p=.332	p=.315
R_{peak}	-.2419	-.1863	-.0376	.1215	.2396	.3339	.4160
	p=.644	p=.724	p=.944	p=.819	p=.648	p=.518	p=.412
AR_{30}	.4861	.5263	.5976	.6814	.7350	.7554	.7839
	p=.328	p=.283	p=.210	p=.136	p=.096	p=.082	p=.065

Table 5.15: Summary of regression results for Modis classification

	b*	Std. Err of b*	b	Std. Err of b	t(4)	p-value
Intercept			-18153	17007	-1..07	0.3459
Q_{40}	0.9167	0.1997	404	88	4.590	0.0101
Area = 404 Q_{40} – 18153 + e (NB Intercept N.S.)						
Multiple R = 0.9167, R^2 = 0.8404, adj. R^2=0.8005, F=21.07 (df 1, 4), p=0.0101						

* regression coefficient for standardised variables (mean = 0, st. dev. = 1)

Summary

Applying an NDVI threshold of 0.75 resulted in total estimated flood areas of up to 107 000ha in 2000. Figure 5.21 shows the classified area of inundation and response at the time of the last image analysed for each flood event against the rolling 40-day inflow volumes. There is still a degree of uncertainty regarding the thresholds used and the areas of response for thresholds of 0.7 and 0.8 are shown to give an indication of the level of uncertainty associated with the method. The relationship between area of response and the 40-day inflow volume is relatively clear. No flood mapping was available to validate the Modis results.

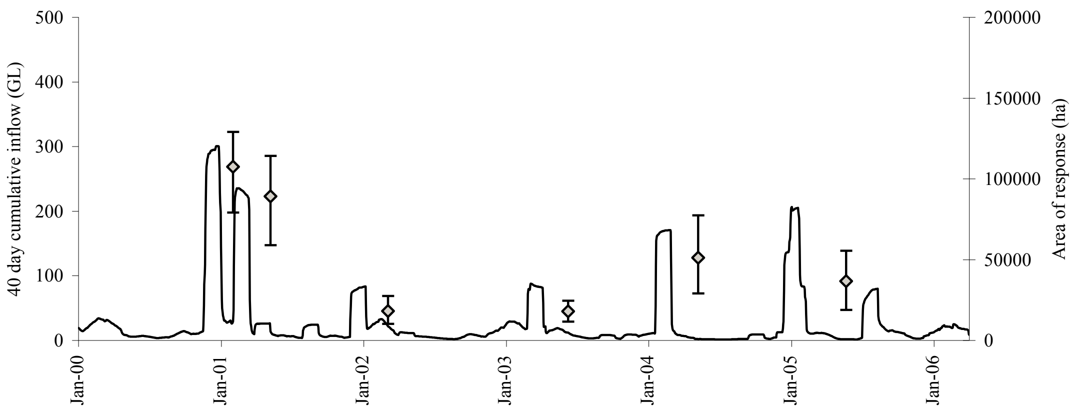

Figure 5.21: Classified area of inundation and response◇ at a threshold of NDVI>0.75 (Modis) to indicate highly responsive vegetation. Error bands are the results for NDVI > 0.7 and NDVI >0.8 to indicate uncertainty associated with the choice of threshold. The area of response is plotted at last day of analysis period following each event and represents the total area of inundation and response from event day = 0 through to last day of last MVC period.

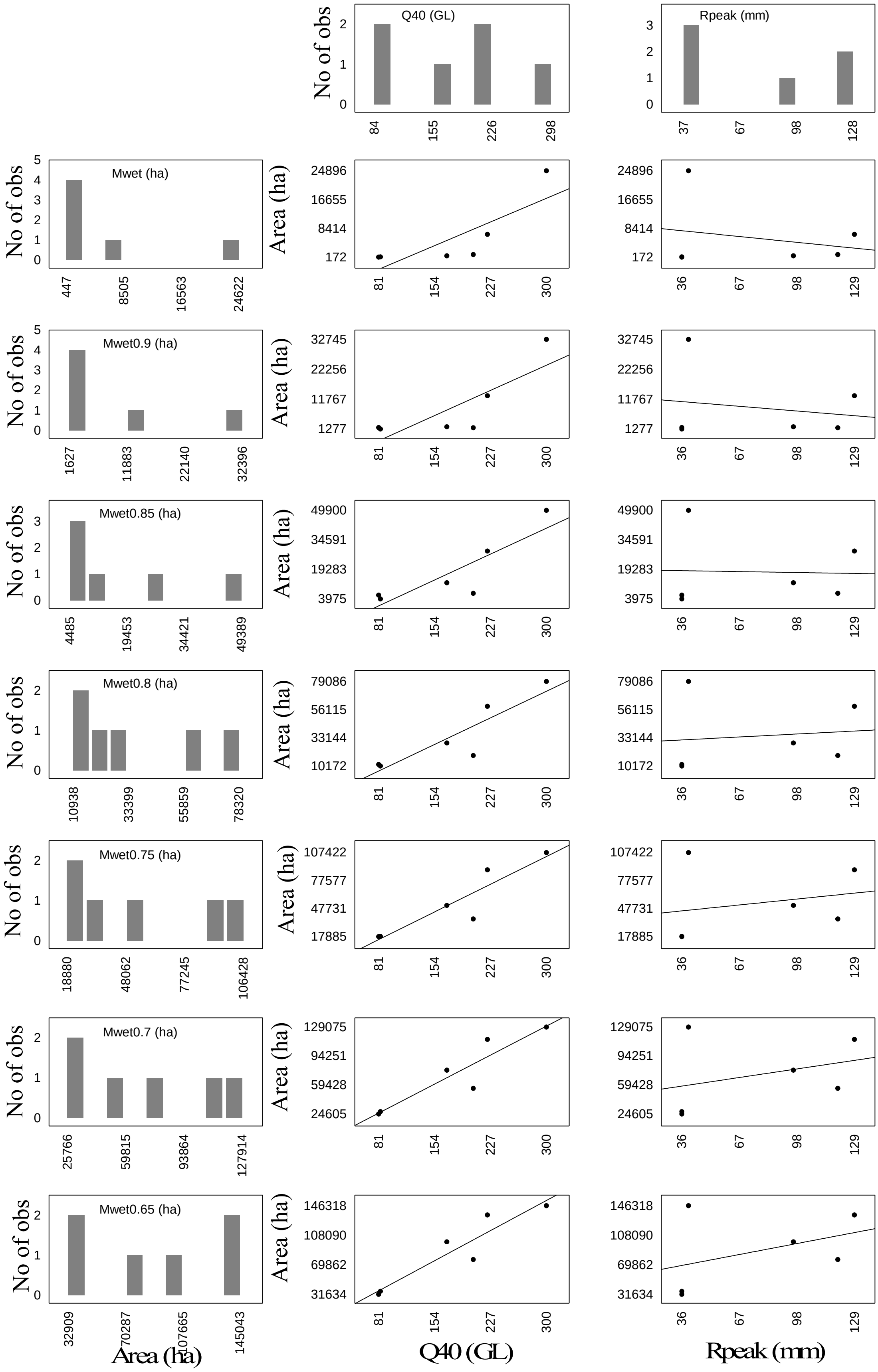

Figure 5.22: Scatter plots for 40-day inflow ($p<0.05$ for all except Mwet) and Modis classified inundated areas. Peak rainfall is also shown but is insignificant in inundated area for the Modis analysis.

5.3.2.3 AVHRR

AVHRR imagery was analysed for 14 events.

Correlation and regression analysis

The area of inundation and response from the decision tree method was significantly correlated with 40-day inflow volumes but not with peak rainfall. The highest correlation was at thresholds of NDVI > 0.6 ($p < 0.001$). Comparison, however, with Landsat, Modis and existing flood mapping (Figure 5.18 and Figure 5.24) indicated that a threshold of 0.52 provides the best estimate of flood and response extent. At NDVI > 0.52 the correlation between area and the 40-day inflow volume was still highly significant ($r=0.70$, $p<0.01$) (Table 5.16 and Figure 5.23).

Regression analysis (backwards stepwise) confirmed the significance ($p<0.01$) of the 40-day inflow volume with removal of all other variables (Table 5.17). The results of the decision tree method for the January 1995 event indicate an outlier in the data set there being a large area of response for a relatively small flood event. This event was removed to determine how much influence it had on the regression analysis. The results (Table 5.18) showed that again 40-day inflow proved to be a significant explanatory variable and the strength of the relationship is increased ($p<0.001$). The January 1995 event occurred after a 3 year dry period with no significant inflow. This resulted in a different level of response, also visible in the results from the Landsat analysis (although not identified as an outlier in that analysis). Unfortunately there are insufficient events with similar drying antecedent conditions to determine the mechanisms responsible for the larger area of response to the January 1995 event in the Gwydir wetlands.

Table 5.16: Correlation matrix for events analysed using AVHRR NDVI decision tree. Significant correlation ($p<0.05$) shown in bold.

	Awet	Awet0.6	Awet0.56	Awet0.52	Awet0.48	Awet0.45
Q_{40}	.1234	**.7755**	**.7521**	**.7002**	**.6461**	**.5961**
	p=.674	**p=.001**	**p=.002**	**p=.005**	**p=.013**	**p=.024**
AQ_{90}	-.2185	-.0362	.0069	.0399	.0337	.0642
	p=.453	p=.902	p=.981	p=.892	p=.909	p=.827
D	-.0098	.1080	.1925	.2501	.2702	.2558
	p=.974	p=.713	p=.510	p=.389	p=.350	p=.377
R_{peak}	.3774	.2456	.2118	.1805	.1535	.1285
	p=.183	p=.397	p=.467	p=.537	p=.600	p=.661
AR_{30}	.1298	.4358	.4593	.4649	.4732	.4544
	p=.658	p=.119	p=.098	p=.094	p=.087	p=.103

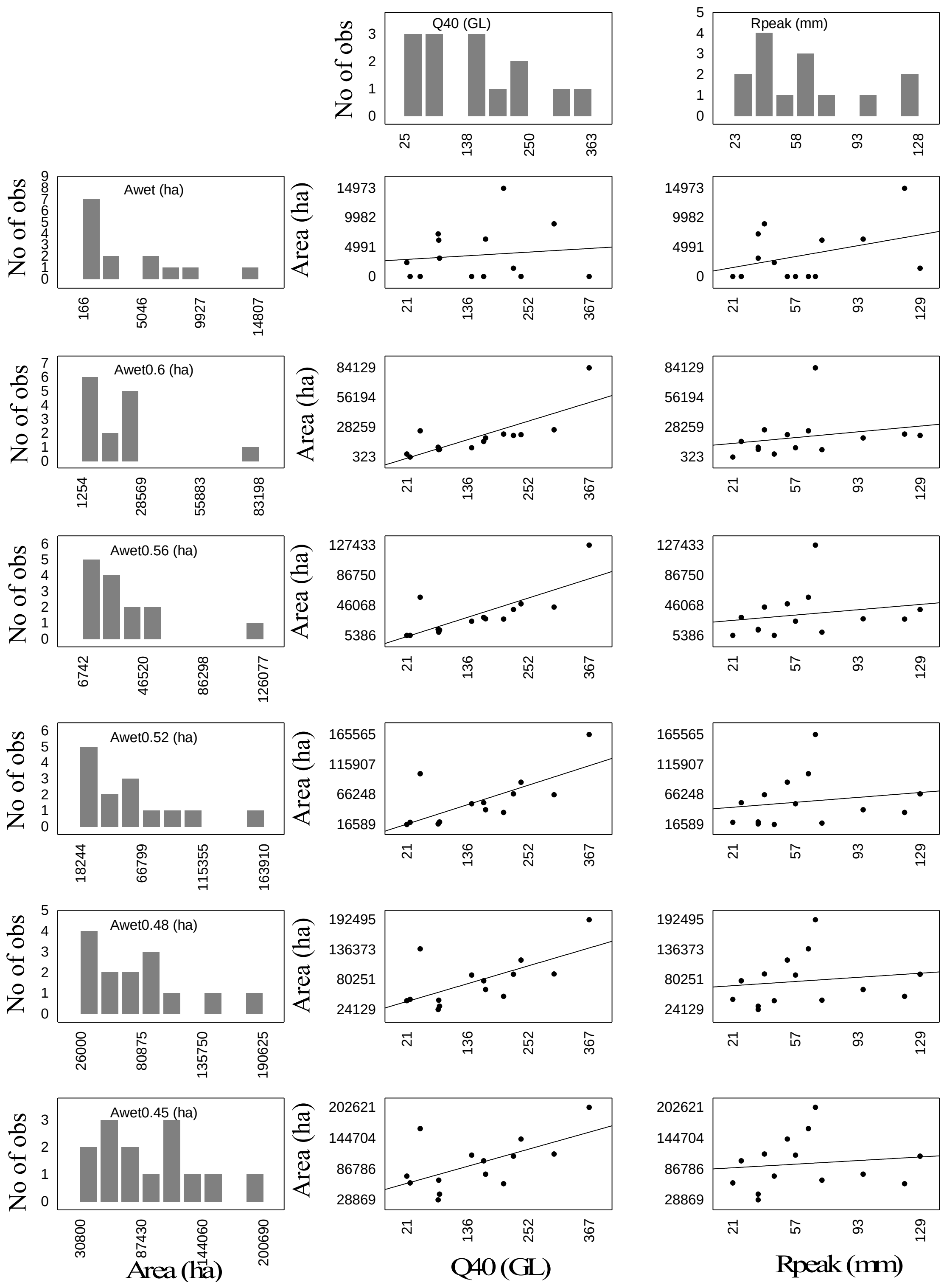

Figure 5.23: Scatter plots for 40-day inflow ($p<0.05$ for all except Awet) and AVHRR classified inundated areas. Peak rainfall is also shown but is insignificant in inundated area for the AVHRR analysis.

Table 5.17: Summary of regression results for AVHRR classification

	b*	**Std. Err of b***	**b**	**Std. Err of b**	**t(12)**	**p-value**
Intercept			11358	15158	0.75	0.4680
Q_{40}	0.7002	0.2061	280	82	3.40	0.0053
Area = $280Q_{40} + 11358 + e$ (NB Intercept N.S.)						
Multiple R = 0.7002, R^2 = 0.4902, adj. R^2=0.4477, F=11.53 (df 1, 12), p=0.0053						

* regression coefficient for standardised variables (mean = 0, st. dev. = 1)

Table 5.18: Summary of regression results (excluding outlier, January 1995)

	b*	Std. Err of b*	b	Std. Err of b	t(12)	p-value
Intercept			-5578	10894	-0.51	0.6187
Q_{40}	0.8781	0.1443	348	57	6.09	0.0001
Area = $348Q_{40} - 5578 + e$ (NB Intercept N.S.)						
Multiple R = 0.8781, R^2 = 0.7710, adj. R^2=0.7502, F=37.03 (df 1, 11), p=0.0001						

* regression coefficient for standardised variables (mean = 0, st. dev. = 1)

Mapped flood events

Validation using the November 1995 event (discussed in detail in 5.3.2.1) was constrained to four MVC AVHRR intervals before the next flood peak entered the system. The thresholds tested for AVHRR were lower than Landsat with NDVI of > 0.6 indicating very high vegetation response. The highest agreement between mapped flood extent and classified extent was for wet pixels (NDVI < 0) and responsive vegetation of NDVI > 0.56 (79% overall accuracy). However the balance of producer and user accuracies and the comparison of total mapped area suggest that 0.52 may be a more appropriate threshold (Table 5.19). Both producer and user accuracy for wet pixels was still low (50% and 51% respectively). The area of mapped response (at $1km^2$ resolution) is around 52 000 ha, similar to the AVHRR classification (using an NDVI threshold of 0.52) that provides an estimated total area of approximately 51 000ha (Figure 5.25).

Table 5.19: November 1995 flood event with mapping undertaken in November and AVHRR NDVI analysis for four MVC periods. Error matrix showing area mapped and predicted and associated errors.

Mapped	NDVI Decision tree				wet		dry	
	Wet (ha)	Dry (ha)	*Total*	Accuracy	producer	users	producer	users
NDVI < 0				76	0	na	100	76
Wet (ha)	0	52136	*52136*					
Dry (ha)	0	163626	*163626*					
Total	*0*	*215763*						
NDVI < 0 or > 0.6				77	12	69	98	78
Wet (ha)	6248	45889	*52136*					
Dry (ha)	2801	160826	*163626*					
Total	*9048*	*206714*						
NDVI < 0 or > 0.56				79	30	63	94	81
Wet (ha)	15619	36517	*52136*					
Dry (ha)	9048	154578	*163626*					
Total	*24668*	*191095*						
NDVI < 0 or > 0.52				76	50	51	85	84
Wet (ha)	26284	25853	*52136*					
Dry (ha)	24883	138743	*163626*					
Total	*51167*	*164596*						
NDVI < 0 or > 0.48				69	70	41	68	88
Wet (ha)	36732	15404	*52136*					
Dry (ha)	52460	111167	*163626*					
Total	*89192*	*126571*						
NDVI < 0 or > 0.45				62	79	37	56	89
Wet (ha)	41257	10880	*52136*					
Dry (ha)	71634	91993	*163626*					
Total	*112890*	*102872*						

For the January 1996 event (discussed in detail in 5.3.2.1) the full 6 MVC periods were used to analyse the AVHRR data with the highest overall accuracy at a threshold of 0.52 (81%) (Table 5.20). Wet producer and user accuracy were reasonable (60 and 68% respectively) while the total area classified as wet was almost 53 000ha compared to just over 60 000ha mapped at the 1km resolution (Figure 5.21b).

Table 5.20: January 1996 flood event with mapping undertaken in January and AVHRR NDVI analysis for six MVC periods.. Error matrix showing area mapped and predicted and associated errors.

Mapped	NDVI Decision tree				wet		dry	
	Wet (ha)	Dry (ha)	*Total*	Accuracy	producer	users	producer	users
NDVI < 0				72	0	na	100	72
Wet (ha)	0	60215	*60215*					
Dry (ha)	0	155655	155655					
Total	*0*	*215871*						
NDVI < 0 or > 0.6				77	21	84	98	76
Wet (ha)	12603	47612	*60215*					
Dry (ha)	2478	153178	*155655*					
Total	*15081*	*200790*						
NDVI < 0 or > 0.56				79	38	76	95	80
Wet (ha)	22837	37379	*60215*					
Dry (ha)	7110	148546	*155655*					
Total	*29946*	*185924*						
NDVI < 0 or > 0.52				81	60	68	89	85
Wet (ha)	35871	24345	*60215*					
Dry (ha)	16912	138743	*155655*					
Total	*52783*	*163088*						
NDVI < 0 or > 0.48				78	76	58	79	89
Wet (ha)	45565	14650	*60215*					
Dry (ha)	32747	122908	*155655*					
Total	*78312*	*137558*						
NDVI < 0 or > 0.45				72	85	50	67	92
Wet (ha)	50951	9264	*60215*					
Dry (ha)	51490	104165	*155655*					
Total	*102442*	*113429*						

For the large event in February 1997 (discussed in detail in Section 5.3.2.1) six MVC periods were used for the AVHRR analysis and highest overall accuracy was for an NDVI threshold of 0.52 (65%). The classified wet/response area at this threshold was 86 607ha which is lower than the mapped area of almost 103 000ha at the 1km resolution, while a threshold of 0.48 overestimates the flood extent (Table 5.21 and Figure 5.25c).

Table 5.21: February 1997 flood event with mapping undertaken in January and AVHRR NDVI analysis for six MVC periods.. Error matrix showing area mapped and predicted and associated errors.

Mapped	NDVI Decision tree				wet		dry	
	Wet (ha)	Dry (ha)	Total	Accuracy	producer	users	producer	users
NDVI < 0				52	0	na	100	52
Wet (ha)	0	102980	102980					
Dry (ha)	0	112783	112783					
Total	0	215763						
NDVI < 0 or > 0.6				58	16	77	96	55
Wet (ha)	16481	86499	102980					
Dry (ha)	4955	107828	112783					
Total	21436	194327						
NDVI < 0 or > 0.56				62	34	72	88	59
Wet (ha)	34794	68187	102980					
Dry (ha)	13465	99318	112783					
Total	48258	167504						
NDVI < 0 or > 0.52				65	56	66	74	65
Wet (ha)	57415	45565	102980					
Dry (ha)	29192	83591	112783					
Total	86607	129156						
NDVI < 0 or > 0.48				64	69	61	59	68
Wet (ha)	71203	31777	102980					
Dry (ha)	46104	66679	112783					
Total	117307	98456						
NDVI < 0 or > 0.45				60	77	55	44	68
Wet (ha)	79390	23591	102980					
Dry (ha)	63662	49120	112783					
Total	143052	72711						

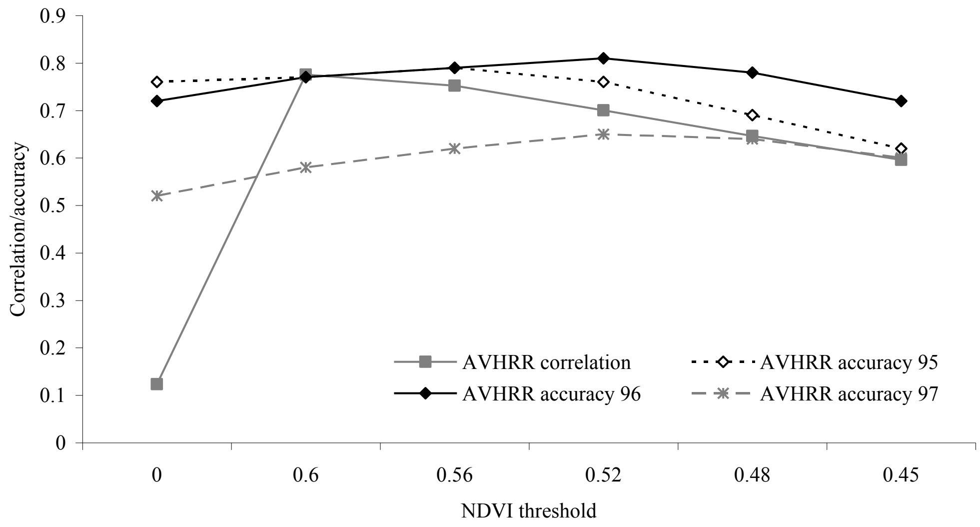

Figure 5.24: Comparison of AVHRR thresholds with 40-day inflow correlations and validation accuracy (area). Threshold of 0.52 was adopted based on comparison with areas mapped for validation events.

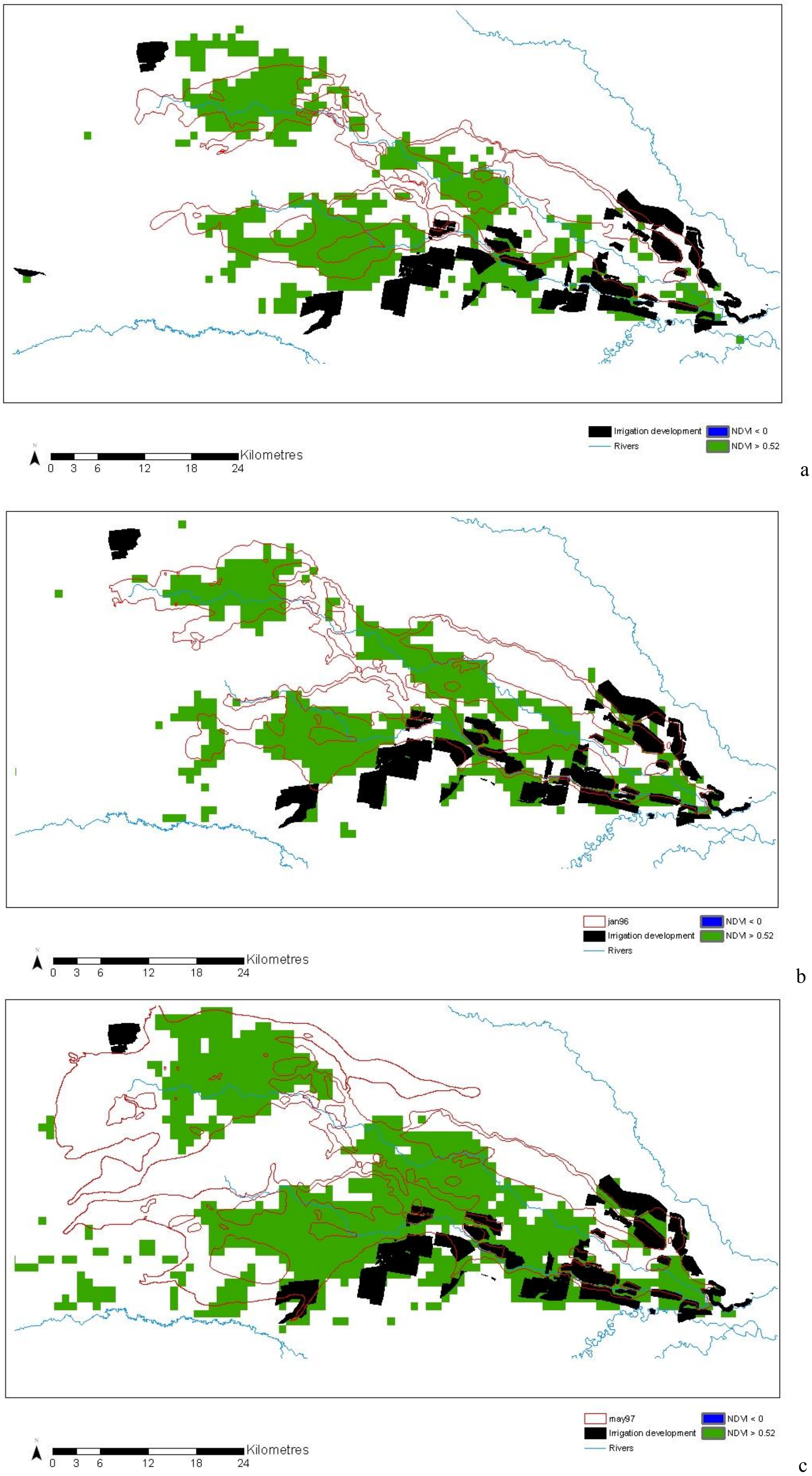

Figure 5.25: AVHRR decision tree classification and mapped flood boundary for a) November 1995, b) January 1996 and c) February 1997 events

Summary

Applying the NDVI threshold of 0.52 resulted in total estimated flood areas of up to 166 000ha in 1998. Figure 5.26 shows the classified area of inundation and response at the time of the last image analysed for each flood event against the rolling 40-day inflow volumes. There is still a degree of uncertainty regarding the thresholds used. The areas of response for thresholds of 0.48 and 0.56 are shown to give an indication of the level of uncertainty associated with the method. Nevertheless the relationship between area of response and the 40-day inflow volume is relatively clear. Comparison with mapped flood events in 1995, 1996 and 1997 showed good agreement in area inundated.

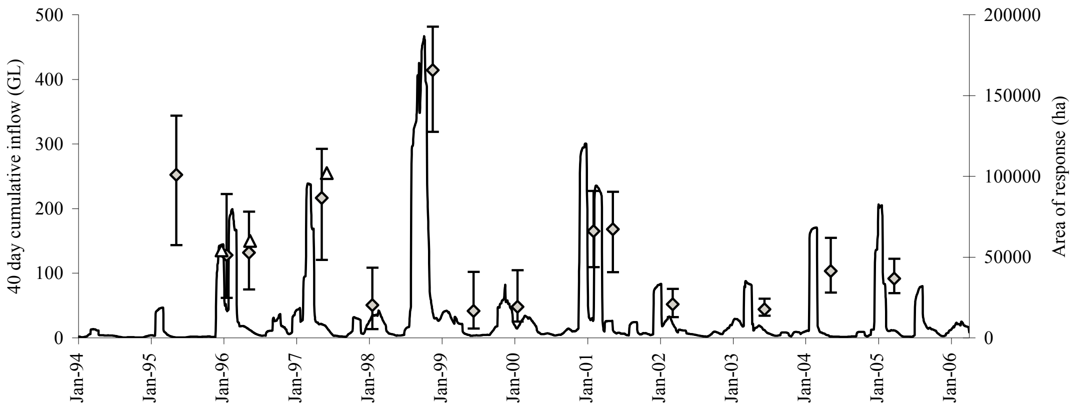

Figure 5.26: Classified area of inundation and response at a threshold of NDVI>0.52 (AVHRR) to indicate highly responsive vegetation. Error bands are the results for NDVI > 0.48 and NDVI >0.56 to indicate the possible levels of uncertainty associated with the choice of threshold. The area of response is plotted at last day of analysis period following each event and represents the total area of inundation and response from event day = 0 through to last day of last MVC period. Validation flood mapping ∆

5.3.2.4 Summary for all sensors

An iterative approach of testing a range of thresholds for vegetation vigour after inundation against 40-day inflow volumes, rainfall and existing flood maps allows estimates of inundated extent in heterogeneous landscapes. For Landsat and Modis, NDVI of 0.75 and greater was highly correlated with inflow volumes while for AVHRR, NDVI greater than 0.52 was the most appropriate. This is consistent with the preliminary results that showed AVHRR NDVI to be lower post-flooding than both Modis and Landsat. The results are also consistent with continental scale maximum NDVI which was approximately 0.6 for AVHRR whilst Modis was around 1.0 (Sandy Berry, ANU, pers. comm.). The range of uncertainty in areas inundated was not consistent between flood events and did not appear to be correlated to magnitude of the flow. Comparison with flood mapping assisted in the selection of NDVI thresholds for vegetation response to flooding using the AVHRR MVC NDVI dataset. The limited Landsat images available for some events resulted in an underestimate of area inundated as vegetation did not have sufficient time to reach maximum NDVI. Despite the differences in spatial resolution and spectral bandwidth, the regression analysis for Modis and AVHRR NDVI show similar results.

Choosing the appropriate NDVI threshold value to extract vegetation response to flooding (as compared to rainfall or seasonal greening events) is not straightforward and a level of uncertainty exists despite high correlation with flow and the use of flood maps. One of the sources of uncertainty is the flood maps themselves. Many historical flood maps are boundaries drawn from on-ground investigation, aerial photography or ‘by eye’ from aerial reconnaissance and tend to concentrate on the furthest extent of the flood peak. Details of higher ground within the boundary, depths and durations are often not documented with the result that the area may be overestimated. Conversely, if mapping is conducted through on-ground field work then a delay of days or even weeks from flood peak exists due to inaccessibility of the floodplain and this could result in underestimation of the flood extent. Ideally flood events can be monitored in real time in the future and compared with the NDVI to determine appropriate thresholds of vegetation response to flooding. This was beyond the scope of this thesis and the timing of flood events during the timeframes also precluded this type of analysis. Future validation may be possible using observations from landowners in the region (Thomas *et al.*, in press) or higher resolution imagery as there is continuous improvement in the accuracy and availability of satellite imagery.

Overall the results suggest a non-linear response to inflows. Plotting the results of Modis and AVHRR (Figure 5.27) indicate little increase in area inundated for 40-day flows up to 100GL (approximately). Once 40-day flows exceed 100GL the area inundated increases significantly.

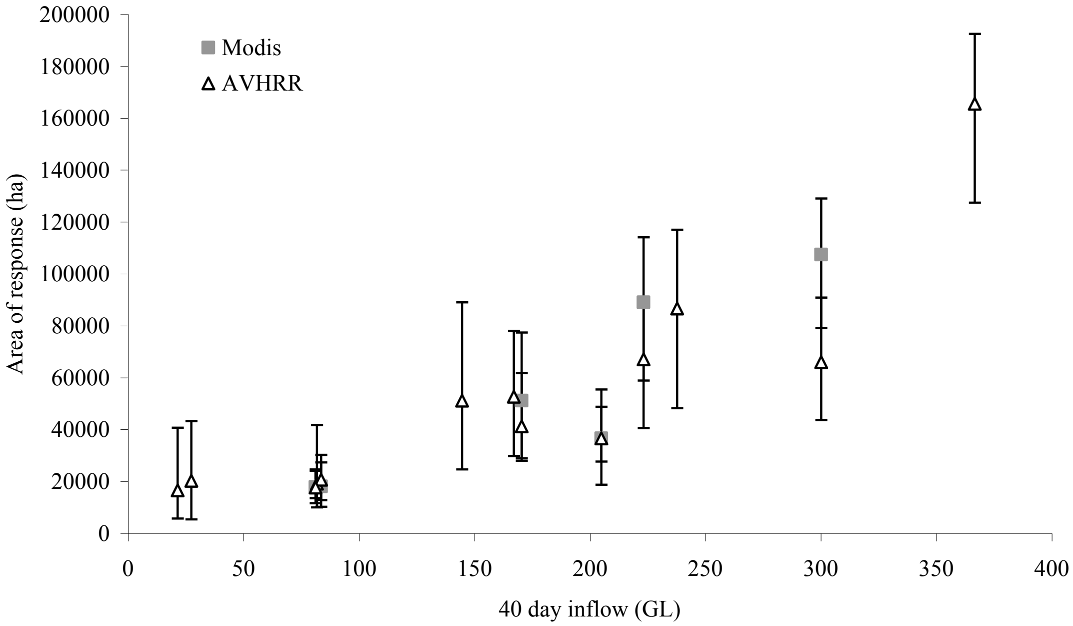

Figure 5.27: Estimated area of inundation and response from Modis and AVHRR image analysis, 1988-2005. Vegetation response threshold of NDVI > 0.75 for Modis, > 0.52 for AVHRR imagery. (excluding AVHRR outlier January 1995). Error bands represent uncertainty associated with choice of threshold.

5.3.3 Landscape units

5.3.3.1 Flood frequency

Combining the inundation and response classifications from all available flood events for each sensor, the estimated flood frequency across the landscape was mapped according to flood event size (inflow volumes as defined in Table 5.5). The remote sensing analysis period is 1988 to 2005, however the flood event frequency corresponds to period post-Copeton Dam, 1977-2008.

Small events, with 40-day inflow volume of less than 25GL, occur in more than 90% of years and result in very low areas of response (note that no events of small or moderately small size were available for analysis with Modis imagery). Very little of the landscape has responded in every event analysed indicating that the small flood events do not always inundate the same locations on the landscape. This could be due to small scale changes to channel capacity or vegetation growth changing the flood distribution patterns of these small floods. The moderately small events (40-day inflows of 25-50GL) occur in 60 to 90% of years and the Landsat and AVHRR analysis provide a similar picture of the consistent response to this size of event. The pattern of inundation and response is along the Gingham and Gwydir channels and centred around the Ramsar listed wetland locations of Old Dromana and Goddards Lease, as well as the 'Raft' area at the eastern edge of the floodplain system (Figure 5.28). Moderate events (40-day inflow 50-100GL) occurring in around 50% of years are also centred along the channels. These, however, extend further across the floodplains and also further west encompassing the Crinolyn Ramsar site on the Gingham Channel (based on the AVHRR analysis). Both the Modis and Landsat analysis suggest that the western half of the wetlands are flooded in 30-50% of years, corresponding to moderately large events (40-day inflow 100-200GL). A wetting response in the broader floodplain occurs in fewer than 30% of years having larger flood events (flood events with 40-day inflow volumes greater than 200GL).

By combining the results from AVHRR, Modis and Landsat a clear indication of the area most frequently inundated is determined (Figure 5.29). Some finer detail is lost, particularly those very small areas that are inundated or responding to inundation in more than 90% of years. The total area responding in more than 60% of years, typically to 40-day flood volumes of less than 50GL, is 2730ha. Connecting these areas is a more contiguous area of 20 780ha that responds in 50-60% of years to 40-day flood volume in the order of 50 to 100GL. It is also evident that floods of up to 100GL in volume are largely connected with the main Gingham and Lower Gwydir channels. Moderately large floods (100 – 200GL over 40-days with a frequency of 30-50% of years) not only extend beyond the boundaries of the more frequently responding areas, but also start to break out along floodways connecting different areas of the floodplains over an additional 71 940ha. As the study area is defined by the largest flood extent, virtually the entire area responds in large floods (>200GL over 40-days with a frequency of <30% of years) with total connectivity across the landscape. Although this analysis is based on post-Copeton Dam data, the presence of several large events during this time provides a good indication of the probable size of 'natural' events as these larger events are largely uncontrolled by weirs through the system. The frequency of events is likely to have been greater pre-dam as indicated by the 'historical climate, no development' scenario in flow modelling undertaken by CSIRO Sustainable Yields project (CSIRO, 2007) which is further discussed in section 7.3.1.

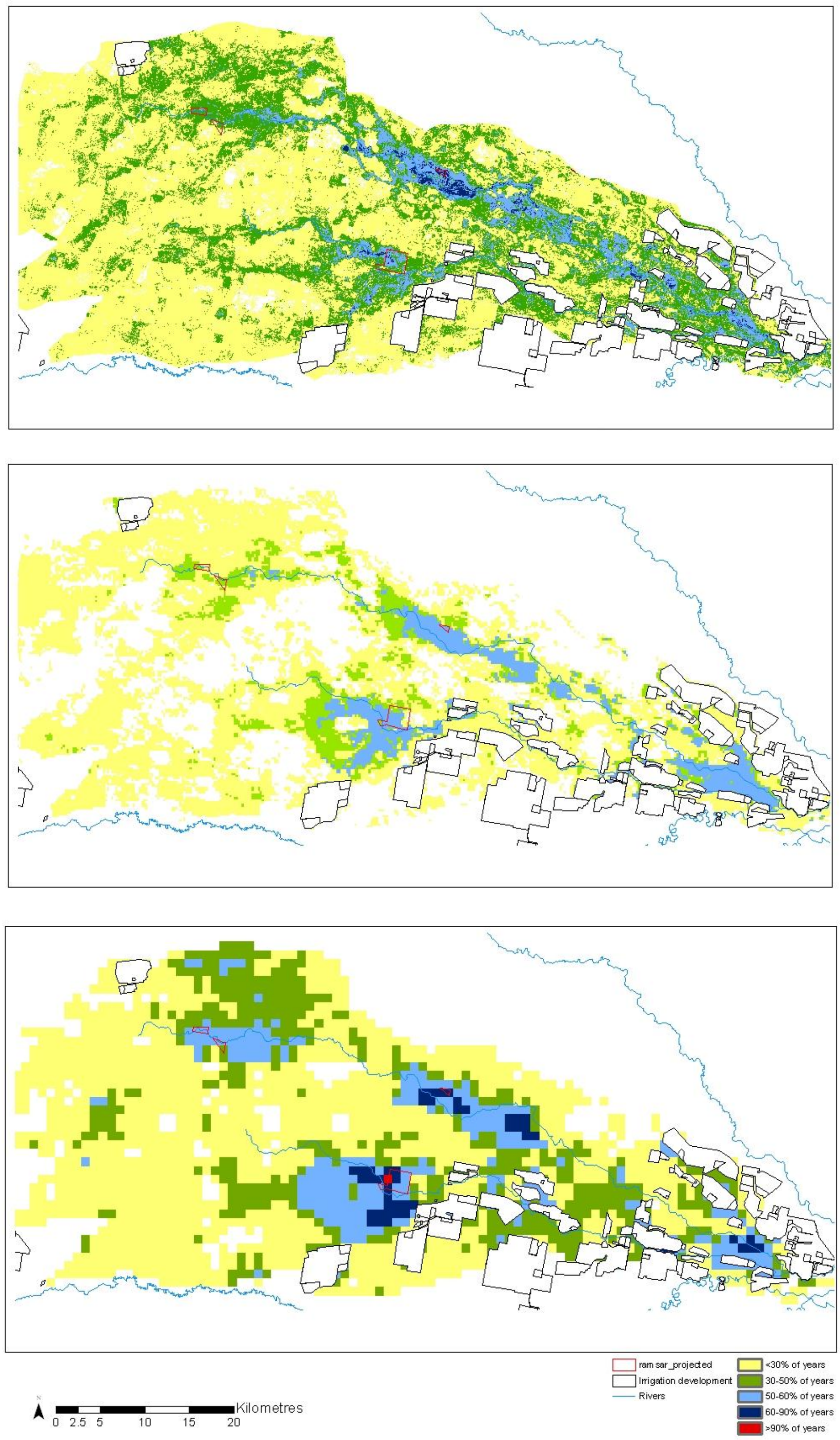

Figure 5.28: Estimated inundation and vegetation response frequency in the Gwydir wetlands from a) Landsat, b) Modis and c) AVHRR NDVI DT classification method. Note that no events with frequencies of >60% of years were analysed for Modis imagery.

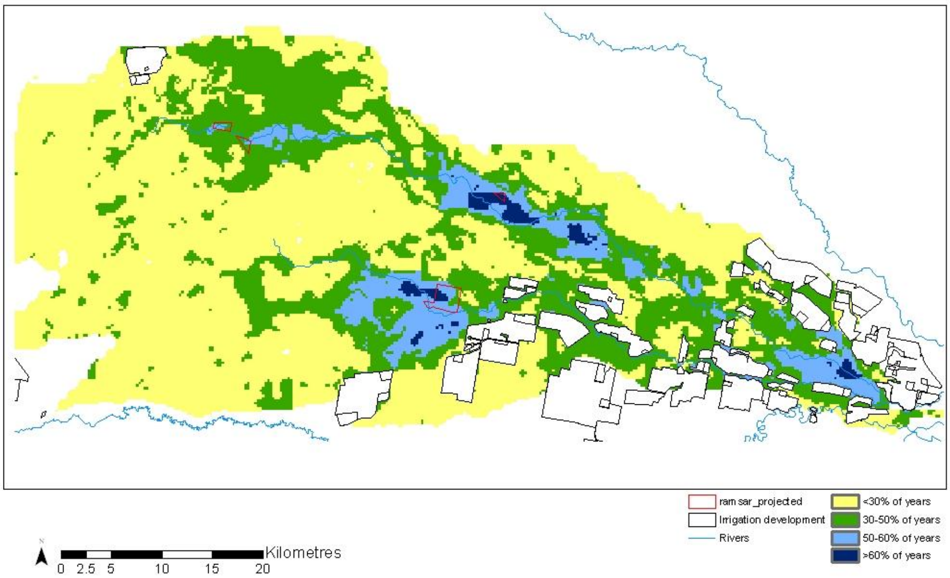

Figure 5.29: Areas connected at different flood frequencies using Landsat, Modis and AVHRR results at 250m^2 resolution. (FF4 is >60% of years, FF3 is 50-60% of years, FF2 is 30-50% of years and FF1 is <30% of years).

5.3.3.2 Connectivity (patches)

The combined results for all sensors and flood events provide a flood frequency classification for each 250m^2 pixel in the study area. Each pixel is assessed for its connection to each of its eight neighbours and each connected patch is then given a unique identifying number. A total of 259 discrete patches were identified ranging in size from single pixels (250m^2) to over 98 000ha. Many of the very small patches were located over the infrequently flooded (FF1) areas and were considered anomalies due to vegetation types, farm dams and other features. These patches are not critical to the analysis of flood behaviour and connectivity so they are combined to form a single large patch connecting the western floodplains. A large number of disconnected patches of FF3 were also found across the western floodplains that were not associated with wetland vegetation types. These were also combined for simplicity to produce the final node-network conceptualisation of the system that includes 17 discrete patches covering 92% of the system. The remaining 8% that is not included is made up of western, unflooded areas of cultivation and non-wetland vegetation types, and some small areas near Gwydir River at Brageen that were found to be unmapped irrigation development. The character of the patches and resulting landscape units are discussed in more detail in Section 5.3.3.3.

The node-network diagram of the Gwydir wetlands (Figure 5.30) forms the basis for the water balance model developed in Chapter 7. The system is first defined along the Gingham Channel (yellow) and the Lower Gwydir River (blue) with reaches separated based on flow gauging locations. In most cases one reach flows directly into the next, however some reaches are indirect (such as downstream of 418066 on the Gwydir channel where the flows distribute into a number of bore drains and undefined floodrunners). Patches are associated with either the reaches directly (as in the FF4_66 patch which is in direct connection to the Gingham Channel) or indirectly (where there is no apparent connection to the channel as in FF4_81), or are connected to other patches (such as FF3_50). Vegetation associations within these patches are described in Section 5.3.3.3. As can be seen, the most frequently flooded areas (FF4) are connected directly to the channel reaches in most cases with less frequently flooded areas generally connected to more frequently flooded areas (i.e. FF4 flow on to FF3). The FF2_6 patch connects many of the more frequently flooded areas of both the Gingham and Gwydir channels while the FF1 patches are largely disconnected due to clearing, cultivation and irrigation development.

5.3.3.3 Landscape units

Overlaying the frequency of flood/response, connectivity and vegetation map (figure 5.3) provides a template for identifying relatively homogenous areas of the landscape with respect to their flood and vegetation response behaviour. The areas flooded and responding to small and moderately small events (Figure 5.31a) cover an area of 2253ha in 29 discrete patches ranging in size from 855ha to 2.5ha. Most of this area contains water dependent vegetation such as spike rush (74%), river red gum associations (13%) and marsh clubrush (5%). A total of 1677ha (74%) of spike rush communities is found in 15 discrete patches. The largest patch of 992ha (4_66) is near the Goddards Lease Ramsar site, and is connected to the Gingham Channel and numerous low flow pathways as it extends for 7-8km along the channel and to a width of 2.2km at its widest. This patch is also contiguous to a 23ha patch of river cooba/lignum association. Approximately 3km upstream of this patch is a contained patch of spikerush (4_81) 290ha in size. This patch appears disconnected from the Gingham Channel or surrounding frequently flooded areas and is surrounded by cultivated areas. A small channel is visible on higher resolution Spot imagery that indicates a possible connection to the channel. Further on-ground investigation would be required to confirm the vegetation type and connectivity. In the Gwydir Raft on the eastern side of the floodplain is a large area (276ha) of coolibah/river red gum which is strongly connected to the Gingham and Lower Gwydir Channels (4_227). On the lower Gwydir a large 302ha patch (4_127) of spikerush is frequently flooded near the Old Dromana Ramsar site and surrounds a large marsh clubrush patch (119ha). An 83ha patch of spike rush (4_188) is also located off the channel to the south west along a flood prone area that has some discontinuous patches of frequently flooded river cooba/lignum, marsh clubrush and bordering cleared cultivated land.

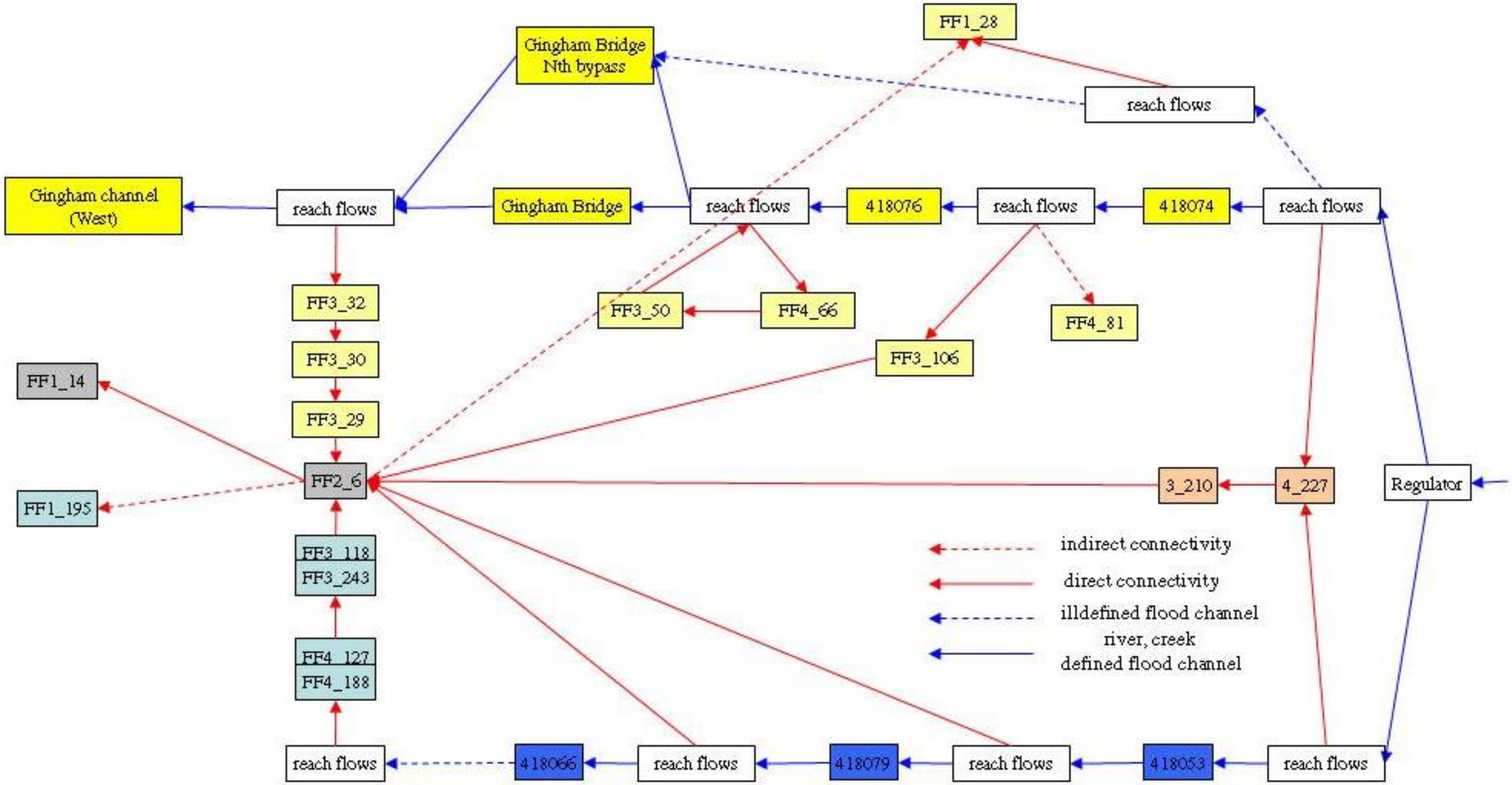

Figure 5.30: Node-link conceptualisation of flood frequency and connectivity of the Gwydir wetlands based on assessment of flooding 1988-2005. Yellow boxes are channels and patches associated with the Gingham Channel while blue boxes are associated with the Lower Gwydir. Orange and grey patches occur over both systems. Solid lines indicated direct connectivity with dashed lines showing indirect or ill-defined connections.

Moderate sized events (Figure 5.31b) result in more contiguous response areas covering more than 16 000ha and ranging in patch sizes from 5 642ha to 2.5ha. The three largest patches are extensions of the more frequently inundated areas. The largest connected patch is located on the Lower Gwydir including the Old Dromana Ramsar site extending west and south west (3_118). This patch includes a large central area of spike rush (2 321ha), marsh clubrush (188ha) and river cooba/lignum (216ha) surrounded by coolibah woodlands (1768ha). There is also a significant area of cleared cultivated land that responds to flooding (1088ha) along with small areas of native grasslands and poplar box associations on the fringes. Another large continuous patch (3_50) is found on the Gingham Channel near the Goddards Ramsar site. It extends westward along the channel comprising a central area of spike rush (1627ha) and connects the areas associated with more frequent events. This patch also contains large areas of coolibah woodlands (1452ha) and river cooba/lignum 321ha) with some smaller areas of cultivated land, belah, poplar box and river redgum associations on the fringes. A large area of river red gum association (1617ha) and smaller areas of coolibah woodland, as well as some cultivated land, also responds to these events in the vicinity of the Gwydir Raft area of the Gingham and Lower Gwydir (3_210). Further west on the Gingham Channel, three patches (3_29, 3_30 and 3_32) are slightly disconnected by cultivated land but form an almost continuous 14km strip of spikerush along the channel itself, spreading to a width of two kilometres at its widest point in the vicinity of the Crinolyn Ramsar site.

Areas associated with moderately large events (Figure 5.31c) form an almost continuous patch over 55 000ha in size. It extends from the Raft area in the east, westward along the Gingham and Gwydir Channels (2_6), connecting the more frequently inundated patches. Much of this area is cleared (24 737ha) or contains coolibah woodlands (12 997ha) although there are also significant areas of spikerush (3062ha) and river cooba/lignum (2699ha).

Most disconnected patches are cultivated land with some patches of coolibah woodland. These are unlikely to be significant wetland areas and are excluded from subsequent analysis (i.e. 2_26, 2_36 and 2_84 in Figure 5.31).

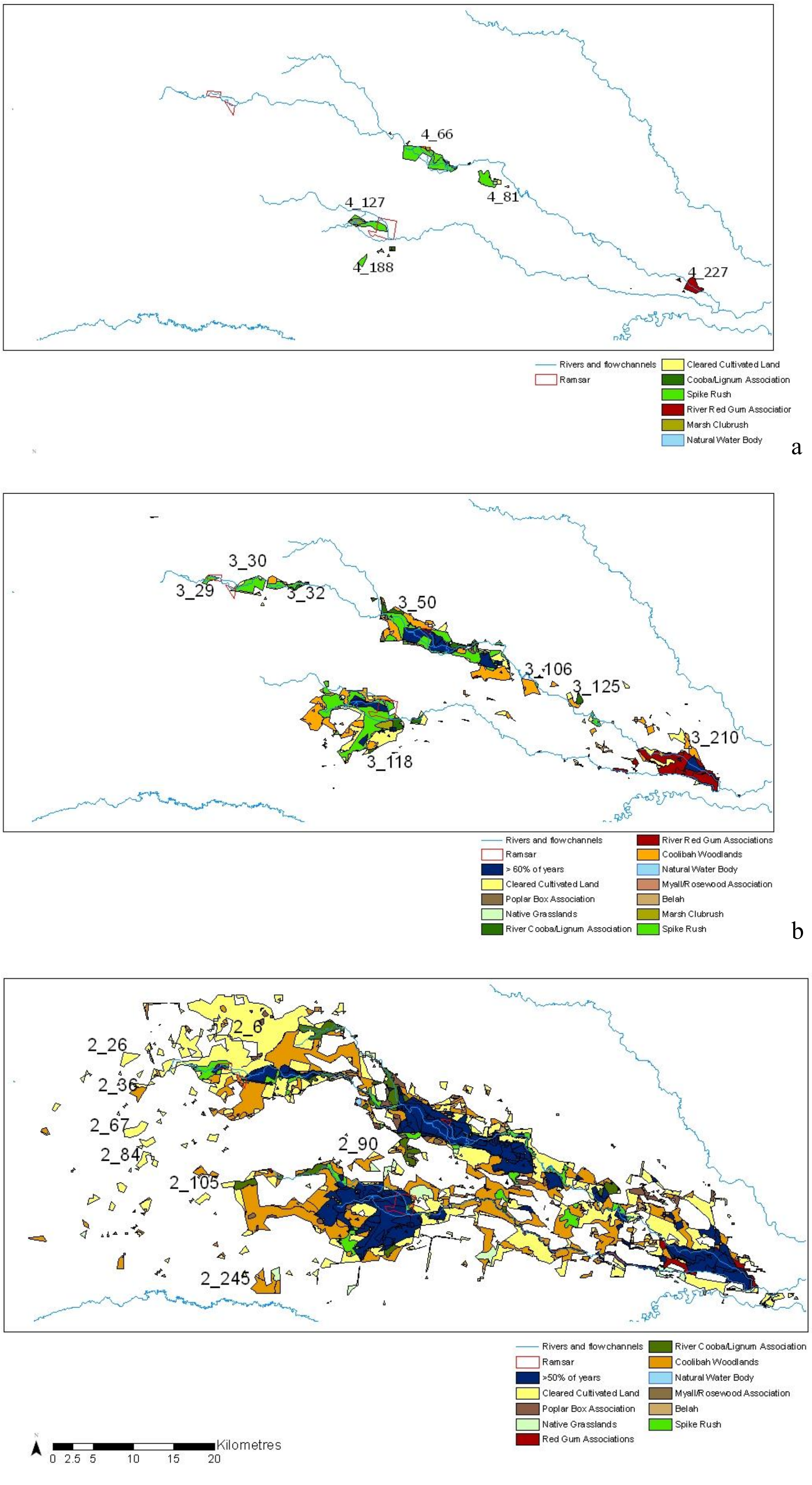

Figure 5.31: Patches associated with event size and vegetation: a) small to moderately small sized events (more than 60% of years), b) moderate sized events (50-60% of years) and c) moderate large events (30-50% of years).

Figure 5.32 shows the distribution of vegetation communities by event size. Marsh clubrush is associated with areas responding to small to moderate flood events. The majority of spikerush and river redgum associations were also found in areas responding to small to moderate events occurring in >50% of years. Interestingly the shrub dominated wetlands (lignum/river cooba) were most commonly associated with the areas flooded 30-50% of the time with only around 20% of this association flooding more than 50% of the time. This shrub dominated wetland is an important nesting habitat for colonial nesting waterbirds in core wetland areas where depth and duration of flooding can sustain breeding events. Lignum can tolerate prolonged flooding and drying and has been found to dominate floodplain areas inundated over frequencies ranging from 1 in 2 years to less than 1 in 10 years (Capon *et al.*, 2009). The tree and shrub dominated floodplain communities such as coolibah, belah, myall/rosewood and poplar box were more commonly associated with the large events. Native grasslands were more commonly found in the areas responding to events occurring <50% of years. The analysis of flood frequency and connectivity here provides a more integrated perspective of the system, indeed a template that matches well with existing knowledge and distribution of vegetation associations in relation to flood frequency as discussed in Sections 2.3.1 and 2.4.4 (Brock and Casanova, 1997; Capon, 2005; Casanova and Brock, 2000; Roberts and Marston, 2000). With such a template it is possible to build a predictive capability of vegetation productivity response that can be used in conjunction with the node-network water balance model.

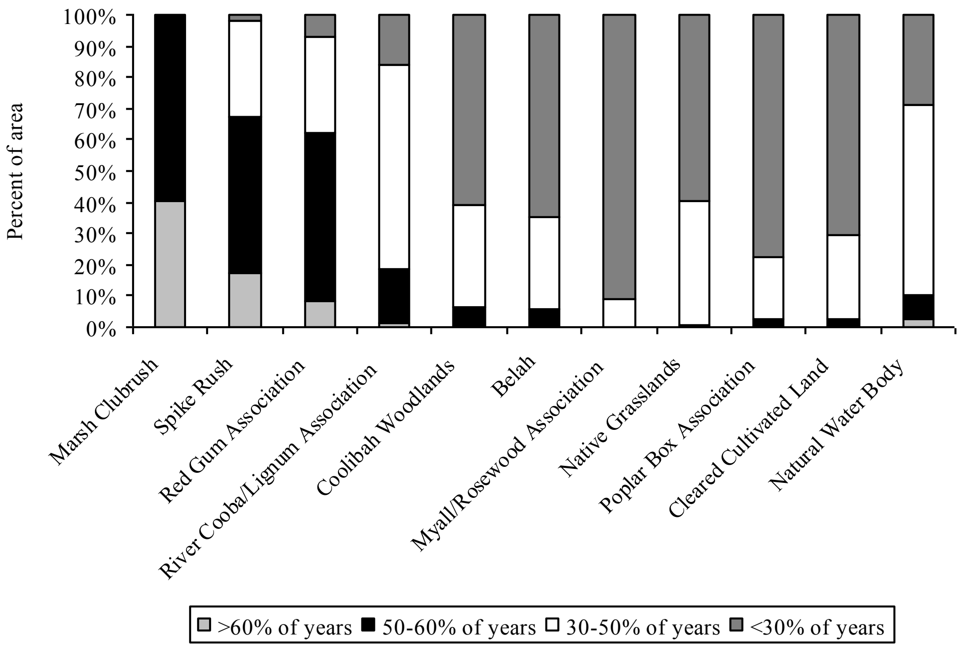

Figure 5.32: Association between mapped vegetation communities and frequency of flooding.

Using the results of this chapter, 42 landscape units were identified (Table 5.22) and mapped for the vegetation response analysis in Chapter 6. The largest units covering 90% of the area of interest as well as a number of smaller units of wetland vegetation communities in the more frequently flooded are included. Therefore, for each patch in the node-network conceptual model, one or more landscape units of particular vegetation community structure occur.

Table 5.22: Identified homogenous landscape units for vegetation response analysis. Patch ID indicates the flood frequency class and the unique connected patch number. Elements are discrete vegetation polygons within a single flood patch.

Patch ID	Vegetation type	Size (ha)	no. elements (tolerance 1km)
2_6	Cleared cultivated	24 737	> 10
2_6	coolibah woodlands	19 997	> 10
2_6	spikerush	3 062	> 10
2_6	river cooba / lignum	2 699	> 10
1_195	coolibah woodlands	2 512	3
3_118	spikerush	2 321	1
3_118	coolibah woodlands	1 768	3
2_6	poplar box	1 677	> 10
3_50	spikerush	1 627	1
3_210	coolibah/river redgum assn (dense)	1 617	1
3_50	coolibah woodlands	1 452	6
2_6	Native Grasslands	1 157	6
3_118	Cleared cultivated	1 088	3
3_210	coolibah/river redgum assn	1 083	7
4_66	spikerush	992	1
1_177	coolibah woodlands	822	1
1_195	Native Grasslands	635	5
2_245	coolibah woodlands	593	1
3_30	spikerush	471	1
3_50	Cleared cultivated	408	5
1_14	river cooba / lignum	381	1
2_6	myall/rosewood	367	7
2_6	belah	342	>10
3_50	river cooba / lignum	321	2
3_106	coolibah woodlands	316	1
2_90	coolibah woodlands	307	1
4_127	spikerush	302	1
4_81	spikerush	290	1
Other significant patches			
3_32	river cooba / lignum	29	1
4_66	river cooba / lignum	23	1
3_125	river cooba / lignum	82	1
3_155	river cooba / lignum	69	1
4_176	river cooba / lignum	20	1
3_118	river cooba / lignum	216	1
3_29	spikerush	103	1
3_32	spikerush	267	1
3_154	spikerush	97	1
4_188	spikerush	83	1
3_118	marsh clubrush	188	1
4_127	marsh clubrush	120	1
4_176	marsh clubrush	9	1
4_227	coolibah/river redgum assn (dense)	276	1
Total		*74 926*	*92%*

5.4 Discussion

This chapter firstly analysed the rainfall and inflow data and extracted a range of metrics that can be used to describe a flood event. Other studies have used peak daily flow to determine the commence-to-flow level of wetlands (Shaikh *et al*., 2001), mean monthly water level or flow (Andersson *et al*., 2003; Sakamoto *et al*., 2007; Zoffoli *et al*., 2008) and average monthly rainfall (Posse *et al*., 2005; Sakamoto *et al*., 2007) or antecedent flows at a range of intervals (Kingsford and Thomas, 2002) to assess inundation and vegetation response relationships. In the Gwydir wetlands the 40-day inflow, which incorporates the peak and recession inflows, and peak rainfall were found to best differentiate between flood events. Antecedent inflows, antecedent rainfall and days since last flooding were also used to describe the flood events but were not found to be significant in any subsequent multiple linear regression modelling relating event metrics to inundated area. The choice of a 40-day flow period requires an extra computational step with each flood peak identified and the total 40-day flow calculated (rather than a reliance on the monthly flow data available in flow data archives). The highly variable timing of flood events compared to seasonal flooding of systems such as the Okavango (Gumbricht *et al*. 2004; McCarthy *et al.* 2003), and the distributed floodplain nature of the Gwydir wetlands as compared to small discrete wetlands connected to the main channel such as the Lower Darling wetlands (Shaikh *et al.* 2001), makes this necessary to adequately describe each event.

As discussed in Section 2.5, there are a number of remote sensing methods used to assess inundated area but most are best suited to open water flooding and do not provide for the productivity response to flooding. The Gwydir wetlands present a challenge of shallow expanses of floodwater that are quickly covered by emergent vegetation. Using a time-series sequence of NDVI allows the open water extent to be mapped as well as the high vigour vegetation response in the months following inundation due to irregular flood events. Multi-spectral approaches using Landsat imagery have been found to be useful in mapping inundation at regular (seasonal) intervals in difficult floodplain environments such as the Macquarie Marshes in Australia (Thomas *et al.*, in press) and the Okavango Delta in Botswana (McCarthy, 2002). Landsat imagery is useful for this application with good spatial resolution but the irregular flood cycles and timing, and the high complexity of the Gwydir wetlands landscape limited its application in this thesis. At the commencement of this research Landsat imagery was also prohibitively expensive for time series analysis within the scope of a PhD. In comparison, the Modis and AVHRR data are freely available at daily time steps over long periods of time. The spectral, spatial and temporal resolution of remote sensing imagery is constantly increasing (Mackay *et al.*, 2009) and it is only very recently that the Landsat archive has been freely available making it a much more useful research tool. Further analysis of the Landsat archive may be warranted to investigate the inundation dynamics of the Gwydir wetlands at finer spatial scales but is outside the scope of this research that is focussed on developing a node-network conceptual model for application to water balance modelling. Similarly the recently acquired LIDAR imagery and associated hydrodynamic analysis for the Gwydir Wetlands will also enhance the detail and level of understanding of the system but was unavailable for this research.

There is inherent uncertainty in any assessment and attempts have been made to include this in the results for the total inundated area of the Gwydir wetlands. This uncertainty is rarely presented in other remote sensing analysis of inundated area regardless of the method used; nor is it presented in maps of flood extent produced in the Gwydir through ground level field investigation or aerial reconnaissance. Although methods for assessing accuracy of geographic classification are well developed (Richards and Jia, 1999), robust data are required to test them. This type of data are not generally available for historic analysis of inundation making detailed error assessment difficult. In the Macquarie Marshes, validation was performed against Landowner records of flooding and against other remotely sensed flood analysis (Thomas *et al.*, in press) while other studies have relied on visual checks of the images (Apan and Sternes, 2006; Gumbricht *et al.*, 2004b).

In the Gwydir, a more iterative approach was taken with results compared to flood maps but also to the flow and rainfall. In the Cumbung Swamp, Lachlan Valley, inundated area was correlated with peak flow and net rainfall (r2 of 0.90) while high NDVI (Landsat MSS) was also highly correlated with flow (r2=0.88) (Shaikh *et al.*, 1998). In the Macquarie Marshes, antecedent flow of 30, 90 and 180 days was significantly correlated with area inundated (r2 of 0.76, 0.66 and 0.77 respectively) (Thomas *et al.*, in press). Correlations between 40-day flow, high NDVI and inundated areas were significant for Landsat, Modis and AVHRR in this study (r2 of 0.69, 0.92 and 0.70 respectively). In non-wetland environments, NDVI was found to be significantly correlated with rainfall (Al-Bakri and Suleiman, 2004) for 10-day and monthly as well as seasonal rainfall and end of season NDVI. Discriminating between rainfed and flood response therefore requires an understanding of how the peak NDVI values differ over the floodplain. Chapter 6 provides some of this understanding; however the classification presented here found that inundated area was not significantly correlated with rainfall in the Gwydir wetlands. An exception occurred when heavy local rainfall occurred in addition to large inflows.

Although the relationship between flow and total inundated area is of interest, the prime purpose of this assessment is to develop a node-network conceptual model of the lower Gwydir in order to model inundation and vegetation response at the landscape and patch scale. By combining the information from multiple sensors and a range of floods, the frequency of flooding for each 250m pixel can be estimated and connected patches identified. The frequency classes encompass relatively broad flow ranges due to the level of uncertainty in the flood assessments. Assigning more detailed frequency classes is possible but does not necessarily improve subsequent water balance modelling. In the Okavango delta, up to 23 units were used initially with the expectation that better representation of the spatial heterogeneity in the system would result in better flood modelling (Wolski *et al.*, 2006). Preliminary runs found that this detailed model performed only slightly better but was over-parameterised and was reduced to just 9 spatial units on the basis of similarities and differences in long-term inundation variation. From the initial identification of over 250 patches in the Gwydir wetlands, the system could be reduced to 17 discrete patches that each represented a relatively homogenous area in relation to flood frequency and connectivity. This is still significantly more than used for the Okavango that could be argued to be a more complex system. The Gwydir is, however, highly modified with the floodplain disconnected due to irrigation infrastructure, land clearing and cropping practices. The system also contains relatively small areas of frequently flooded wetlands amongst less frequently inundated floodplains. These discrete areas need to be recognised within the node-network model. In practicality, the connected patches identified in the Gwydir wetlands are similar to the concept of hydrogeomorphic units (HGMU) (Maltby *et al.* 2009) used in wetland classification in Europe. HGMUs are considered to by functionally homogenous landscape units with respect to their hydrogeomorphology, hydrology and soils. Vegetation is not used in the definition of HGMUs due the dependence on land use and management however the hydrogeomorphology and hydrological linkages across the floodplain in the Gwydir wetlands has also been altered by landuse through the advent of laser levelling, levee bank development and bore drain construction. For these reasons the functioning of the landscape with regards to vegetation is also considered important in the Gwydir and hence the basic landscape unit includes the vegetation.

As discussed in Zoffoli *et al.* (2008) wetland functioning can refer to both the hydrological behaviour of the wetland and the annual greenness cycle of vegetation. Taking the patch analysis a step further, each patch is subdivided into landscape units of similar flood frequency and vegetation association. This provides a template for further analysis of vegetation response to flooding in Chapter 6. The vegetation associations may also influence the accuracy of inundated area using the time-series NDVI decision tree approach taken. For some associations, such as the river redgum forest of the Gwydir Raft, dense evergreen canopy cover precludes the remotely sensed detection of open water inundation while the vigour of the canopy may not reach the high values of the macrophyte wetlands. Variable response depending on antecedent conditions may also influence the assessment. Macrophyte species have been found to increase in biomass if exposed to regular periods of inundation and drying (Brock and Casanova, 1997; Nielsen and Chick, 1997) and these wetting/drying cycles are also thought to enhance nutrient release. Therefore, areas may have greater vegetation vigour for floods after dry periods compared to flooding that occurs continuously or without sufficient time between for these drying processes to occur.

5.5 Conclusions

Flood events are highly variable in the Gwydir wetlands with daily inflow peaks of up to 112GL recorded during the study period. These flood events are best described by inflows over a 40-day period coupled with 90-day antecedent flows, days since last event, peak rainfall and antecedent rainfall. Since the completion of Copeton Dam, 40-day inflow of 100GL is exceeded in 5 out of every 10 years.

As for many expansive floodplain and wetland systems, the landscape complexity, rapid vegetation response, canopy cover and shallow water depths make flood extent mapping problematic. By coupling open water and temporal vegetation response using NDVI satellite image products, the inundated extent relevant to vegetation productivity can be estimated for a range of flood events. The NDVI product provides a relatively robust measure of landscape productivity through time and is useful for temporal analysis but the selection of appropriate threshold of high vegetation productivity response is critical. For both Modis and Landsat, NDVI of 0.75 provided the best measure of flood related vegetation response, while for AVHRR a lower threshold of 0.52 was most appropriate. Uncertainty due to the thresholds chosen is variable.

Combining the estimated flood extent for a range of flood frequencies and connectivity analysis provides a method of classifying the landscape for water balance modelling. The most frequently flooded areas, responding in more than 60% of years, only cover a relatively small area of the floodplain. The 2730ha includes the most permanent wetland areas and is associated with water dependent macrophyte vegetation such as marsh clubrush and spikerush as well as river redgum communities. These areas are in direct connection to the Gingham Channel or Lower Gwydir River. Surrounding and connecting these areas are slightly less frequently flooded patches totalling over 20 000ha and responding to events in the order of 50 to 100GL. Only in events greater than 100GL do broader areas of floodplain become connected with secondary floodways occurring between the Gingham Channel and Lower Gwydir River.

Although remote sensing has been used in a large number of wetland systems to map inundation this is not generally applied to developing node-network conceptual models of the system. In this chapter, inundation mapping of a range of flood events has been analysed to produce a node-network conceptual model of the Gwydir Wetlands. This model provides a framework for the further development of a water balance model in Chapter 7. The inundation mapping has also been linked to vegetation community structure to provide the template for vegetation response to flooding in the following chapter.

Chapter 6: Vegetation response

6.1 Introduction

Phenological cycles of green-up, maturity, senescence and dormancy are controlled primarily by temperature and soil moisture (Zhang *et al.*, 2001) and can be seen in the normalised difference vegetation index (NDVI) time series (Figure 4.2). As discussed in Chapter 2, NDVI is directly related to the fraction of photosynthetically active radiation (fPAR) and is a good indicator of primary productivity (Box *et al.*, 1989; Glenn *et al.*, 2008; Myneni and Williams, 1994; Pettorelli *et al.*, 2005; Posse *et al.*, 2005). At regional scales, primary productivity is mainly correlated with precipitation but is also influenced by temperature, soil fertility, disturbance, successional status and soil water capacity (Posse *et al.*, 2005; Scanlon *et al.*, 2002). Local topographic features can influence the soil properties and water availability at small spatial scales (Posse *et al.*, 2005).

As discussed briefly in Chapter 4, this chapter uses time series of fPAR (calculated from NDVI) to assess the phenological attributes of each landscape unit defined in Chapter 5. In floodplain wetlands where productivity is linked to the flood-pulse, many of the phenological attributes can be linked to the characteristics of the flood assessment described in Chapter 5. A distinct pattern in the temporal fPAR response may occur in response to the flooding, as compared to adjacent landscapes that respond to other seasonal climatic conditions including climate driven soil moisture (as compared to inundation driven soil moisture).

This chapter, therefore, aims to characterise the vegetation productivity response of each landscape unit to inundation. The relationship between vegetation productivity, as measured by the fPAR time-series, inflow and climate, is analysed with the objective of developing multiple linear regression (MLR) models of fPAR response for each landscape unit. As overviewed in Chapter 4, the outcomes from this Chapter can be combined with the node-network conceptual model in Chapter 5 to develop an Inundation and Vegetation Response Model (IVRM) for the Gwydir wetlands in Chapter 7.

6.2 Methods

For each landscape unit identified in Chapter 5 the time series NDVI is extracted and converted to fPAR. The 16-day maximum value composite (MVC) values from both AVHRR and Modis are used to create a time series from 1992 to 2007 covering a range of flood events. Climate data (rainfall and evaporation) is used to develop a soil moisture index and, along with inflow at a variety of time steps, all are tested for significance in driving fPAR response. The data analysis of fPAR response includes both exploratory analysis to understand the patterns of response, as well as multiple linear regression analysis to derive quantitative models of this response. The analysis concentrates on the more frequently flooded, core wetland areas, but results for all landscape units are included. An overview of the analysis flow in this chapter is shown in Figure 6.1.

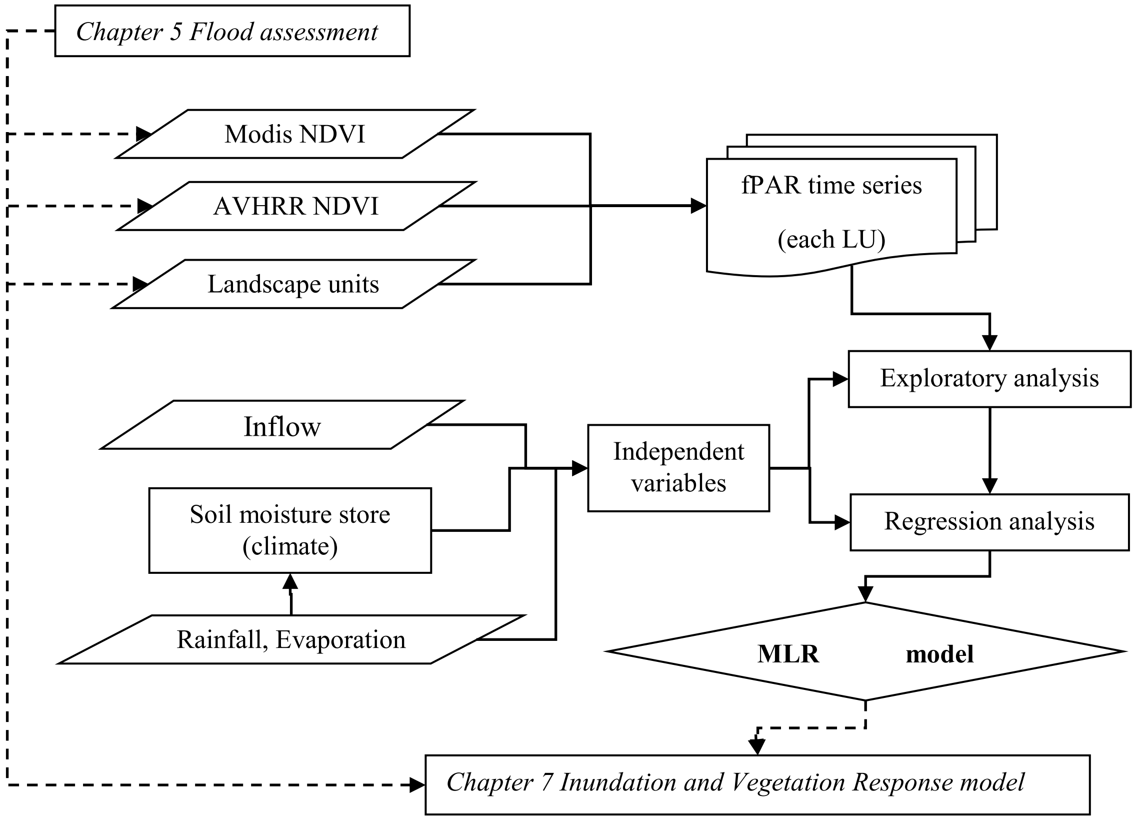

Figure 6.1: Flow chart of vegetation response (fPAR) analysis in this chapter and linkages (dotted lines) with Chapters 5 and 7.

6.2.1 Landscape units and time series NDVI

A total of 42 landscape units (LU) are identified in Chapter 4 covering 92% of the study area. Each LU has a unique combination of flood frequency (FF), patch (connected flood areas) and vegetation community (for example 4_66spikerush is FF 4, patch 66 and mapped as spikerush association). For each pixel within each LU, NDVI is extracted for the Modis and AVHRR data records. As used in previous chapters, the data are comprised of 16-day maximum value composite (MVC) periods with 23 periods per year. Modis at 250m^2 covering the period 2000-2008, while AVHRR is a nominal 1km^2 spatial resolution from 1992 through to 2005.

Data were extracted from a remote sensing software package (ENVI) and imported to spreadsheet format (Excel) for manual data checking. Following manual clean up NDVI were converted to fPAR and the mean fPAR for each LU for each MVC period was calculated for both Modis and AVHRR data. Converting the raw NDVI values to fPAR allows better comparison between different sensors and represents a more consistent indicator of the greening response (Berry and Roderick, 2002; Roderick *et al.*, 1999).Unlike the previous chapter where the main purpose of the analysis was to identify flooded and responsive areas using NDVI, this chapter models the vegetation productivity (as fPAR) response to inflow and climate.

6.2.1.1 fPAR Conversion

The NDVI data are converted to fPAR using the methods proposed by Roderick *et al.* (1999) and Berry and Roderick (2002). Equation 6.1 describes the conversion of NDVI values (V) to fPAR (F). Roderick *et al.* (1999) assumed that very low NDVI values are likely to be cloud contaminated, however they can often be associated with open water flooding. The NDVI values were reviewed for cloud contamination and other erroneous data in Chapter 4 and any retained negative values are assumed to be flooded pixels and, for the purpose of the vegetation assessment, are set to 0. Soil-adjustments (Berry and Roderick 2002) are then applied (Equation 6.2). Parameters used in the equation are determined from the time series Modis and AVHRR data sets such that V_{max} is the 95th percentile of maximum pixel NDVI values and F_{max} is the theoretic maximum fPAR proposed by Roderick *et al.*(1999). Table 6.1 shows the parameter values used to convert the Modis and AVHRR NDVI values to fPAR.

$$F_i = V((F_{\max} - F_{\min})/(V_{\max} - V_{\min})) + F_{\min}$$

where
$F = fPAR$
$V = NDVI$

Equation 6.1

$$F_v = (F_i - V_{soil})/(F_{\max} - V_{soil})$$

Equation 6.2

Table 6.1: Parameters used to convert Modis and AVHRR NDVI values to fPAR

	Description	Modis	AVHRR
Vmax	95%ile of pixel maximum NDVI values	0.9624	0.7614
Vmin	Minimum NDVI observed*	0	0
Fmax	theoretical maximum fPAR	0.95	0.95
Fmin	theoretical minimum fPAR	0	0
Vsoil	Bare soil estimate NDVI	0.15	0

* NDVI values of less than 0 are observed in areas of inundation. These have been set to 0 for the vegetation analysis.

6.2.1.2 Time series fPAR

The Modis fPAR is used where available and supplemented using the AVHRR fPAR to produce a nearly continuous time series from 1992-2008. The AVHRR data may slightly underestimate the maximum fPAR due to the difference in the sensor bandwidths and spatial resolution, however for exploratory and comparison purposes it does provide a reasonable extension to the Modis data (as discussed in section 2.5). For more detailed analysis (MLR) or benchmarking purposes, the Modis fPAR is used.

6.2.2 Soil moisture and inflows

The primary aim of this chapter is to determine the relationship between soil moisture derived from rainfall and evapotranspiration processes, inflow and vegetation response. Two indicators of climate are used. Rainfall and pan evaporation (Et) from the Moree BoM station are aggregated to the 16-day MVC periods. Climate driven soil moisture status (SMS) is modelled from the Gwydir ICMS model (Powell, 2005). The SMS is based on rainfall, evaporation and soil characteristics to give a simple index of soil moisture status from 0 (dry) to one (saturated) (Figure 6.2). The soil water is considered saturated when at field capacity and dry when at wilting point. Field capacity is estimated initially at 250mm for cracking clay soils (Humphreys and Edraki, 2003). Evapotranspiration (Et) loss is proportional to soil moisture with Et approximating pan evaporation at field capacity down to 0 at wilting point (Apan and Sternes, 2006; Humphreys and Edraki, 2003; Murphy and Lodge, 2001).

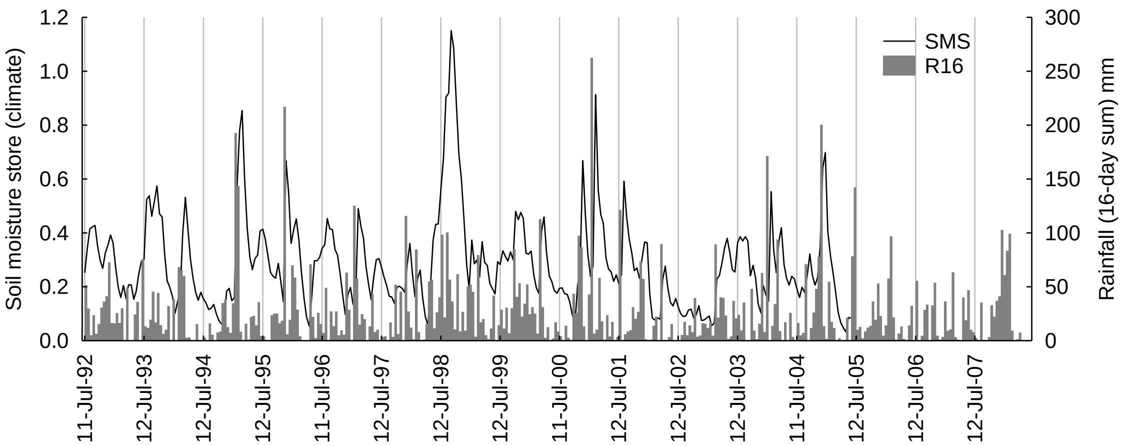

Figure 6.2: Climate derived soil moisture status for the Lower Gwydir (based on BoM rainfall and pan Et records from Moree) and 16-day rainfall. Note the SMS is not available for the period 2005-2007.

The fPAR response analysis is based primarily on inflows at Gwydir River at Yarraman. Although there are closer gauges to some of the LUs, the measurement of large flows becomes problematic as discussed in previous chapters (i.e. Section 3.4). As the flows move westward through the Gwydir wetlands, the channel dimensions become smaller and bankful capacity diminishes. In large flows much of the water spreads out across the floodplain and the relationships between water depth and flow become more difficult to determine. The Gwydir River at Yarraman gauge has a large channel cross section and can measure flows in excess of 50 000ML/day with good reliability. The results in Chapter 5 suggest that a 40-day inflow best describes the flood events in the Gwydir. Vegetation response occurs over a period of time, so lag effects of inflow are important. For this reason, other inflow periods are tested including the cumulative 16-day inflow that coincides with the fPAR MVC interval.

The flow data are skewed and a log transformation is used to normalise the datasets to ensure that the normality assumption underlying the multiple regression analysis is met. Lags of up to a total of 200 days antecedent flow are included in the analysis but only 120 days was found to be significant. The resultant data sets for analysis are shown in Figure 6.3. Soil moisture store and log flow are significantly correlated for the 40-day inflow (Q40) and the antecedent 40-day inflow ($Q40_{-1}$) ($P<0.05$) (Figure 6.4).

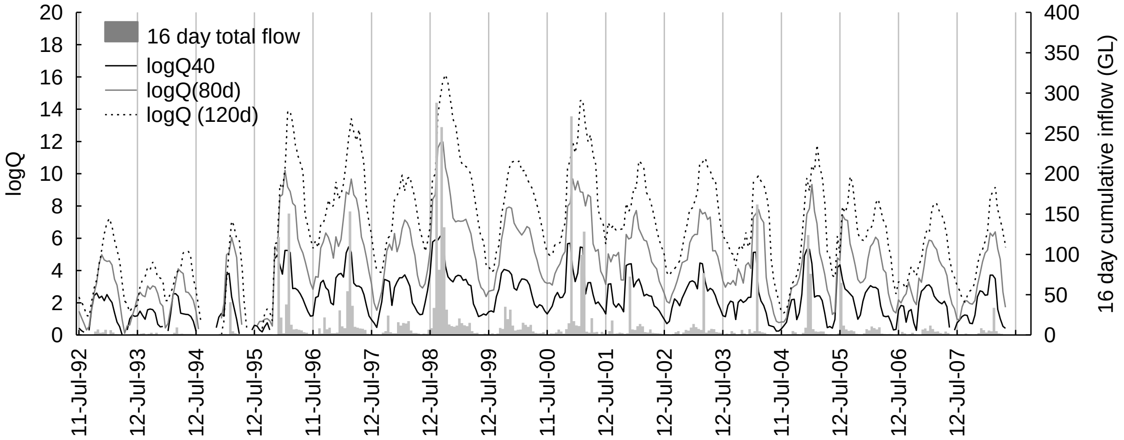

Figure 6.3: Inflow at Gwydir River at Yarraman gauge 1992-2008.

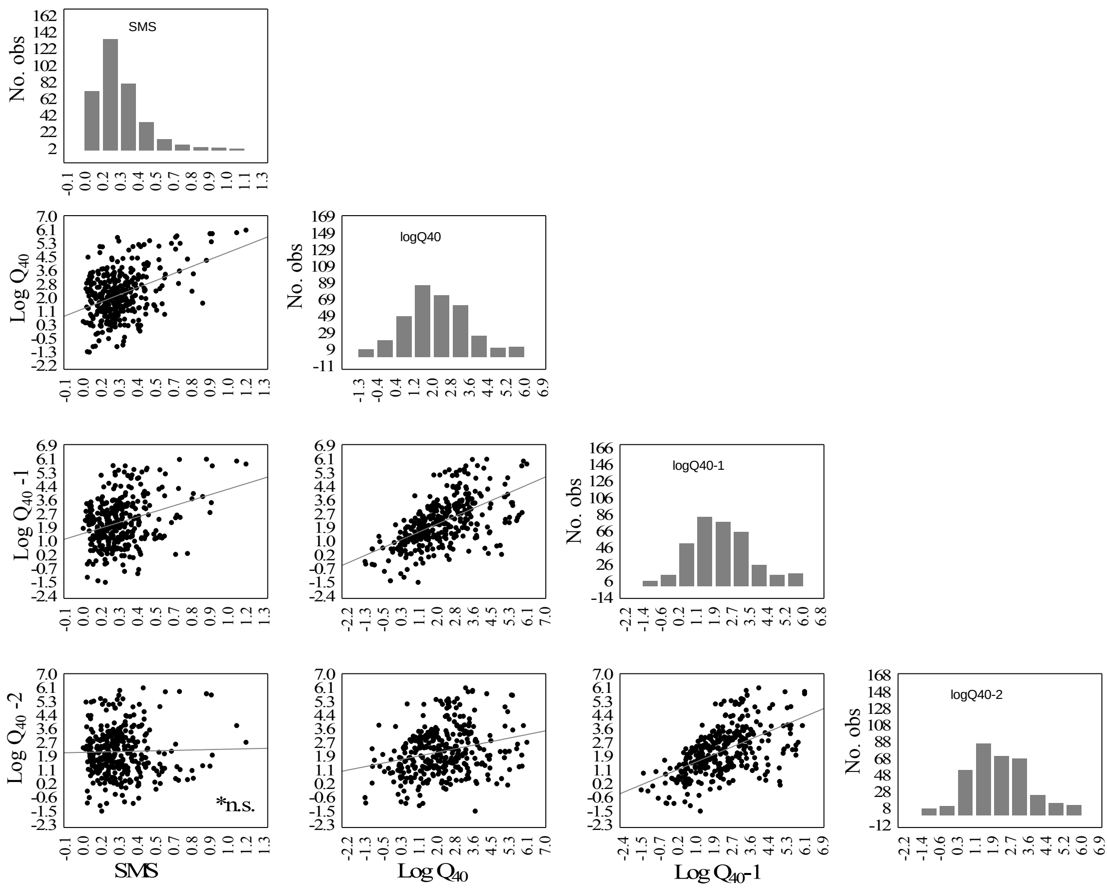

Figure 6.4: Scatterplots and histograms of soil moisture store and log flow at Gwydir River at Yarraman. All correlations are significant at $p<0.05$ with the exception of SMS and logQ_{40}-2 which is not significant.

6.2.3 Data Analysis

6.2.3.1 Exploratory analysis

The mean fPAR values for each LU, flood frequency, patch and vegetation community identified in Chapter 5 are compared using a simple univariate analysis of variance ANOVA in Statistica (StatSoft Inc, 2009) to determine if the population means are significantly different. Scheffe's Test is used in a post-hoc analysis to identify homogenous groups (StatSoft Inc, 2009). Temporal fPAR patterns are compared between different LUs using the time series fPAR data. The more frequently flooded wetlands are the primary focus as these areas are more likely to be influenced by water management activities and the target of environmental watering strategies. . Average monthly fPAR for a range of LUs are compared to the monthly patterns for both flow and soil moisture. Typical phenology response to inundation is proposed for each LU using benchmark flood events.

6.2.3.2 Multiple Linear Regression

The fPAR response to climate driven soil moisture (SMS) and inflow is modelled using multiple linear regression (MLR). The intercept is included in the model and a range of independent variables including soil moisture and inflows at a range of lag intervals are assessed for significance in Statistica (StatSoft Inc, 2009) (Eq. 6.3). The models are developed using the Modis dataset for the period 2000-2005 and tested against the combined AVHRR and Modis fPAR dataset. The regression of order n (to be determined) is shown in Equation 6.3 below.

$$\begin{aligned}
&F_t = I + \beta_1 S_t + \beta_2 Q_t + \beta_3 Q_{t-1} + \beta_4 Q_{t-2} + \ldots\ldots + \beta_n Q_{t-(n-2)} + \varepsilon_t \\
&where \\
&F_t = fPAR\ at\ time\ step\ t \\
&I = intercept \\
&S_t = soil\ moisture\ store(SMS)\ at\ time\ step\ t \\
&Q_t = inflow\ at\ time\ step\ t \\
&\varepsilon_t = model\ residual\ at\ time\ step\ t\ (\varepsilon\ ind.\ distribution) \\
&\beta_i = parameters
\end{aligned}$$

Equation 6.3

The significant variables in the MLR model are also plotted to provide a visualization of the relationships. A surface is fitted to the XYZ coordinate data using the bicubic spline smoothing procedure (StatSoft Inc, 2009). In these surface plots, X and Y are the totals for the significant inflow lags and soil moisture variables respectively while Z is the dependent fPAR values.

6.3 Results

A total of 42 LUs were identified in Chapter 4 for analysis of vegetation response to flooding. Of these 38 have good AVHRR and Modis time series with the remaining four LUs being too small or of a shape that did not provide sufficient separation from surrounding LUs at the resolution of the satellite imagery.

6.3.1 fPAR Modis and AVHRR

The conversion of Modis and AVHRR NDVI to fPAR provided a normalised dataset that represents vegetation productivity across the LUs. The fPAR values for the AVHRR record are marginally lower than for Modis (Figure 6.5), but there were slight differences in the period of record which partially account for this as well as spatial and spectral resolution differences between the sensors. Over all LUs, fPAR varied from close to 0 as a non-outlier minimum, to a few outlier maximums around or just exceeding 1.0. Median and 25th to 75th percentiles were similar for both sensors.

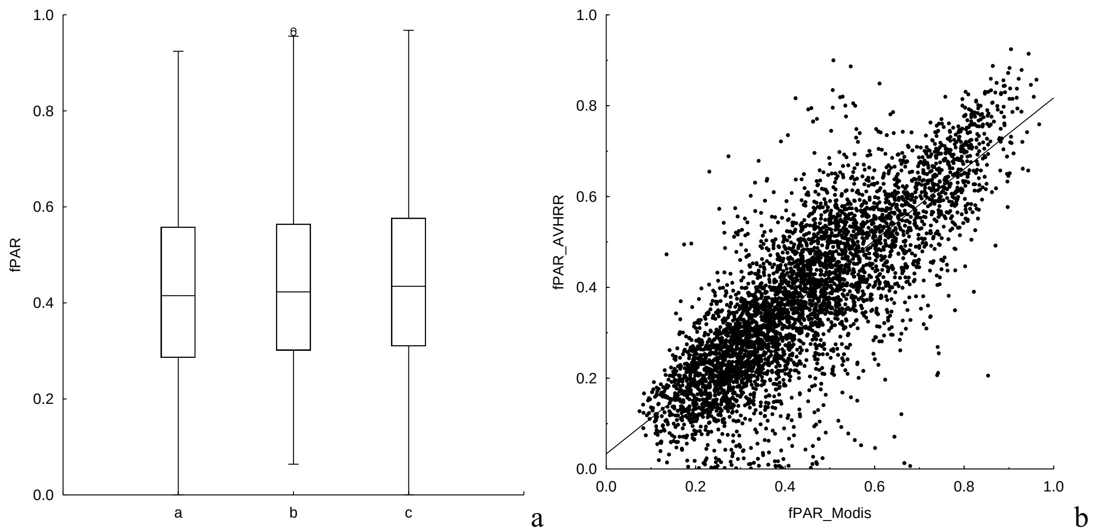

Figure 6.5: Box plot of fPAR values for a) fPAR AVHRR, b) fPAR Modis and c) combined fPAR time series. Scatter plot of common period of record for fPAR Modis and fPAR AVHRR.

All LUs have a high range of fPAR values as shown in Figure 6.6. The lowest median fPAR values tend to occur in the least frequently flooded LUs with most LUs exceeding fPAR of 0.8 at maturity. Phenology patterns can be detected, with some events showing high response across most LUs (i.e. 2000/1), while other events resulted in high response in some LUs and no response in others (i.e. 2002/3) (Figure 6.7).

With this high degree of variability and large number of the LUs, a simple ANOVA was used to test the significance of the population means. The results (Table 6.2) demonstrate that the population means are significantly different ($p<0.01$) with the Scheffe test (Table 6.3) identifying a number of possible homogenous groups. Although the population means between some LUs may be similar, the distribution of the fPAR values through time may still be different and the separate LUs are retained for the vegetation analysis. Flood frequency, patches and vegetation communities were also all significantly different in the ANOVA test ($p<0.01$) indicating that all factors contribute to differences between the LUs.

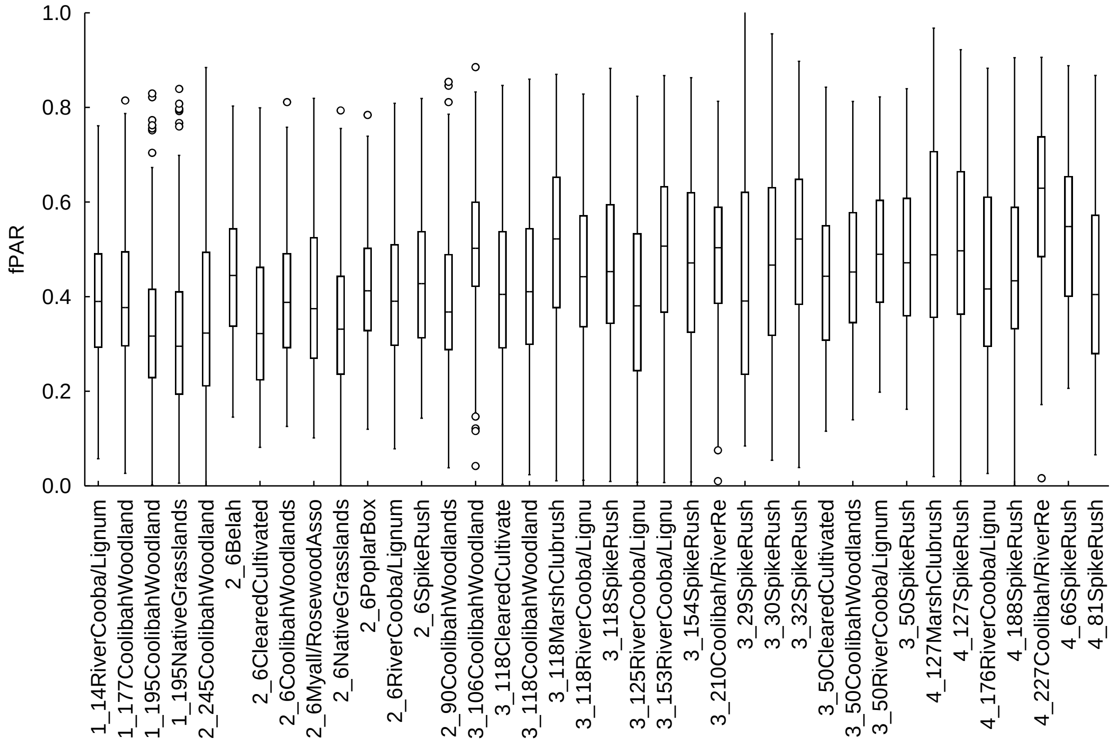

Figure 6.6: Box plot of fPAR variability for each landscape unit, n = 365

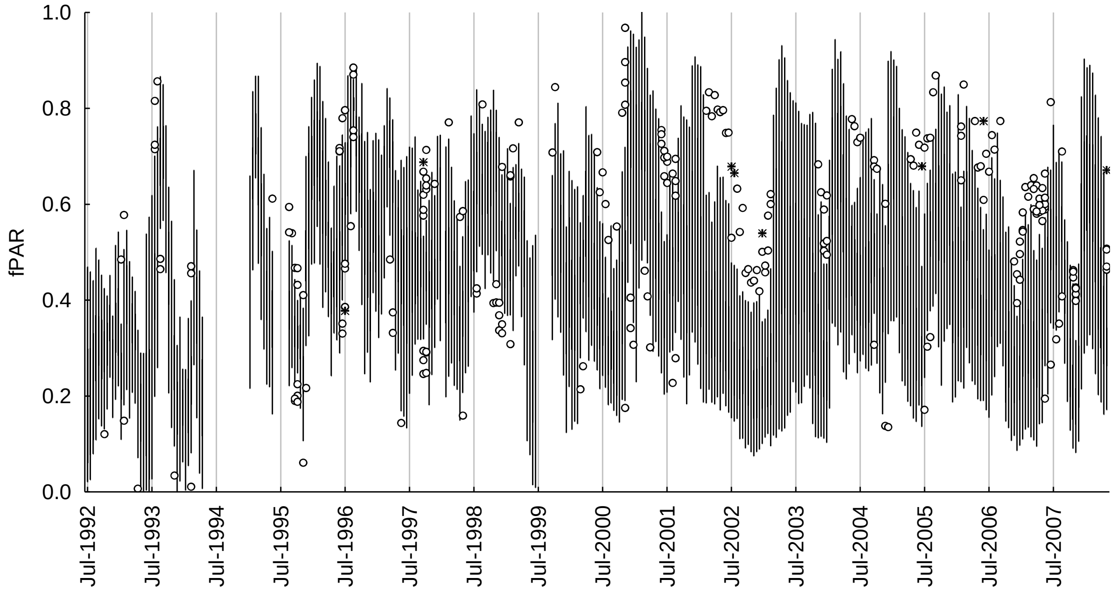

Figure 6.7: Time series of fPAR (all landscape units combined) showing median, quartiles, non-outliers, outliers o and extremes *, n = 38

Table 6.2: ANOVA test of significance of fPAR time series results for 38 identified landscape units.

	SS	Degr. of Freedom	MS	F	p
Intercept	2578.59	1	2578.59	88717.32	0.00
Landscape_unit_2	50.76	37	1.372	47.20	0.00
Error	378.55	13024	0.029		

Table 6.3: Scheffe test of homogenous groups. α = 0.05 (non-exhaustive search). Error: Between MS = .02907, df = 13024

Landscape unit	Mean fPAR	1	2	3	4	5	6	7	8	9	10	11	12	13
1_195nativegrasslands	0.3116	**												
1_195coolibahwoodland	0.3291	**	**											
2_6nativegrasslands	0.3471	**	**	**										
2_6clearedcultivated	0.3485	**	**	**										
2_245coolibahwoodland	0.3590	**	**	**	**									
1_177coolibahwoodland	0.3930	**	**	**	**	**								
1_14river cooba/lignum	0.3940	**	**	**	**	**	**							
2_90coolibahwoodlands	0.3959	**	**	**	**	**	**							
2_6coolibahwoodlands	0.3981	**	**	**	**	**	**							
2_6myall/rosewoodAsso	0.4018	**	**	**	**	**	**	**						
3_125river cooba/lignum	0.4023	**	**	**	**	**	**	**						
2_6river cooba/lignum	0.4079		**	**	**	**	**	**	**					
2_6PoplarBox	0.4142		**	**	**	**	**	**	**					
3_118clearedcultivate	0.4235			**	**	**	**	**	**	**				
4_81spikerush	0.4266			**	**	**	**	**	**	**	**			
3_29spikerush	0.4272			**	**	**	**	**	**	**	**	**		
2_6spikerush	0.4276			**	**	**	**	**	**	**	**	**		
3_50clearedcultivated	0.4340			**	**	**	**	**	**	**	**	**		
3_118coolibahwoodland	0.4352			**	**	**	**	**	**	**	**	**		
2_6belah	0.4426				**	**	**	**	**	**	**	**		
4_176river cooba/lignum	0.4507				**	**	**	**	**	**	**	**	**	
3_118river cooba/lignum	0.4565					**	**	**	**	**	**	**	**	
3_50coolibahwoodlands	0.4637					**	**	**	**	**	**	**	**	
4_188spikerush	0.4720					**	**	**	**	**	**	**	**	
3_154spikerush	0.4746					**	**	**	**	**	**	**	**	
3_118spikerush	0.4769					**	**	**	**	**	**	**	**	
3_30spikerush	0.4827					**	**	**	**	**	**	**	**	
3_50spikerush	0.4860					**	**	**	**	**	**	**	**	
3_210coolibah/river redgum	0.4870						**	**	**	**	**	**	**	
3_50river cooba/lignum	0.4951							**	**	**	**	**	**	
3_153river cooba/lignum	0.4985								**	**	**	**	**	
3_106coolibahwoodland	0.5082									**	**	**	**	
4_127spikerush	0.5113									**	**	**	**	**
3_32spikerush	0.5168									**	**	**	**	**
3_118marshclubrush	0.5195										**	**	**	**
4_127marshclubrush	0.5207											**	**	**
4_66spikerush	0.5393												**	**
4_227coolibah/river redgum	0.6052													**

6.3.2 MLR exploratory analysis

The results from initial MLR analysis indicates that adjusted R^2 values for rainfall of up to 10 lag intervals is higher than for the soil moisture store when the fPAR is modelled based on these parameters alone. However, when combined with flow, the SMS performs slightly better (Figure 6.8) and provides a simpler model structure. Similarly model fit was optimised using the log of 40-day cumulative inflow with lags of 0 (Q, 0-40-days), lag 1 (Q_{-1}, 40-80-days) and lag 2 (Q_{-2} 80-120-days) significant depending on the LU. Further lag intervals of inflow were insignificant for all LU.

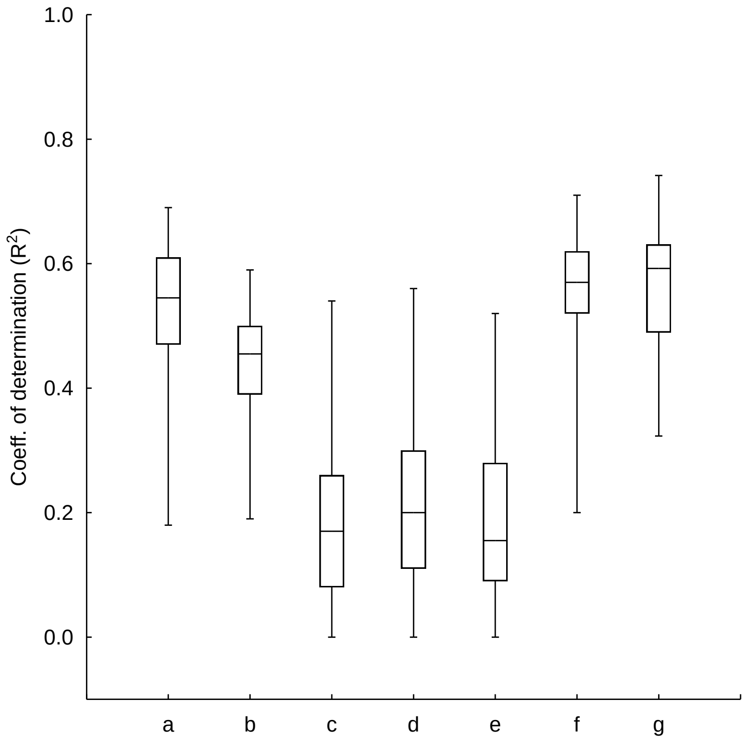

Figure 6.8: Box plots of the coefficient of determination (adjusted R^2) for the different MLR models of fPAR response for a) 16-day cumulative rainfall and Et including significant lag intervals, b) modelled soil moisture status, c) 16-day log inflow including sig. lag intervals, d) 40-day log inflow including sig. lag intervals, e) 120d log inflow, f) sig. rainfall, et and 40-day inflow, and g) sig. SMS and 40-day inflow. n=38

6.3.3 Vegetation response characteristics

Landscape units corresponding to the more frequently inundated wetlands have been analysed in detail, as well as some contrasting LUs in less frequently flooded areas or of other vegetation types. A summary of all other LUs are included after the detailed results. The LUs that are examined in detail are grouped geographically into:

- The Lower Gwydir frequently flooded (FF 3 and 4) areas of marsh clubrush and spikerush.
- The frequently flooded (FF 3 and 4) spikerush areas of the Gingham Channel, east of Gingham Bridge.
- The frequently flooded (FF 3) spikerush areas of the Gingham Channel, west of Gingham Bridge.
- Less frequently flooded spikerush (FF 2) and native grasslands (FF 1).
- The Gwydir 'Raft' areas of coolibah and river redgum (FF 3 and 4).

6.3.3.1 Lower Gwydir

The frequently flooded areas of the lower Gwydir (4_127 and 3_118) include the major area of marsh clubrush and surrounding spikerush water meadows and included the 'Old Dromana' Ramsar site and IMEF vegetation monitoring sites. The property 'Old Dromana' has recently been acquired as a wetland reserve. The flood response of the marsh clubrush landscape units contain a diverse range of species dominated by the amphibious functional groups (fluctuation responders and tolerators) such as marsh clubrush (*Bulboschoenus fluviatilis*), spikerush and tall spikerush (*Eleocharis plana and E. sphacelata*), typha (*Typha domingensis*), water couch (*Paspalum distichum*), *Persicaria decipiens*, *Ranunculus undosus*, *Potamogeton tricharinatus* and *Azolla filiculoides* (Unpublished IMEF data, DLWC). The spikerush vegetation (Figure 6.9a) is similar but has a higher proportion of spikerush (*E. plana*) and water couch. In terms of productivity, the main difference between the two LUs is the presence of almost 100% cover of spikerush, water couch and other lower growing species in both LUs, but with an 'overstory' of the taller rushes such as marsh clubrush and typha in the marsh clubrush LU. During dry periods, some of these species may persist as non-productive litter cover (Figure 6.9b). The difference between 4_127 and 3_118 is the frequency of flooding which also influences the community structure.


a

b

Figure 6.9: The frequently flooded (4_127) spikerush dominated landscape unit of the lower Gwydir showing a) 100% vegetation cover dominated by spikerush (*Eleocharis plana)* and water couch (*Paspalum distichum)* and b) chlorotic water couch cover. (source: Mawhinney, DLWC)

The fPAR time series of these LUs show responsive vegetation that can be highly productive with maturity peaks occurring in most years, and some years recording two distinct green-up periods (Figure 6.10). The central, more frequently flooded areas (4_127) reach higher fPAR peaks exceeding 0.90 for five and three events for marsh clubrush and spikerush respectively and 0.8 for 13 and nine events respectively. The slightly less frequently flooded surrounding LUs (3_118) did not exceed 0.90 in any events with the marsh clubrush exceeding 0.8 on 10 occasions while the spikerush only exceeded 0.8 for six events. Minimum values were lowest for the most frequently flooded LUs. This may be due to an increased duration and depth of flooding, where the minimum values are due to open water and reduce the raw NDVI values prior to a rapid increases in fPAR. Alternatively the low values could be due to a less productive dormancy vegetation community due to a lack of terrestrial species when there is low soil moisture.

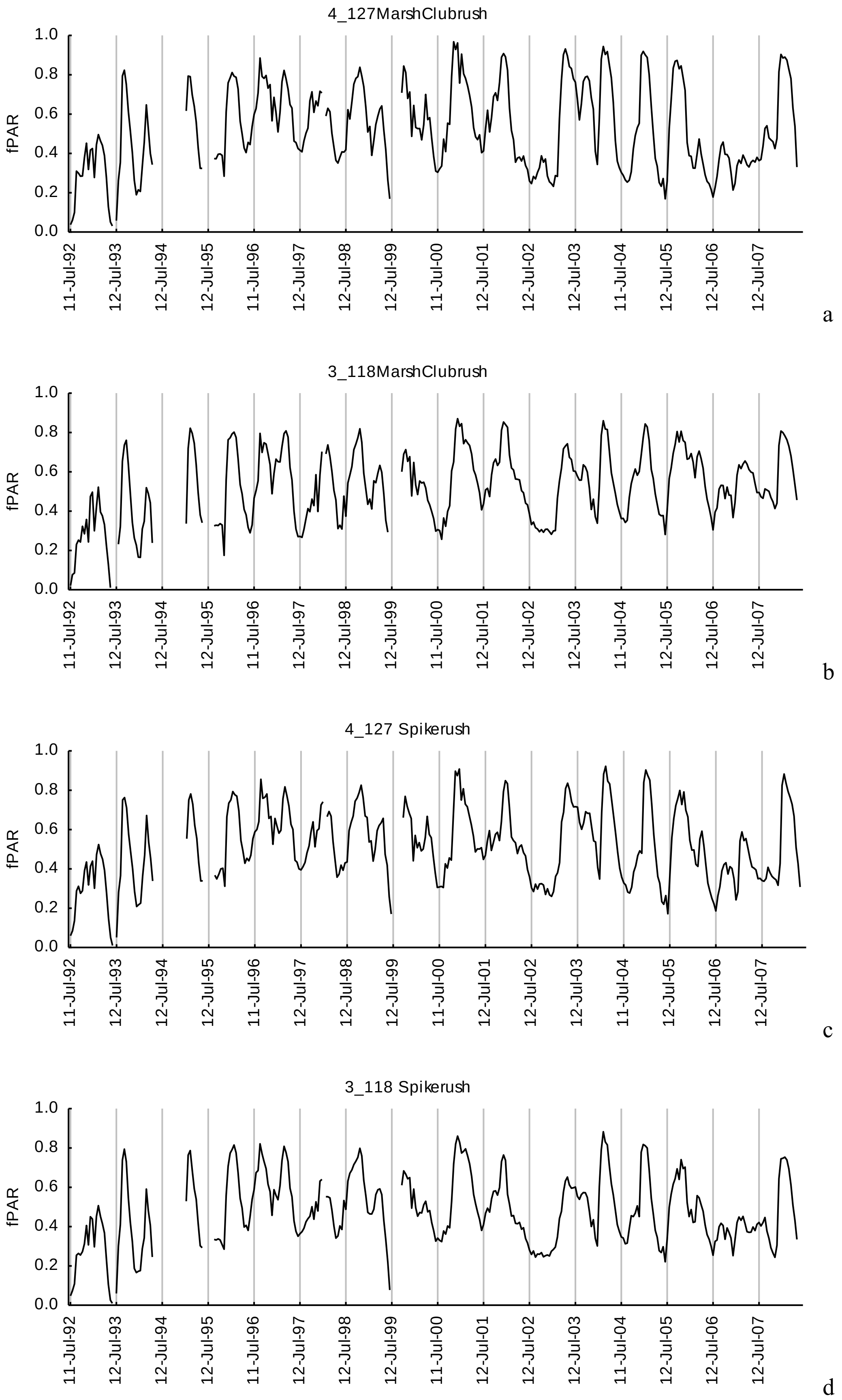

Figure 6.10: Time series fPAR of frequently flooded landscape units of the lower Gwydir. a) 4_127 marsh clubrush, b) 3_118 marsh clubrush, c) 4_127 spikerush, and d) 3_118 spikerush.

Productivity of the marsh clubrush and spikerush LUs in the Lower Gwydir peaks in the warmer months although there is high variability from year to year. The frequently flooded 4_127 LUs can remain highly productive throughout the spring and summer months (Figure 6.11a) and follow a similar annual pattern to inflow Figure 6.12a. The slightly less frequently flooded 3_118 LUs tend to peak in February and March in line with the peak inflows (Figure 6.11b). The cooler months have much lower productivity for the frequently flooded wetland LUs. In contrast the infrequently flooded native grassland LUs (Figure 6.11a and section 6.3.3.4) tend to peak in late winter (August) with a secondary peak in February in a similar pattern to the climate driven soil moisture.

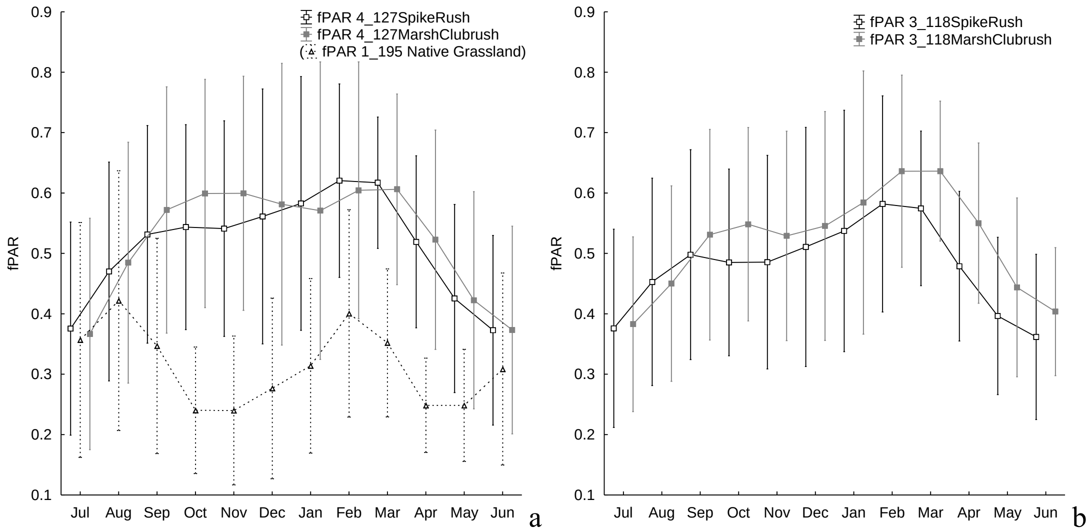

Figure 6.11: Mean monthly fPAR (±st dev) 1992-2008. a) 4_127 LUs and rarely flooded 1_195 grassland LU for comparison b) 3_118 LUs

Extracting a 'typical' response pattern from the time series can be problematic as events tend to merge into one another or be interrupted by subsequent events. The inflow event that occurred in 2003/4 is one of the best separated events, occurring after a relatively dry period. Of a size that resulted in flood response over much of the floodplain (FF 1, 2, 3 and 4) it is a good event to compare the response of the different LUs. Extracting the time series of fPAR for this event it can be seen that the frequently flooded (FF=3 and 4) LUs of spikerush and marsh clubrush responded in a very similar pattern as shown in Figure 6.12b. (Note that dates correspond to the start of the 16-day MVC period). Greenup onset commenced on the 1st January 2004 with a rapid increase in fPAR over two 16-day MVC periods before maturity from the 2nd February to the 21st March. The peak occurred around 0.94 or 0.92 (4_127 LUs) or slightly less (0.88 and 0.86 for the 3_118 LUs). Senescence occurred over five MVC periods before dormancy onset on the 9th June at around 0.41 fPAR. The most frequently flooded marsh clubrush appeared to have a slightly longer and higher maturity than the other LUs but fell to slightly lower (dormancy) fPAR values.

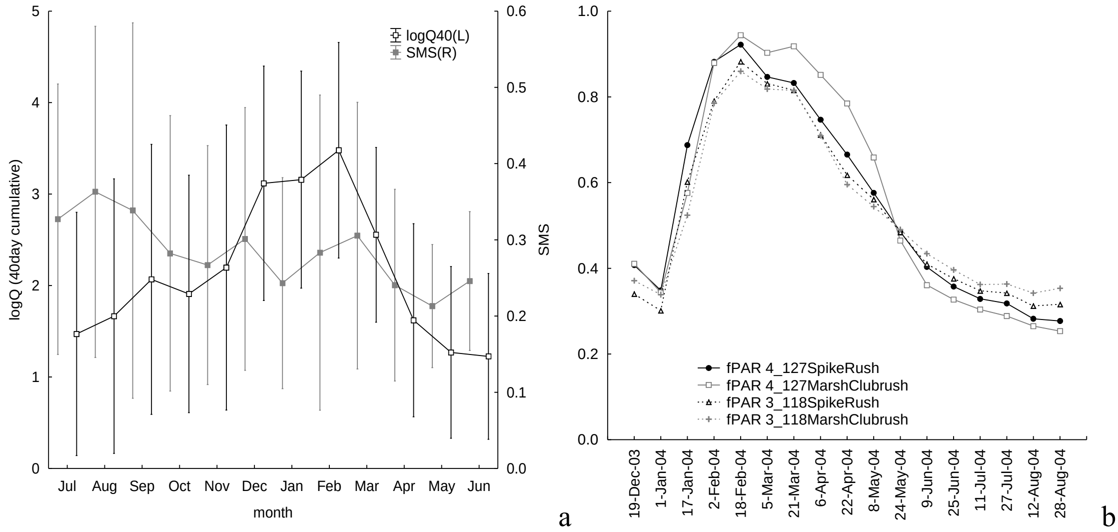

Figure 6.12: a) Mean SMS and inflow (40-day cumulative) monthly distribution (±st. dev)1992-2008. b) fPAR response 2003/4 for frequently flooded landscape units of the lower Gwydir

The results of multiple linear regression analysis (Table 6.4) indicate a significant relationship between fPAR, SMS and antecedent inflows of up to 80 days (Q at 0-40 days and Q_{-1} at 40-80 days) for the most frequently flooded LUs. For the surrounding LUs SMS and the Q_{-1} flows are significant. For all LUs the intercept is also significant, ranging from 0.16 to 0.22. The model fit is fair to good (adjusted R^2 of 0.55 to 0.71) and represents most periods of response quite well in terms of both magnitude and timing.

The model overestimates fPAR for the largest flood event (exceeding 1.0 in 1999) as shown by the time series and scatter plots of the observed and modelled fPAR (Figure 6.13). The fPAR is also underestimated during the 2002-3 period, particularly for the 4_127 LUs, which coincides with the delivery of small environmental flow releases targeted at these LUs.

Table 6.4: Multiple linear regression results for frequently flooded LUs of the lower Gwydir.

Landscape unit	**Intercept**	**SMS**	**lnQ**	**lnQ_{-1}**	**lnQ_{-2}**	**Adj. R^2**	**St. Error**
4_127spikerush	**0.18**	**0.59**	**0.0297**	**0.0539**	0.0042	0.63	0.12
4_127marshclubrush	**0.16**	**0.71**	**0.0262**	**0.0611**	0.0050	0.55	0.15
3_118spikerush	**0.16**	**0.65**	0.0145	**0.0522**	0.0052	0.71	0.09
3_118marshclubrush	**0.22**	**0.49**	0.0148	**0.0588**	0.0085	0.62	0.10

Significant variables shown in bold ($p<0.05$), Q is 40-day cumulative inflow

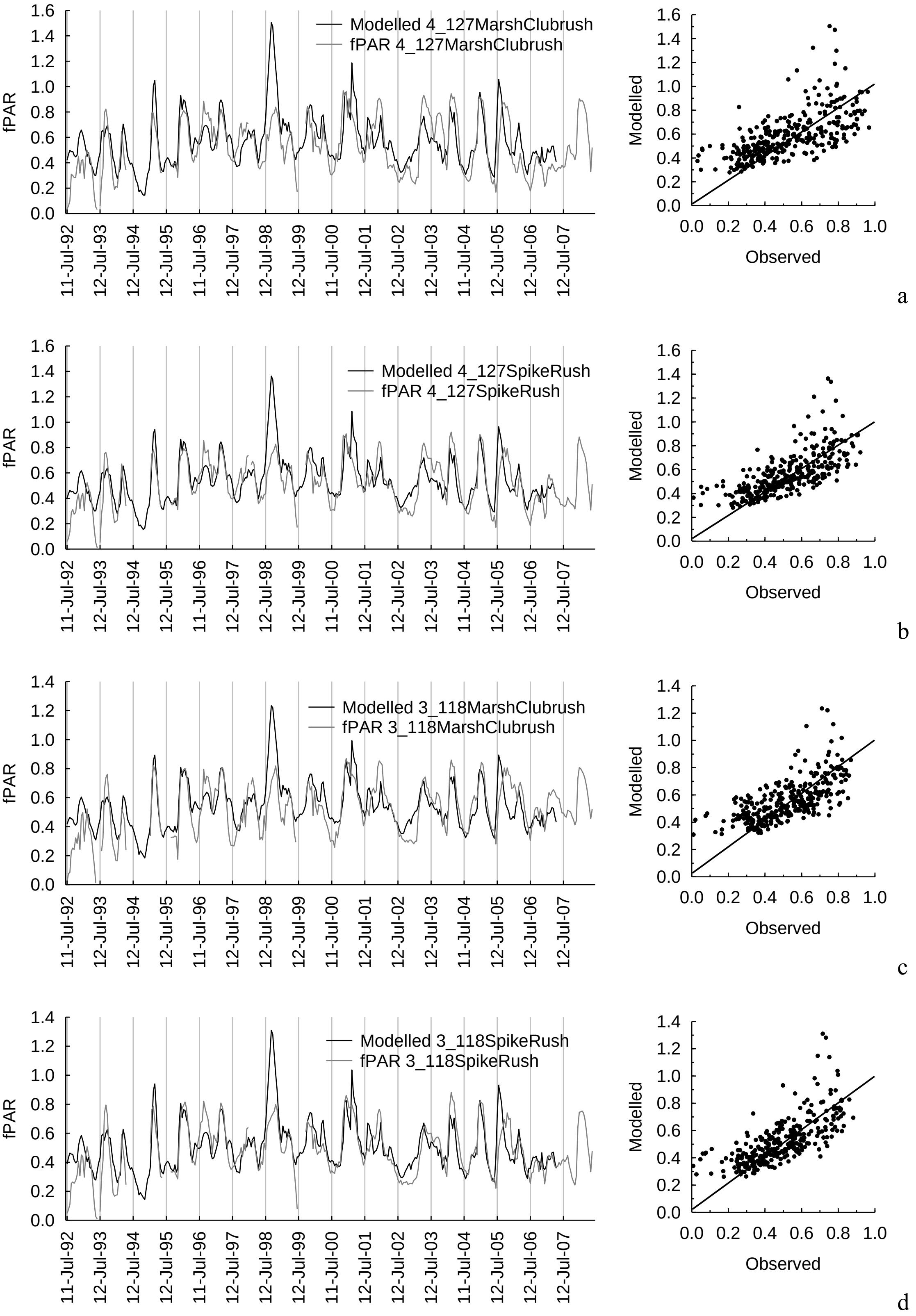

Figure 6.13: Time series and scatter plots of the observed (grey) and modelled (black) fPAR for frequently flooded LUs of the lower Gwydir a) 4_127 marsh clubrush, b) 4_127 spikerush, c) 3_118 marsh clubrush and d) 3_118 spikerush. 1:1 line shown on scatter plots.

As an exploratory tool, these relationships are visualised further using XYZ surface plots with a bicubic spline smoothing procedure (StatSoft Inc, 2009). The surface plots provide a visual tool to help understand the possibly non-linear response and relationships between fPAR, SMS and inflows. For example in figure 6.14a, the highest fPAR values (dark green) are associated with highest inflows (logQ) and moderate SMS. Low FPAR values (red) are seen at low inflows regardless of SMS values. There are areas of the surface plot with no 'dots' which are area of no data. Interpretations of these areas are undertaken with caution.

Examining the relationship between inflow (40-day cumulative inflow at significant lag intervals), SMS and fPAR for the frequently flooded marsh clubrush LU indicates a peak of fPAR for mid to high inflows with only small increases of fPAR at very high inflows. For 4_127 marsh clubrush (Figure 6.14a) and 4_127 spikerush (Figure 6.14b) the relationship to flow is generally linear. For the less frequently flooded 3_118 LUs (Figure 6.14 c and d), however, there may be a breakpoint dependent on SMS. This is difficult to visualise in the scatter plots shown in Figure 6.15 that indicate a linear minimum fPAR value in relation to flow, particularly for $\ln Q_{-1}$, with high variability above this. The relationship between fPAR and SMS alone is not clear. There were no periods of high SMS with low flow so it is not possible to be confident about the role of high soil moisture alone in driving fPAR response, nevertheless moderate SMS does contribute to higher fPAR during moderate to high flows. A combination of moderate to high inflow volumes with mid-range SMS provide conditions suitable for highest fPAR response in these LUs. The surrounding marsh clubrush that is flooded slightly less frequently (3_118) does not reach the same peak fPAR (Figure 6.14c). The surface plot and scatter plots (Figure 6.15) suggest that maximum fPAR is reached at moderate inflows and SMS, with increasing inflow or SMS beyond this point not resulting in increasing fPAR. The depression of fPAR at high inflows/SMS may be caused by the depression of raw NDVI values due to the presence of open water flooding (so not 'real' in the sense of reduced productivity of the vegetation), and/or a reduction in productivity due to the presence of flooding.

It could be suggested that non-linear model fits may better represent the response. But the uncertainty in the data source itself and in the large range of other environmental variables not considered within the model structure (and for which information is not available at this time) limit the confident identification of more complex model structures.

In summary, the model assessment undertaken here reveals likely fPAR response to flows in the small to moderately large range. The response is not always linear and capping the modelled results at the theoretic maximum fPAR of 1.0 is necessary for very large floods. The MLR does not provide good estimation at very low flows such as targeted environmental flows. More generally, the exploratory analysis suggests that given ideal soil moisture in the midrange of the SMS and seasonality (September through to March) the most frequently flooded areas of marsh clubrush and spike rush should respond to a flood event quickly, reaching maximum fPAR in excess of 0.9 within 2-3 MVC periods (32-48 days). Maximum fPAR may last up to 48 days before senescence where fPAR drops to dormancy of around 0.4 over a period of up to 80 days. At this point, the rate of decline in fPAR values slow. The surrounding slightly less frequently flooded LU have a similar pattern of response however the maturity values are slightly lower (0.86-0.88).

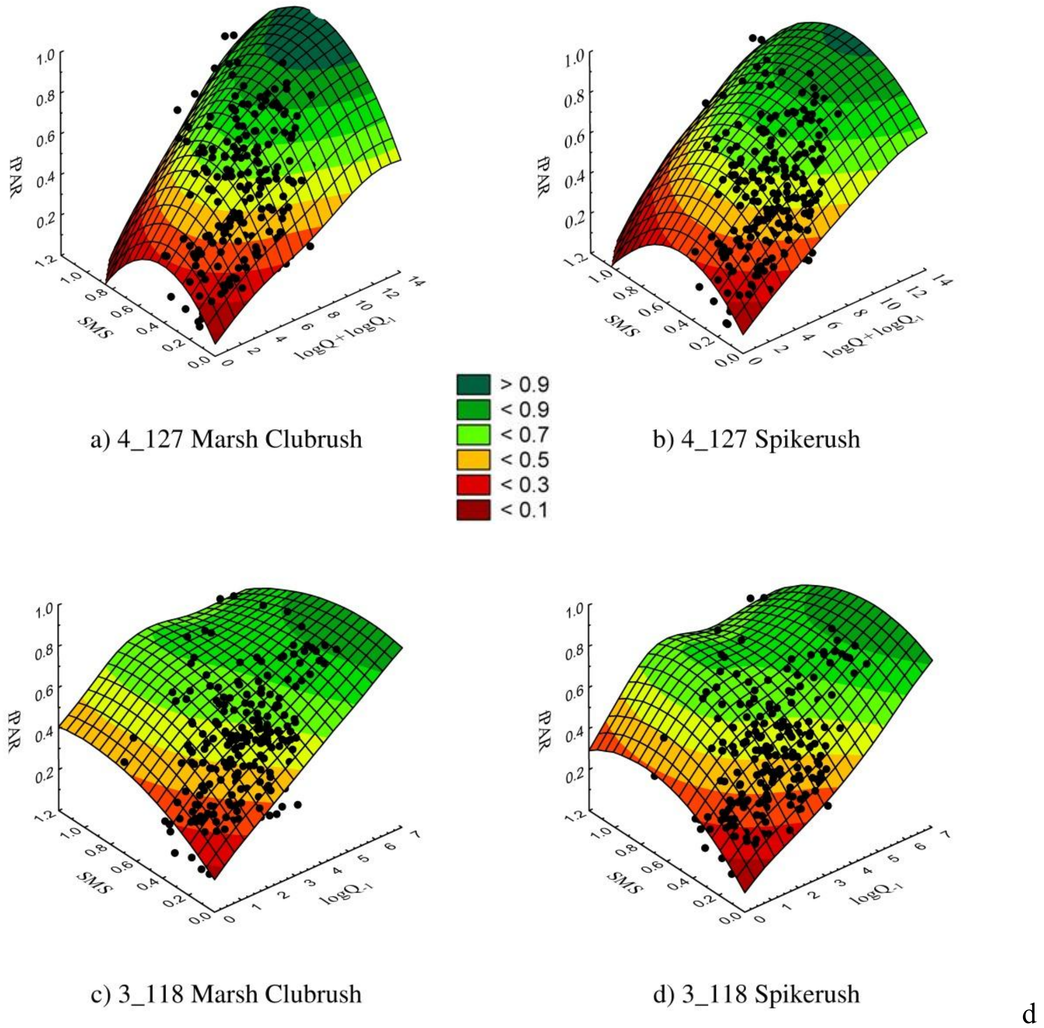

Figure 6.14: Surface plots of fPAR response in the Lower Gwydir landscape units in relation to soil moisture status (SMS) and significant inflows (Q).

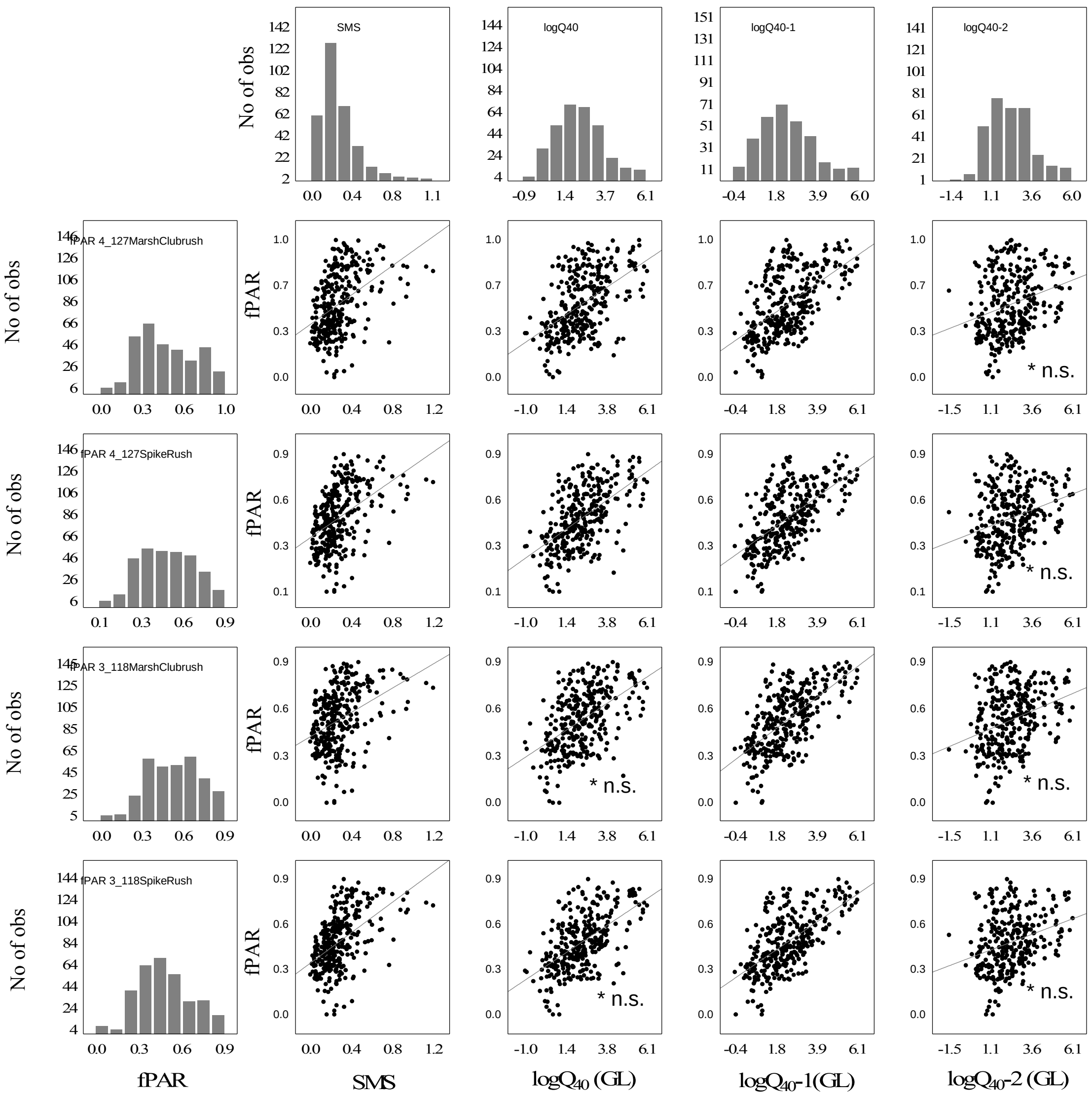

Figure 6.15: Scatterplot of fPAR response in the lower Gwydir marsh clubrush landscape units in relation to soil moisture status and inflows. Note that non-significant variables in the MLR model are labelled as *n.s. Histograms display the distribution of each variable of the analysis period.

6.3.3.2 Gingham east

Three frequently flooded wetland LUs were identified in the area of the Gingham channel and floodplains, between the Gwydir ‘Raft’ and Gingham Bridge. The LUs are all mapped as spikerush wetlands. The frequently flooded 4_66 spikerush is highly connected to the Gingham channel and includes the Goddards Lease Ramsar site. Surrounding this area is a slightly less frequently flooded spikerush LU (3_50) extending through to the Gingham Waterhole to the west. There is a slightly different community structure to the Lower Gwydir spikerush LU although it is still dominated by the amphibious functional groups (Unpublished IMEF data, NSW DLWC). On the other hand the invasive water hyacinth (*Eichhornia crassipes*) can dominate during periods of extended flooding, forming a highly productive cover over open water areas that can persist for long periods (Figure 6.16). At various times water hyacinth has been controlled by spraying, mechanical removal or by 'drying out' some areas by controlling inflows. Another LU (4_81 spikerush) is located off the Gingham channel and appears disconnected but is mapped as spikerush.

Figure 6.16: Invasive water hyacinth (*Eichhornia crassipes*) in the Gingham wetlands. (Source Fulford, DLWC)

The main area of frequently flooded spikerush (4_66) peaks at an fPAR of 0.86, but only exceeded an fPAR of 0.8 on seven occasions over the 16 years of record (Figure 6.17a). The response patterns from 1995 to 1999 are not as clear as for the lower Gwydir LUs, the area maintaining a moderately high fPAR (between 0.5 and 0.75) for most of this period. The other large frequently flooded LU (4_81 spikerush, Figure 6.17b) shows a slightly different pattern with similar peaks of around 0.84 but the minimum values have been lower since 2000 and the time from greenup to dormancy appears to be of shorter duration. This LU, although mapped as spikerush, appears disconnected from the Gingham Channel and warrants further field investigation that is beyond the scope of this thesis.

The large LU (3_50spikerush, Figure 6.17c) surrounding 4_66 is still highly connected to the Gingham Channel. The fPAR time series results are similar to those for the 4_66 LUs with slightly lower peak of 0.82 and only four periods exceeding 0.8. Minimum values are also slightly lower but the time series does show a similar trend through 1995-1999 where values stayed in the moderate range of 0.5 to 0.75 for the most part. This pattern may be due to the water hyacinth invasion as the plant is quite persistent through time but it is difficult to determine with any certainty.

The monthly mean fPAR values (Figure 6.18a) show their peaks tend to occur in late summer with high variability. The mean fPAR is highest and standard deviation lower in the most frequently flooded LU (4_66). Again the 4_81 LU shows some results that suggest a different response pattern to other spike rush LUs, with lower fPAR means and higher standard deviations indicating higher variability. The mean fPAR through the year for all three LUs is similar to the annual flow pattern rather than the SMS (Figure 6.12).

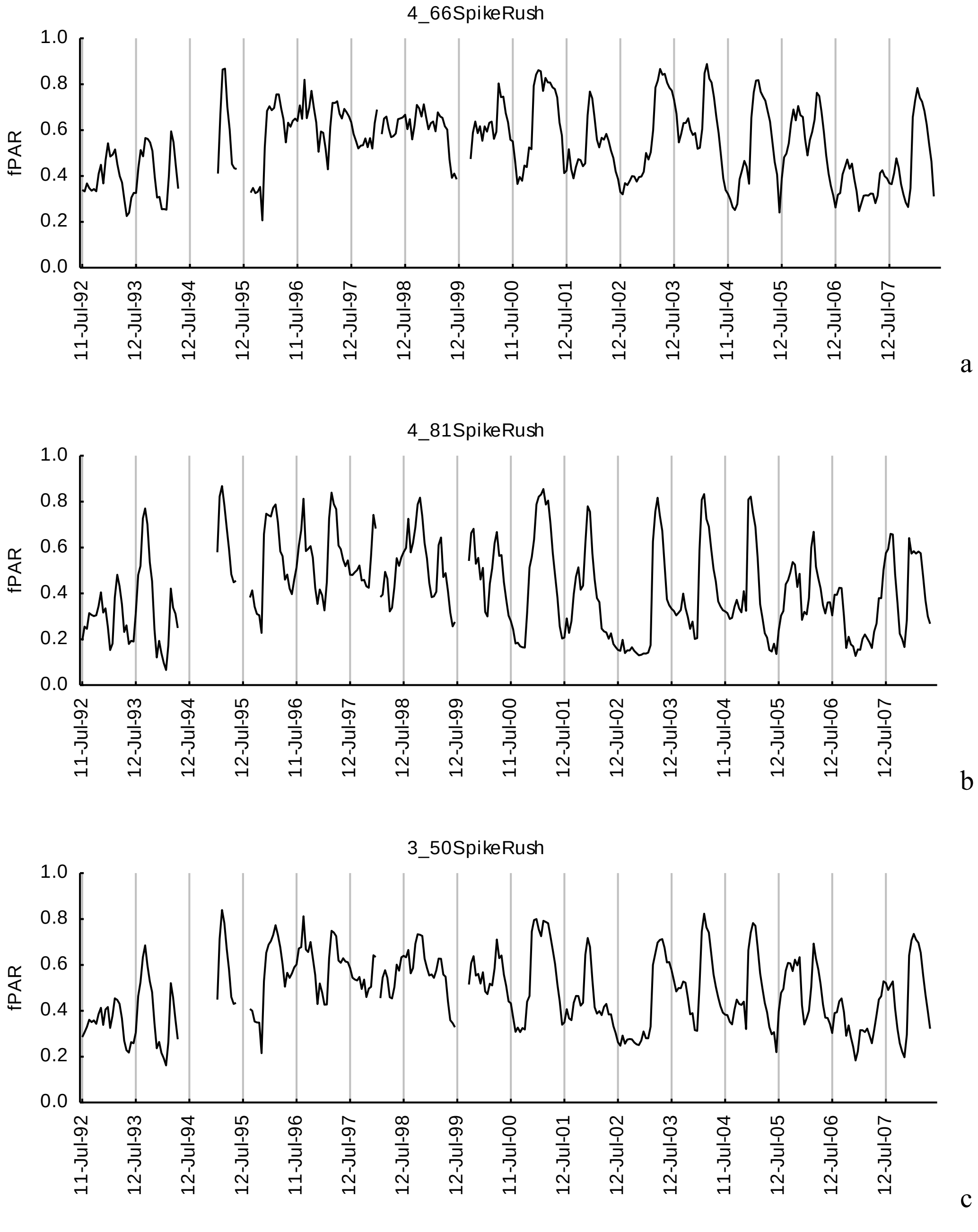

Figure 6.17: Time series fPAR for frequently flooded spike rush landscape units of the eastern Gingham Channel. a) 4_66 spikerush, b) 4_81 spikerush and c) 3_50 spikerush.

The response pattern for the 2003/4 flood event (Figure 6.18b) was similar to the Lower Gwydir frequently flooded spikerush LUs although 4_66 had a higher fPAR at green-up onset. The peak fPAR was reached in three MVC periods at 0.83 for 4_81 and 3_50 spikerush LUs, and 0.89 for 4_66 spikerush. The duration of maturity was slightly shorter than the Lower

Gwydir with fPAR values falling within one to two MVC periods from the peak; however dormancy onset occurred at the same time as the Lower Gwydir at similar fPAR values. Again the LU with the highest peak fPAR fell to a slightly lower dormancy onset fPAR than the other LUs.

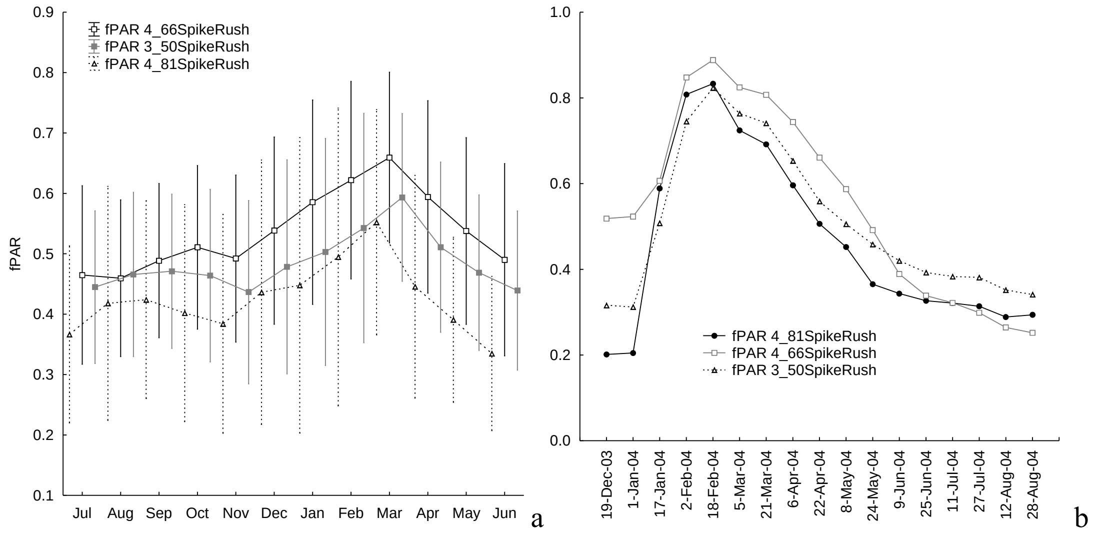

Figure 6.18: a) Mean monthly fPAR (±st dev) for frequently flooded spikerush landscape units of the eastern Gingham Channel. b) Response pattern for the 2003/4 flood event

The MLR analysis for the frequently flooded spikerush LUs of the eastern Gingham Channel showed good model fit (R^2 of 0.68-0.74) (Table 6.5). The 4_81 spikerush LU is the only LU with a non-significant intercept. The highest intercept (0.22) occurred in the 4_66 spikerush LU while the less frequently flooded 3_50 spikerush has a slightly lower intercept (0.15). SMS was significant for all LUs. Antecedent flows at Q and Q_{-1} were significant for 4_81, but a more delayed response was seen in the 4_66 and 3_50 LUs where Q_{-1} and Q_{-2} were significant in the MLR model.

The time series comparison of MLR modelled and observed fPAR (Figure 6.19) reveals that the model represents the patterns reasonably well up to 1995 and after 1999 but overestimates the maturity peaks and dormancy troughs between 1995 and 1999.

Exploring the relationship between fPAR, SMS and significant flow periods, the LU connected to the east Gingham Channel (4_66 and 3_50 spikerush) indicate the possibility of a breakpoint - further inflows or SMS have little impact on the fPAR giving a flat top appearance to the surface plots (Figure 6.20a and b). The scatter plots of flow versus fPAR indicate a linear relationship between a minimum fPAR value and inflow; however the highest fPAR values can occur over a range of flows. The relationship with SMS is not as clear, there being a wide scatter of points.

The 4_81 spikerush LU has a quite different surface plot (Figure 6.20c) indicating a flow breakpoint that triggers higher fPAR response. The flow versus fPAR scatter plot (Figure 6.21) does not show the same linear minimum pattern as the other LUs.

Table 6.5: MLR results for the frequently flooded spikerush landscape units of the eastern Gingham Channel

Landscape unit	**Intercept**	**SMS**	**lnQ**	**lnQ_{-1}**	**lnQ_{-2}**	**R^2**	**St. Error**
4_81spikerush	-0.03	**0.70**	**0.0206**	**0.0716**	0.0112	0.68	0.12
4_66spikerush	**0.22**	**0.31**	0.0056	**0.0681**	**0.0421**	0.70	0.09
3_50spikerush	**0.15**	**0.60**	-0.0043	**0.0602**	**0.0181**	0.74	0.08

Significant variables shown in bold ($p<0.05$), Q is 40-day cumulative inflow

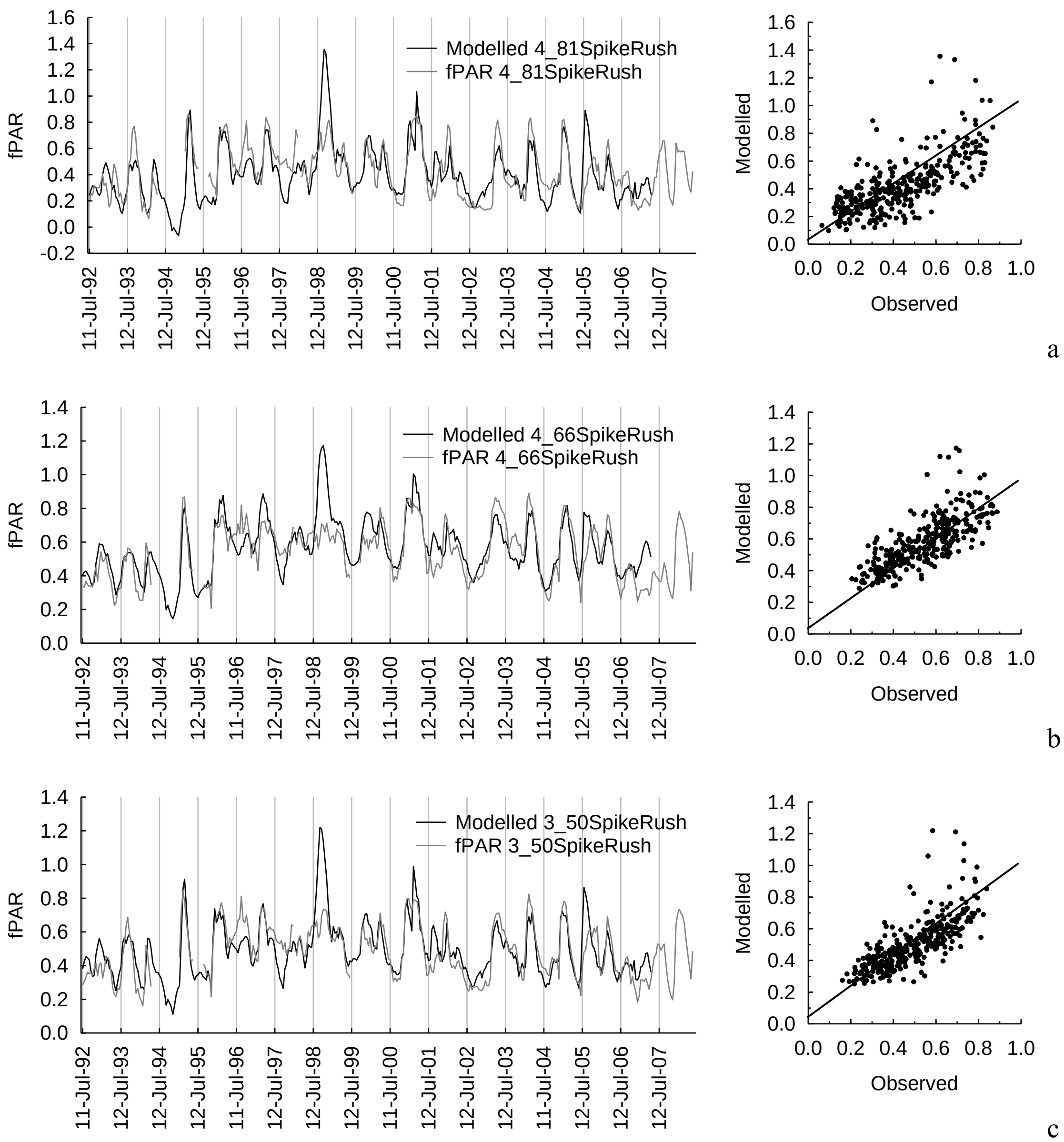

Figure 6.19: Observed and modelled fPAR time series and scatter plots for the frequently flooded spike rush landscape units of the eastern Gingham Channel a) 4_66 spikerush, b) 4_81 spikerush and c)3_50 spikerush. 1:1 line shown on scatter plots.

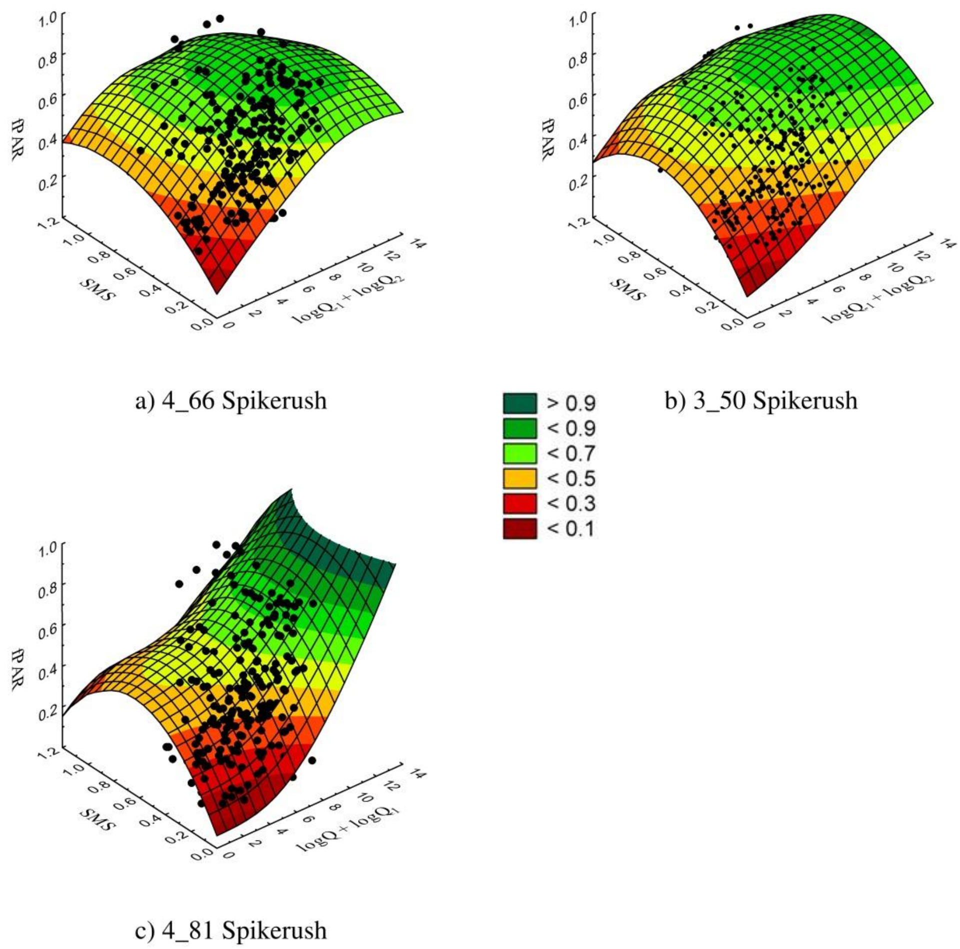

Figure 6.20: Surface plots of fPAR response in the spikerush vegetation landscape units of the eastern Gingham in relation to soil moisture status and inflows a) 4_66 spikerush b) 3_50 spikerush and c) 4_81 spikerush

In summary LU 4_81 spikerush does not follow the same productivity patterns as other frequently flooded spikerush LUs. Given ideal conditions of moderate to high SMS and inflows in the warmer months, the frequently flooded 4_66 spikerush LU can exceed an fPAR of 0.85 at maturity while the surrounding 3_50 spikerush LU displays maturity around 0.82. Maturity occurs within 2-3 MVC periods of green-up onset. The rate of senescence is similar to that of the lower Gwydir spikerush LUs although duration of maturity may be slightly shorter. In contrast to the Lower Gwydir LUs, both 4_66 and 3_50 spikerush LUs can maintain moderate fPAR through successive years. For both 4_66 and 3_50 spikerush LUs, intercept, SMS and inflow at Q_{-1} and Q_{-2} are significant in the MLR model, the adjusted R^2 values being 0.70 and 0.74 respectively.

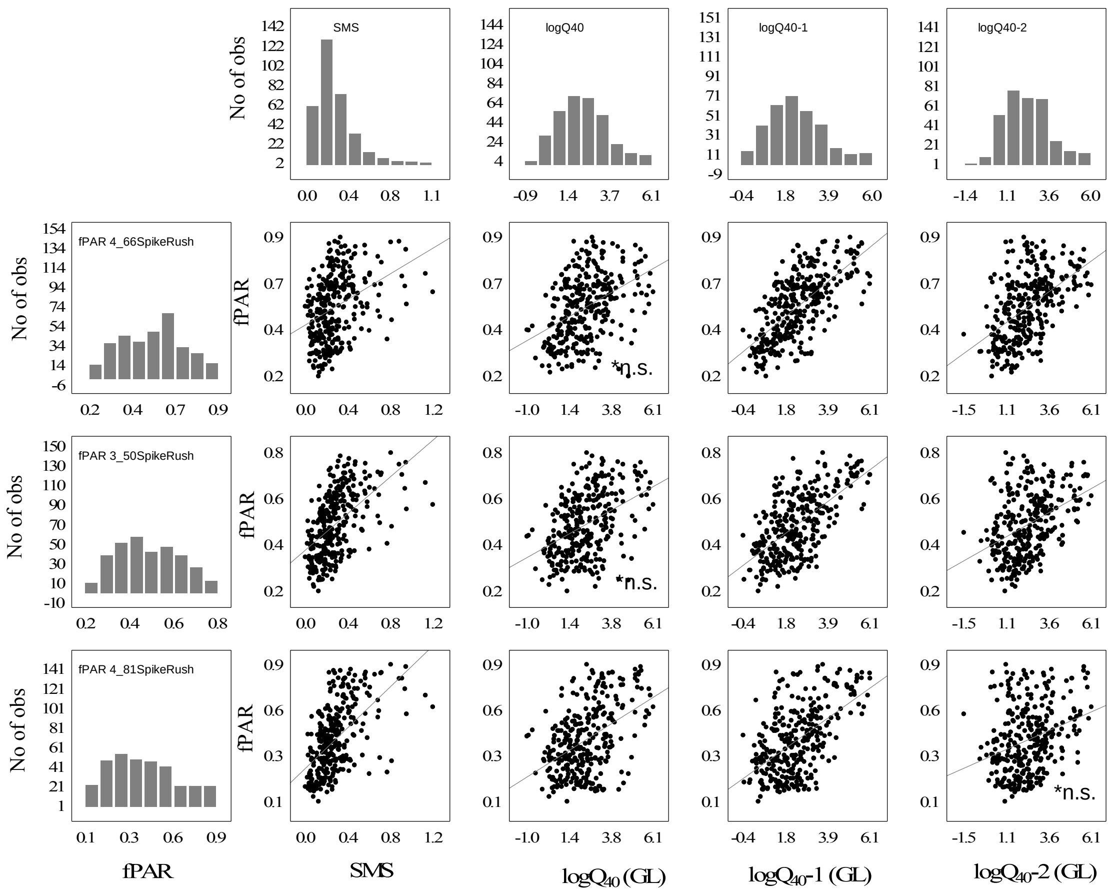

Figure 6.21: Scatterplot of the Eastern Gingham spikerush landscape unit in relation to soil moisture status and inflows. Note that non-significant variable in the MLR model are labelled as *n.s.

6.3.3.3 Gingham west

Downstream (west) of Gingham Bridge are further spikerush dominated LUs associated with the Gingham Channel. These LUs have a slightly lower flood frequency than the eastern spikerush LUs and are dominated by water couch and spikerush during and after flooding (Unpublished IMEF data, NSW DLWC). However they also have a higher proportion of the invasive weed lippia (*Phyla canescens*) which is a low growing amphibious fluctuation tolerator that can form a thin blanket-like ground cover excluding many other species. Lippia can persist during short periods of flooding and is more drought tolerant than the other amphibious wetland species (Mawhinney, 2003). It does occur throughout the Gwydir but appears more prevalent as flood frequency decreases.

Moving from east (3_32) to west (3_29), the number of events that exceeded an fPAR value of 0.8 drop from five events to 3 events and events exceeding an fPAR value of 0.7 drop from 12 to 10 (Figure 6.22). The LUs do not show the same range of fPAR values from year to year as the more frequently flooded areas and the phenology pattern is less clear in many years. Also apparent in the time series fPAR is the variability in the response patterns through time.

This may be due to changing flow regime, a shift in vegetation type (i.e. from more 'wetland' responsive to more terrestrial species or increased dominance of lippia) or changing landuse.

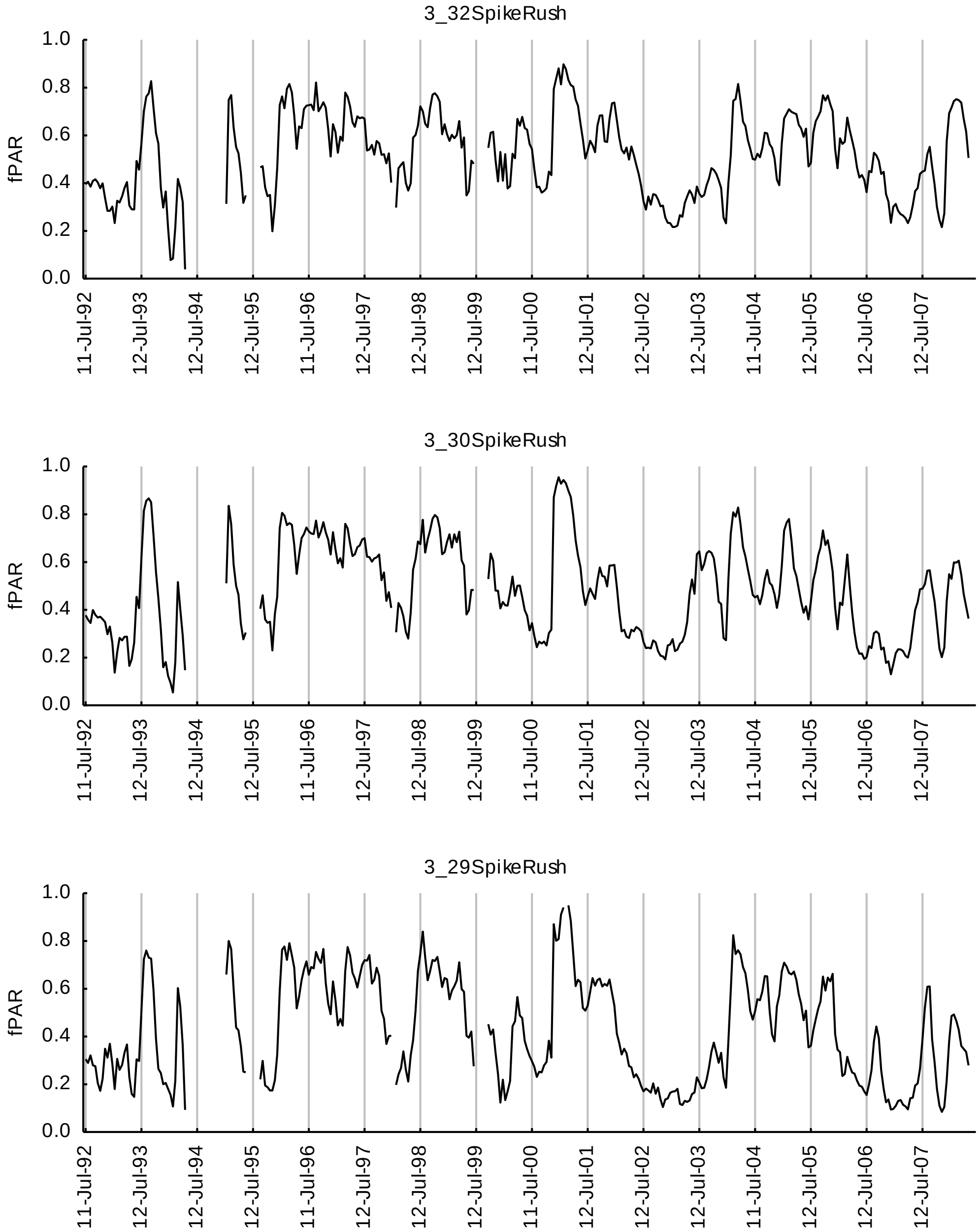

a

b

c

Figure 6.22: Time series fPAR of spikerush Landscape Units associated with the western Gingham Channel, downstream of Gingham Bridge a)3_32 spikerush, b) 3_30 spikerush and c) 3_29 spikerush.

The mean monthly fPAR is highly variable with small peaks occurring in September and March (Figure 6.23a). The easternmost LU has higher mean fPAR for all months while the western most LU (3_29) has the highest variability. The 2003/4 event shows a slightly slower rate of response in comparison to the eastern Gingham and Lower Gwydir spikerush LUs, reaching a maturity fPAR of 0.83 in three composite periods. Dormancy onset occurred one period later than the eastern LUs with high fPAR values (0.47 to 0.5) persisting again. This is suggestive of vegetation that can maintain productivity with lower soil moisture conditions compared to the more frequently flooded LUs. Peak fPAR has been higher in previous events (2000/2001) and is capable of exceeding 0.9 under ideal conditions.

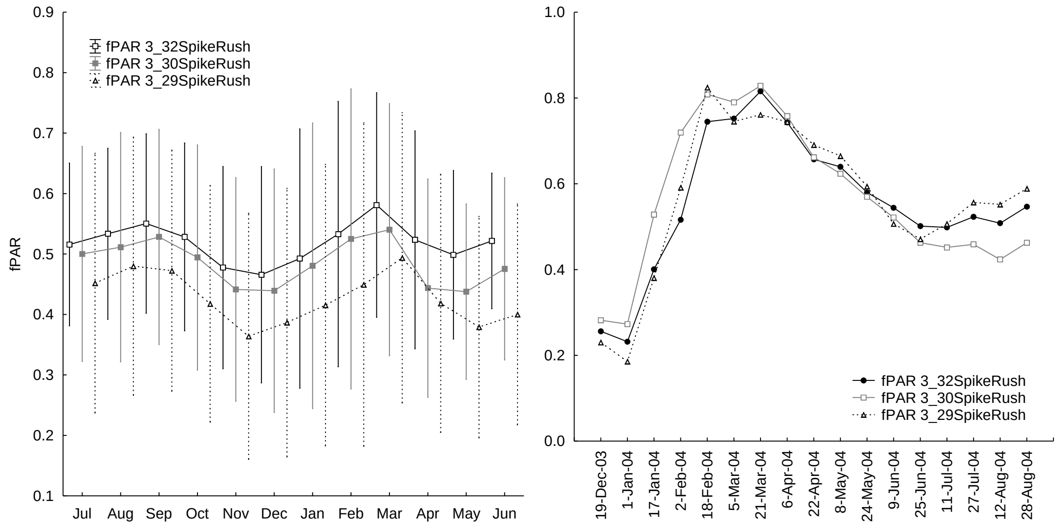

Figure 6.23: a) Mean monthly fPAR (±st dev) and b) 2003/4 fPAR response for the western Gingham Channel spikerush landscape units.

The coefficient of determination for the MLR model was lower than for the more eastern LUs ranging from 0.52 to 0.32 (Table 6.6). Intercept, SMS and flow for lnQ_{-1} were all significant ($p<0.05$). Flow was also significant at lnQ and lnQ_{-2} for 3_32 and at lnQ for 3_30. There was a significant negative relationship between fPAR and lnQ at 0-40 days for LU 3_32 and 3_30; however the relationship was positive at lnQ_{-1} for all LUs and at lnQ_{-2} for 3_32.

Table 6.6: MLR results for western Gingham spikerush LUs

Landscape unit	Intercept	SMS	lnQ	lnQ_{-1}	lnQ_{-2}	R^2	St. Error
3_32spikerush	**0.31**	**0.47**	**-0.0321**	**0.0418**	**0.0269**	0.34	0.14
3_30spikerush	**0.20**	**0.79**	**-0.0314**	**0.0502**	0.0168	0.52	0.14
3_29spikerush	**0.17**	**0.78**	-0.0228	**0.0385**	0.0149	0.32	0.19

Significant variables shown in bold ($p<0.05$), Q is 40-day cumulative inflow

The poor model fit from the MLR is highlighted in the poor representation of the response patterns of the fPAR time series in the western Gingham spikerush LUs (Figure 6.24). From 1995 to 1998 the model results underestimate the peaks, while through 2002 and 2003 fPAR is overestimated. A number of factors may contribute to the poorer model fit in these LUs including the distance from the source (inflow) gauge, the nature of the landscape and channel structure where small interference can result in quite dramatic changes in flow paths and inundation, and changes in landuse and vegetation types as some areas have been cleared and more terrestrial species may occur.

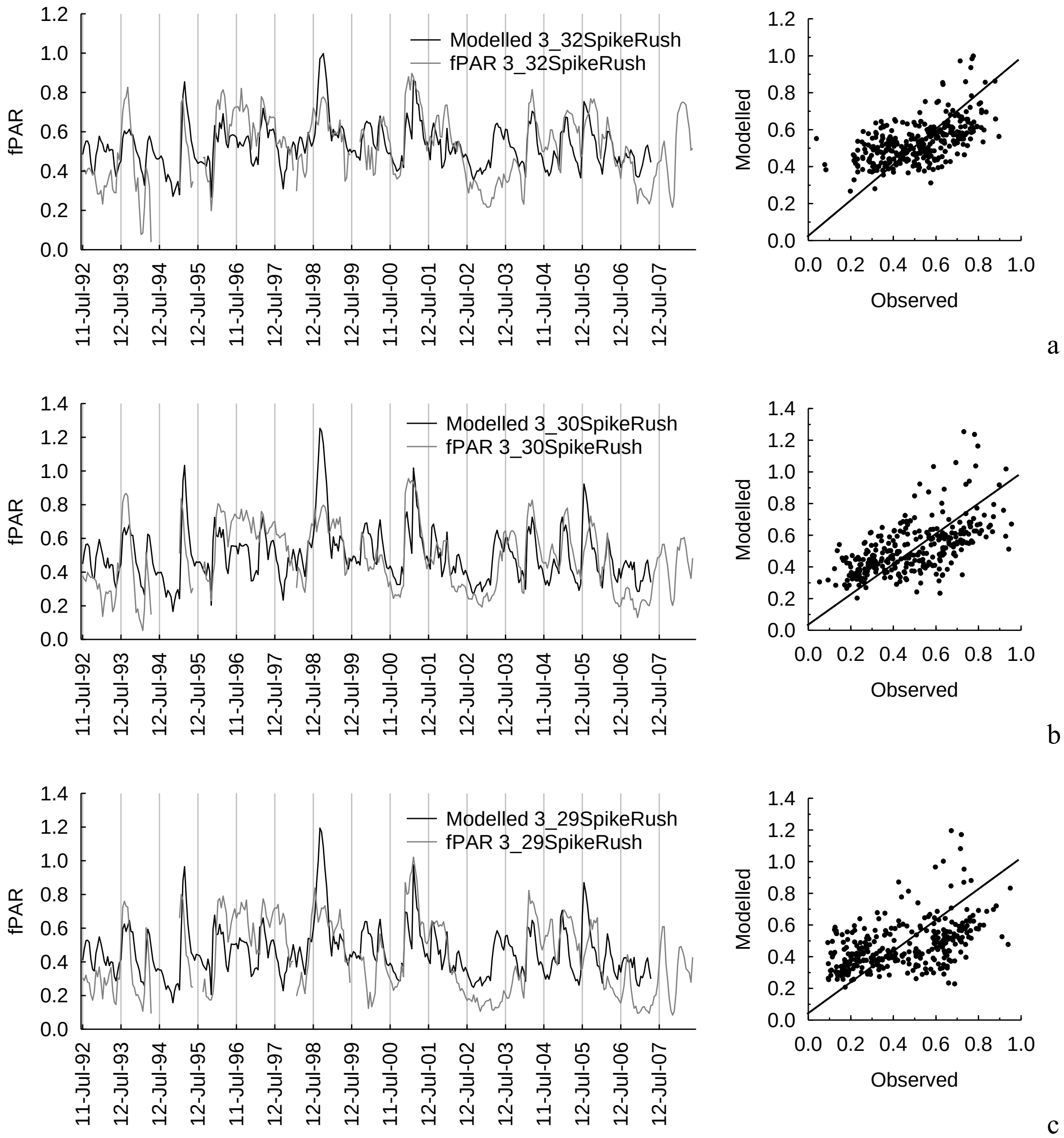

Figure 6.24: Observed and modelled fPAR time series and scatter plots for frequently flooded spike rush landscape units of the western Gingham Channel a) 3_32 spikerush, b) 3_30 spikerush and c) 3_29 spikerush. 1:1 line shown on scatter plots.

The surface plots for these LUs suggest that there is a breakpoint for inflow with a linear relationship above a threshold of around 12 for the combined log of Q, Q_{-1} and Q_{-2} for the eastern-most LU (3_32). For LU 3_30 the breakpoint relates to a log flow of 8 for $Q + Q_{-1}$ while the LU 3_29 is related to $\ln Q_{-1}$ with a breakpoint of 4.5. At low flows, SMS is unlikely to drive high fPAR response.

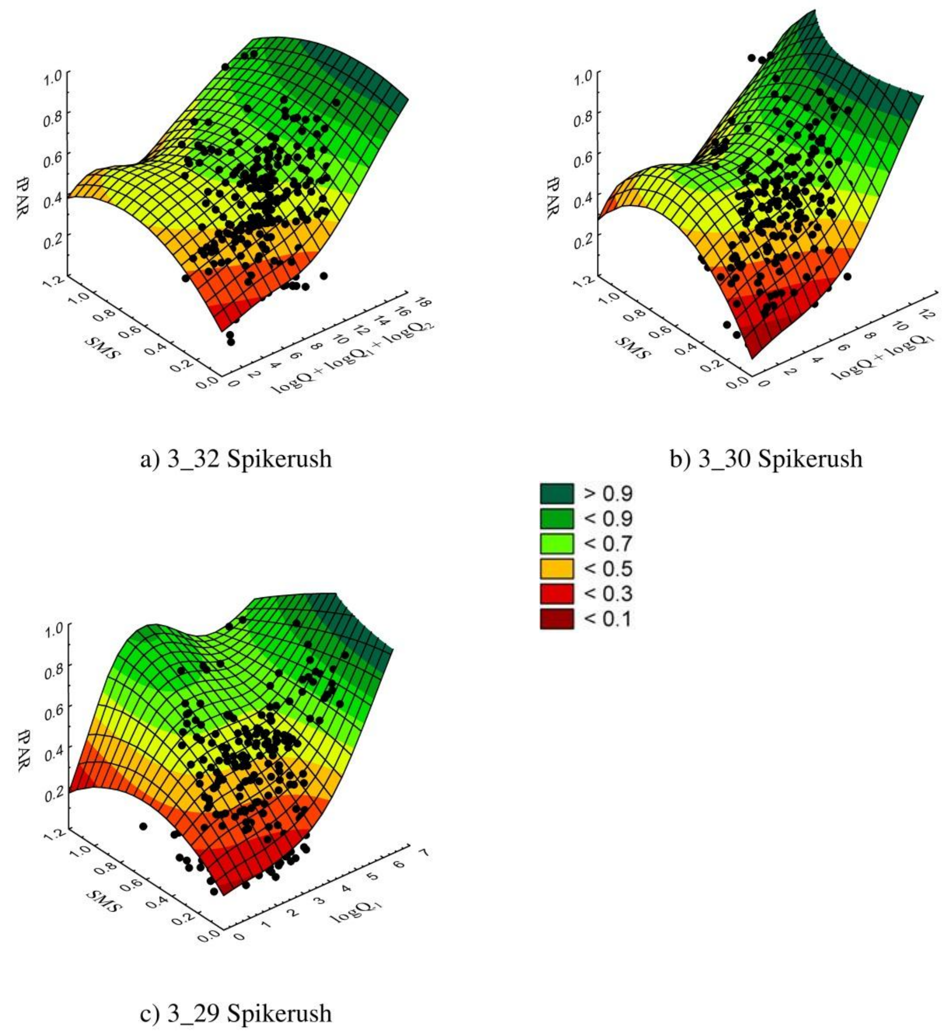

Figure 6.25: Surface plots of fPAR response of spikerush LUs west of Gingham Bridge in relation to soil moisture status and inflows. a) 3_32 spikerush, b) 3_30 spikerush and c) 3_29 spikerush.

In summary the spikerush LUs west of Gingham Bridge can reach high fPAR at maturity but for the period of record this occurs infrequently. There is a clear gradient from east to west with lower fPAR values to the west. The annual pattern of response is less pronounced compared to spikerush LU to the east, with small peaks occurring in September and March but high variability in all months. The LUs have a slightly slower rate of response and may also have a higher and more persistent dormancy fPAR. The relationship with flow and SMS is uncertain but does suggest large inflows are required to drive high fPAR response. The MLR model fit was poor for 3_32 and 3_29 (0.34 and 0.32 respectively) and only fair for 3_30. The model does not therefore provide a reliable predictor of events.

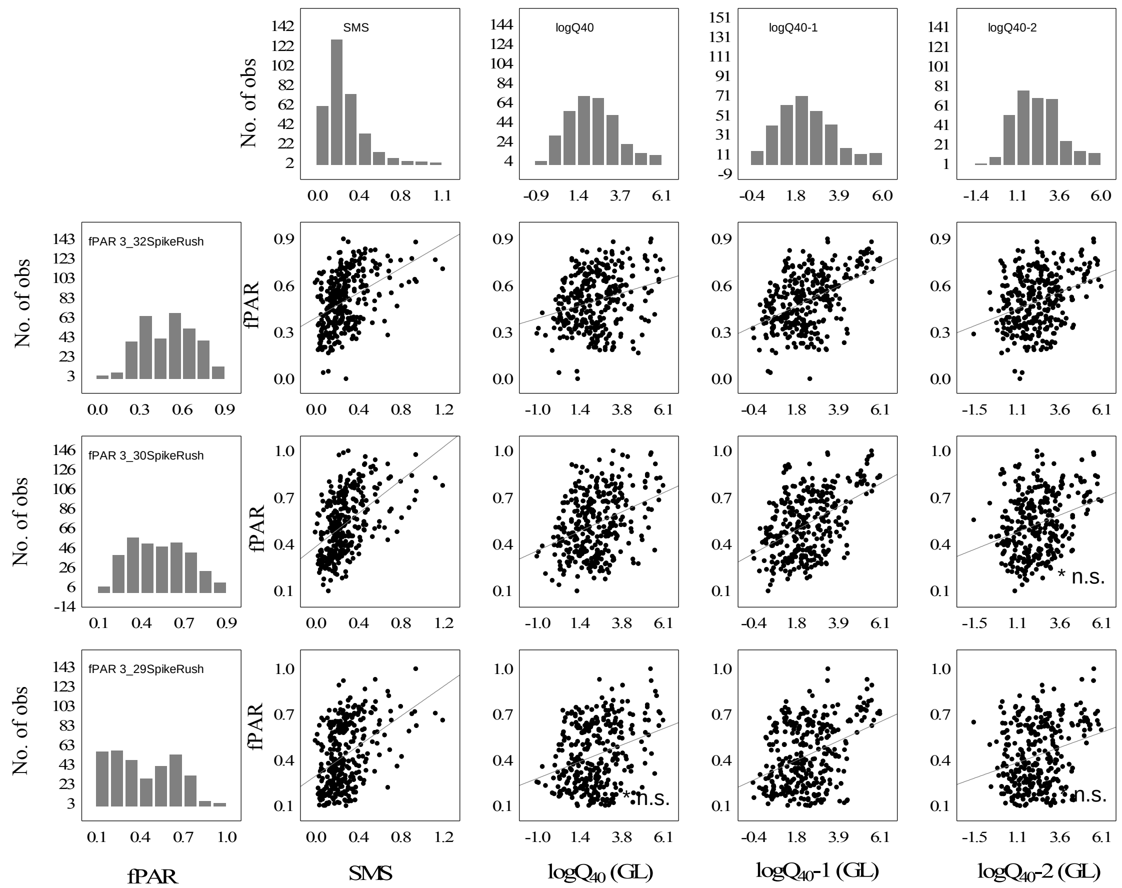

Figure 6.26: Scatterplot of spikerush LUs west of Gingham Bridge in relation to soil moisture status and inflows. Note that non-significant variable in the MLR model are labelled as *n.s.

6.3.3.4 Broader floodplain macrophytes and grasslands

The less frequently inundated areas of spikerush and infrequently flooded native grasslands provide a comparison to the fPAR response and MLR modelling for more frequently flooded wetland LUs. The 2_6 spikerush LU fringes some of the more frequently flooded spikerush LUs in both the Gingham and Lower Gwydir. It would contain similar species to those found in the FF3 spikerush LUs but most likely with an increased proportion of lippia and terrestrial species. Detailed monitoring information is not available for these LUs. Exceeding the peak fPAR of 0.8 on only one occasion in 1996 the response peak is generally closer to a fPAR of 0.7. The dormancy fPAR rarely falls below 0.2 suggesting that the LU has a vegetation cover with some greenness persisting most of the time. The infrequently flooded native grassland LU can respond to peak fPAR of 0.84 (1996) but only exceeded 0.7 on two occasions (1996 and 1998) with peaks of 0.5 – 0.6 more common. The native grassland LU has the lowest dormancy fPAR of any of the LU examined so far, dropping below 0.2 in most years.

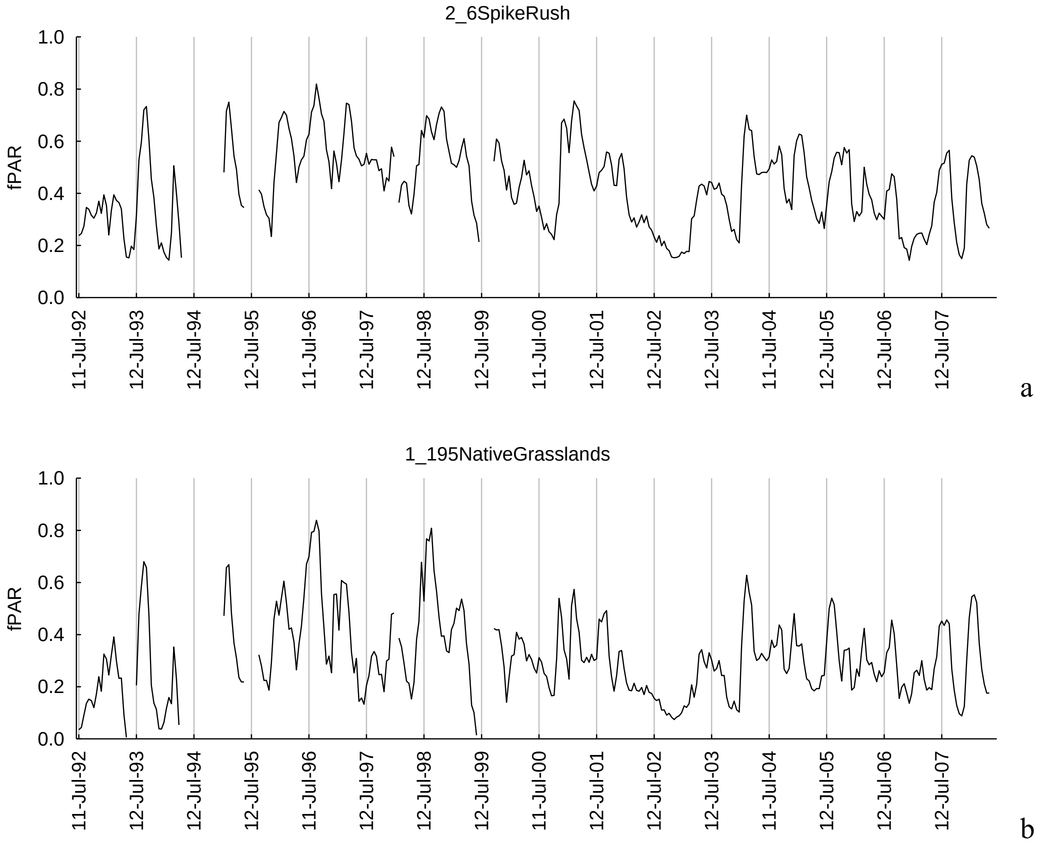

Figure 6.27: Time series fPAR of a) 2_6 spikerush and b) 1_195 native grasslands.

The mean monthly fPAR peaks in August and March in a pattern that has more in common with SMS rather than flow. Lowest fPAR in the grassland LU (1_195) tends to occur in October, November, April and May rather than in the coldest months of June and July for the more frequently flooded wetland LUs (Figure 6.28). The green-up onset and time to reach maturity for the 2003/4 event is similar to other LUs but the peak is lower (0.7 and 0.63 for 2_6 and 1_195 respectively) (Figure 6.28). Senescence commences and dormancy occurs much sooner (22nd April compared to 9th or 25th June for other LUs) however the dormancy fPAR remains at relatively constant level rather than the gradual decease seen in other LUs suggesting a much more persistent, and perhaps terrestrial, vegetation community.

The MLR results show that intercept, SMS and log Q and lnQ-1 are significant for the 2_6 spikerush LU ($p<0.05$) with a reasonable model fit (R^2 of 0.68), while only intercept and SMS are significant for the 1_195native grassland LU with a poor model fit (R^2 of 0.48, Table 6.7).

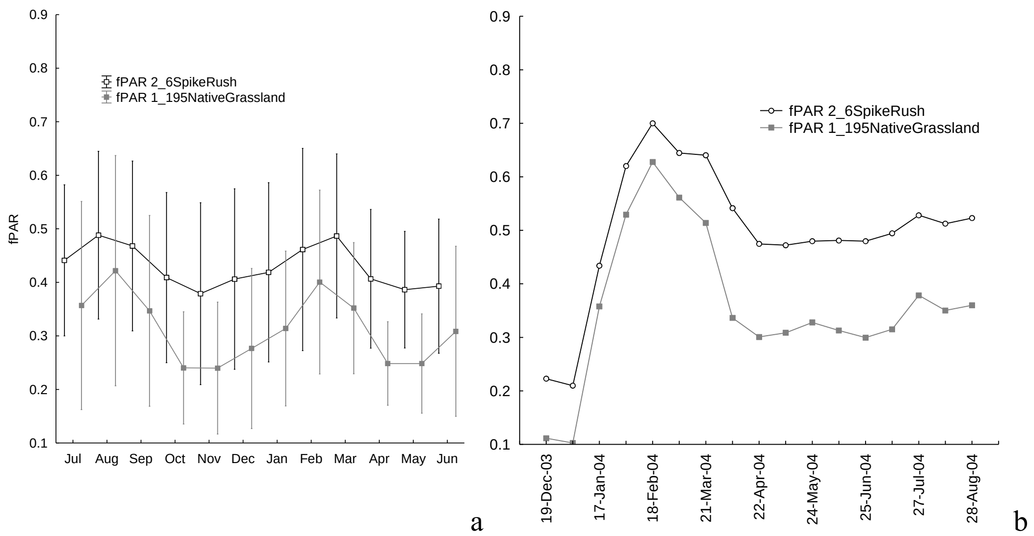

Figure 6.28: a)Mean monthly fPAR (±st dev) and b) 2003/4 fPAR response for 2_6 spikerush and 1_195 native grassland landscape units.

Table 6.7: MLR results for 2_6 spikerush and 1_195 grassland landscape units

Landscape unit	Intercept	SMS	lnQ	lnQ_{-1}	lnQ_{-2}	R^2	St. Error
2_6spikerush	**0.20**	**0.75**	**-0.0241**	**0.0300**	0.0038	0.62	0.09
1_195nativegrasslands	**0.14**	**0.57**	-0.0039	0.0052	-0.0021	0.48	0.09

Significant variables shown in bold ($p<0.05$), Q is 40-day cumulative inflow

Inspection of modelled versus observed time series of fPAR (Figure 6.29) shows a reasonably good representation of most events for the 2_6 spikerush LU, although the events of 1995 and 1996 are underestimated in the model while the 1998 event is overestimated. The surface plot and scatter plots (Figure 6.30) indicate a generally linear relationship between significant inflows and fPAR, with a weak breakpoint suggested around 7 (log Q + lnQ_{-1}), and a weak linear relationship with SMS up to 0.5 with no increase in fPAR above this level.

MLR results for 1_195 native grassland LU tend to underestimate maturity fPAR and overestimate the dormancy fPAR values. The surface plot gives a completely different shape to any other LU with fPAR more strongly related to SMS (Figure 6.30).

The less frequently flooded spikerush and native grasslands rarely exceed 0.8 at maturity with response maturity closer to 0.7 (2_6 spikerush) or 0.5 to 0.6 (native grasslands). Dormancy fPAR may also be more persistent suggesting a terrestrial groundcover with productivity at lower soil moisture conditions compared to wetland species such as spikerush and marsh clubrush. In contrast to other LUs, the native grassland fPAR tends to be lowest in October, November, April and May with a pattern more closely aligned to the SMS annual means. The MLR was fair for 2_6 spikerush (R^2 0.62) with intercept, SMS and flow at Q (negative) and Q_{-1}

significant in the model. The native grassland LU had a lower coefficient of determination (R^2 = 0.48) with only the intercept and SMS significant in the MLR model.

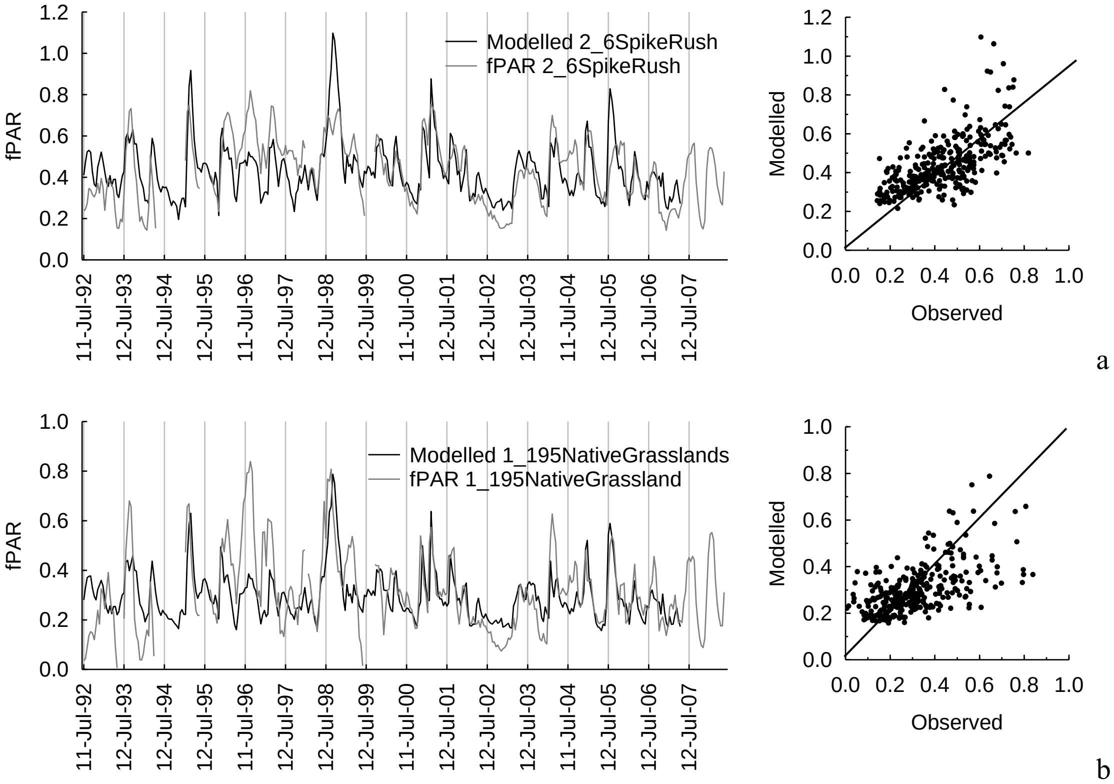

Figure 6.29: Observed and modelled fPAR time series and scatter plots for a) 2_6 spikerush and b) 1_195 native grassland landscape units. 1:1 line shown on scatter plots.

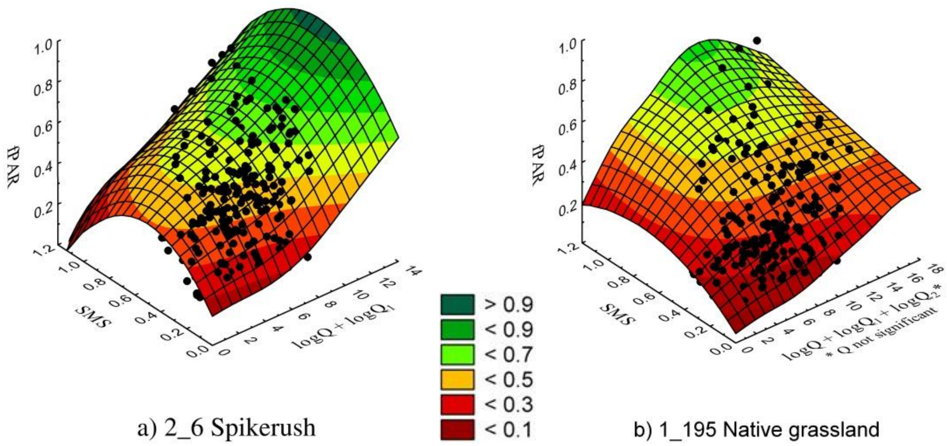

Figure 6.30: Surface plot of fPAR response in relation to flow and SMS in a) 2_6 spikerush and b) 1 _195 native grassland landscape units

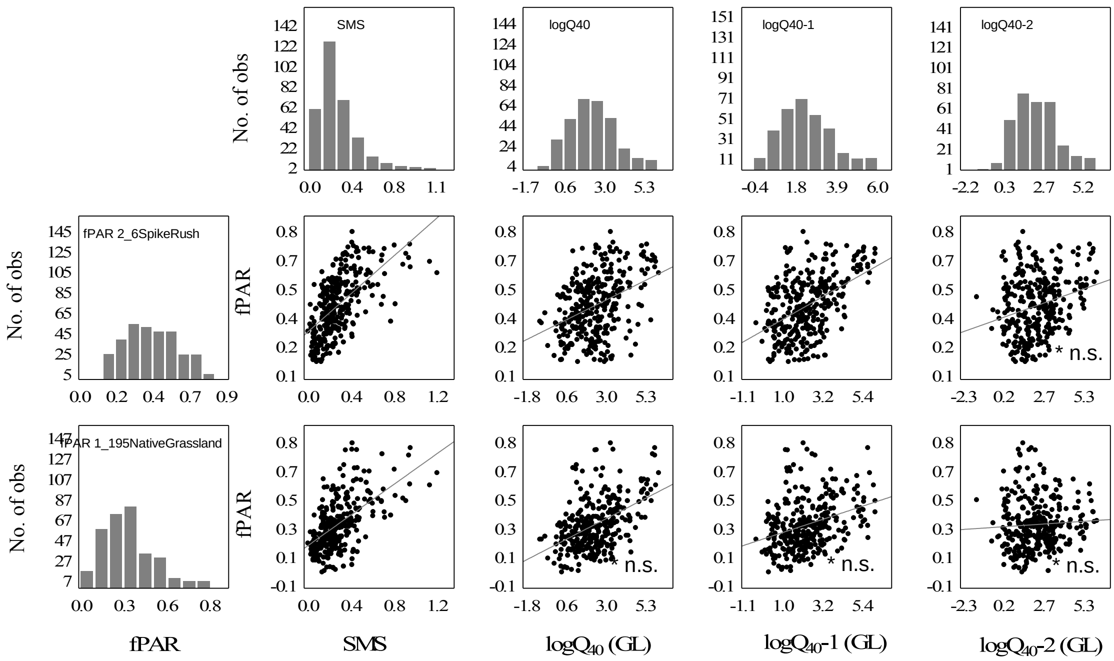

Figure 6.31: Scatterplot of 2_6 spikerush and 1_195 native grassland LUs in relation to soil moisture status and inflows. Note that non-significant variables in the MLR model are labelled as *n.s.

6.3.3.5 Gwydir 'Raft' coolibah and river redgum landscape units

The last of the LUs to be examined in detail is the frequently flooded areas with moderate to dense canopy cover of the Gwydir Raft (Figure 6.32). Most of the monitoring undertaken in the Gwydir wetlands has focussed on the macrophyte dominated spikerush and marsh clubrush communities and there is no detailed information on the Gwydir 'Raft'. The fPAR time series of the 4_227 coolibah and river redgum LU in Figure 6.33a show a much higher dormancy fPAR in comparison to the spikerush and marsh clubrush LUs, with maturity fPAR exceeding 0.8 on seven occasions and 0.7 in most years. Dormancy fPAR is greater than 0.4 and can be maintained over 0.6 for several years. The surrounding 3_210 coolibah and river redgum LU (Figure 6.33b) has slightly lower maturity fPAR and dormancy fPAR values.

Figure 6.32: Aerial photograph of river redgum and coolibah vegetation associated with the Gwydir Raft floodplains

The mean monthly fPAR still peaks in March but the difference between the months is much less than for the spikerush and marsh clubrush LUs and the standard deviation are lower. The pattern of response for the 2003/4 event also has a much higher green-up onset, particularly for 4_227 LU, and maturity fPAR values of 0.89 and 0.76 for 4_227 and 3_210 respectively. The rate of senescence is much slower than any other LUs, fPAR persisting at high to moderate levels for both LUs (Figure 6.34).

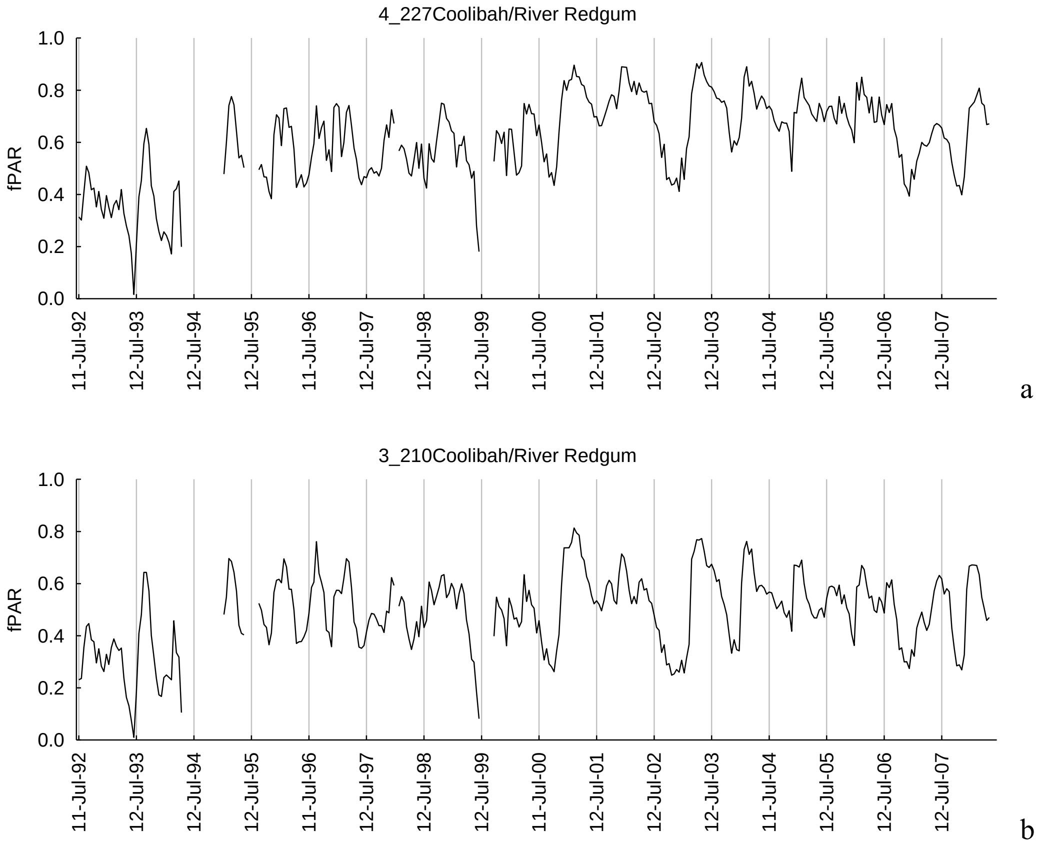

Figure 6.33: Time series fPAR of frequently flooded coolibah/river redgum landscape units associated with the ‘Raft’, downstream of Tyreel regulator a) 4_227 coolibah/river redgum and, b) 3_210 coolibah/river redgum.

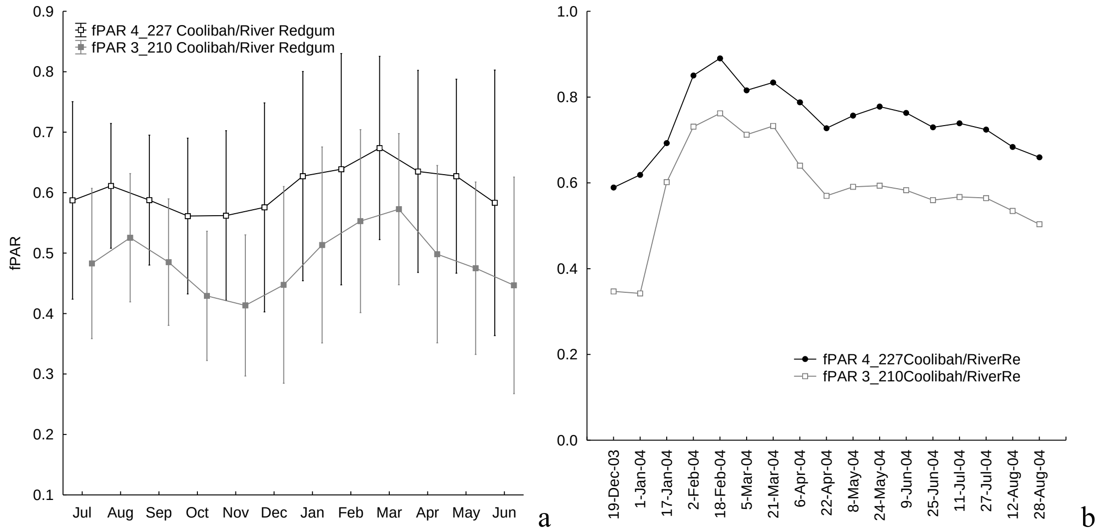

Figure 6.34: a) Mean monthly fPAR (±st dev) and b) 2003/4 fPAR response for coolibah/river redgum landscape units in the 'Raft'.

Model results were poor to fair with R^2 of 0.46 (4_227) and 0.59 (3_210). Intercept, SMS and flow at Q, Q_{-1} and Q_{-2} were all significant in the model ($p<0.05$) (Table 6.8). The modelled time series fit to the observed for 4_227 appears better after 2000. The model was developed using the Modis 2000-2005 time series compared to the AVHRR time series pre-2000. It is not certain whether the better fit to the Modis data are an artefact of the spectral resolution of the sensors and the nature of the vegetation type, or due to the different flood/climate patterns. Overall the periods of maturity and of dormancy are not particularly well represented and the model should be used with caution in those LUs with dense canopy cover.

Surface plot suggest a linear relationship with higher fPAR values associated with higher SMS and higher inflows. This may be due to the canopy cover itself where areas of open water may not reduce the raw NDVI as much as for some other LUs and/or the longer period of response (or depression during prolonged flooding) by woody vegetation. The coolibah/river red gum vegetation LUs also maintains very high fPAR values throughout the period of record. Coupled with low correlation with inflows and SMS this vegetation community may be accessing water from other sources such as groundwater as would be expected as these are evergreen trees.

Table 6.8: MLR results for the coolibah/river redgum landscape units of the Gwydir 'Raft'.

Landscape unit	**Intercept**	**SMS**	**lnQ**	**lnQ_{-1}**	**lnQ_{-2}**	**R^2**	**St. Error**
4_227coolibah/river redgum	**0.54**	**0.36**	**-0.0265**	**0.0294**	**0.0292**	0.46	0.09
3_210coolibah/river redgum	**0.30**	**0.57**	**-0.0243**	**0.0375**	**0.0255**	0.59	0.09

Significant variables shown in bold ($p<0.05$), Q is 40-day cumulative inflow

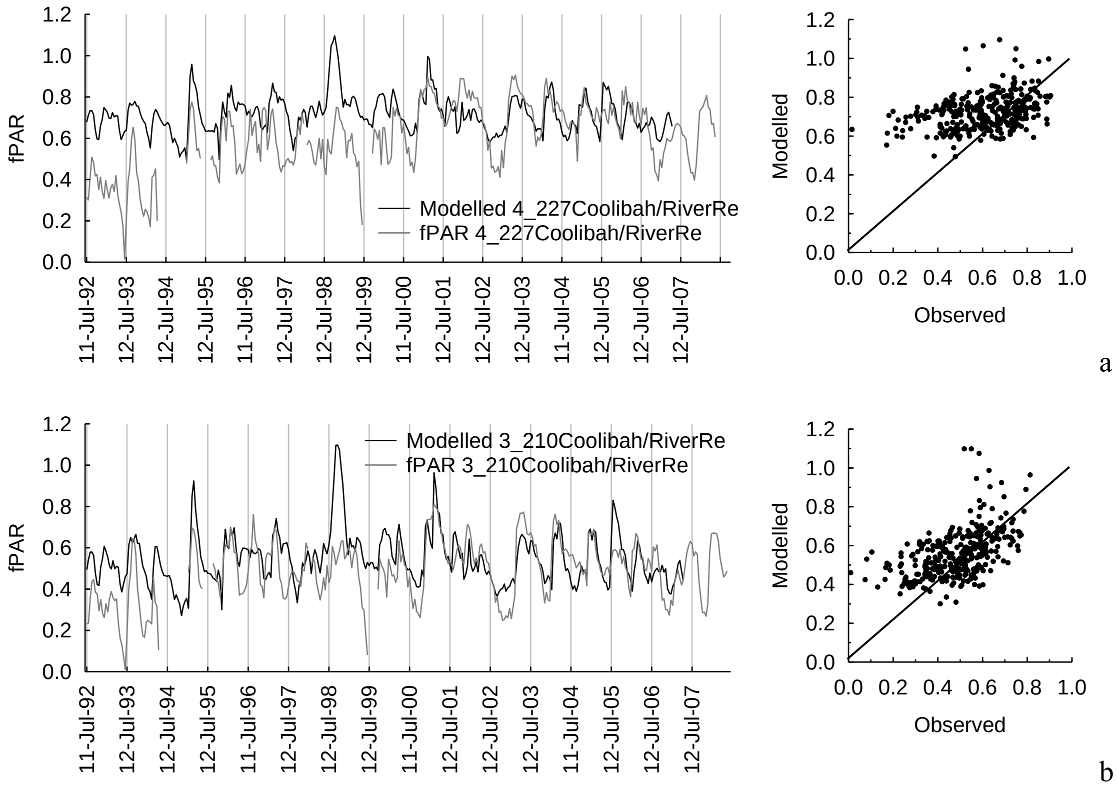

Figure 6.35: Observed and modelled fPAR time series and scatter plots for a) 4_227 coolibah/river redgum and b) 3_210 coolibah/river redgum landscape units of the Gwydir 'Raft'. 1:1 line shown on scatter plots.

The coolibah/river redgum LUs of the Gwydir Raft maintain higher dormancy fPAR values as well as high fPAR at maturity resulting in the highest mean fPAR of any of the LUs. The mean monthly fPAR shows less variability between months. The MLR model is only fair (R^2 of 0.46 and 0.59 with high intercept and the SMS and flow at Q (negative), Q_{-1} and Q_{-2} all significant. These LUs are highly persistent as expected from a relatively dense tree canopy cover.

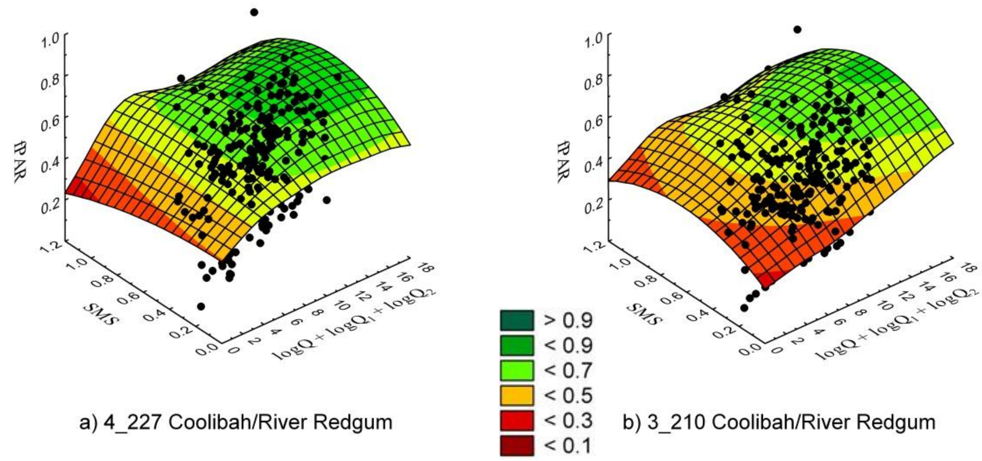

Figure 6.36: Surface plots of fPAR response to flow and SMS in 4_227 coolibah/river redgum and b) 3_210 coolibah/river redgum landscape units.

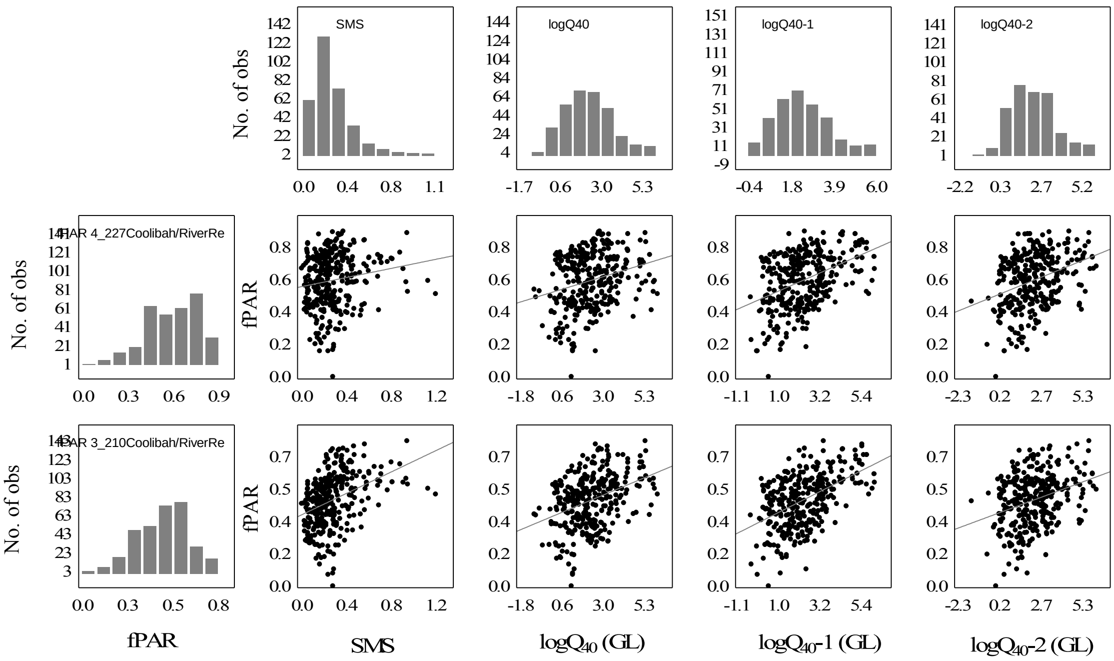

Figure 6.37: Scatterplots of frequently flooded coolibah and river redgum LUs of the Gwydir Raft in relation to soil moisture status and inflows. Note that non-significant variables in the MLR model are labelled as *n.s.

6.3.3.6 Other landscape units

The time series of fPAR values for the remaining LUs are modelled using the MLR method. The coefficient of determination (R^2) range; from greater than 0.7 for some of the more frequently flooded spikerush (4_188), river cooba/lignum (3_118) and open coolibah woodland (3_50) LUs; to less than 0.45 particularly for the less frequently flooded LUs (1_14, 1_195 and 1_177) (Table 6.9). The 4_176 river cooba/lignum LU also has a poor model fit of only 0.40.

Table 6.9 shows the intercept and SMS values that are significant for all LU. Flow at $\log Q_{-1}$ is significant for most LU while Q yields a negative relationship where significant, indicating that event inflows initially reduce fPAR at green-up onset (most likely due to the presence of open water) before fPAR increases at a lag of 40 or more days. Flow at Q_{-2} is only significant for four LUs, including 3_50 river cooba/lignum, 3_153 river cooba/lignum, 3_106 coolibah and 2_6 cleared and cultivated. The 2_6 cleared and cultivated LU has the poorest model fit of all LU (0.35) and negative relationships with flow at Q and Q_{-2}, suggesting that fPAR decreases with increasing flow.

Table 6.9: MLR results for the other landscape units of the Gwydir wetlands.

Landscape unit	**Intercept**	**SMS**	**lnQ**	**$\ln Q_{-1}$**	**$\ln Q_{-2}$**	**R^2**	**st Error**
4_188spikerush	**0.15**	**0.66**	0.0136	**0.0618**	-0.0017	0.71	0.10
4_176river cooba/lignum	**0.18**	**0.60**	-0.0045	**0.0593**	-0.0082	0.40	0.15
3_50river cooba/lignum	**0.27**	**0.65**	**-0.0359**	**0.0464**	**0.0209**	0.69	0.08
3_118river cooba/lignum	**0.15**	**0.50**	0.0083	**0.0609**	0.0025	0.71	0.08
3_50coolibahwoodlands	**0.12**	**0.69**	-0.0056	**0.0531**	0.0123	0.72	0.09
3_50clearedcultivated	**0.15**	**0.77**	-0.0147	**0.0381**	0.0021	0.59	0.11
3_154spikerush	**0.18**	**0.78**	**-0.0324**	**0.0605**	0.0189	0.59	0.13
3_153river cooba/lignum	**0.32**	**0.49**	-0.0165	**0.0490**	**0.0202**	0.56	0.10
3_125river cooba/lignum	**0.12**	**0.84**	0.0002	**0.0324**	-0.0068	0.62	0.11
3_118coolibahwoodland	**0.11**	**0.76**	0.0086	**0.0428**	0.0024	0.67	0.10
3_118clearedcultivated	**0.15**	**0.66**	0.0112	**0.0463**	-0.0127	0.60	0.11
3_106coolibahwoodland	**0.26**	**0.65**	**-0.0281**	**0.0545**	**0.0182**	0.62	0.10
2_6river cooba/lignum	**0.21**	**0.66**	**-0.0299**	**0.0333**	0.0045	0.57	0.09
2_90coolibahwoodlands	**0.16**	**0.63**	-0.0096	**0.0401**	0.0029	0.59	0.10
2_6PoplarBox	**0.24**	**0.57**	**-0.0266**	**0.0225**	0.0066	0.57	0.08
2_6nativegrasslands	**0.12**	**0.61**	0.0001	**0.0205**	0.0031	0.62	0.08
2_6myall/rosewoodAsso	**0.11**	**0.67**	-0.0150	**0.0351**	0.0069	0.58	0.10
2_6coolibahwoodlands	**0.16**	**0.66**	**-0.0142**	**0.0307**	0.0046	0.63	0.08
2_6clearedcultivated	**0.28**	**0.71**	**-0.0387**	0.0008	**-0.0230**	0.35	0.13
2_6belah	**0.28**	**0.63**	**-0.0400**	**0.0280**	0.0077	0.59	0.08
2_245coolibahwoodland	**0.09**	**0.67**	0.0066	**0.0242**	-0.0025	0.49	0.12
1_14river cooba/lignum	**0.24**	**0.53**	**-0.0286**	**0.0204**	0.0131	0.46	0.09
1_195coolibahwoodland	**0.19**	**0.55**	-0.0105	0.0074	-0.0036	0.45	0.09
1_177coolibahwoodland	**0.33**	**0.66**	**-0.0386**	-0.0057	0.0038	0.42	0.10

Significant variables shown in bold ($p<0.05$)

Q is 40-day cumulative inflow

6.4 Discussion

The 16-day MVC period for both Modis and AVHRR provided good estimation for the phenology patterns in the Gwydir LUs. Different time series patterns of fPAR response were found depending on the frequency of flooding, the location and the vegetation types. In other studies, 16-day MVC Modis imagery also allowed for the estimation of subtle changes in vegetation phenology and estimation of green-up onset, maturity and dormancy (Lupo *et al.*, 2007; Sakamoto *et al.*, 2007; Zhang *et al.*, 2003). In the Gwydir, some years show two periods of maturity coinciding with peaks in flow in February and a smaller peak in September, retaining relatively high fPAR throughout the warmer months and lowest fPAR tending to occur in the colder months of July. In contrast the infrequently flooded native grasslands peak in August and February, but the lowest fPAR values tend to occur in October-November and April-May, coinciding with the lowest SMS. This pattern is similar to that found in flooding Pampa grasslands where two production peaks occur in spring and autumn with summer water deficits accounting for a summer decrease in NDVI (Posse *et al.*, 2005). It should be noted that many studies use the NDVI values as a surrogate for productivity and the relationships should be similar to the fPAR used in this thesis.

In wetlands associated with the Parana River Delta in South America, 8km^2 AVHRR NDVI time series correlated with water level and records of local rainfall (Zoffoli *et al.*, 2008). Using a Spearman correlation matrix the NDVI time series was found to correlate more strongly with either the ENSO patterns, having a complex NDVI pattern that related to the fluvial regime, or a more regular annual pattern controlled by tidal patterns or precipitation. The Parana study did not attempt to model the time series response. In the Parana River delta wetlands there is a clear reduction in NDVI during periods of high water level. This contrasts with the short term flooding and rapid vegetation response patterns seen in the Gwydir. The interannual variability due to the action of flood pulses of different intensity and duration in the Parana River delta, however, is similar to the variability found in the Gwydir.

In the Cumbung Swamp, Lachlan Valley, Australia, NDVI was also correlated with flow volumes into the swamp (Shaikh *et al.*, 1998). The highest correlations were for high NDVI response and were associated with typical flood dependent vegetation communities such as Common Reed (*Phragmites australis)* and river redgum. Moderate NDVI values had low correlation with flow and were associated with species such saltbush (*Atriplex nummularia*) where cover attributes are more dependent on the rainfall (Shaikh *et al.*, 1998). A similar pattern of correlations was found in the Gwydir where high fPAR was associated with wetland dependent species and were correlated with flow. Although river redgum exhibited high fPAR values, the correlations with flow were much weaker than for emergent macrophyte vegetation.

The variations in peak fPAR for different LUs with the same mapped vegetation community in the Gwydir are likely to be due to the proportional mix of species. Taller emergent species can co-exist with lower emergents and groundcovers to form a highly productive community in the marsh clubrush dominated LUs, while adjacent spikerush LUs may be missing the taller emergent species. Algae may also occur on or near the water surface which can also increase productivity however IMEF data from the Gwydir wetlands suggests that algae growth or mats are not a dominant feature (unpublished IMEF data, NSW DLWC). The tendency of the LUs with the highest maturity fPAR to have lower dormancy fPAR also suggests a vegetation community highly responsive to flooding but not as tolerant of drying. Similarly, some LUs with lower frequency of flooding exhibit higher and more persistent fPAR at dormancy, suggestive of a terrestrial evergreen vegetation community. The analysis of the LUs of the Gwydir demonstrated that phenology patterns may be used to identify LUs that may exhibit patterns that differ from similar LUs, or from recent data, and warrant further on-ground monitoring. Time series vegetation indices can provide indicators of landscape change processes (Lupo *et al.*, 2007; Pettorelli *et al.*, 2005). As more events are covered by the Modis imagery the phenology patterns of specific LUs in the Gwydir can be documented with increasing certainty, thereby providing a benchmark to assess changes in response patterns to changing flow regimes or vegetation types.

The relationship between the AVHRR NDVI and rainfall was tested in East Africa using 10-day rainfall (significant for up to 8 lag periods), aggregated monthly rainfall and a soil moisture index. The best result was found for aggregated monthly rainfall with average R^2 of 0.36 but up to 0.8 for some locations, while the soil moisture index had an average R^2 of only 0.17 but up to 0.7 for some locations (Eklundh, 1998). In another study (Al-Bakri and Suleiman, 2004) the mean seasonal rainfall was found to have the most significant influence on NDVI with log and power law relationships giving the highest correlations, suggesting a non-linear NDVI response to rainfall. In the Gwydir the exploratory analysis does suggest that relationships between fPAR and soil moisture may be non-linear but the nature of the relationship may depend on the LU. In many cases it could be argued that the relationship may contain breakpoints and be more complex. Despite this, the rainfall and evaporation aggregated to 16 days (including lag intervals) and the modelled climate driven soil moisture (SMS) are both significant in the linear relationship with fPAR response, with average R^2 of 0.53 (maximum of 0.69) and 0.43 (maximum of 0.59) respectively. Eklundh (1998) does argue that the impact of non-stationarity in the rainfall and NDVI data and the impact of autocorrelation may result in elevated R^2 values. These factors were not considered explicitly in this thesis and may require further consideration if these types of models are further developed.

Ground validation of the pixels (i.e. 1km^2 or 250m^2) remains problematic (Lupo *et al.*, 2007) and the field programs for monitoring vegetation are typically species-specific and collected at scales not compatible with the coarser resolution of remote sensing observations (Zhang *et al.*, 2003). In the course of this analysis for the Gwydir wetlands, field vegetation data from the IMEF program (Chessman and Jones, 2001) were used to attempt to validate the remotely sensed data but was found to have these same problems (Powell et al. 2007). The data were reported in terms of vegetation cover and species but the 'greenness' of productivity may not relate directly to vegetation cover. It appears that through the period of senescence in the spikerush and marsh clubrush LUs, vegetation cover and community structure may remain unchanged even though the vegetation yellows and becomes chlorotic. Penuelas *et al.* (1993) reported that *Ludwigia sp.* may exceed 0.8 (NDVI) when healthy but less than 0.6 when chlorotic showing that productivity falls despite retaining 100% cover.

6.5 Conclusions

Using the fPAR time series for LUs in the Gwydir wetlands the response to soil moisture, due to local rainfall and evapotranspiration, and inflows can be assessed in relation to vegetation productivity. The phenological cycles of green-up, maturity, senescence and dormancy could be detected and quantified for individual LUs with differences identified based on flood frequency, vegetation type and location. All LUs showed high variability in mean monthly fPAR values, however there were pattern similarities between frequently flooded LUs and the seasonality of inflows. In contrast, infrequently flooded native grasslands exhibited mean monthly fPAR values that were similar to the SMS monthly distribution. The results for the Gwydir indicate that time series remotely sensed vegetation indices such as the Modis and AVHRR NDVI can be applied to characterising vegetation productivity patterns in macrophyte wetlands.

Rainfall and evaporation provided better regression fits than estimated soil moisture store when modelling fPAR time series against climate alone. However when combined with flow it was found that the soil moisture store variable combined with inflow functions provided the best model fit with an average adjusted R^2 of 0.57 and exceeding 0.7 for some LUs. The inflow functions were the log of 40-day inflow at lags of 0 (0-40 days), -1 (40-80 days) and -2 (80-120 days). Flows beyond 120 days were not significant in fPAR response for any LU and inflows were not significant at all in the infrequently flooded native grasslands. The use of exploratory graphic tools such as surface plots provided some evidence that the relationship between climate, flow and fPAR response may not be linear. The response may have breakpoints where it changes and these patterns may vary between LUs. Considering the number of other factors that would influence vegetation response including seasonality, the distance from the gauge, landuse and provision of environmental flows targeted at particular locations, the MLR model provides a good basis for comparison of fPAR response to different inflow scenarios for many of the LUs. For some LUs, particularly those less frequently flooded and to the west of the study area, the results were less satisfactory. One of the main reasons is likely to be the distance from the inflow gauge used because the relationship between flow gauges becomes weaker as a flood travels across the landscape.

In Chapter 7, a simple water balance model based on conceptual models developed in earlier work (Powell, 2005; Powell *et al.*, 2008) is further developed using the results from the flow and inundation analysis in Chapter 5. The multiple linear regression model of fPAR response developed in this chapter is applied to inflows to the water balance model.

Chapter 7: Developing an inundation and vegetation response model

7.1 Introduction

The research presented in Chapters 5 and 6 provide some insight into the flood behaviour and vegetation productivity response in the Gwydir wetlands. The floodplain landscape of Chapter 5 was characterised by flood frequency and connectivity using remote sensing analysis to help provide homogenous patches in relation to the water balance. Patches are also subdivided by vegetation community to provide a template of relatively homogenous landscape units (LUs) that can be expected to respond in similar spatial and temporal dimensions to the flood pulse. Using these LUs, Chapter 6 developed an understanding of the temporal response of vegetation productivity as measured by the fraction of photosynthetically active radiation (fPAR) and modelling this response to inflow and climate drivers.

In this chapter, this information is used to develop a water balance model of the Gwydir wetlands downstream of Gwydir River at Yarraman gauge and to link the multiple linear regression (MLR) models of vegetation response to inflows and rainfall (Figure 6.1). A node-network approach is used to model the water balance through the Gwydir wetlands. Node-network approaches are commonly used to assess resource management problems in general (Letcher and Jakeman, 2003; Letcher *et al.*, 2007; Letcher *et al.*, 2004; Podger and Hameed, 2000; Simons *et al.*, 1996) and can be used to manage environmental flows in particular (Whigham and Young, 2001). In the Gwydir wetlands a decision support system (Ibis) has been developed which links node-network water balance model outputs to ecological response using discrete Bayesian network models, regression equations and/or empirical models (Merritt *et al.*, 2010). The ecological attributes considered in Ibis relate to indicators of bird, fish and vegetation response at a species or community scale. The Ibis ecological models are Bayesian models of species-specific response at the event scale. In contrast, the new work in this thesis could contribute by enhancing the knowledge of variables at the nodes used in the water balance model, identifying landscape units relevant to the existing vegetation models and by the addition of the overall productivity model of vegetation response.

The inundation and vegetation response model (IVRM) developed in this chapter is verified using observed flow data where available and behaviour is tested against the observed vegetation productivity. As many parameters in the IVRM are based on expert opinion, the sensitivity of the model to some of these parameters is tested and the uncertainties discussed.

The IVRM is used to model a range of inflow and climate change scenarios drawn from the CSIRO Sustainable Yields (SY) project (CSIRO, 2007), and the possible impacts of these scenarios on the water balance and vegetation productivity in the Gwydir wetlands is discussed. The IVRM also has application to further research to link vegetation productivity response to local flood behaviour and to develop discrete Bayesian networks and other models for use in decision support systems such as the Ibis DSS.

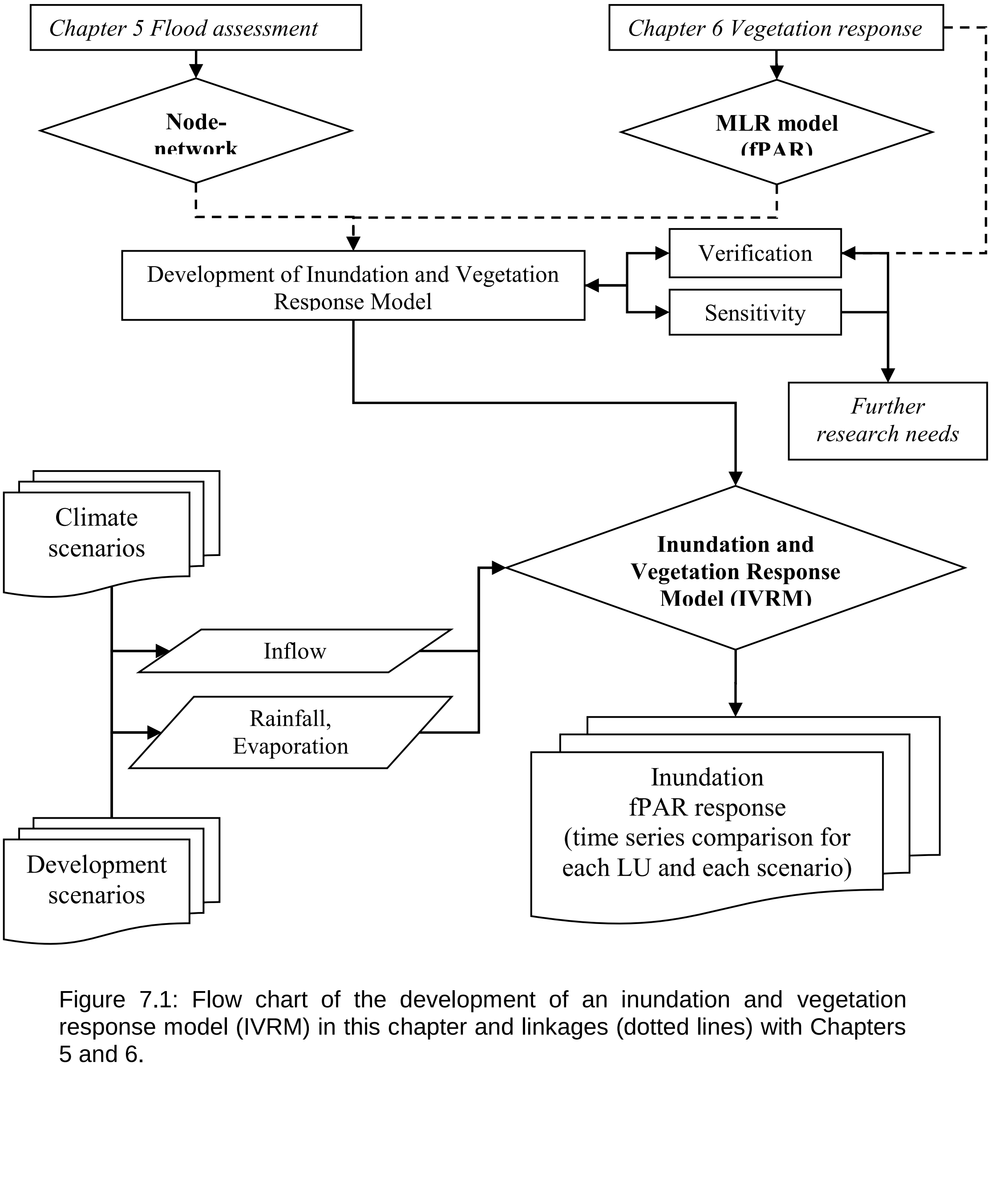

Figure 7.1: Flow chart of the development of an inundation and vegetation response model (IVRM) in this chapter and linkages (dotted lines) with Chapters 5 and 6.

7.2 Development of an inundation and vegetation response model

The IVRM is developed following the ten steps approach to model development delineated in Jakeman *et al.* (2006) and applied in Welsh (2008) and Robson *et al.* (2008) to a groundwater modelling problem and a hydro-ecological one, respectively. The purpose of the model is to improve our understanding of the system, to apply the knowledge base developed within the thesis and to explore the predictive capacity of water balance and vegetation response models in water management and climate change scenario applications.

The IVRM is developed in the Integrated Component Modelling System (ICMS) and is limited to the lower Gwydir wetlands downstream of the Gwydir River at Yarraman gauge. ICMS is a model-building and delivery environment developed by CSIRO Land and Water (Reed *et al.*, 1999) to facilitate the rapid development of catchment models. Catchment and/or processes are represented by classes and objects that can be linked, building up a sequence of processes to be executed. The IVRM focuses on the more frequently flooded parts of the landscape defined in Chapter 5 with particular emphasis on the macrophyte-dominated landscape units.

7.2.1 Water balance model

The water balance model of the IVRM is based on a number of different component models which route and calculate the water balance across the landscape and is a development of the Gwydir floodplain model (Powell, 2005; Powell *et al.*, 2008). As shown in Figure 7.2 the water balance model includes channel, wetland and floodplain components with water routed from one object to the next depending on the volume of water held within each. In the IVRM each object represents a node or a spatial area of the landscape and has a specific model (such as a channel, wetland or floodplain model) as well as individual object parameters. Figure 7.3 shows the full system model and linkages between the objects which was developed from the outcomes of Chapter 5, specifically the node-link conceptualisation in figure 5.30.. Each of the objects and their component models are described below.

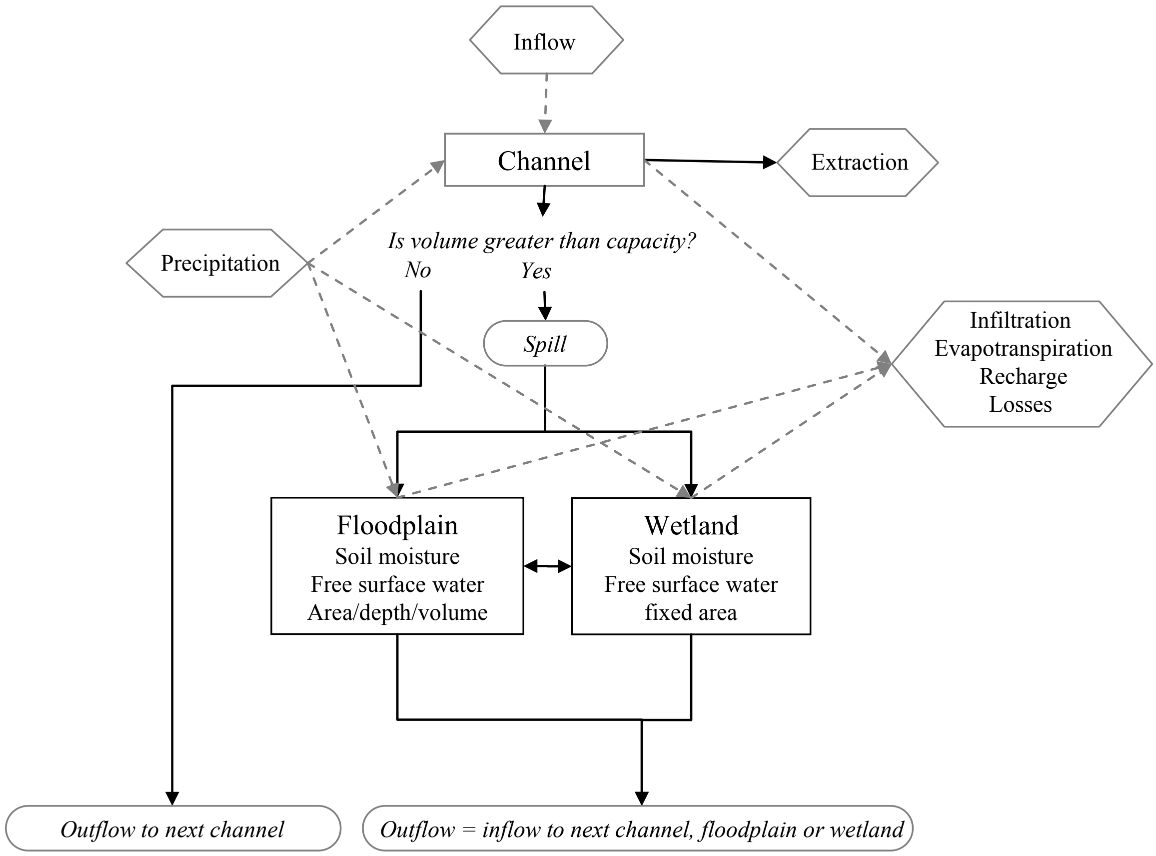

Figure 7.2: Components of the floodplain water balance model (Powell, 2005; Powell *et al.*, 2008).

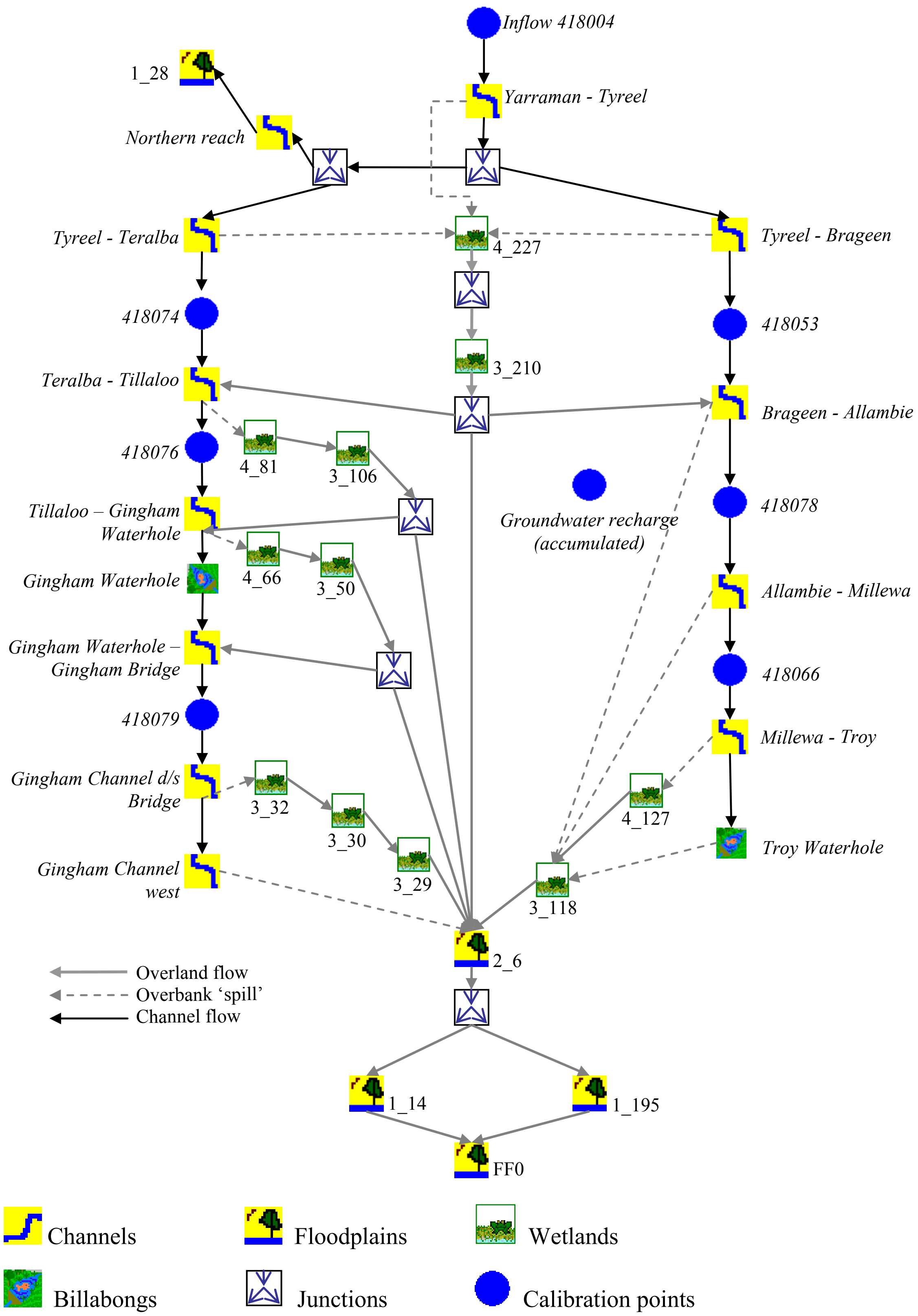

Figure 7.3: System view of the Gwydir wetlands IVRM. All overland flow, wetlands and floodplains also link to groundwater recharge (links not shown).

7.2.1.1 Channels

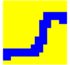 The channel objects within the model route water through defined river, creek or constructed channels. Each channel is described by the reach capacity (daily flow ML/d) as estimated from gauging stations or expert knowledge (Table 7.1). Losses (or gains) from each channel reach include evaporation and rainfall over the surface area of the channel reach, estimated regulated water extractions, constant losses to account for stock watering and general farm or household water use, and deep drainage and bank wetting losses proportional to flow. Volume in excess of capacity is 'spilled' into connected wetlands or floodplains while the remaining volume is routed to the next channel reach.

Table 7.1: Parameters used in the channel objects for Gwydir IVRM

Reach	**Calibration gauge**	**Capacity (ML/day)**	**Loss proportion**	**Length (km)**	**Width (m)**
Yarraman - Tyreel	na	50000	0.2	8.27	65
Gingham					
Tyreel-Teralba	418074	9000	0.2	11.4	25
Teralba-Tillaloo	418076	2000	0.2	34.6	8
Tillaloo – Gingham WH	none	400	0.25	31.7	10
Gingham WH – Gingham Bridge	418079	4000	0.25	4.9	25
Gingham West	none	200	0.3	30	10
Gingham West1	none	50	0.4	30	5
Lower Gwydir					
Tyreel-Brageen	418053	9000	0.2	26.2	40
Brageen-Allambie	418078	4000	0.2	16.0	20
Allambie-Millewa	418066	800	0.25	7.1	15
Millewa – wetlands	none	100	0.25	17.3	5
Northern Reach					
Northern Reach	none	500	0.3	40	5

7.2.1.2 Wetlands (FF4 and FF3)

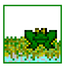 The wetland model components are represented as a bucket model with a predetermined area and maximum depth and can be conceptualised using the 'egg carton' analogy, as mentioned in Chapter 2, wherein the landscape is a "*a collection of depressions rather like an egg carton, but where the depressions are irregularly shaped, have varying depths and are separated by divides of varying height*" (Jones *et al.*, 2008). The area is determined from analysis of the connected patches in Chapter 5. The frequently flooded (FF4 and FF3) patches are considered as relatively homogenous wetlands (i.e. the *depressions*). Depths (maximum and threshold) are estimated from IMEF monitoring data where available (Mawhinney, pers. comm.) or from expert opinion and personal knowledge. All parameters

used in the Gwydir wetland components of the IVRM are shown in Table 7.2. Depending on the volume held within a wetland, four discrete states are modelled as shown in Table 7.3.

Table 7.2: Parameters used in the wetland objects of the Gwydir IVRM

Patch	**Area (A)** **km^2**	**Maximum depth (m)** **mm**	**Threshold depth (t)** **mm**	**Outflow rate** β	**Field Capacity** **mm**	**Et factor f**
4_227	3	500	50	0.75	250	1
3_210	36	400	50	0.5	250	1
4_127 188	5	400	200	0.3	250	1
3_118	56	400	200	0.3	250	1
4_66	10	500	300	0.3	250	1
4_81	3	400	200	0.4	250	1
3_50	40	400	100	0.5	250	1
3_32	5	400	200	0.5	250	1
3_30	6	400	200	0.5	250	1
3_29	1	400	200	0.5	250	1
3_106	3	400	100	0.5	250	1

Table 7.3: Wetland states using in the IVRM

State	**Description**	**Freewater F_t**	**Depth D_t**	**Soilwater SW_t**	**Effective Et**	**Outflow O_t**
1	Not flooded. Vt <= FC * Area	0	0	V_t/A	$SW_t/FC*f*Et$	0
2	Flooded, depth <= threshold (flooded, no outflow)	V_t-(SW_t*A)	F_t/A	FC*A	f*Et	0
3	Flooded, threshold<depth<=maxdepth (flooded and spilling)	V_t-(SW_t*A)	F_t/A	FC*A	f*Et	$\beta*(F_t–(t*A)$
4	Flooded, depth > maxdepth (flooded and spilling)	V_t-(SW_t*A)	F_t/A	FC*A	f*Et	F_t-(A*m)

V_t = Volume at time t (ML)
A = Area (km^2)
β = outflow rate
m = maximum depth

FC = Field capacity of soil
f = Et factor (1 is pan Et at Moree)
t = threshold depth

7.2.1.3 Floodplain (FF2 and FF1)

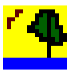

Unlike the wetlands, floodplains are generally larger areas where both the area inundated and depth can vary dramatically depending on the flood event. The less frequently flooded patches (FF2 and FF1) are defined as floodplains in the model with a generalised volume/area/depth relationship. As for the wetland components, soil water is calculated within the floodplain model. This is a little more complicated as the variable area of inundation is necessarily represented by two soilwater 'buckets'. The area that has not been influenced by recent inundation has a climate driven soil moisture profile, while areas that have had surface inflows have additional water available to the soil profile. When water is routed to the floodplain object, soil water over the initial estimation of inundated area is filled first. The remaining volume of 'freewater' (F) is used to calculate the final inundated area (A) as shown in Equation 7.1. If the depth is greater than a threshold depth (T) then water is routed out of the floodplain object at a rate (Beta) of the available freewater. If the depth is less than the threshold depth then a slower rate (Beta1) of outflow is used. The parameters used in the floodplain objects of the Gwydir IVRM are shown in table 7.4.

$$A_t = \sqrt{2A_{max}D_{max}} * \sqrt{F}_t \qquad \text{Equation 7.1}$$

Table 7.4: Parameters used in the floodplain objects of the Gwydir IVRM

Patch	**Max Area (A) km^2**	**Maximum depth (D) mm**	**Threshold depth (T) mm**	**Beta**	**Beta1**	**FC mm**	**Et factor f**
2_6	648	200	100	0.4	0.05	250	1.1
1_28	133	200	100	0.5	0.1	250	1.3
1_14	988	200	100	0.5	0.1	250	1.3
1_195	87	200	100	0.5	0.1	250	1.3
FF0	1000	200	100	0.5	0.1	250	1.3

7.2.1.4 Billabong

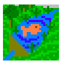

Billabongs are natural depressions within or adjacent to channels that hold near permanent water at depths that generally preclude emergent vegetation, except along the margins (Figure 7.4). Although an important feature of the system, these billabongs hold small volumes of water at fairly constant, but shallow, depths. The model used is also a simple bucket type with outflows occurring over a depth threshold. The major loss is through evapotranspiration from the open water surface.


a

b

Figure 7.4: Billabongs in the Gwydir wetlands a) Troy waterhole and b) Gingham waterhole

7.2.1.5 Junctions

The junction model allows distribution of water in several ways. If a commence to flow (CTF) is not set (CTF = 0) then the water is distributed based on proportion of inflow. If a CTF is set then inflows below a CTF will follow one set of rules, while above a CTF another set of rules can be adopted, as shown in Table 7.5. The CTF is simply a trigger for a specific action but does equate to real world commence to flow (or commence to fill) which describe the flow (or level) required for water to flow into or fill a wetland, effluent channel or cut-off billabong feature (to name but a few geomorphic features to which this term may be applied).

Junctions are also used to route water to groundwater storage. In the CSIRO SY report (CSIRO, 2007), eastern portions of the Gwydir River and Gingham Channel downstream of Moree are assessed as high losing streams (high hydraulic conductivity zone, 5 to 50m/day) while the western portions are medium to low losing streams. Estimated recharge for the lower Gwydir Alluvium is between 40 and 60GL/yr (most years) which includes the Mehi River. With limited information available water is simply routed as a percentage of the outflows to groundwater storage. The model is calibrated to give an average volume over the seven years used for model testing. This volume is approximately 20-40GL/yr that equates to a cumulative volume of 140 – 280GL for the seven year period to approximate the recharge from the Gwydir and Gingham alone.

Table 7.5: Rules governing outflow from the Junction model of the IVRM

CTF	CTF1	Inflow (I)	Outflow1 (O1)	Outflow2 (O2)	Outflow3 (O3)	Outflow4 (O4)
0			P1*I	P2*I	P3*I	P4*I
>0		< CTF	I	0	0	0
>0	0	>= CTF	P1*I	P2*I	P3*I	P4*I
>0	1	>= CTF	CTF	P1*(I-O1)	P2*(I-O1)	P3*(I-O1)

I = Inflow
P = Proportion
CTF – Commence to flow level

7.2.1.6 Calibration points

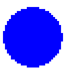

For calibration and model testing the modelled flow or depth to gauged or measured time series or point data is compared. Table 7.1 and Figure 7.3 show the calibration points used for the channel reaches in the Lower Gwydir model.

7.2.2 Vegetation model

Vegetation productivity is linked to total system inflows and the climate driven soil moisture status. Climate driven soil moisture status (SMS), which is defined as a proportion of field capacity, is stored as a global object available to all model components and is based on input rainfall and pan-evaporation. Cumulative inflows are also calculated for each antecedent period from the inflows at Gwydir River at Yarraman gauge. There were included as global objects in the model structure. Both are made available to all objects in the IVRM. Each wetland and floodplain model includes the multiple linear regression (MLR) equation of fraction of photosynthetically active radiation (fPAR) response, linked to the global SMS and cumulative flows for the most productive or largest landscape unit. The MLR model can drive fPAR beyond the maximum as discussed in Chapter 6. The MLR fPAR output from the IVRM is capped at a maximum of 1.

Table 7.6: Landscape patches and associated landscape units used in the MLR fPAR model within the IVRM.

Patch	Model	Landscape unit	Intercept	SMS	lnQ40	$lnQ40_{-1}$	$lnQ40_{-2}$
4_81	Wetland	4_81spikerush	-0.03	**0.70**	**0.0206**	**0.0716**	0.0112
4_66	Wetland	4_66spikerush	**0.22**	**0.31**	0.0056	**0.0681**	**0.0421**
4_227	Wetland	4_227coolibah/river redgum	**0.54**	**0.36**	**-0.0265**	**0.0294**	**0.0292**
4_127	Wetland	4_127marshclubrush	**0.16**	**0.71**	**0.0262**	**0.0611**	0.0050
3_50	Wetland	3_50spikerush	**0.15**	**0.60**	-0.0043	**0.0602**	**0.0181**
3_32	Wetland	3_32spikerush	**0.31**	**0.47**	**-0.0321**	**0.0418**	**0.0269**
3_30	Wetland	3_30spikerush	**0.20**	**0.79**	**-0.0314**	**0.0502**	0.0168
3_29	Wetland	3_29spikerush	**0.17**	**0.78**	-0.0228	**0.0385**	0.0149
3_210	Wetland	3_210coolibah/river redgum	**0.30**	**0.57**	**-0.0243**	**0.0375**	**0.0255**
3_118	Wetland	3_118spikerush	**0.16**	**0.65**	0.0145	**0.0522**	0.0052
3_106	Wetland	3_106coolibahwoodland	**0.26**	**0.65**	**-0.0281**	**0.0545**	**0.0182**
2_6	Floodplain	2_6spikerush	**0.20**	**0.75**	**-0.0241**	**0.0300**	0.0038
1_195	Floodplain	1_195nativegrasslands	**0.14**	**0.57**	-0.0039	0.0052	-0.0021
1_14	Floodplain	1_14river cooba/lignum	**0.24**	**0.53**	**-0.0286**	**0.0204**	0.0131

SMS = Soil moisture status (proportion of field capacity)

Q40 = 0 - 40-day antecedent cumulative inflows (GL)

$Q40_{-1}$ = 40 – 80-day antecedent cumulative inflows (GL)

$Q40_{-2:}$ = 80-120-day antecedent cumulative inflows (GL)

7.2.3 Verification

The IVRM is run using the full model construct driven by daily flow for Gwydir River at Yarraman (418004) and routing through the Tyreel junction on a 40% to Gingham and 60% to Gwydir split. Without any detailed information on weir operations the 40/60 split has been adopted for the model 'base-case' as it provided the best overall fit to downstream gauges.

Model error assessment is presented where there is observed data available for comparison. The root of the mean square error (RMSE) and coefficient of determination (r^2) are used to evaluate the goodness of fit to observed data (Costelloe *et al.*, 2005; Legates and McCabe, 1999). For the IVRM the time delays in the system have not been replicated. Generally these delays are in terms of days and are of a complexity that is beyond the requirements of this model. Verification and further model evaluation is therefore based both on the daily model outputs but also on the 16-day maximum value composite (MVC) periods and/or with cumulative data where appropriate, to reduce the effects of minor differences in timing.

7.2.3.1 Channels

Model fit was poor for most sites at the daily time-step but was generally good for the MVC 16-day time-step (Table 7.7). This was to be expected with the model not attempting to replicate the relatively short time delays through the system. In addition the model is optimised to fit the majority of flows through the time-series and may therefore under or overestimate the peak flows.

Table 7.7: Model performance at daily and 16-day maximum value composite periods of the channel reaches in the Gwydir IVRM

Gauge	Daily			16-day MVC		
	n	**RMSE**	**r^2**	**n**	**RMSE**	**r^2**
418074	2222	396	0.80	146	167	0.95
418076	1973	417	0.50	131	322	0.74
418079	2321	592	0.32	150	361	0.75
418053	2422	540	0.70	156	196	0.92
418066	2408	133	0.45	157	74	0.73
418078	2191	297	0.75	144	139	0.92

Gingham Channel at Teralba 418074

The Gingham Channel at Teralba (418074) has a maximum gauged stage of 3.4m and a maximum recorded stage of over 3.8m (mean daily) rated at over 9000ML/day (Figure 7.7). With only two gaugings for flows greater than 1000ML/d there is some uncertainty for the conversion of gauge height to flow at higher flows. The model fit to this gauge is very good with timing and quantity well represented by the model at both daily and MVC periods (Figure 7.6).

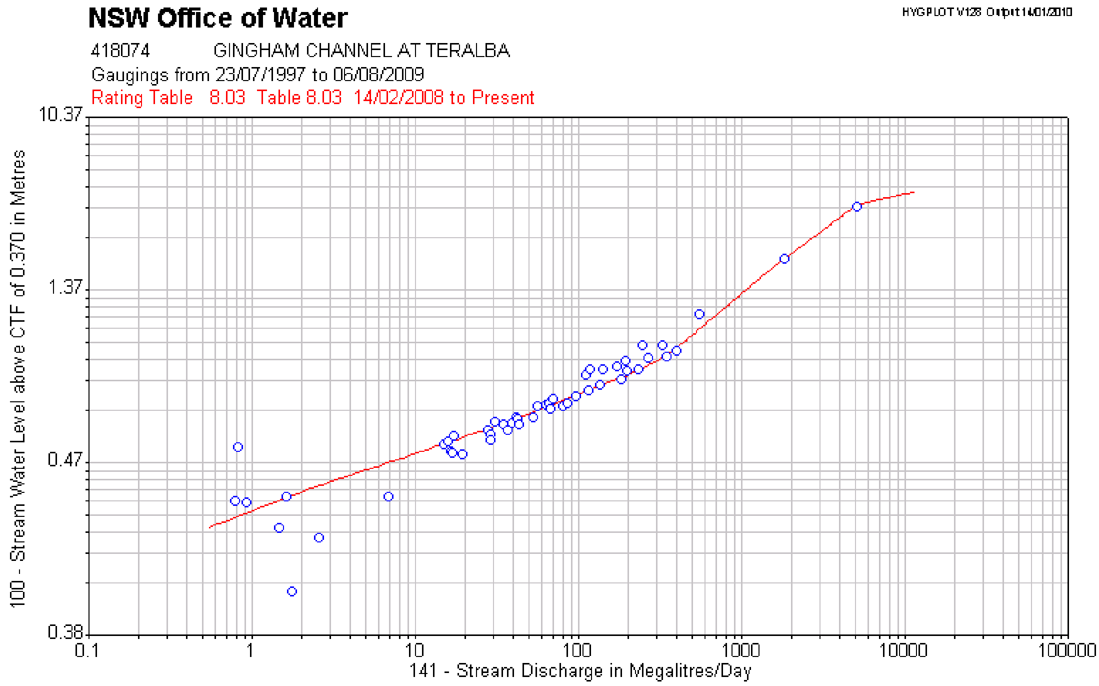

Figure 7.5: Gaugings and rating curve for Gingham Channel at Teralba (418074) (NSW Water Information, http://waterinfo.nsw.gov.au/ accessed Jan 2010)

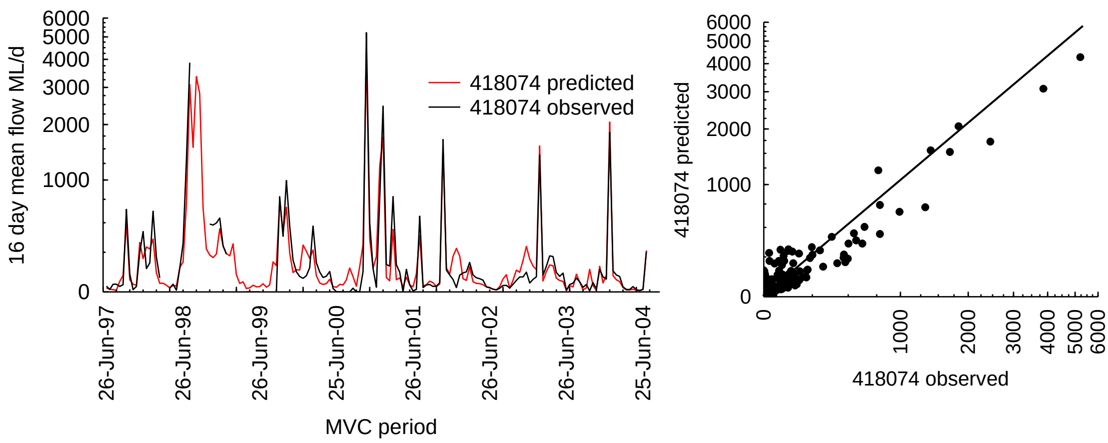

Figure 7.6: Comparison of predicted and observed flow for 418074 at 16-day time-step for the Gwydir IVRM. 1:1 line shown on scatterplot.

Gingham channel at Tillaloo (418076)

The maximum gauged stage at Gingham channel at Tillaloo (418076) is 1.2m (approx. 800ML/day) with the maximum peak in observed data of 1.82m (mean daily gauge height is rated at approx. 7225ML/day). With only two ratings carried out over 300ML/day, the rating curve for this gauge leaves a large degree of uncertainty in values greater than this. There are also some clear shifts in the rating curve that are most likely due to changes in channel cross-section over time (Figure 7.7) adding to the uncertainty in observed flow data. The 16-day model fit shown in Figure 7.8 is reasonable considering this uncertainty in the observed data and the periods of missing data from the gauge when numerous small peaks are modelled (i.e. July- December 2001, September – November 2002, January-March 2003, October- December 2003)

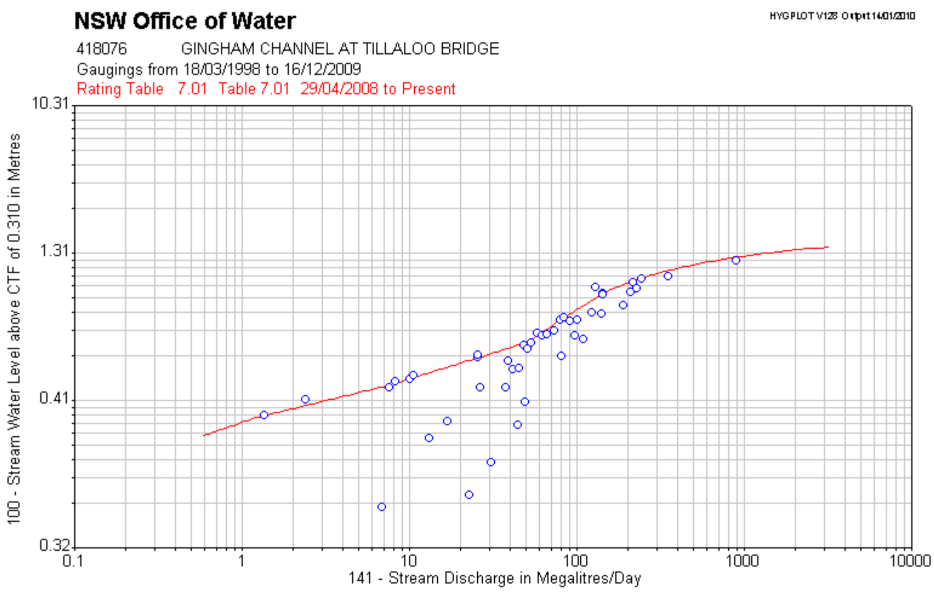

Figure 7.7: River gauging and rating curve for the Gingham Channel at Tillaloo (NSW Water Information, http://waterinfo.nsw.gov.au/ accessed Jan 2010).

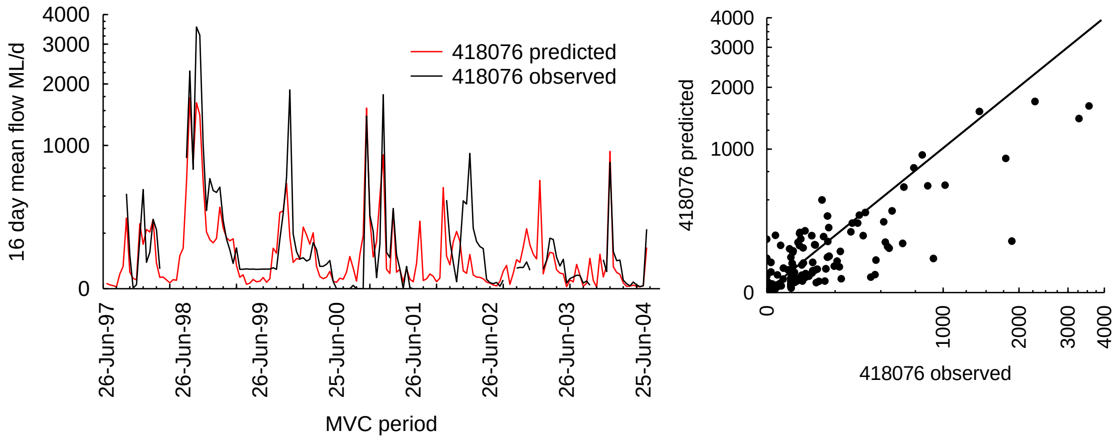

Figure 7.8: Comparison of observed and predicted flow for 418076 at 16-day time-step for the Gwydir IVRM. 1:1 line shown on scatterplot.

Gingham Channel at Gingham Bridge (418079)

The Gingham Channel at Gingham Bridge (418079) has a maximum gauged stage of 1.83m and less than 4000ML/day. The maximum observed gauge height is 2.7m (10 362ML/day). Examining the rating curve for this gauge (Figure 7.9) leaves a large degree of uncertainty in the highest values with only two gaugings conducted over 1000ML/d. The daily time-step correlation between observed and predicted flows is poor due to the time-lags through the system. The 16-day time-step fit is much better but the peaks are under estimated in the model (Figure 7.10).

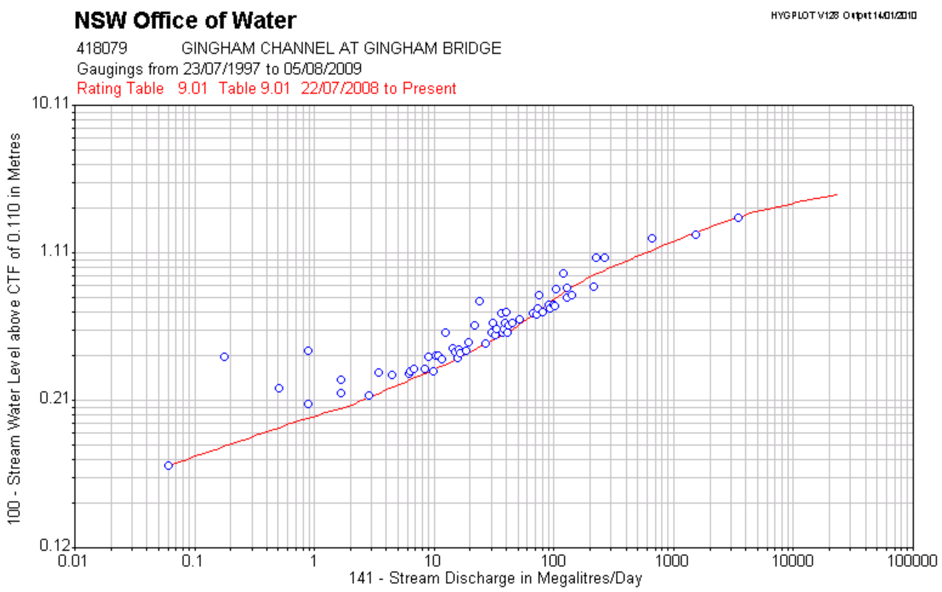

Figure 7.9: Gaugings and rating curve for Gingham Channel at Gingham Bridge 418079 (NSW Water Information, http://waterinfo.nsw.gov.au/ accessed Jan 2010).

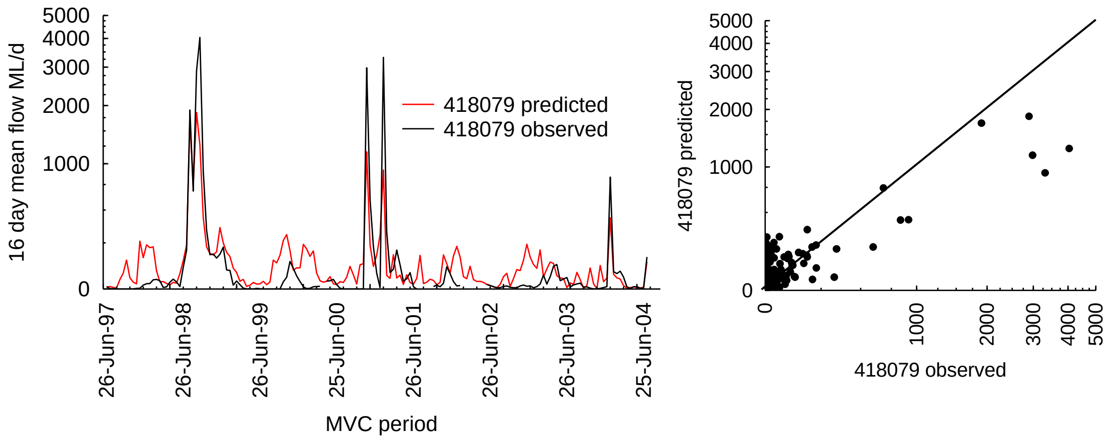

Figure 7.10: Comparison of observed and predicted flow for 418079 at 16-day time-step for the Gwydir IVRM. 1:1 line shown on scatterplot.

Gwydir River at Brageen Crossing (418053)

The first reliable gauge on the Gwydir River below Tyreel regulator is at Brageen Crossing (418053). This gauge is well gauged with a maximum gauged stage of 4.9m but there is some uncertainty for flows over 8000ML/day (Figure 7.11) due to a lack of gaugings undertaken at higher flows. Model fit is good for this gauge with the 16-day time-step well represented as shown in Figure 7.12.

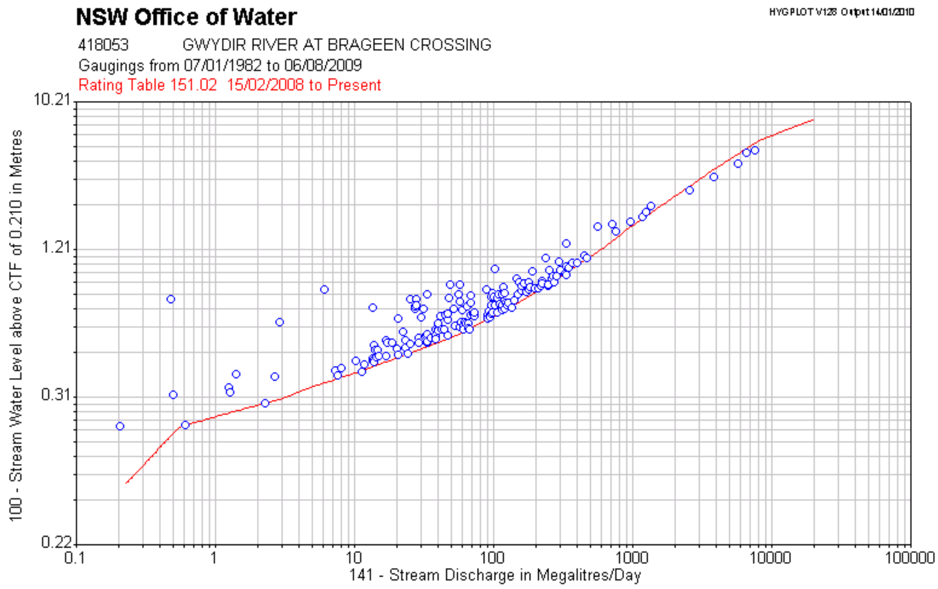

Figure 7.11: Gaugings and rating curve for Gwydir River at Brageen Crossing 418053 (NSW Water Information, http://waterinfo.nsw.gov.au/ accessed Jan 2010).

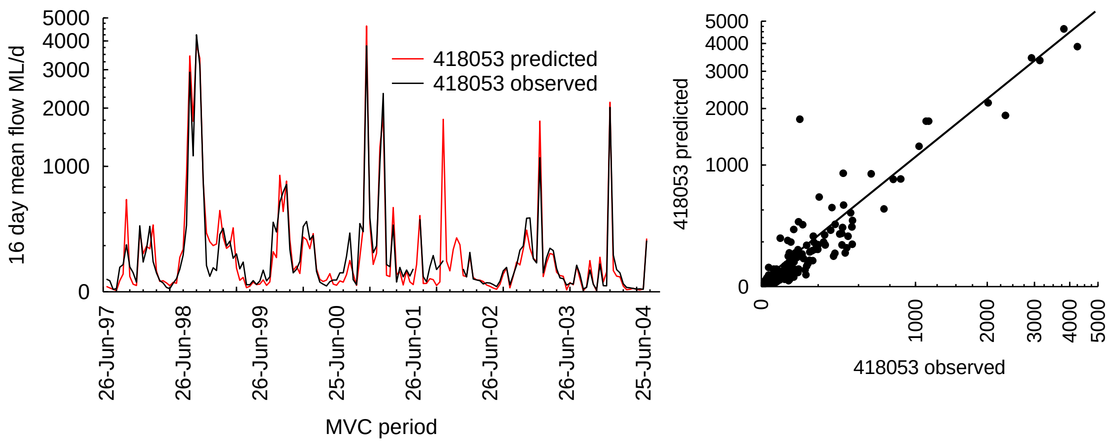

Figure 7.12: Observed and predicted flow for the Gwydir River at Brageen 418053 for the Gwydir IVRM. 1:1 line shown on scatterplot.

Gwydir River at Allambie Bridge (418078)

The rating curve for Gwydir River at Allambie Bridge (418078) shows a stable river cross-section with reliable measurement of flows up to 4000ML/d and a maximum gauged stage of 3.3m (Figure 7.13). Model fit is good for both daily and 16-day time steps (Figure 7.14).

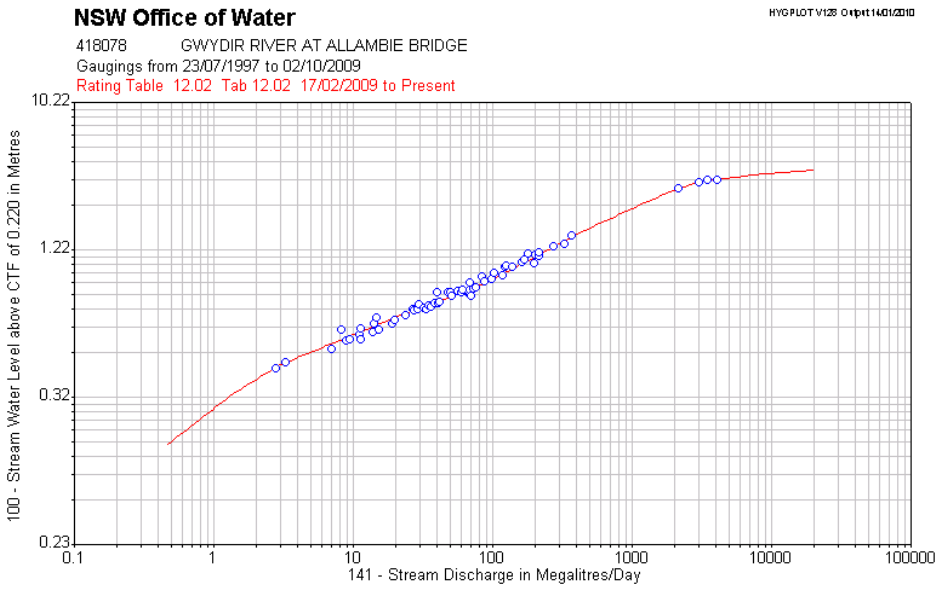

Figure 7.13: Gaugings and rating curve for Gwydir River at Allambie Bridge 418078 (NSW Water Information, http://waterinfo.nsw.gov.au/ accessed Jan 2010).

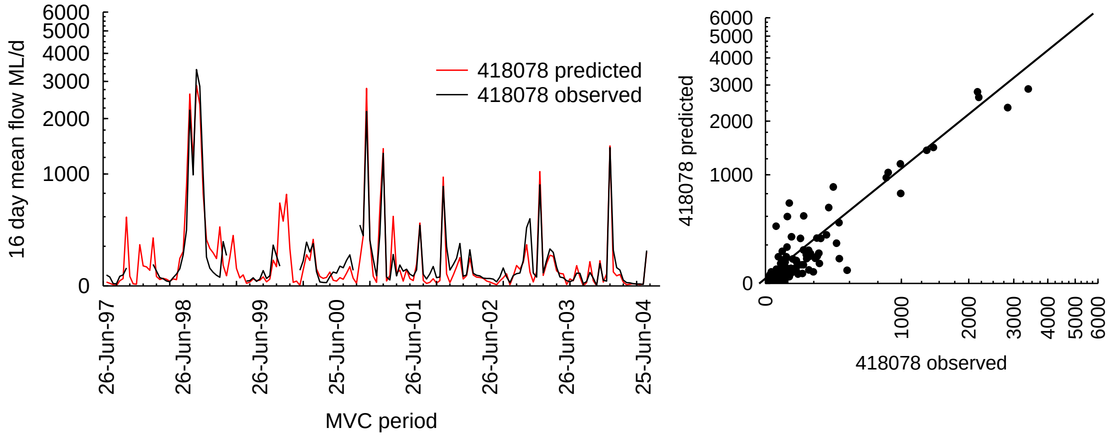

Figure 7.14: Observed and predicted flow for the Gwydir River at Allambie Bridge 418078 for the Gwydir IVRM. 1:1 line shown on scatterplot.

Gwydir River is at Millewa 418066

The last gauge on the Gwydir River is at Millewa 418066 and has been gauged to approximately 300ML/day. There is evidence of a shift in channel cross-section and high degree of uncertainty in flows greater than 300ML/day due to a lack of high flow gaugings (Figure 7.15). Model fit is poor for daily flows (r^2 < 0.5) but reasonable-good for 16-day time-step (Figure 7.16).

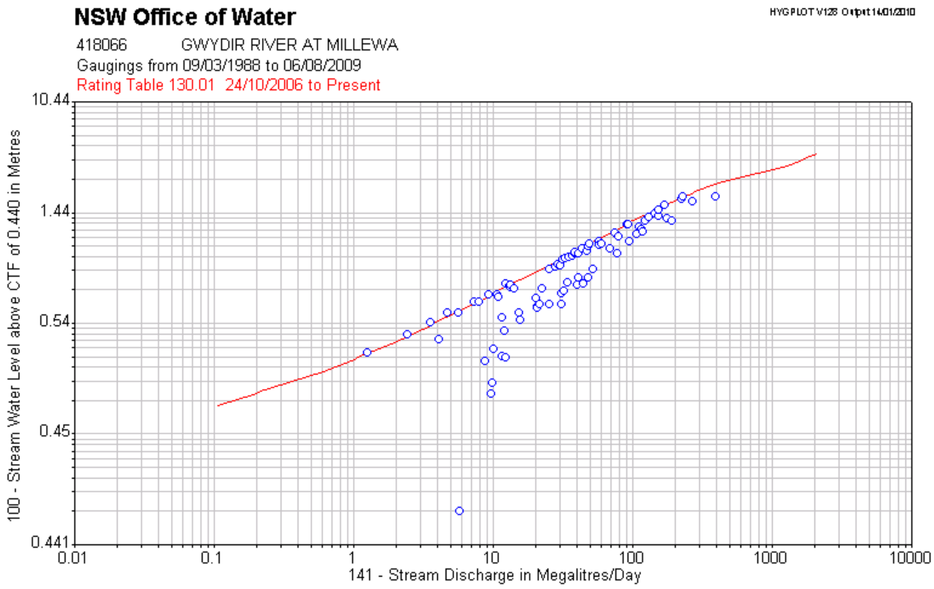

Figure 7.15: Gaugings and rating curve for Gwydir River at Millewa 418066 (NSW Water Information, http://waterinfo.nsw.gov.au/ accessed Jan 2010).

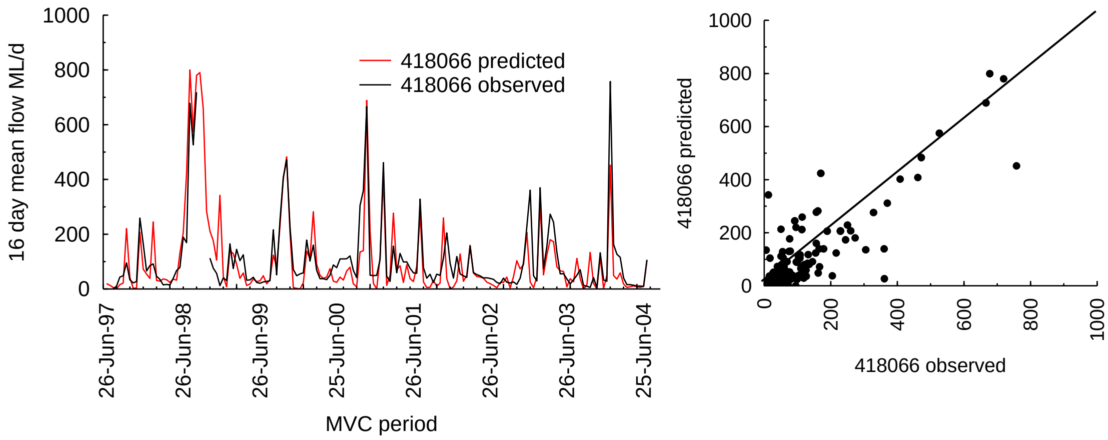

Figure 7.16: Observed and predicted flow for the Gwydir River at Millewa 418066 for the Gwydir IVRM. 1:1 line shown on scatterplot.

7.2.3.2 Wetlands and floodplains

There is limited data to verify the wetland and floodplain objects of the IVRM. Three methods are used to verify the depth and duration represented in the model:

1. The depth is compared to gauged depth data for one location on the floodplain.
2. The total area inundated in the IVRM is compared to the flood and response analysis of Chapter 5 in this thesis.
3. Each object is compared to the fPAR of vegetation within the landscape unit with a subjective assessment of depth, duration and vegetation response.

The only observed time series data available for the wetland depth is for one location that is located at the ‘rookery’ on the Gingham channel (418083). The gauge has been operational since October 2001 and has had some reliability problems resulting in periods of missing data. The gauge is also affected by upstream dams and/or backwater effects so can only be used as a guide. This coincides with the FF4_66 landscape unit in direct connectivity with the Tillaloo-waterhole channel reach. Model fit of wetland depth was reasonable for the 2000/2001 event but poor for subsequent events as shown in Figure 7.17. The fit was optimised for the 2000/1 event as the 2002/3 event peak was altered due to the construction of drainage pathways upstream of the gauge. This highlights the sensitivity of flood distribution to small scale landscape changes.

The total area inundated is compared with the results of remote sensing analysis of flood and response areas from Chapter 5, figures 5.19, 5.21 and 5.26 (Figure 7.18). Of the nine events for which data are available, five of the events fell within the error bounds of the remotely sensed analysis. Of the other four events, the modelled extent exceeds the remotely sensed estimate in three cases. The modelled area was smaller than the remotely sensed estimate in one case but this occurred very early in the model run and may reflect start-up effects associated with the model itself. The largest events show good agreement with remotely sensed estimates but the moderate to smaller events are over-estimated in the model. The model does overestimate some flow peaks in moderate events, but may also underestimate the ‘losses’ through the system in the moderate events and this may be linked to stock and domestic demand, inaccurate estimates of extractions, movement of surface water to groundwater or the volume/area estimates for the western floodplains. The 2002 and 2003 events are the worst represented and occurred during relatively dry climatic conditions suggesting the model may also underestimate rates of drying, groundwater recharge and/or soil moisture deficits.

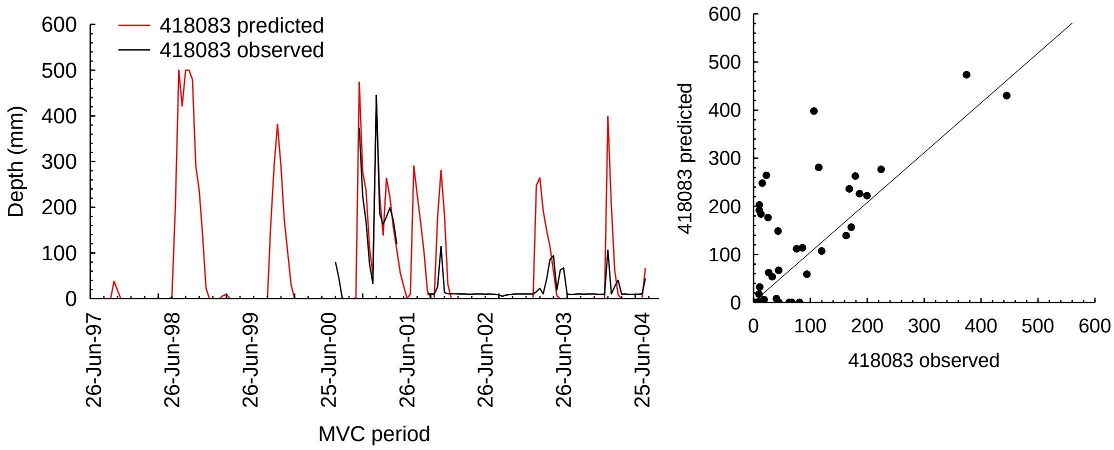

Figure 7.17: Comparison of modelled maximum depth (red) in FF4_66 landscape unit and the gauged data (black) from the Gingham Channel at Rookery floodplain gauge for the Gwydir IVRM (Daily: n=1279, RMSE = 60, r^2 = 0.52, MVC: n=83, RMSE = 70, r^2= 0.63).

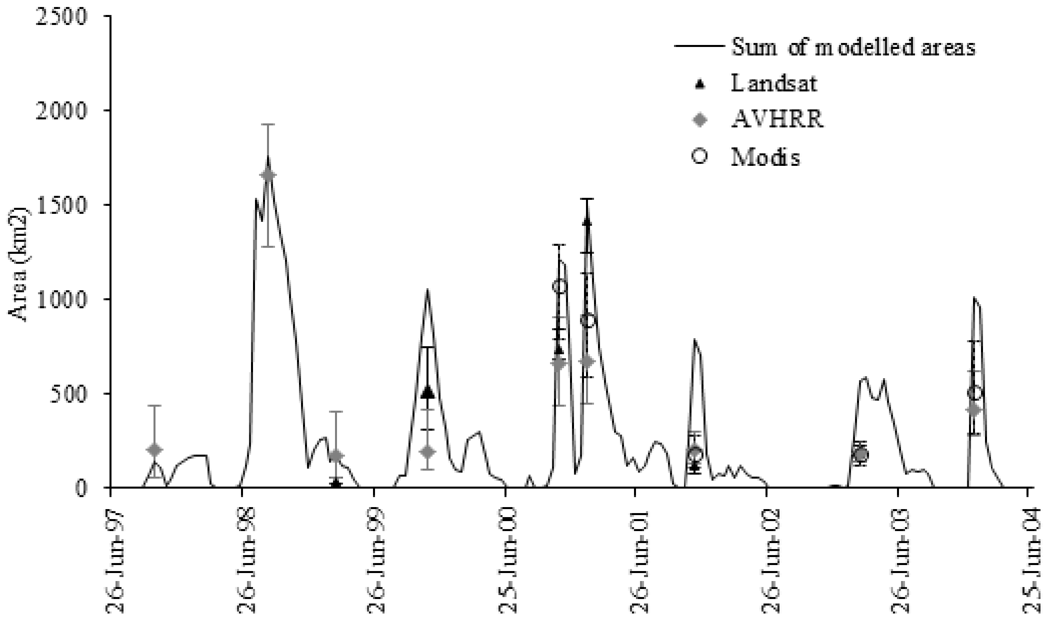

Figure 7.18: Sum of all wetland and floodplain areas inundated in the IVMR compared to results of remote sensing analysis of flood events (Chapter 5, figures 5.19, 5.21 and 5.26).

The wetland and floodplain areas can also be compared to the observed fPAR time series (see Chapter 6, Section 0) as a 'reality' check of the flood behaviour of each landscape unit. As discussed in Chapter 6, high fPAR response in wetlands and floodplains is expected to be in response to flooding while soil moisture also contributes to some level of response but of less vigour. By examining the fPAR response in comparison to modelled depth in the wetlands and to both the depth and area in floodplains, the model behaviour can be further evaluated.

The Gwydir Raft river redgum and coolibah woodlands are split into two landscape units: a small area of dense river redgum 4_227 and a broader area of river redgum and coolibah

3_210. The vegetation productivity of these areas has relatively poor MLR model fit using soil moisture and inflows (Chapter 5). The results of the IVRM indicate that inundation only occurred on six and four occasions for the 4_227 and 3_210 LUs respectively (Figure 7.19). This is likely to be an underestimate due to the relatively high channel capacity used in the IVRM for the adjacent Gingham Channel between Tyreel regulator and Teralba gauging station. The channel may have suffered significant decrease in capacity due to the Raft itself that would increase the frequency of flooding in these LUs. The impact of channel capacity in this reach on adjacent LUs is tested further in the sensitivity analysis in section 7.2.4. Periods of low observed fPAR do correlate quite well with periods of low modelled soil water depth (SWD) with declining fPAR in 2000 and 2002. Similarly, the free surface water and/or rise in soil water depths modelled from 2000 onwards did correlate with a rapid response in fPAR in both LUs. This suggests that these LUs do rely on surface flooding or high soil moisture for high productivity rather than deeper groundwater sources.

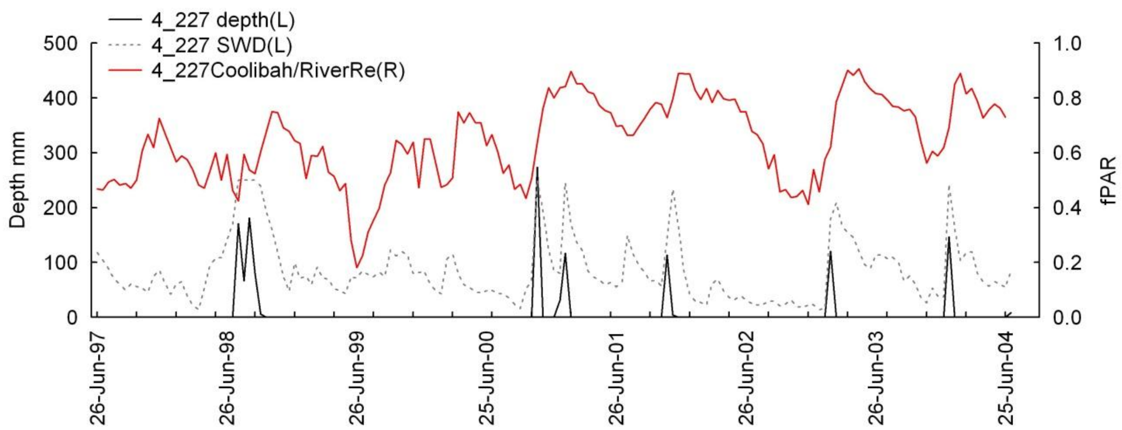

a)

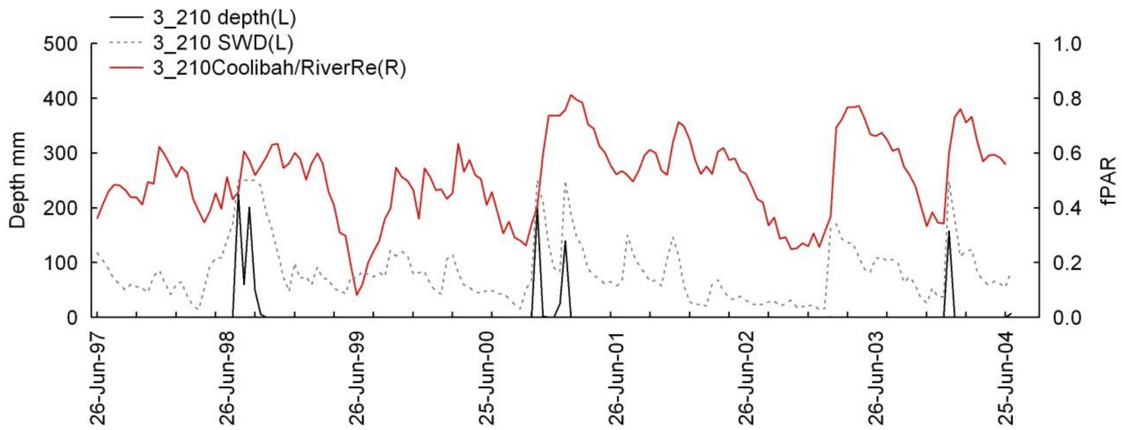

b)

Figure 7.19: Modelled inundation depth (depth, solid black line) and soil water depth (SWD, dotted black line) of the Gwydir Raft in comparison to observed fPAR values (red) of the a) 4_227 and b) 3_210 coolibah / river redgum landscape units.

In the Lower Gwydir the frequently flooded wetlands of Old Dromana and adjacent properties include the 4_127/4_188 and 3_118 patches and the marsh clubrush and spikerush landscape units. Results of the IVRM indicate that flooding occurred very frequently in the 4_127 patch and the soil profile is likely to be saturated for long periods of time as a consequence (Figure 7.20). Inundated periods (where depth > 0) generally coincided well with the peaks in productivity of the marsh clubrush landscape unit. Similarly periods not inundated and with decreasing soil moisture also agreed with decreased productivity.

The 3_118 patch is expected to inundate less frequently than the 4_127 patch and although this behaviour is exhibited generally in the modelled outputs there are some events that appear to be poorly represented. For example during 1997/8, a moderate response in productivity is not matched by inundation but a lower peak in productivity in 1999/2000 occurs during a period modelled as inundated (Figure 7.21). This may partially be explained by the antecedent conditions with lower fPAR responses following periods of low soil water depth compared to higher fPAR responses following wetter antecedent conditions.

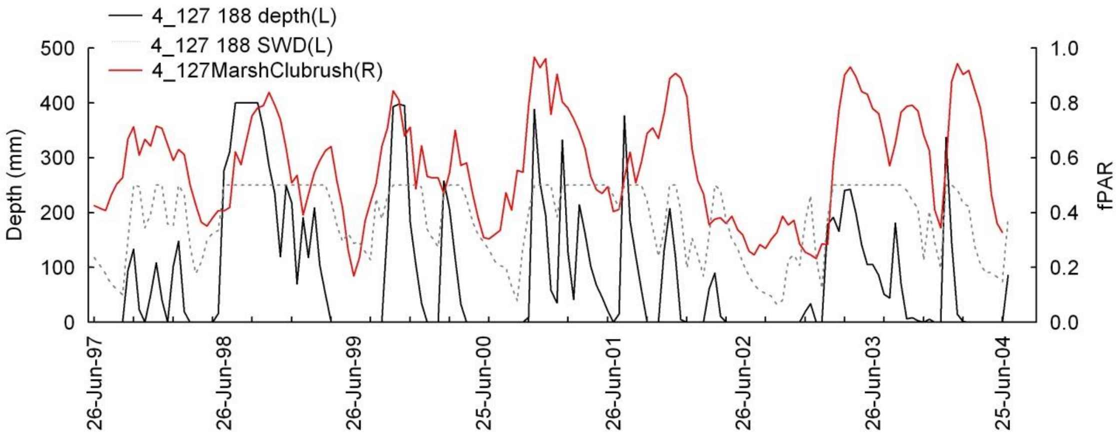

Figure 7.20: Modelled surface water depth and soil water depth (SWD) and observed fPAR in the 4_127 patch of the Gwydir IVRM.

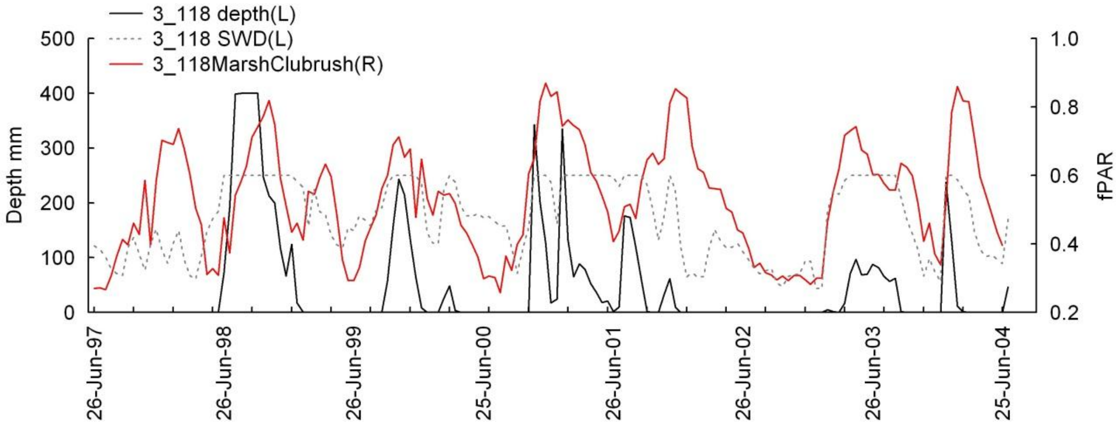

Figure 7.21: Modelled surface water depth and soil water depth (SWD) and observed fPAR in the 3_118 patch of the Gwydir IVRM.

On the Gingham Channel the main area of interest is the 4_66 patch that includes an area of spikerush and key waterbird breeding areas. As discussed in Chapter 6, the observed fPAR in the 4_66 Spike rush landscape unit was maintained at a moderate productivity for the 1997/1999 period without any high peaks or periods of senescence. This may have been due to prolonged flooding but this is not indicated by the depths modelled in the IVRM (Figure 7.22). The other explanation could be modification of the site and/or the provision of targeted low flow to the site to prolong bird breeding events in 1998 and 1999 by artificially prolonging the flooding event (Foster, pers. com.) This type of activity cannot be replicated in the model. The patterns after 2000/2001 appear to better match the fPAR productivity. The depression in fPAR in winter of 2001 is likely due to cold temperatures rather than lack of water.

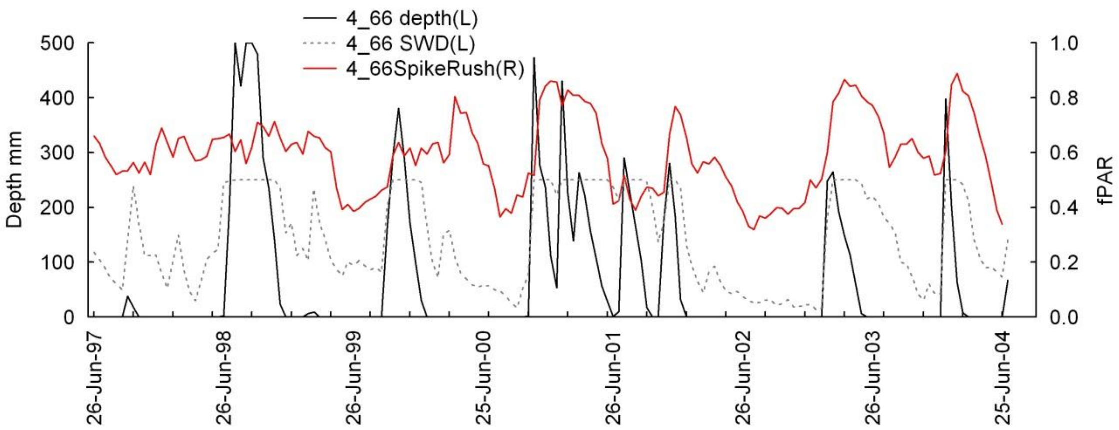

Figure 7.22: Modelled surface water depth and soil water depth (SWD) and observed fPAR in the 4_66 patch of the Gwydir IVRM.

Further west on the Gingham Channel is the 3_30 patch associated with the Crinolyn Ramsar site. The modelled inundation behaviour displays generally good agreement with the periods of high fPAR of the spikerush LU (Figure 7.23). The underlying fPAR pattern, particularly after 2000, appear to be associated with soil water depth. This could reflect a terrestrial vegetation component that is more capable of responding modestly to soil water availability than the wetlands species.

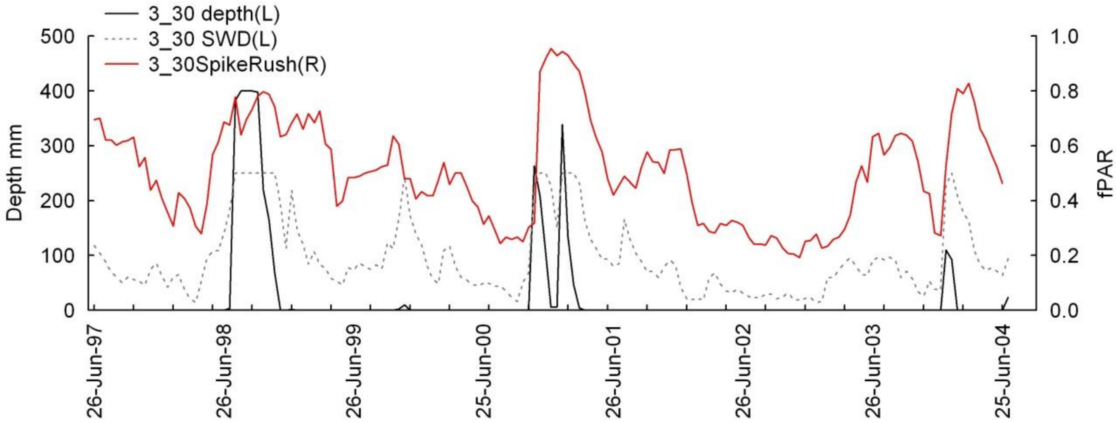

Figure 7.23: Modelled surface water depth and soil water depth (SWD) and observed fPAR in the 3_30 patch of the Gwydir IVRM.

The less frequently flooded areas of the 2_6 patch surround the wetlands of the Gingham and Gwydir and are modelled as a single large floodplain with varying area and depth depending on the volume of water available. Also modelled for these floodplains is the soil water depth due to climate (rainfall/Et) alone for unflooded areas. Under the area flooded the soil water depth is assumed to be saturated. The maximum area is over 600 km^2 but the model outputs only reach around 400 km^2 (Figure 7.24). This is likely to be an underestimate of the total area flooded in the larger 1998 flood event. The patch includes areas of spikerush that are likely to be in the most frequently flooded areas of the whole patch. The larger fPAR peaks correspond with large areas of sustained inundation. Some periods of inundation occur without fPAR peaks showing high response, which may indicate an overestimate of flooding in the water balance. This could be due to the amalgamation of a large area into a single patch. The inundation frequency classes used in Chapter 5 identified this large area as a single connected patch that encompasses areas on both eastern and western portions of the Gingham and Gwydir and across the intervening floodplains. In reality the inundation behaviour may still be influenced by the operation of the Tyreel regulator as well as the large range of inflows represented by the flood frequency class. Further model development should re-examine this patch in particular and consider splitting the single patch into better spatial representation.

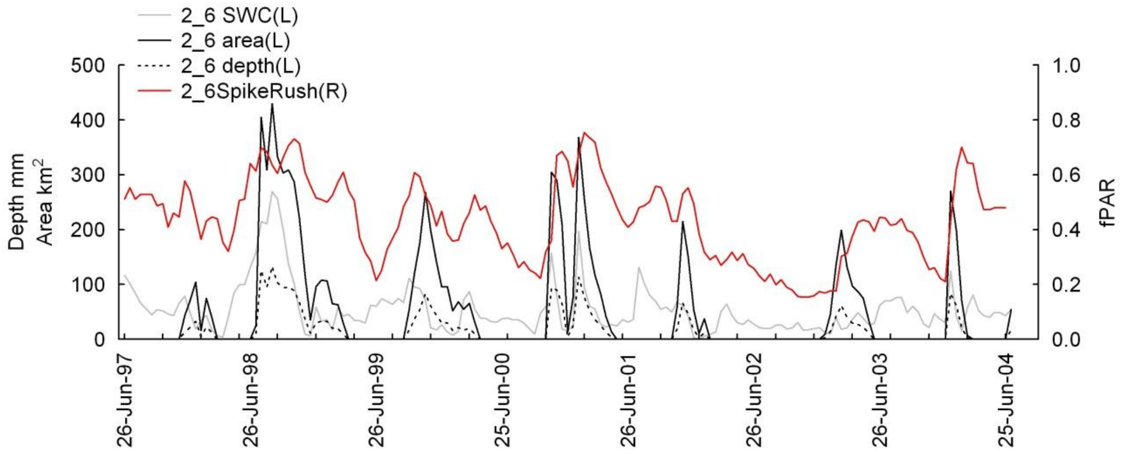

Figure 7.24: Modelled surface water depth, area flooded and climate driven soil water (SWC) and observed fPAR in the 2_6 patch of the Gwydir IVRM.

The broader floodplain includes an area of native grassland (1_195) that is infrequently flooded. Results of the MLR modelling of fPAR response in Chapter 6 indicate that fPAR is driven by soil moisture rather than inundation in this LU. Although fPAR does correlate quite closely with the modelled soil water depth due to rainfall alone, the peak observed fPAR occur at times when a small area of inundation is modelled (Figure 7.25). Unlike most of the other LUs examined, the rate of senescence in the native grasslands is very rapid and does not show extended maturity after inundation.

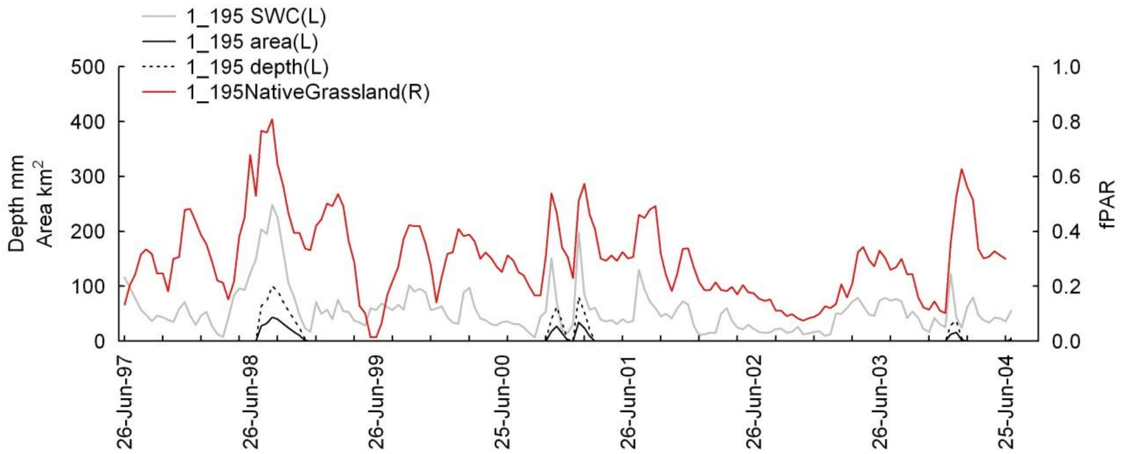

Figure 7.25: Modelled surface water depth, flooded area and climate driven soil water (SWC) and observed fPAR in the 1_195 patch of the Gwydir IVRM.

The IVRM also includes a theoretical floodplain (FF0) that represents outflows from all objects or 'excess' water. The largest area occurs in the 1998 flood event where an extra 500km^2 of inundation is modelled (Figure 7.26). As this event produced an outflow to the Barwon River to the west it is reasonable that the IVRM produced an excess volume of water during this event. Similarly outflows may have occurred in 1999/2000, 2000/2001 and possibly in the 2003/4 events. It would be expected that the FF1 floodplains would be inundated during these events, which did not always occur in the model. Further evaluation of the rates of outflow and/or thresholds within some of the wetland and floodplain objects is undertaken in the sensitivity analysis in section 7.2.4 to determine critical factors.

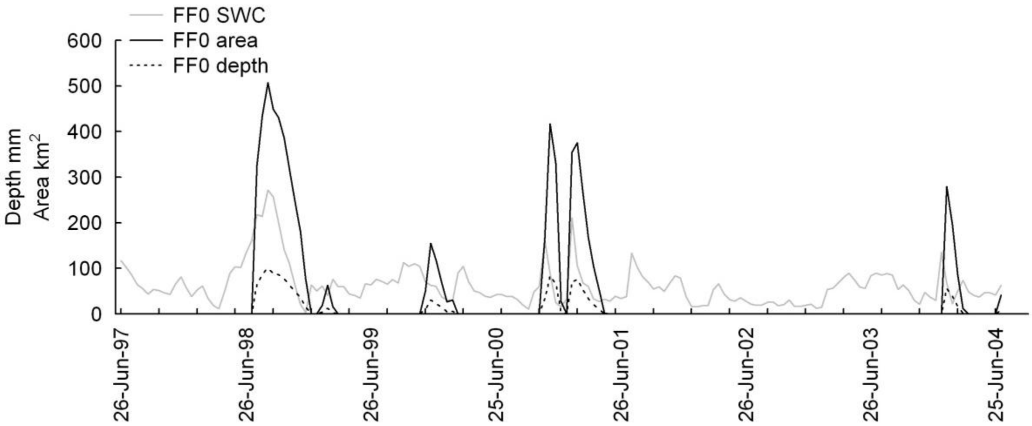

Figure 7.26: Modelled surface water depth, flooded area and climate driven soil water (SWC) and observed fPAR in the FF0 patch of the Gwydir IVRM.

One aspect of the IVRM, generally excluded from routing models, is the inclusion of simple soil moisture accounting. Comparing the modelled soil moisture resulting from climate (rainfall and Et) alone to the modelled soil moisture under flooded areas indicates the contribution that this can make to vegetation response. In the frequently flooded areas of the Lower Gwydir (4_127 and 4_188) the modelled soil moisture is frequently saturated and rarely decreases to similar values to those of climate driven soil moisture. Even in periods when there is no surface inundation, vegetation productivity is likely to remain higher for prolonged periods than non-flooded areas. Similarly wetland areas further west (3_32 on the Gingham Channel for example) have higher soil moisture than does climate alone but much less than the more frequently flooded wetlands (Figure 7.27).

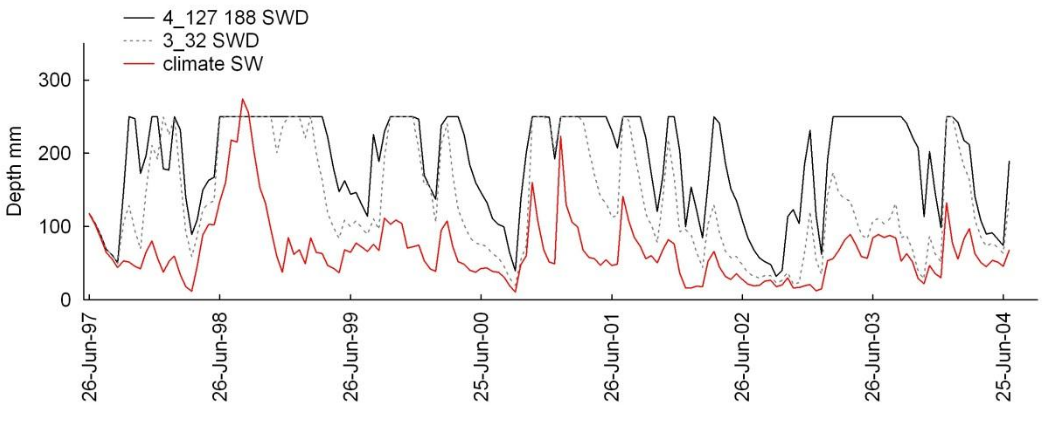

Figure 7.27: Modelled soil moisture (in mm) due to climate alone (climate SW) and due to climate and surface water flooding (4_127 188 SWD and 3_32 SWD) of the Gwydir IVRM.

7.2.3.3 Groundwater storage

A very simple 'loss' to groundwater is included in the IVRM. This is based on the information in the CSIRO SY report (CSIRO, 2007) which reports an estimated recharge of 40 000 to 60 000ML/yr (including the Mehi River) to the Lower Gwydir alluvium. The report also identifies the stream reaches most likely to contribute to this recharge. The cumulative volume held in the groundwater storage (no outflows) component of the IVRM is in the order of 220 000ML over the 7 year period, or an average of 31 500ML/yr (Figure 7.28). This is a similar order of magnitude to that reported in the CSIRO SY report, allowing for some portion to be recharged through the Mehi River that is not accounted for in the IVRM. The IVRM uses a simple routing of a percentage of the outflows from each object into groundwater storage, so recharge occurs predominantly during periods of high flow and flooding. There is no data to test this against, however the CSIRO SY report does suggest that it is during these times that recharge is most likely to occur.

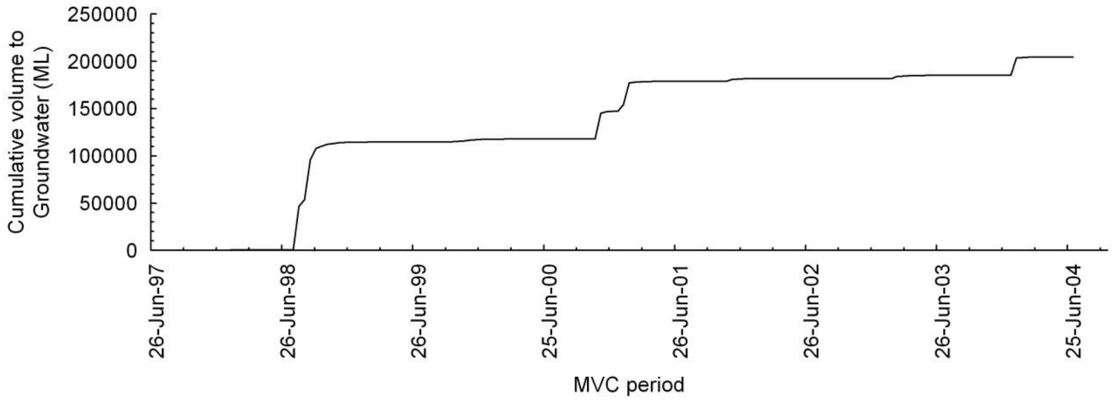

Figure 7.28: Cumulative recharge to groundwater over the modelled period 1997 to 2004 estimated from the IVRM.

7.2.3.4 Vegetation response

The vegetation MLR model is based on total inflows to the system and climate driven soil moisture. This section evaluates the MLR model's capacity to predict the fPAR response of individual LU within the IVRM structure. The sensitivity to inflows and climate is evaluated in Section 7.2.4 and the scope for enhancing the vegetation response models using local water balance outputs of the IVRM (or other hydrodynamic models of the system) is discussed further in Sections 7.2.5 and 7.4

Observed and predicted fPAR response is compared to evaluate if the MLR model is functioning as expected. The results (see Figure 7.29) for 1997-2004 are consistent with those found in Chapter 6, confirming the MLR was correctly input to the IVRM. Overall the pattern of fPAR response also highlights the differences between the flood frequency patches with relatively consistent results for similar vegetation types (Figure 7.29). The river redgum LU stands out with the highest persistent fPAR while the least frequently flooded LU (a grassland) provides a predominantly climate driven response reference point.

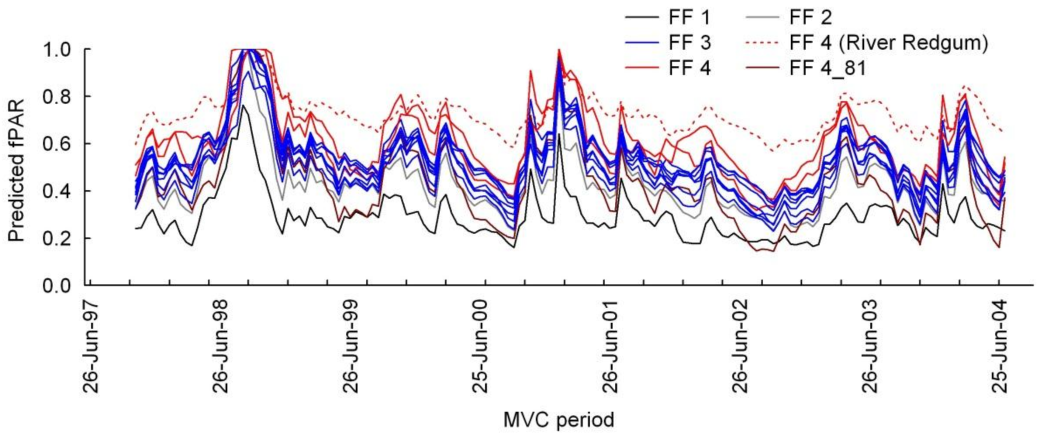

Figure 7.29: Modelled fPAR response based on multiple linear regression to climate driven soil moisture and inflows at Yarraman gauge.

7.2.4 Sensitivity

The sensitivity of the IVRM to various input parameters is tested in this section. Of particular interest are the parameters that have high uncertainty or little data to support their values. These parameters include:

- Channel capacity through the Gingham Channel in the Tyreel to Teralba reach.
- The field capacity of the soil (in particular the assumed depth of soil beneath the river red gum communities of the Gwydir Raft).
- Both maximum and threshold depth of wetlands.
- Measures of evapotranspiration.

A range of values are tested for each of these parameters and the outputs reported in terms of days inundated for various wetlands and floodplains (where depth > 0).

7.2.4.1 Tyreel-Teralba capacity

A high degree of uncertainty exists about the capacity of this channel reach through the ‘Raft’ area. Assumed to be 9000ML/day based on the downstream Teralba gauge, it may be much lower at various locations. The sensitivity of this parameter on the depth of the adjacent 4_227 patch and downstream wetlands is tested for capacities in the range of 500 to 12 000ML/d. Channel capacity set between 3 000 up to 12 000ML/d has little impact on the number of days inundated in adjacent or downstream wetlands (Figure 7.30). Below 3 000ML/d there is a significant increase in the number of days inundated in adjacent wetlands (4_227 and

3_210). Below 2000ML/d there is a large decrease in the number of days inundated in downstream wetlands of the Gingham Channel (4_66) but little impact on the wetlands of the Lower Gwydir (4_127 and 4_188). This indicates that further information is required to establish the minimum channel capacity through this reach. It also highlights the impact on downstream wetlands if the 'Raft' accumulation continues to decrease the channel capacity below 3 000 ML/day.

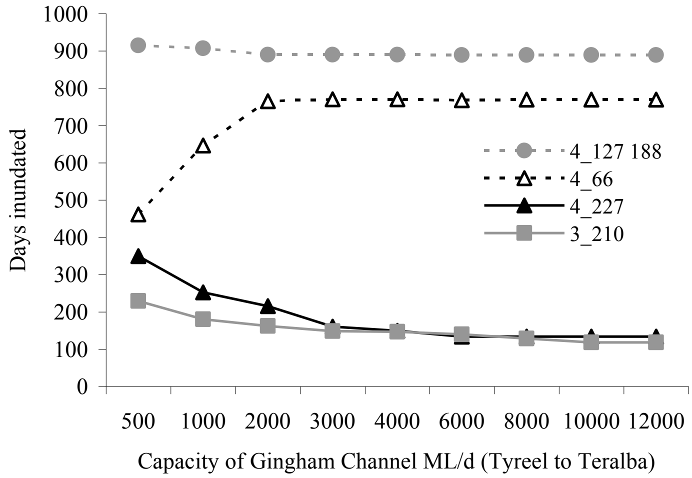

Figure 7.30: Sensitivity of the days inundated in four wetlands patches to changes in channel capacity in the Gwydir IVRM.

7.2.4.2 Field capacity

The field capacity (plant available water capacity) of the soil profile was set at 250mm for the cracking clay soils of the Gwydir floodplains. This is an estimate based on reported values for this soil type (Humphreys and Edraki, 2003) and does not take into consideration some of the complexities of cracking clays and water availability. Effective soil depth of a metre was used in the development of the IVRM for the macrophyte vegetation communities but there is little published information on the root depth of these communities. The effective soil depth under the river red gum communities of the Gwydir Raft may be much greater with the deeper root systems. During the course of the IVRM development and analysis, further information on the soils in the study area was published. The results of the soil survey found that plant available water in the Gwydir wetlands was likely to be in the order of 140-160mm in the upper metre of the soil profile (EAS Systems, 2009). To test the sensitivity of the IVRM to the field capacity of these landscape units, total field capacity from 50mm to 500mm was tested which would account for not only different field capacity, but also different root depths. The results shown in Figure 7.31 indicate that field capacity has little impact on the days inundated for the river red gum landscape units until the field capacity is reduced to less than 150mm. The change in field capacity of the 4_227 and 3_210 patches has negligible impact on downstream wetlands.

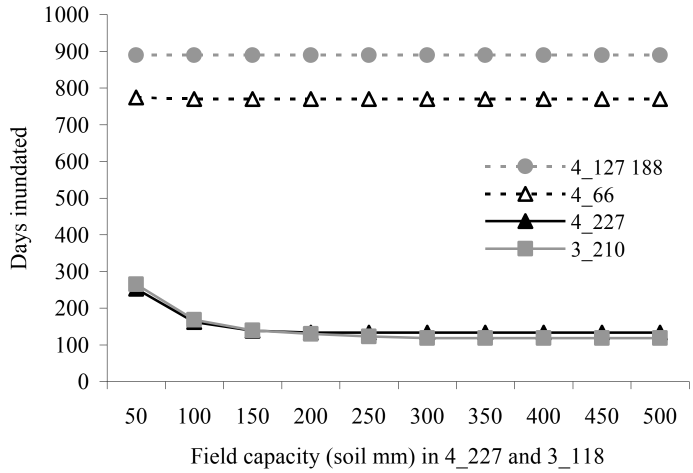

Figure 7.31: Sensitivity of days inundated to the field capacity of the 4_227 and 3_118 patches in the Gwydir IVRM.

7.2.4.3 Maximum and threshold depth of wetlands

When depth exceeds the parameter value for maximum depth, all excess water is routed to the next object. When depth is greater than the threshold depth, excess water is routed at a rate β to the next object. When depth is less than the threshold, all water is retained within the wetland with losses primarily due to evapotranspiration processes. The maximum and threshold depths have a high degree of uncertainty, with most wetlands set to a maximum depth of between 300 and 500mm and with threshold depths varying between 50 and 300mm. Sensitivity to these parameters is tested in two frequently flooded wetlands (4_127/188 and 4_66) and one less frequently flooded wetland (3_32).

The maximum depth has little impact on the number of days inundated (Figure 7.32) but the threshold depth has a significant impact on days inundated and, along with the outflow rate β, are the most important parameters influencing the inundation behaviour of wetlands (Figure 7.33 and Figure 7.34 respectively). Currently the threshold depth and outflow rates for most objects are estimated from personal knowledge gained from site visits between 1997 and 2004, as well as from the scant gauging data available from the Gingham Channel at Rookery site. Further research on these parameters would enhance the model development in the future.

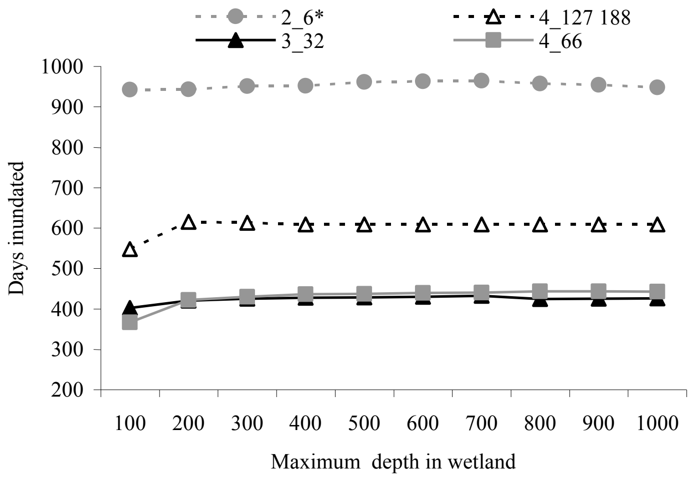

Figure 7.32: Sensitivity of days inundated to maximum depth in wetland patches of the Gwydir IVRM.

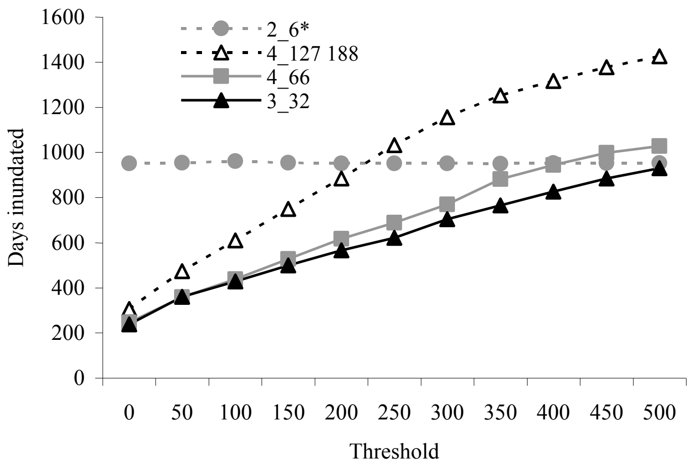

Figure 7.33: Sensitivity of days inundated in wetland patches, and adjacent floodplains, to threshold depth for outflow in the wetlands of the Gwydir IVRM.

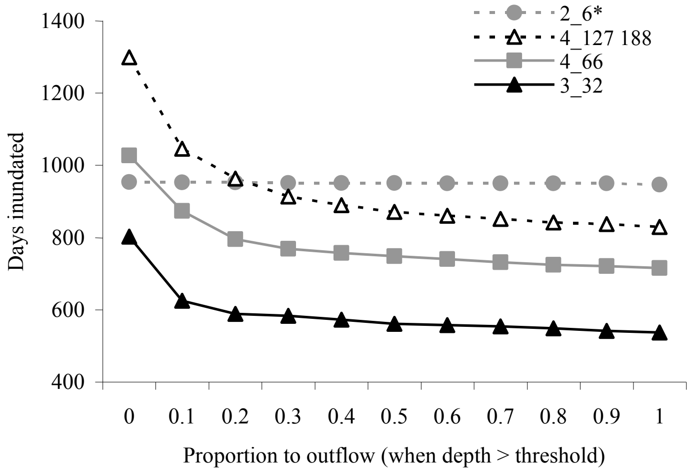

Figure 7.34: Sensitivity of days inundated in wetland patches, and adjacent floodplains, to the rate of outflow for depths above threshold in wetlands of the Gwydir IVRM.

7.2.4.4 Evapotranspiration

Evapotranspiration rates are estimated in the IVRM as a multiplicative factor of pan evaporation that is obtained from the Moree BoM observations. In other river models, potential evapotranspiration is calculated using a Penman-Montieth equation or, as in recent Murray Darling basin sustainable yields assessments, it is based on the SILO climate surfaces using Morton's wet environment evapotranspiration algorithms (Chiew *et al.*, 2008). Testing the sensitivity of the days inundated in the frequently flooded (4_127) and less frequently flooded (3_29) wetland patches to evaporation indicates that the potential Et used in the sustainable yields assessment gives a similar result to using ~0.75*pan evaporation at the Moree BoM station. The number of days inundated is quite sensitive to the range of evaporation factors tested, as shown in Figure 7.35.

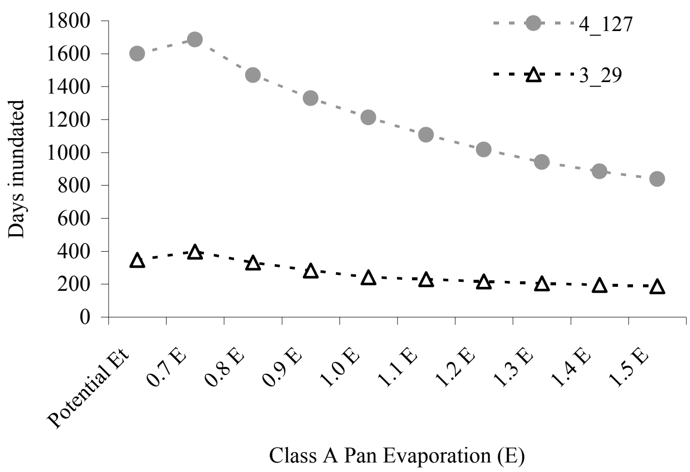

Figure 7.35: Sensitivity of days inundated in wetland patches of the Gwydir IVRM to measures of evapotranspiration.

7.2.5 Summary of model development

The IVRM aims to provide depth and duration of inundation across the wetlands and floodplains of the lower Gwydir linked to inflows and climate. The results of the flood analysis in Chapter 5 and vegetation productivity in Chapter 6 provide a landscape analysis of the system response that is used to develop the IVRM framework.

At a daily time step, the model routes flows through channels with only a fair to reasonable fit to observed data. The model fit is improved considerably at the 16-day time step when aligned with the maximum value composites NDVI data. The r^2 values range from 0.73 to 0.95 depending on the channel reach. There are also uncertainties in the observed (gauged) flow data, particularly at high flows, that impact on the verification of the model.

The total areas inundated in wetlands and floodplains matches the remote sensing evaluations in Chapter 5 (fig. 5.27) relatively well for moderate to large events. Comparison of modelled depth in a wetland with limited depth gauged data shows good fit for some events but poor fit for others. Significant issues associated with channel changes upstream and downstream of the gauged site highlight a potential issue in attempting to model this system. Even small channel structure changes that can be undertaken by land managers can dramatically alter flood behaviour. Given this complexity the IVRM should be used for comparative purposes only to evaluate changing climate and inflow scenarios or possibly to look at potential impacts of large scale changes in channel capacity, rather than attempting to model individual events.

To overcome the lack of data to calibrate and test the validity of the IVRM, the observed vegetation productivity (fPAR) response is used. With an understanding that soil moisture and flooding drives the fPAR response in different landscape units (Chapter 6) the time series of productivity can be compared to modelled depth as a reality check of behaviour. Only qualitative at this stage, the use of vegetation productivity does show promise for testing water balance models in these types of systems.

The IVRM is quite sensitive to some parameter changes such as threshold depths and proportional outflows for wetland and floodplains. The IVRM includes soil moisture accounting and is quite sensitive at low estimates of field capacity. However the model is relatively insensitive to field capacity above 150mm. Channel capacity can influence adjacent wetlands but the follow-on effects to downstream wetlands and floodplains are relatively small.

The IVRM was developed using pan evaporation data from the closest BoM site at Moree. Comparison with estimated potential areal evapotranspiration (CSIRO, 2007) reveals large differences (~30%) in the datasets. The IVRM has largely adopted 100% of the pan evaporation values and up to 130% in western sites that would appear to be a large overestimate compared to potential areal evapotranspiration. Meteorological methods such as the Penman-Montieth equation have been shown to underestimate evapotranspiration in natural wetlands over the growing season (Lott and Hunt, 2001). Evapotranspiration can vary spatially and temporally in wetlands due to soil moisture in the root zone, vegetation senescence and the type of vegetation community (Lott and Hunt, 2001). Further research of the treatment and application of evapotranspiration in the IVRM is warranted given the sensitivity and uncertainty of this factor.

The multiple linear regression model for fPAR response is currently linked directly to inflows to the system and climate-driven soil moisture. The IVRM differentiates among vegetation types and different flood frequency patches and can be linked to climate change and/or inflow scenarios. Further development is needed to link the fPAR response directly to patch scale depth and duration of flooding and soil moisture. Similarly the IVRM does not implicatively include the uncertainties and errors that have been reported throughout analysis sections of this thesis. Any future development of the IVRM should include these uncertainties.

7.3 Applying the model

The main purpose of the IVRM is to capture the outcomes from remote sensing flood and vegetation analysis and to provide a tool for using a variety of inflow and/or climate scenarios to predict the changes in depth and duration of inundation and vegetation response. Input data from the CSIRO SY project (CSIRO, 2007) are used to run the IVRM for a range of scenarios to demonstrate possible applications of the model. This application is not an indepth evaluation of the impacts of climate change on the Gwydir wetlands.

7.3.1 Scenario comparison

A range of scenarios are tested from the CSIRO SY data for 418004 (Yarraman gauge) and associated climate. The IVRM runs use the CSIRO daily input data for rain, potential areal evapotranspiration and flow. Extraction estimates were not available so the estimates used in the IVRM development are adopted. The IVRM is run for the same 1997-2004 period as invoked in the model development using the following CSIRO scenarios.

Base case: IVRM as developed and testing with observed input data from Yarraman gauge and Moree BoM station.

Scenario P: Historical climate, no development (i.e. no headwater storage and no extractions).

Scenario A: Historical climate and current development uses the historical daily rainfall time series data and calculated potential evapotranspiration. Current development for river system modelling comprises the dams, weirs and licence entitlements in the latest State agency models, updated to 2005 levels of large farm dams.

Scenario C: Future climate and current level of development is used to assess the range of likely climate conditions around the year 2030. Three variants are used in the river modelling. A dry, a mid (best estimate of the median) and a wet variant.

Table 7.8: Environmental indicator values for pre-development and current events (>100GL/month) in the Gwydir wetlands and percent change under climate change scenarios (CSIRO, 2007)

Indicators	P	A	Cdry	Cmid	Cwet
			% change from A		
Average between	1.3	2.3	52	-1	-39
Maximum between	7.0	11.5	65	-4	-53
Ave flood volume/yr	211	123	-50	-20	72
Ave flood volume/event	316	342	43	-20	19

P – pre-development
A - current
C – current development level for 2030 climate change scenarios.

The IQQM model evaluation (CSIRO, 2007) indicated good performance of modelled steam flow for the Gwydir River between Pinegrove and Pallamallawa. Average flows were over-estimated by 8 to 15% for these reaches. In the lower distributaries Carole, Gil Gil and Mehi performance was moderate to reasonable. The reaches of the lower Gwydir (Yarraman, Tyreel, Brageen and Millewa) were not evaluated.

7.3.2 Results

The results are presented as exceedance curves for modelled depth in selected wetland and floodplain patches and for modelled fPAR response. Notable in a comparison of the base case and Scenario A is that the depth and the calculated MLR fPAR are higher in Scenario A than the base case. Inflows at Yarraman for the period of observed flows (1977-2006) are very similar. The rainfall used for the Yarraman reach is approximately 10% higher than those used in the IVRM development (observed data from Moree BoM) while the potential areal evapotranspiration used in the IQQM model is 30% lower than the BoM Et used in the IVRM development and calibration. The correlation between potential evapotranspiration calculations and pan evaporation observations is poor for many Australian sites (Chiew and McMahon, 1992) and highlights a potential issue in model development using observed pan evaporation data. The PeT used in the CSIRO modelling is based on the SILO climate surface using Morton's wet environment evapotranspiration algorithms. Due to the differences in input data, the scenarios are only compared to each other and not to the development model.

In the most frequently flooded patch on the Lower Gwydir (4_127), modelled depth in the predevelopment scenario with no extractions was at a maximum for over 80% of the time and the patch was inundated for 99% of the time, only drying out once in the 7 year period (Figure 7.36). Under scenario A this core wetland would be expected to be wet 77% of the time while future climate scenarios range from remaining wet 63% of the time in the C dry scenario to 83% of the time for the Cwet scenario.

The MLR fPAR results (Figure 7.37) reflect the differences in flow and climate-driven soil moisture. Using the results from Section 5.3.3.1, a 'good' wetland productivity of greater than 0.9 fPAR can be expected for marsh clubrush. This level of response is found less than 14% of the time in the current scenario while the predevelopment condition indicates that productivity may remain at or above 0.9 fPAR for over 47% of the time. Climate change scenarios indicate that productivity greater than 0.9 fPAR could range from over 20% of the time for Cwet to less than 8% of the time for Cdry. Under the predevelopment scenario fPAR remains above 0.5 100% of the time compared to less than 78% of the time in the climate change Cdry scenario.

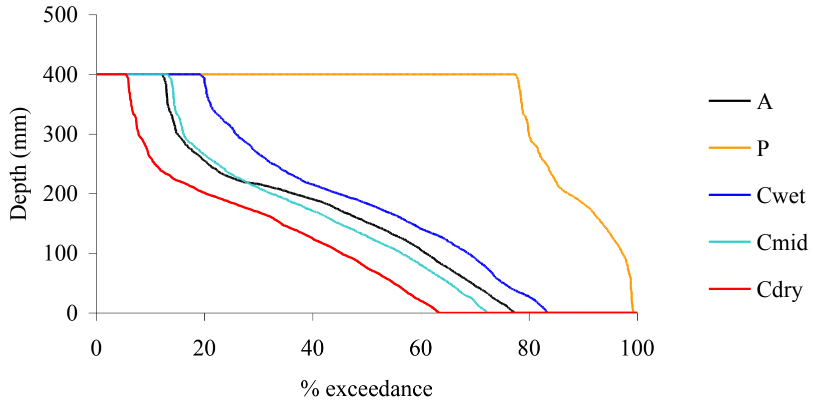

Figure 7.36: Comparison of the IVRM outputs for percent exceedance in modelled depth for frequently flooded 4_127 patch on the lower Gwydir for scenarios A, P, Cwet, Cmid and Cdry.

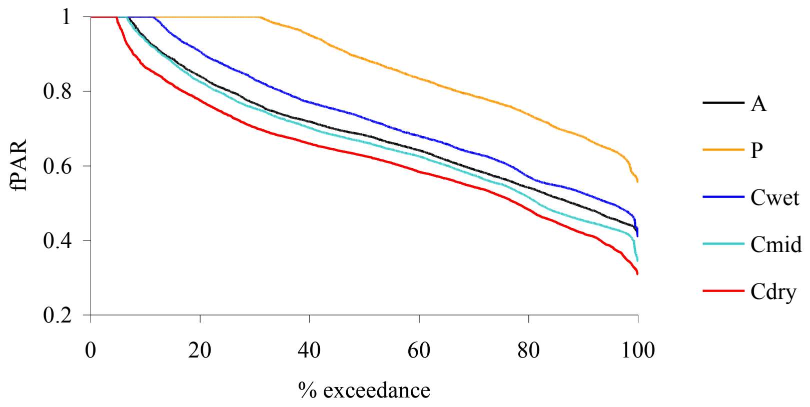

Figure 7.37: Comparison of the IVRM outputs for percent exceedance in modelled fPAR for frequently flooded 4_127 patch on the lower Gwydir for scenarios A, P, Cwet, Cmid and Cdry.

Consider now a slightly less frequently flooded spikerush dominated wetland in the Gingham Channel west of Gingham Bridge (3_30). The scenarios again show more frequent flooding under a predevelopment scenario where the IVRM indicated the patch would be wet 93% of the time and at maximum depth over 50% of the time. Scenario A indicates that the current situation is to remain wet for just 30% of the time with maximum depths only 4% of the time. Under climate change scenarios this patch could remain wet between 47% of the time (Cwet) and just 11% of the time (Cdry).

Anecdotal information (Foster, pers. comm.) suggests that this area has been considerably drier under post-development conditions and is showing signs of terrestrial weed invasion as well as a shift in community composition away from species such as marsh clubrush. If the productivity of the lower Gwydir marsh clubrush LU is used as a benchmark then only under predevelopment scenario does the modelled productivity exceed 0.9 fPAR more than 10% of the time. This is closer to the current development scenario in the more frequently flooded 4_127 patch that maintains a healthy marsh clubrush community. Productivity for Scenario A, Cmid and Cdry all exceed 0.9 fPAR less than 6% of the time which suggests that a community structure similar to that of 4_127 is unlikely.

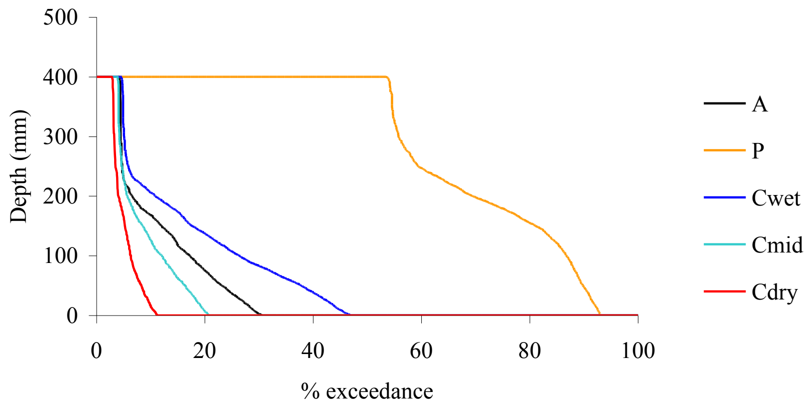

Figure 7.38: Comparison of the % exceedance in modelled depth for 3_30 patch on the Gingham Channel, west of Gingham Bridge for scenarios A, P, Cwet, Cmid and Cdry.

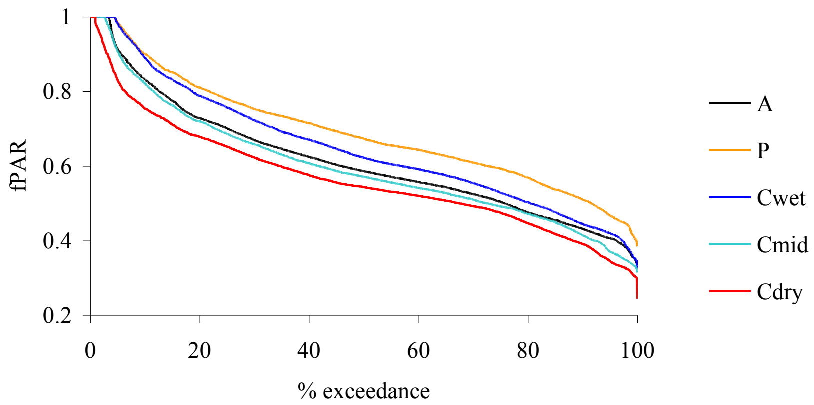

Figure 7.39: Comparison of the % exceedance in modelled fPAR for 3_30 patch on the Gingham Channel, west of Gingham Bridge for scenarios A, P, Cwet, Cmid and Cdry.

This is a simple example of how the IVRM can be used to evaluate flow and/or climate scenarios. Understanding the current condition of the wetlands and comparing, in a relative sense, the outputs of the model may provide insight into the flows and climate required to maintain the wetland vegetation.

The predevelopment scenarios appear to provide large areas of flooding for long periods of time but this is consistent with a simple monthly water balance model that has demonstrated that flooding flows would have occurred in the Gwydir for 192 months during 93 years under predevelopment flows (Bennett and Green, 1993). Considering that historical depths in the lower Gwydir wetlands could be "*up to the saddle-flaps in water and it is about 4 miles across*" (Bennett and Green, 1993) it would take around 4-6 months at that depth to evaporate (assuming 0 inflows and potential evaporation rates as modelled in IQQM). Using this information it is conceivable that some of the Gwydir wetlands remained virtually permanently wet through the 1997-2004 period as modelled by the IVRM.

7.4 Discussion

Node-network approaches are commonly used as a modelling framework for assessing water allocation problems (Letcher *et al.*, 2007; Letcher *et al.*, 2004; Podger and Hameed, 2000; Simons *et al.*, 1996) and have been applied to environmental flow decision support systems (Merritt *et al.*, 2010; Whigham and Young, 2001; Young *et al.*, 1999; Young *et al.*, 2003). The models represent river basins as a series of nodes which may be where water extraction or management impacts are aggregated for a region (Letcher *et al.*, 2007) or where a particular environmental value may be assessed (Young *et al.*, 2000). In the development of the IVRM in this thesis, the wetland and floodplain nodes have been defined by the similarities in flood frequency and connectivity (patches), thus providing a framework that is defined by the very inundation characteristics that are to be modelled. These nodes are also subdivided into landscape units that define the vegetation characteristics to be modelled.

The basic concept behind the water balance model is very similar to those used other node-network models for ecological response. Whigham and Young (2001) described the storage unit with input and output pipes, where the outputs pipes drain water at either linear rates based on threshold, or exponential decay based on volume at the daily time step. In the Okavango Delta, the system is represented as a set of inter-linked linear reservoirs and models the water balance at a monthly time step (Wolski *et al.*, 2006). The outflow for each reservoir is linearly related to the volume of water stored above a certain threshold volume (the outlet level) (Wolski *et al.*, 2002). Whereas the water balance approach of Whigham and Young (2001) Environmental Flows Decision Support System (EFDSS) regards each storage unit as a fixed area, Wolski *et al.* (2002) use the water balance model to provide reservoir volumes which are then related to inundated area using volume-area curves, and finally transferred to a flood distribution map using flood maps derived from classification of satellite imagery (McCarthy *et al.*, 2003). In the Gwydir wetlands, a composite approach has been taken where smaller 'wetland' units (i.e. the more frequently flooded FF4 and FF3 nodes) are treated as fixed area buckets much like the Whigham and Young (2001) approach. The more expansive, less frequently inundated 'floodplain' patches (FF2 and FF1 nodes) are conceptualised more like the Wolski *et al.* (2002) approach using an area/volume relationship. In both cases the outflow is proportional to the volume held within the node. The water balance component of the IVRM also includes simple soil moisture accounting due to both the local rainfall and evapotranspiration processes, and from inundation. This accounting is not included in any of the water balance models reviewed but is valuable both in assessing vegetation response and the role of antecedent conditions.

Although the flood assessment of Chapter 5 provides a good assessment of the connected patches and their flood frequencies there is still a high level of uncertainty in the inundated area to volume relationships in the Gwydir. Rather than over-parameterise the node-network water balance model to replicate the GIS approach of the Okavango hybrid reservoir-GIS model, the approach taken for the Gwydir IVRM in this thesis is to use a generic volume/area relationship. The IVRM provides an estimate of the area of each identified floodplain patch inundated and an average depth but not an explicit spatial distribution beyond the patch analysis scale.

The Landsat mapping of annual inundation undertaken by Thomas *et al.* (in press) in the Macquarie Marshes is currently being applied to the Gwydir wetlands, while the NSW Government is also developing a more detailed IQQM model of the Gwydir catchment. The outcomes of these projects may provide the level of resolution required to further extend the Gwydir IVRM to provide a spatial distribution of inundation. The Gwydir IVRM models run at the daily time step but the results indicate that reliability at that temporal resolution is quite poor. At the 16-day time step (which matches the input vegetation response data from maximum value composite fPAR data) the model performance is much better. Adding temporal delays into the node-network model could improve the model fit to observed flow data, but is unlikely to improve the inundation estimates. Unlike the lagoon and flow through floodplain wetlands of the Border Rivers which are highly connected to the main river channel (Whigham and Young, 2001), the Gwydir Wetlands and Okavango Delta (McCarthy, 2002) tend towards being a distributary alluvial fan at the end of the river system. The time step chosen for model development can therefore be longer as total volumes are more important in the total inundated area than peak daily flows. Peak daily flows may still influence the FF4 wetlands in small floods as they rely on immediate overbank flooding.

The Ibis decision support system (Merritt *et al.*, 2010) was initially developed using a prototype of the water balance model (Merritt *et al.*, 2010; Powell *et al.*, 2008) presented in this thesis. Following completion of a more detailed IQQM model of the Gwydir wetlands by the NSW Office of Water, the Ibis model now used daily outputs from the IQQM model. The IQQM model is restricted to surface water flows and inundation and does not include a soil water component although the distribution of flows and broad understanding of the connected patches developed in this thesis helped inform the IQQM development. The water balance outputs from IQQM are summarised into event metrics specific to the ecological functions. For example for some native fish species, the flow pulse through the channel reaches is thought to trigger spawning (Wilson *et al.*, 2009). For each flow event (defined by a flow threshold) the maximum flow pulse, time of year and the probability of overbank flow are extracted and related using a Bayesian decision network (BDN) to link factors influencing spawning (Merritt *et al.*, 2010). The EFDSS (Whigham and Young, 2001) models vegetation using response functions for each influencing variable. Each vegetation stage is calculated monthly with the final assessment being given annually. Both Ibis and EFDSS rely largely on expert opinion, based on monitoring and research data where available, in developing the BDNs and response functions. The vegetation productivity model in the IVRM in this thesis is linked to inflows and soil moisture from local rainfall and evapotranspiration processes. The model is a quantitative regression model and provides a time series estimate of the phenology cycles for each landscape unit that is a subdivision of the patches (nodes). Unlike the EFDSS or Ibis approach, the IVRM does not currently model individual species response. It could, however, easily be adapted to link to BDNs or response functions from Ibis or EFDSS. In fact, the quantitative estimate of vegetation productivity and water balance of the IVRM coupled with species specific BDNs or response functions would provide the ideal combination for assessing ecological response. If a water management scenario shows a suitable response for an ecological attribute (from a BDN for example) combined with broader landscape unit vegetation productivity response, this would provide a higher level of confidence in the overall model outputs.

In Section 7.3 the model is applied to predicting the relative outputs for a range of scenarios. The scenarios have been run for a short time sequence (7 years) due to a lack of extraction data to run the model for longer under current levels of development. There is no limitation, if the data are available, to running the model for 100 years or more. Given the uncertainty in some of the model components it is important the scenario outputs are reviewed in a relative sense. It was evident in running the predevelopment scenario provided by CSIRO (2007) that the Gwydir wetlands were much wetter than they are under current development levels. The outputs from the scenario runs also demonstrated the difference in relative flooding and vegetation response between the wetlands closest to the inflows from the Gwydir River and those further west. Again, in a relative sense, the outputs can demonstrate what changes are required to improve the productivity (and by conjecture, the vegetation community structure) of some of the more degraded wetland areas. In the Border Rivers, the vegetation model for river redgum was applied over a 50 year time period based on 1993 development levels (Whigham and Young, 2001). The results demonstrated the outputs of the response in relation to regeneration, maintenance and condition of river redgum at two sites but other flow/climate scenarios were not demonstrated in the pilot study.

The IVRM does not consider the impacts of climate change (or water management scenarios) on the geomorphology of the Gwydir wetlands. In the Macquarie Marshes the potential impacts and adaptations of climate change were considered qualitatively in relation to the geomorphology (Rogers *et al.*, 2010). In a climate with less rainfall and greater evapotranspiration, and a hydrological regime with reduced large flood frequency and variability, overbank flooding would be reduced. This is likely to cause greater drying of the floodplain and extensive cracking of the soils on the periphery of wetlands. Low flows may increase due to ongoing river regulation that could encourage in-channel erosion and increased sediments in the water column. These sediments would accumulate at the end of channels in the core wetlands (Rogers *et al.*, 2010). It is likely that these same processes would occur in the Gwydir wetlands. The Gwydir Raft could continue to silt up and further decrease channel capacity at the eastern edge of the system, resulting in greater overbank flooding of the river redgum communities but less flows through to the western wetlands. Sediment deposition could also change the character and flood patterns, particularly in the most frequently flooded (FF4 and FF3) wetlands. Rogers *et al.* (2010) also highlight the impact of drier antecedent conditions on the inundated area from overbank flooding. This aspect of climate change is included in the IVRM as soil moisture is accounted for and included in the water balance model, and the climate change scenario includes both the modelled inflows, rainfall and evaporation. This again highlights the importance of including soil moisture accounting in floodplain models.

7.5 Conclusions

The landscape scale analysis of flood frequency and connectivity provides a template for the development of a node-network water balance model. The model includes the channels, wetlands and floodplains of the Gwydir wetlands and the linkages between these parts of the landscape. Wetlands are modelled as simple buckets with fixed area based on the patch analysis of Chapter 5 (section 5.3.3.2). Floodplains have a maximum area, also defined through the patch analysis, but the area changes depending on the volume of water contained within the floodplain using a simple volume/area curve. Both wetlands and floodplains include soil moisture accounting and connectivity to groundwater. Vegetation response, as measured by the fraction of photosynthetically active radiation (fPAR), is modelled directly from inflows to the system and soil moisture from local rainfall and evapotranspiration processes. The vegetation response model is based on the multiple linear regression models developed in Chapter 6 of this thesis. Together, these models form the inundation and vegetation response model (IVRM) of the Gwydir wetlands.

The IVRM is verified using observed daily flow and depth where available. Much of the wetlands have no depth data and are verified using the observed fPAR time-series and the knowledge of vegetation response to inundation developed in section 6.3.3. Although the groundwater component of the IVRM is very simple at this stage, the cumulative recharge to the alluvial aquifer is similar to that reported in CSIRO (2007). Model sensitivity is assessed against those parameters that have limited data such as channel capacity, soil field capacity, and depth of water in wetland and evapotranspiration processes. Of these, channel capacity through the Gwydir Raft, the threshold depth at which outflows occur from wetlands, the rate of outflow from wetlands and the evapotranspiration rates can all impact significantly on modelled inundation of downstream wetlands and floodplains. Further research or data acquisition is warranted to improve the model performance for these parameters.

The Gwydir IVRM can be applied to test a variety of scenarios. In this chapter, predevelopment, current development and three climate change scenarios were used to test the predictive capacity of the model. Comparing the scenarios highlighted the large reduction in overall duration and depth of flooding from predevelopment to current levels of development. As an example of the application of this type of model, the exceedence for fPAR values in a frequently flooded wetland were compared. A high vigour response of over 0.9 fPAR occurred over 47% of the time under predevelopment scenarios compared to just 14% currently, with climate change scenarios varying from 20% to less than 8%.

There is a range of other ecological models that could easily be linked to the IVRM, while the vegetation productivity model in the IVRM provides a new approach that can be coupled with existing vegetation species scale BDNs or suitability type models to improve the confidence in the outputs. The node-network conceptualisation of the IVRM may also be linked to more detailed hydrological or hydrodynamic analysis of the Gwydir wetlands that provided a robust landscape scale framework.

Chapter 8: Conclusions

8.1 Overview

This thesis integrates hydrological and ecological understanding, remote sensing analysis, statistical methods, and good modelling practice to provide a tested Inundation and Vegetation Response Model for a floodplain wetland system. This fulfils the aims of this thesis. The Gwydir wetlands, NSW, Australia, is representative of a floodplain wetland system in a dryland setting, and provides the case study for this thesis. The methods developed within this thesis are equally applicable to a range of floodplain wetland systems and address the major knowledge gaps identified.

The Gwydir floodplain and wetlands are reliant on flows from the upstream catchment. This catchment is heavily regulated with water resource developments including a large headwater storage, numerous weirs and regulating structures, diversions and channel alterations and floodplain development for irrigated agriculture. The Gwydir wetlands include a range of ecological values with some core wetlands listed under international agreements for the protection of wetlands and migratory waterbirds.

The Gwydir wetlands are a classic example of one of the management challenges within Australia; how to manage flows for achieving environmental benefits whilst still providing for an economically feasible irrigation industry. To address this, an improved ecological understanding of the benefits of flows into the Gwydir wetlands is critical. As a first step an understanding of how these flows move across the landscape has been used to develop a conceptual model of the wetlands in relation to inflows and climate. Following on from this, a landscape scale understanding of vegetation response has been developed to supplement existing site and species scale knowledge. Finally a means of translating these research findings and knowledge into a model that can assess a range of inflow and climate options or scenarios is produced.

8.2 Summary and outcomes

The research findings from this thesis are summarized in Table 8.1. The major outcome is the development of a landscape scale node-network model that allows river inflows and climate variables to be characterised as ecologically relevant variables, being inundation depth, duration and extent, and vegetation response. To develop this conceptual model, a method was proposed and tested which integrates classification of open water and vegetation response from remotely sensed normalised difference vegetation indices (NDVI). A range of flood events were mapped and summarised into homogenous patches with respect to flood frequency and connectivity in a similar way to the wetland functional classification used in the USA and Europe. Due to the inundation dynamics, the patches are divided into two types of nodes that function quite differently: wetlands that are a fixed area and flood in more than 5 in 10 years (post-development), and floodplains which have an area/volume relationship and are generally much larger in area and flood in less than 5 in 10 years. Patches are subdivided by vegetation association and the resulting landscape units used to develop models of vegetation productivity response measured as the fraction of photosynthetically active radiation (fPAR).

The Inundation and Vegetation Response Model is implemented and verified using existing flow and depth data. The flood mapping and vegetation productivity response results from this thesis are also used to verify the model. Sensitivity is tested and the model is applied to predicting inundation and vegetation response outcomes from a range of scenarios.

Table 8.1: Summary and outcomes from analysis chapters of the thesis.

Analysis	Summary and outcomes
Chapter 5: Flood assessment	
Appropriate flow and climate metrics to characterise flood events	Flow metrics relating to peak, total and antecedent inflows as well as antecedent and peak event rainfall and the days since last flood event may all be used to describe inflow events to floodplain wetland systems. In the Gwydir wetlands, flood events are best characterised by the 40-day event inflow, antecedent 90-day inflow, peak daily rainfall, 30-day antecedent rainfall and the days since last flood event
Mapping floods in shallow wetlands dominated by emergent macrophytes	Multi-temporal decision tree method developed to map both the open water flood extent and the resulting high vigour vegetation response to flooding. This method can be applied to any large areas of inundation with rapid emergence vegetation response and uses readily available NDVI from Modis and AVHRR and Landsat imagery. A range of floods are analysed with full results presented in Appendix 2. The largest flood extent of over 166 000ha occurred in 1998. The area of response for floods of 20 to 100GL (40-day total inflow) was around 20 000ha while larger floods saw a relatively linear increase in corresponding area inundated.
Landscape scale analysis of homogeneity in relation to flood frequency and connectivity	The mapping results are compiled and each pixel is characterised by flood frequency from those flooded in more than 60% of years (FF4) to those flooded in less than 30% of years (FF1). Pixels are assessed for connectivity to each of eight neighbours with all connected pixels forming a discrete ‘Patch’. These patches are further subdivided by vegetation associations to form ‘landscape units’. Over 250 patches were identified but this was reduced to 17 patches which covered 92% of the study area including all wetland vegetation. The patch analysis is used to develop a conceptual node-network model of the Gwydir wetlands based on 17 patches.

Analysis	Summary and outcomes
Chapter 6: Vegetation response	
Vegetation response measures developed	Time-series of vegetation productivity is developed from the NDVI records for each landscape unit. Productivity is measured as the fraction of photosynthetically active radiation (fPAR) which is a reliable indicator of productivity.
Vegetation response characterised	Phenological attributes are extracted from the time-series of fPAR for each landscape unit including green-up, maturity, senescence and dormancy. In the Gwydir case study, the most frequently flooded marsh clubrush LU has the highest fPAR response regularly exceeding a fPAR value of 0.9. The spikerush LUs also show high maturity fPAR. There is a trend of reduced fPAR response from east to west.
Vegetation response modelled	Multiple linear regression analysis can be used to model fPAR response to flow and soil moisture. Different landscape units show different relationships depending on flood frequency and vegetation associations.
Chapter 7: Inundation and Vegetation Response Model (IVRM) development	
Node-network water balance model	Node-network model includes the major channel reaches, wetlands (defined as connected patches inundated in more than 5 out of 10 years) and floodplains (connected patches inundated less than 5 out of 10 years). Daily water balance includes both surface water inundation and soil water components as well as groundwater recharge. The model is verified from gauged flow and depth data, reported groundwater recharge estimates, the flood assessment and vegetation responses developed in this thesis.
Vegetation response	The multiple linear regression model is coded into the IVRM and linked to inflows and soil moisture due to local rainfall and evapotranspiration. Linked to the most productive landscape unit of each node, the time series fPAR can be modelled for each scenario (of inflow and climate).
Sensitivity analysis	Sensitivity analysis can be undertaken for any parameters and can be used to identify further research needs. For the Gingham Channel between Tyreel and Teralba the Gwydir Raft can reduce capacity and the model is sensitive to capacity of less than 2000ML/day. The field capacity of the soil is dependent on soil type and the root depth that can vary depending on vegetation. The model is relatively insensitive to field capacity unless it is reduced below 150mm. This suggests that inclusion of some soil moisture accounting is important in water balance modelling in the Gwydir wetlands. The threshold depth of wetlands and the rate of outflow are important parameters to which the model is sensitive. Further work is required to define these parameters. Modelled inundation is also very sensitive to evapotranspiration (Et) rates and some uncertainty exists in the best method to apply for this system. It is likely that traditional methods of Et calculation may underestimate the Et rates from vegetated wetlands.

Analysis	Summary and outcomes
Chapter 7: cont.	
Scenario modelling	THE IVRM can be used to run scenarios related to inflow and climate. In the Gwydir case study, the CSIRO sustainable yield (2007) modelled inflow, rainfall and Et is used to run five scenarios. A current development, historical climate P pre development, historical climate Cwet current development, 2030 climate change scenario (wet) Cmid current development, 2030 climate change scenario (mid) Cdry current development, 2030 climate change scenario (dry) Scenario P results in inundation in the most frequently flooded nodes for over 99% of days. In comparison, scenario A may only inundate these same nodes for less than 77% of days while future climate scenarios range from 63% to 83% of days. This translates to fPAR response exceeding 0.9 fPAR for over 47% of the time in scenario P, less than 14% under scenario C with climate changes scenarios ranging from 20% to less than 8%.

8.3 Future directions for model development

The conceptual node-network model provides an important advance in modelling. However, more detailed Landsat mapping of annual inundation and LiDAR mapping and hydrodynamic studies could strengthen outcomes from this thesis. This additional information will still need to be conceptualised and summarised to be useful to further model development.

The flood assessment methods can be applied to a range of floodplain wetland systems and could provide a consistent classification across the Murray-Darling Basin floodplains and wetlands regardless of the seasonality, duration and depth of flooding, as it does not rely on the open water extent. This would require testing of the method in other floodplain systems. Unlike tradition mapping techniques, the methods can be applied retrospectively to give the areas responding to flooding, and using the NDVI and fPAR approach, can provide a benchmark of that response. Node-network conceptualisation from the patch analysis can also supplement existing information and be used to further develop water balance or flow models such as IQQM. The role of soil water in floodplain wetland systems should be considered in such models.

The model development also highlighted some areas where there are still knowledge gaps that affect model parameterisation and performance. In the Gwydir wetlands, better data on the channel capacity of some reaches is required while monitoring of depths across the wetlands and floodplains is also needed to help establish the threshold depths and assist to parameterise the outflow rates, as well as to calibrate and verify the model performance. Further information on groundwater linkages would also be useful. A better understanding of the soil moisture and evapotranspiration processes in floodplain wetlands would improve the model structure particularly for the floodplain and wetland nodes. Although sensitivity analysis and some uncertainties are reported throughout sections of this thesis, these have not been fully coded into the IVRM and are another area for future development. The methods and models developed in this thesis could be further developed using time-series GIS tools and DSS software to be readily reapplied to other floodplain wetlands. But a good understanding of remote sensing, GIS, model development and of the floodplain wetland system itself is required to utilise the methods presented in this thesis.

The outcomes of this thesis provide a quantitative model of vegetation productivity response to inflows and climate. Further development of this model to relate the productivity response to inundation depth and duration for each landscape unit would enhance the model. In addition, the integration with existing Bayesian decision networks or species scale response models would be of great value to increase confidence in the model outcomes. The wealth of knowledge at site scale as well as glasshouse experimental data could also be integrated into the model to provide a full range of vegetation responses linked directly to the water balance model. Finally, other ecological values in floodplain wetlands such as waterbirds, aquatic vertebrates and invertebrates should be identified and the linkages between them included in the model structure.

8.4 Concluding remarks

Many Australian and overseas catchments contains large areas of valuable wetlands. The area and condition of many of these wetlands have been diminished over the last century due to a combination of land use impacts and river regulation. This indicates that it is not possible to sustain the same area of wetlands, maintaining the same level of diversity and condition using dramatically less water. This thesis focuses on identifying the current linkages between flow, climate and the landscape in floodplain wetlands, and on characterising the vegetation productivity response in these systems.

The assessment framework presented here can be applied not only in the Gwydir wetlands, but also to other inland floodplain wetland systems. It takes a holistic view of an ecosystem, and explores how a wetting regime influences structure and function. The flood pulse in these systems provides the lateral overflow of water to inundate floodplains and wetlands, in turn providing the physicochemical environment for rapid and highly productive vegetation response. The temporal component of these flood pulses is also important to sustain the types of vegetation that have evolved, with different vegetation communities associated with different flood frequencies, while drying cycles also have a role in nutrient cycling of the organic matter produced insitu. Vertical connectivity to soil moisture and groundwater also influence inundation and vegetation response. The landscape scale approach uses the lateral, temporal and vertical connectivity, critical to the floodplain wetland functioning, to inform the development of a node-network model.

The spatial and temporal scales used in the assessment and modelling structures are specific to the geomorphology and hydrology of the case study catchment, but the principles and methods can be applied to floodplain wetland systems in general. As remote sensing technology provides more and more detail at a range of resolutions, and much of the on-ground monitoring efforts are centred towards site and species-specific assessment, the overall form, function and connectivity of the system can be lost in the detail. To make informed decisions about the management of these systems, with regards to managed inflows, the system firstly needs to viewed as a whole as presented in this thesis. Once the landscape scale inundation behaviour and vegetation productivity response can be quantified, the detail at finer resolutions can filled in where required.

References

Al-Bakri, J. T. and Suleiman, A. S., 2004. NDVI response to rainfall in different ecological zones in Jordan, *International Journal of Remote Sensing,* **25**: 3897-3912.

Allan, A. and Lovett, S., 1997. *Impediments to managing environmental water provisions*, Bureau of Resource Sciences, Canberra.

Andersson, L., Gumbricht, T., Hughes, D., Kniveton, D., Ringrose, S., Savenije, H., Todd, M., Wilk, J. and Wolski, P., 2003. Water flow dynamics in the Okavango River Basin and Delta an prerequisite for the ecosystem of the Delta, *Physics and Chemistry of the Earth*, **28**: 1165-1172.

Apan, A. and Sternes, P., 2006. Mapping and spatio-temporal analysis of flooded and inundated areas in the Lower Balonne Floodplain, Queensland, Australia., *WSEAS Transactions on Environment and Development*, **2**: 360-367.

Arthington, A. H., 1995. *State of the rivers in the cotton growing areas. Northern NSW and the Border Rivers with Queensland*, Occasional Paper No.02/95, Canberra, Environment Protection Association, Cotton Research and Development Corporation, Murray-Darling Basin Commission and LWRRDC, Land and Water Resources Research and Development Corporation.

Baldwin, D. S. and Mitchell, A. M., 2000. The effects of drying and re-flooding on the sediment and soil nutrient dynamics of lowland river-floodplain systems: a synthesis, *Regulated Rivers: Research & Management*, **16**: 457-467.

Barrett, D., Byrne, G. and Senarath, U., 2005. *The 250m 16 day vegetation index product (MOD13Q1) for Australia. A comparison with AVHRR normalised difference vegetation index*, CSIRO Land and Water, Canberra.

Barton, I. J. and Bathols, J. M., 1989. Monitoring floods with AVHRR, *Remote sensing of the environment*, **30**: 89-94.

Beeton, R. J. S., Buckley, K. I., Jones, G., Morgan, D., Reichelt, R. E., Trewin, D. and (2006 Australian State of the Environment Committee), 2006. *Australia State of the Environment 2006, Independent report to the Australian Government Minister for the Environment and Heritage*, Department of Environment and Heritage, Canberra.

Benger, S. N. 1997. *Remotely sensed determination of flood surface gradients for hydrological modelling of semi-arid floodplains* Proceeding of the International Geoscience and Remote Sensing Symposium, Singapore.

Bennett, M. and Green, A. J., 1993. *Preliminary assessment of the Gwydir wetland water needs*, Department of Water Resources, Sydney.

Bennett M and McCosker R (1994*) Estimating environmental flow requirements of wetlands.* In Proceedings of the Environmental Flows Seminar, Artarmon., pp. 9-16

Berry, S. L. and Roderick, M. L., 2002. Estimating mixtures of leaf functional types using continental-scale satellite and climatic data, *Global Ecology and Biogeography*, **11**: 23-29.

Blom, C. and Voesenek, L., 1996. Flooding: The survival strategies of plants, *Trends in Ecology & Evolution*, **11**: 290-295.

Boresjo Bronge, L. and SwedPower, A. B., 2004. *Satellite remote sensing for estimating leaf area index, FPAR and primary production. A literature review*, Swedish Nuclear Fuel and Waste Management Company, Stockholm.

Boulton, A. J. and Brock, M. A., 1999. *Australian freshwater ecology: Processes and management*., Gleneagles Publishing, Glen Osmond, SA.

Boulton, A. J. and Lloyd, L. N., 1991. Macroinvertebrate assemblages in floodplain habitats of the lower River Murray, South Australia., *Regulated Rivers: Research and Management,* **6**: 183-201.

Boulton, A. J. and Lloyd, L. N., 1992. Flooding frequency and invertebrate emergence from dry floodplain sediments of the river Murray, Australia., *Regulated Rivers: Research & Management*, **7**: 137-151.

Bowen, S. and Simpson, S., 2009. *Changes in extent and condition of the vegetation communities of the Gwydir wetlands and floodplain 1996-2008*. Final report to NSW Wetland Recovery Program, Department of Environment, Climate Change and Water, Sydney.

Box, E. O., Holben, B. N. and Kalb, V., 1989. Accuracy of the AVHRR vegetation index as a predictor of biomass, primary productivity and net CO2 flux, *Plant Ecology*, **80**: 71-89.

Brinson M M (2009) The United States HGM (Hydrogeomorphic) Approach. In *The Wetlands Handbook* (Eds, Maltby E and Barker T). Wiley-Blackwells, pp. 486-512.

Brock, M., Nielsen, D. L. and Crossle, K., 2005. Changes in biotic communities developing from freshwater wetland sediments under experimental salinity and water regimes, *Freshwater Biology*, **50**: 1376-1390.

Brock, M. A., 1991. Mechanisms for maintaining persistent populations of Myriophyllum variifolium J. Hooker in a fluctuating shallow Australian lake, *Aquatic Botany*, **39**: 211-219.

Brock, M. A. and Casanova, M. T., 1997. Plant life at the edges of wetlands; ecological responses to wetting and drying patterns., In *Frontiers in Ecology: Building the Links* (Eds, Klomp, N. and Lunt, I.) Elsevier Science, Oxford, pp. 181-192.

Bryant, R. G., 1999. Application of AVHRR to monitoring a climatically sensitive playa. Case study: Chott El Djerid, southern Tunisia, *Earth Surface, Processes and Landforms*, **24**: 283-302.

Bunn, S. E. and Arthington, A. H., 2002. Basic principles and ecological consequences of altered flow regimes for aquatic biodiversity, *Environmental Management*, **30**: 492-507.

Bureau of Meteorology, 2004. Moree, NSW: Daily weather observations, Available at: www.bom.gov.au (accessed December 2004).

Bureau of Meteorology, 2010. Moree, NSW: Weather observations, Available at: www.bom.gov.au (accessed October 2010).

Caddy, H., 2004. *Lower Gingham Watercourse data collection and flood study: Draft Phase A report*. NSW Department of Land and Water Conservation, Sydney.

Capon, S. and Brock, M. A., 2006. Flooding, soil seed bank dynamics and vegetation resilience of a hydrologically variable desert floodplain., *Freshwater Biology*, **51**: 206-223.

Capon, S. J., 2003. Plant community responses to wetting and drying in a large arid floodplain, *River research and applications*, **19**: 509-520.

Capon, S. J., 2005. Flood variability and spatial variation in plant community composition and structure on a large arid floodplain, *Journal of Arid Environments*, **60**: 283-302.

Capon, S. J., James, C. S., Williams, L. and Quinn, G. P., 2009. Responses to flooding and drying in seedlings of a common Australian desert floodplain shrub: Muehlenbeckia florulenta Meisn. (tangled lignum), *Environmental and Experimental Botany*, **66**: 178-185.

Casanova, M. T. and Brock, M. A., 2000. How do depth, duration and frequency of flooding influence the establishment of wetland plant communities?, *Plant Ecology*, **147**: 237-250.

Chauhan, M. and Gopal, B., 2005. Vegetation structure and dynamics of a floodplain wetland along a subtropical regulated river, *River research and applications*, **21**: 513-534.

Chessman, B. and Jones, H., 2001. *Integrated monitoring of environmental flows: design report.*, Department of Land and Water Conservation, Parramatta.

Chiew, F. H. S. and McMahon, T. A., 1992. An Australian comparison of Penman's potential evapotranspiration estimates and class A evaporation pan data., *Australian Journal of Soil Research*, **30**: 101-112.

Chiew, F. H. S., Teng, J., Kirono, D., Frost, A. J., Bathols, J. M., Vaze, J., Viney, N. R., Young, W. J., Hennessy, K. J. and Cai, W. J., 2008. *Climate data for hydrologic scenario modelling across the Murray-Darling Basin. A report to the Australian Government from the CSIRO Murray-Darling Basin Sustainable Yields Project*, CSIRO, Australia.

Chopping, M. J., 1998. *BRDF applications in semiarid grassland monitoring with the AVHRRs*, http://www.csam.montclair.edu/~chopping/index.php. (assessed March 2006).

Costelloe, J. F., Grayson, R. B., Argent, R. M. and McMahon, T. A., 2003. Modelling the flow regime of an arid zone floodplain river, Diamantina River, Australia, *Environmental Modelling & Software*, **18**: 693-703.

Costelloe, J. F., Grayson, R. B. and McMahon, T. A., 2005. Modelling stream flow for use in ecological studies in a large, arid zone river, central Australia, *Hydrological processes*, **19**: 1165-1183.

Cox, S. J., Sivertsen, D. P. and Bedward, M., 2001. Clearing of native woody vegetation in the New South Wales northern wheatbelt: Extent, rate of loss and implications for biodiversity conservation, *Cunninghamia*, **7**: 101-155.

Cronk, J. K. and Fennessy, M. S., 2001. *Wetland plants: biology and ecology*, CRC Press, Boca Raton, FL

CSIRO, 2007. *Water availability in the Gwydir. A report to the Australian Government from the CSIRO Murray-Darling Basin Sustainable Yields Project*. CSIRO, Australia.

Department of Environment and Conservation, 2003. *New South Wales State of the Environment 2003*, Department of Environment and Conservation, Sydney.

Department of Infrastructure Planning and Natural Resources, 2004a. *Draft exhibition document: Lower Gingham Watercourse floodplain management plan V1.4*, Department of Infrastructure, Planning and Natural Resources, Tamworth.

Department of Infrastructure Planning and Natural Resources, 2004b. *Water Sharing Plan for the Gwydir Regulated River Water Source (as amended 1 July 2004)*. Sydney,

Department of Water and Energy, 2007. *Pinneena 9.2: New South Wales Surface Water Archive*, NSW Department of Water and Energy, Sydney.

Di Bella, C. M., Paruelos, J. M., Becerra, J. E., Bacour, C. and Baret, F., 2004. Effect of senescent leaves on NDVI-based estimates of fAPAR: experimental and modelling evidences., *International Journal of Remote Sensing*, **25**: 5415-5427.

EAS Systems, 2009. *Gwydir Wetlands - Soil Survey, Report 22317.35447 prepared for River and Wetlands unit*, DECC, Sydney

Eklundh, L., 1998. Estimating relations between AVHRR NDVI and rainfall in East Africa at 10-day and monthly time scales, *International Journal of Remote Sensing*, **19**: 563-568.

Environment Australia, 2001. *A Directory of Important Wetlands in Australia, Third Edition.*, Environment Australia, Canberra.

Field, C. B., Randerson, J. T. and Malmstrom, C. M., 1995. Global net primary production: Combining ecology and remote sensing, *Remote Sensing of Environment*, **51**: 74-88.

Finlayson, B. L., Hall, R. and Bayliss B (1998) *Regional review of wetland management issues: wet-dry tropics of northern Australia.* LWRRDC Occasional Paper. LWRRDC National Wetlands R&D Program, Canberra

Finlayson, C. M. and Rea, N. (1999) Reasons for the loss and degredation of Australian wetlands. *Wetlands Ecology and Management* **7**: 1-11

Frazier, P. S. and Page, K. L., 2000. Water body detection and delineation with Landsat TM data, *Photogrammetric Engineering and Remote Sensing*, **66**: 1461 - 1465.

Froend, R. H. and McComb, A. J., 1994. Distribution, productivity and reproductive phenology of emergent macrophytes in relation to water regimes at wetlands of south-western Australia, *Australian Journal of Marine and Freshwater Research*, **45**: 1491-1508.

Gallo, K., Ji, L., Reed, B., Dwyer, J. and Eidenshink, J., 2004. Comparison of MODIS and AVHRR 16-day normalized difference vegetation index composite data, *Geophysical Research Letters*, **31**: L07502.

Gallo, K., Ji, L., Reed, B., Eidenshink, J. and Dwyer, J., 2005. Multi-platform comparisons of MODIS and AVHRR normalized difference vegetation index data, *Remote Sensing of Environment,* **99**: 221-231.

Glenn, E. P., Huete, A. R., Nagler, P. L. and Nelson, S. G., 2008. Relationship between remotely-sensed vegetation indices, canopy attributes and plant physiological processes: What vegetation indices can and cannot tell us about the landscape., *Sensors*, **8**: 2136-2160.

Goetz, S. J., 1997. Multi-sensor analysis of NDVI, surface temperature and biophysical variables at a mixed grassland site, *International Journal of Remote Sensing*, **18**: 71-94.

Gordon, N. D., A, M. T., Finlayson, B. L., Gippel, C. J. and J, N. R., 2004. *Stream hydrology: an introduction for ecologists,* John Wiley & Sons Ltd, Chichester, UK.

Green, A. J. and Bennett, M., 1991. *Wetlands of the Gwydir Valley: Progress Report,* Department of Water Resources, Parramatta.

Gumbricht, T., McCarthy, J. and McCarthy, T. S., 2004a. Channels, wetlands and islands in the Okavango Delta, Botswana, and their relation to hydrological and sedimentological processes, *Earth Surface, Processes and Landforms*, **29**: 15-29.

Gumbricht, T., McCarthy, T. S. and Bauer, P., 2005. The micro-topography of the wetlands of the Okavango Delta, Botswana, *Earth Surface, Processes and Landforms*, **30**: 27-39.

Gumbricht, T., Wolski, P., Frost, P. and McCarthy, T. S., 2004b. Forecasting the spatial extent of the annual flood in the Okavango delta, Botswana, *Journal of Hydrology*, **290**: 178-191.

Harmel, R. D., Cooper, R. J., Slade, R. M., Haney, R. L. and Arnold, J. G., 2006. Cumulative uncertainty in measured streamflow and water quality data for small watersheds, *Trans ASABE*, **49**: 689-701.

Harmel, R. D., Smith, D. R., King, K. W., Slade, R. M. and Smith, P. (Eds.), 2008. *Data uncertainty estimation tool for Hydrology and water quality (DUET-H/WQ): Estimating measurement uncertainty for monitoring and modelling applications* Proceedings of the iEMSs Fourth Biennial Meeting: International Congress on Environmental Modelling and Software (iEMSs 2008), Barcelona, Catalonia.

Harmel, R. D. and Smith, P. K., 2007. Consideration of measurement uncertainty in the evaluation of goodness-of-fit in hydrologic and water quality modelling, *Journal of Hydrology*, **337**: 326-336.

Huete, A., Didan, K., Miura, T., Rodriguez, E. P., Gao, X. and Ferreira, L. G., 2002. Overview of the radiometric and biophysical performance of the MODIS vegetation indices, *Remote Sensing of Environment*, **83**: 195-213.

Huete, A., Justice, C. and van Leeuwen, W., 1999. *MODIS Vegetation Index (MOD13): Algorithm theoretical basis document*. (http://modis .gsfc.nasa.gov/data/atbd/atbd_mod13.pdf).

Humphreys, E. and Edraki, M., 2003. *Deep drainage and crop water use for irrigated annual crops and pastures in Australia - a review of determinations in fields and lysimeters.*, CSIRO Land and Water, Griffith.

Hunter, N. M., Bates, P. D., Horritt, M. S. and Wilson, M. D., 2007. Simple spatially-distributed models for predicting flood inundation: A review, *Geomorphology*, **90**: 208 - 225.

Jain, S. K., Saraf, A. K., Goswami, A. and Ahmad, T., 2006. Flood inundation mapping using NOAA AVHRR data, *Water Resources Management*, **20**: 949-959.

Jain, S. K., Singh, R. D., Jain, M. K. and Lohani, A. K., 2005. Delineation of flood-prone areas using remote sensing techniques, *Water Resources Management*, **19**: 333-347.

Jakeman, A. J., Letcher, R. A. and Norton, J. P., 2006. Ten iterative steps in development and evaluation of environmental models, *Environmental Modelling & Software*, **21**: 602-614.

James, C. S., Capon, S. J., White, M. G., Rayburg, S. C. and Thoms, M. C., 2007. Spatial variability of the soil seed bank in a heterogeneous ephemeral wetland system in semi-arid Australia, *Plant Ecology*, **190**: 205-217.

James, C. S., Thoms, M. C. and Quinn, G. P., 2008. Zooplankton dynamics from inundation to drying in a complex ephemeral floodplain-wetland, *Aquatic Sciences*, **70**: 259-271.

Johnson, W., 2004. *Breeding of colonially nesting waterbirds*. Unpublished report, NSW National Parks and Wildlife Service, Dubbo.

Johnston, R. M. and Barson, M. M., 1993. Remote sensing of Australian wetlands: An evaluation of Landsat TM data for inventory and classification, *Australian Journal of Marine and Freshwater Research*, **44**: 235-252.

Jones, K. L., Poole, G. C., O'Daniel, S. J., Mertes, L. A. K. and Stanford, J. A., 2008. Surface hydrology of low-relief landscapes: Assessing surface water flow impedance using LIDAR-derived digital elevation models, *Remote Sensing of Environment*, **112**: 4148-4158.

Julien, M., Storrie, A. and McCosker, R. (Eds.), 2004. *Lippia, Phyla canescens, an increasing threat to agriculture and the environment*. Fourteenth Australian Weeds Conference Papers and Proceedings,

Junk, W. J., Bayley, P. B. and Sparks, R. E., 1989. The Flood Pulse Concept in River-Floodplain Systems, *Canadian special publication of fisheries and aquatic sciences*, **106**: 110-127.

Kelleway, J., Mazumder, D., Wilson, G. and Kobayashi, T., 2010a. Using isotopic techniques to assess trophic structure in northern Murray-Darling Basin wetlands., In *Ecological Response Modelling in the Murray-Darling Basin* (Eds, Saintilan, N. and Overton, I. C.) CSIRO Publishing, Melbourne, pp. 85-102.

Kelleway, J., Mazumder, D., Wilson, G., Saintilan, N., Knowles, L., Iles, J. and Kobayashi, T., 2010b. Trophic structure of benthic resources and consumers varies across a regulated floodplain wetland, *Marine and Freshwater Research*, **61**: 430-440.

Kennard, M. J., Pusey, B. J., Olden, J. D., Mackay, S. J., Stein, J. L. and Marsh, N., 2010. Classification of natural flow regimes in Australia to support environmental flow management, *Freshwater Biology*, **55**: 171-193.

Kerr, J. T. and Ostrovsky, M., 2003. From space to species: ecological application for remote sensing, *Trends in Ecology & Evolution*, **18**: 299-305.

Keyte, P., 1994. *Lower Gwydir Wetland Plan of Management 1994 to 1997. Report by NSW Department of Water Resources for the Lower Gwydir Wetland Steering Committee.*, NSW Department of Water Resources, Sydney.

King, E. A., 2003. *The Australian AVHRR data set at CSIRO/EOC: Origins, processes, holdings and prospects,* CSIRO Earth Observation Centre Report 2003/04, Canberra.

Kingsford, R. T., 2000. Ecological impacts of dams, water diversions and river management on floodplain wetlands in Australia., *Austral Ecology*, **25**: 109-127.

Kingsford, R. T. and Johnson, W., 1998. Impact of water diversions on colonially-nesting waterbirds in the Macquarie Marshes of Arid Australia., *Colonial Waterbirds*, **21**: 159-170.

Kingsford, R. T. and Norman, F. I., 2002. Australian waterbirds - products of the continent's ecology, *Emu*, **102**: 47-69.

Kingsford, R. T. and Thomas, R. F., 2002. Use of satellite image analysis to track wetland loss on the Murrumbidgee River floodplain in arid Australia, 1975-1998., *Water Science and Technology*, **45**: 45-53.

Legates, D. R. and McCabe, G. J., 1999. Evaluating the use of "goodness-of-fit" measures in hydrologic and hydroclimatic model validation, *Water Resources Research*, **35**: 233-241.

Letcher, R. and Jakeman, A. J., 2003. Application of an Adaptive Method for Integrated Assessment of Water Allocation Issues in the Namoi River Catchment, Australia, *Integrated Assessment*, **4**: 73-89.

Letcher, R. A., Croke, B. F. W. and Jakeman, A. J., 2007. Integrated assessment modelling for water resource allocation and management: A generalised conceptual framework, *Environmental Modelling & Software*, **22**: 733-742.

Letcher, R. A., Jakeman, A. J. and Croke, B. F. W., 2004. Model development for integrated assessment of water allocation options., *Water Resources Research*, **40**: W05502 doi 05510.01029/02003WR002933.

Lott, R. B. and Hunt, R. J., 2001. Estimating evapotranspiration in natural and constructed wetlands, *Wetlands*, **21**: 614-628.

Lupo, F., Linderman, M., Vanacker, V., Bartholome, E. and Lambin, E. F., 2007. Categorization of land-cover change processes based on phenological indicators extracted from time series of vegetation index data, *International Journal of Remote Sensing*, **28**: 2469-2483.

Lytle, D. A. and Poff, N. L., 2004. Adaptation to natural flow regimes, *Trends in Ecology & Evolution*, **19**: 94-100.

Mackay, S. J., Finlayson, C. M., Fernandez-Prieto, D., Davidson, N., Pritchard, D. and Rebelo, L.-M., 2009. The role of Earth Observation (EO) technologies in supporting implementation of the Ramsar Convention on Wetlands, *Journal of Environmental Management*, **90**: 2234-2242.

Maltby, E. (1989) Soils and wetland functions. In *Conservation and Management of Greek Wetlands. Proceedings of a Greek Wetland Workshop*. (Ed. Gerakis, P. A.) pp. 61-78. IUCN, Gland, Switzerland: Thessaloniki, Greece.

Maltby, E., Barker, T. and Linstead, C. (2009) Development of a European Methodology for the Functional Assessment of Wetlands. In *The Wetlands Handbook*. (Eds Maltby, E. and Barker, T.) pp. 513-544. Wiley-Blackwells

Mawhinney, W., 2003. Restoring biodiversity in the Gwydir wetlands through environmental flows., *Water Science and Technology*, **48**: 73-81.

McCarthy, J. (2002) *Remote sensing for detection of landscape form and function of the Okavango Delta Botswana.* PhD Thesis, Department of Land and Water Resources Engineering, Royal Institute of Technology, Stockholm.

McCarthy, J., Gumbricht, T. and McCarthy, T. S., 2005. Ecoregion classification in the Okavango Delta, Botswana from multitemporal remote sensing, *International Journal of Remote Sensing*, **26**: 4339-4357.

McCarthy, J., Gumbricht, T., McCarthy, T. S., Frost, P., Wessels, K. and Seidel, F., 2003. Flooding patterns of the Okavango wetland in Botswana between 1972 and 2000, *Ambio*, **32**: 453-457.

McCosker, R., 1994a. *Lippia (Phyla nodiflora). An invasive plant of floodplain ecosystems in the Murray-Darling Basin*., University of New England, Armidale.

McCosker, R. (1994b) *The preparation of a plan of management for the Gingham Watercourse*. Masters Thesis, University of New England, Armidale.

McCosker, R., 1996. *Gwydir Wetlands ecological response to flooding. 1995-1996*., LANDMAX Natural Resource Management Services.

McCosker, R., 1999. *Gwydir Wetlands ecological response to flooding. 1997.*, LANDMAX Natural Resource Management Services.

McCosker, R., 2001a. *Gwydir Wetlands ecological response to flooding. 1998.,* LANDMAX Natural Resource Management Services.

McCosker, R., 2001b. *Gwydir Wetlands ecological response to flooding. 2000-2001.*, LANDMAX Natural Resource Management Services.

McFeeters, S. K., 1996. The use of Normalised Difference Water Index (NDWI) in the delineation of open water features, *International Journal of Remote Sensing,* **17**: 1425-1432.

Merritt, W., Powell, S., Pollino, C. and T, J., 2010. Ibis: a decision support system for managers of environmental flows into wetlands, In *Ecological Response Modelling in the Murray-Darling Basin* (Eds, Saintilan, N. and Overton, I. C.) CSIRO Publishing, Melbourne, pp. 85-102.

Mertes, L. A. K., 1997. Documentation and significance of the perirheic zone on inundated floodplains, *Water Resources Research*, **33**: 1749-1762.

Mertes, L. A. K., 2002. Remote sensing of riverine landscapes, *Freshwater Biology*, **47**: 799-816.

Mitsch, W. J. and Gosselink, J. G., 2000. *Wetlands*, John Wiley & Sons, New York.

Mohamed, Y. A., Bastiaanssen, W. G. M. and Savenije, H. H. G., 2004. Spatial variability of evaporation and moisture storage in the swamps of the upper Nile studied by remote sensing techniques, *Journal of Hydrology*, **289**: 145-164.

Murphy, S. R. and Lodge, G. M. (Eds.), 2001. Plant density, litter and bare soil effects on actual evaporation and transpiration in autumn. *Proceedings of the 10th Australian Agronomy Conference*, Hobart.

Myneni, R. B. and Williams, D. L., 1994. On the relationship between FAPAR and NDVI, *Remote Sensing of Environment*, **49**: 200-211.

Nanson, G. C. and Croke, J. C., 1992. A genetic classification of floodplains, *Geomorphology*, **4**: 459-486.

Nielsen, D. L. and Chick, A. J., 1997. Flood-mediated changes in aquatic macrophyte community structure., *Marine and Freshwater Research*, **48**: 153-157.

NSW Department of Environment Climate Change and Water, 2010. *NPWS is ready and committed to improving health of wetland property.* Media release, 26 Oct 2010.

NSW Department of Land and Water Conservation (1996). *Northern NSW Cotton Development Shapefile*, ANZLIC unique identifier ANZNS0359090012, DLWC, Gunnedah

NSW Department of Land and Water Conservation, 2000. *Cap & Pipe the Bores*, Sydney,

Ordoyne, C. and Friedl, M. A., 2008. Using MODIS data to characterize seasonal inundation patterns in the Florida Everglades, *Remote Sensing of Environment*, **112**: 4107-4119.

Paget, M. J. and King, E. A., 2008. MODIS *Land data sets for the Australian region*, CSIRO Marine and Atmospheric Research Internal Report No. 004.

Penuelas, J., Gamon, J. A., Griffin, K. L. and Field, C., 1993. Assessing community type, plant biomass, pigment composition and photosynthetic efficiency of aquatic vegetation from spectral reflectance, *Remote Sensing of Environment*, **46**: 110-118.

Pettorelli, N., Vik, J. O., Mysterud, A., Gaillard, J., Tucker, C. J. and Stenseth, N. C., 2005. Using the satellite-derived NDVI to assess ecological responses to environmental change, *Trends in Ecology & Evolution*, **20**: 503-510.

Pezeshki, S. R., 2001. Wetland plant responses to soil flooding, *Environmental and Experimental Botany*, **46**: 299-312.

Pietsch, T. J. (2006) Fluvial geomorphology and late quaternary geochronology of the Gwydir fan-plain. PhD Thesis, School of Earth and Environmental Sciences, University of Wollongong.

Podger, G. and Hameed, T. 2000. Use of IQQM to develop environmental flow rules for the Lachlan regulated river system Hydro 2000, 3rd International Hydrology and Water Resources Symposium, Perth, WA, Australia.

Poff, N. L., Allan, J. D., Bain, M. B., Karr, J. R., Prestegaard, K. L., Richter, B. D., Sparks, R. E. and C, S. J., 1997. The Natural Flow Regime: A paradigm for river conservation and restoration, *Bioscience*, **47**: 769-784.

Poff, N. L., Richter, B. D., Arthington, A. H., Bunn, S. E., Naiman, R. J., Kendy, E., Acreman, M., Apse, C., Bledsoe, B. P., Freeman, M. C., Henriksen, J., Jacobson, R. B., Kennen, J. G., Merritt, D. M., O'Keeffe, J. H., Olden, J. D., Rogers, K., Tharme, R. E. and Warner, A., 2010. The ecological limits of hydrologic alteration (ELOHA): a new framework for developing regional environmental flow standards, *Freshwater Biology*, **55**: 147-170.

Poole, G. C., 2002. Fluvial landscape ecology: addressing uniqueness within the river discontinuum, *Freshwater Biology*, **47**: 641-660.

Posse, G., Oesterheld, M. and Di Bella, C. M., 2005. Landscape, soil and meteorological influences on canopy dynamics of northern flooding Pampa grasslands, Argentina, *Applied Vegetation Science*, **8**: 49-56.

Powell, S. J. 2005) *Modelling flood dynamics in a regulated floodplain wetland.* Masters Subthesis, Integrated Catchment, Assessment and Management Centre, The Australian National University, Canberra, 98pp.

Powell, S. J., Croke, B. F. W. and King, E. A. 2007. Modelling ecosystem response to flooding: a remote sensing approach. *MODSIM 2007 International Congress on Modelling and Simulation*. Modelling and Simulation Society of Australia and New Zealand, Christchurch, New Zealand.

Powell . J., Croke, B. F. W., King, E. A., Barrett, D. J., Berry, S. and Mawhinney W (2007) Characterising flood response of wetland and floodplain vegetation using temporal NDVI profiles. In *Joint meeting of the New Zealand Freshwater Sciences Society and the Australian Society for Limnology*. Queenstown, New Zealand (poster)

Powell, S. J., Letcher, R. A. and Croke, B. F. W., 2008. Modelling floodplain inundation for environmental flows: Gwydir wetlands, Australia, *Ecological Modelling*, **211**: 350-362.

Price, J., Gross, C. L. and Whalley, W., 2010. Prolonged summer flooding switched dominance from the invasive weed Lippia (Phyla canescens) to native species in one small, ephemeral wetland., *Ecological Management and Restoration*, **11**: 61-63.

Quan, W., Masataka, W., Seiji, H. and Shogo, M., 2003. Using NOAA AVHRR Data to Assess Flood Damage in China, *Environmental Monitoring and Assessment*, **82**: 119-148.

Ramberg, L. and Wolski, P., 2008. Growing islands and sinking solutes: processes maintaining the endorheic Okavango Delta as a freshwater system, *Plant Ecology,* **196**: 215-231.

Ramsar Convention Secretariat, 2004. *The Ramsar Convention Manual: a Guide to the Convention on Wetlands* (Ramsar, Iran, 1971), 3rd ed., Gland, Switzerland., Ramsar Convention Secretariat.

Rayburg, S., Thoms, M. and Neave, M., 2009. A comparison of digital elevation models generated from different data sources, *Geomorphology*, **106**: 261-270.

Reed, M., Cuddy, S. M. and Rizzoli, A. E., 1999. A framework for modelling multiple resource management issues--an open modelling approach, *Environmental Modelling and Software*, **14**: 503-509.

Reid, M. A. and Quinn, G. P., 2004. Hydrologic regime and macrophyte assemblages in temporary floodplain wetlands: implications for detecting responses to environmental water allocations, *Wetlands*, **24**: 586-599.

Richards, J. A. and Jia, X., 1999a. *Remote Sensing Digital Image Analysis. An Introduction.*, Springer, Berlin Heidelberg New York.

Roberts, J., 1993. *Water Management options for Gwydir Valley wetlands*, Griffith, CSIRO Division of Water Resources.

Roberts, J. and Marston, F., 2000. *Water regime of wetland and floodplain plants in the Murray-Darling Basin: A source book of ecological knowledge.*, CSIRO Land and Water, Canberra.

Roberts, J. and Marston, F., 2011. *Water regime of wetland and floodplain plants: a source book for the Murray-Darling Basin*, National Water Commission, Canberra.

Roberts, J., Young, B. and Marston, F., 2000. *Estimating the water requirements for plants of floodplain wetlands: a guide.* Occasional Paper 04/00, Land and Water Resources Research and Development Corporation, Canberra.

Robertson, A. I., Bacon, P. and Heagney, G., 2001. The responses of floodplain primary production to flood frequency and timing, *Journal of Applied Ecology*, **38**: 126-136.

Robson, B. J., Hamilton, D. P., Webster, I. T. and Chan, T., 2008. Ten steps applied to development and evaluation of process-based biogeochemical models of estuaries, *Environmental Modelling & Software*, **23**: 369-384.

Roderick, M. L., Noble, I. R. and Cridland, S. W., 1999. Estimating woody and herbaceous vegetation cover from time series satellite observations. GCTE/LUCC RESEARCH LETTER, *Global Ecology and Biogeography*, **8**: 501-508.

Rogers, K., Ralph, R. and Imgraben, S., 2010. Water requirements of biota, geomorphology and climate change in the Macquarie Marshes, In *Ecosystem response modelling in the Murray-Darling Basin* (Eds, Saintilan, N. and Overton, I. C.) CSIRO Publishing, Melbourne, pp. 85-102.

Sakamoto, T., Nguyen, N. V., Kotera, A., Ohno, H., Ishitsuka, N. and Yokozawa, M., 2007a. Detecting temporal changes in the extent of annual flooding within the Cambodia and the Vietnamese Mekong Delta from MODIS time-series imagery, *Remote Sensing of Environment*, **109**: 295-313.

Scanlon, T. M., Albertson, J. D., Caylor, K. K. and Williams, C. A., 2002. Determining land surface fractional cover from NDVI and rainfall time series for a savanna ecosystem, *Remote Sensing of Environment*, **82**: 376-388.

Schmugge, T. J., Kustas, W. P., Ritchie, J. C., Jackson, T. J. and Rango, A., 2002. Remote sensing in hydrology, *Advances in Water Resources*, **25**: 1367-1385.

Scholz, O. and Boon, P. I., 1993. Biofilms of submerged River Red Gum (Eucalyptus camaldulensis Dehnh. Myrtaceae) wood in billabongs: an analysis of bacterial assemblages using phospholipid profiles, *Hydrobiologia*, **259**: 169-178.

Scott, A., 1997. *Relationships between waterbird ecology and river flows in the Murray-Darling Basin.* Technical Report No. 5/97, CSIRO Land and Water, Canberra.

Shaikh, M., Brady, A. T. and Sharma, P. K., 1998. Applications of remote sensing to assess wetland inundation and vegetation response in relation to hydrology in the Great Cumbung Swamp, Lachlan Valley, NSW, Australia., In *Wetlands for the Future* (Eds, McComb, A. J. and Davis, J. A.) Gleneagles Publishing.

Shaikh, M., Green, D. and Cross, H., 2001. A remote sensing approach to determine environmental flows for wetlands of the Lower Darling River, New South Wales, Australia., *International Journal of Remote Sensing*, **22**: 1737-1751.

Sheng, Y., Gong, P. and Xiao, Q., 2001. Quantitative dynamic flood monitoring with NOAA AVHRR., *International Journal of Remote Sensing*, **22**: 1709-1724.

Siebentritt, M., 1999. *Fish and the Lower Gwydir Floodplain*, Wetland Care, Australia.

Silva, T. S. F., Costa, M. P. F. and Melack, J. M., 2009. Annual net primary production of macrophytes in the eastern Amazon floodplain, *Wetlands*, **29**: 747 - 758.

Simons, M., Podger, G. and Cooke, R., 1996. IQQM--A hydrologic modelling tool for water resource and salinity management, *Environmental Software*, **11**: 185-192.

Sims, N. C., 2007. *A method for spectrally calibrating Landsat TM images for change detection*. Client Report No. 1796, Ensis (CSIRO and SCION).

Smith, D. I. (1998) Water in Australia. Oxford University Press, Melbourne.

Spencer, J. A., 2010. *Historical records of waterbirds and fish populations in the Gwydir Wetlands, final report for the NSW Recovery Program*, Rivers and Wetlands Unit, Department of Environment, Climate Change and Water NSW, Sydney.

Steven, M. D., Malthus, T. J., Baret, F., Xu, H. and Chopping, M. J., 2003. Intercalibration of vegetation indices from different sensor systems, *Remote Sensing of Environment*, **88**: 412-422.

Stowe, L. L., Davis, P. A. and McClain, E. P., 1999. Scientific Basis and initial evaluation of the CLAVR-1 global clear/cloud classification algorithm for the Advanced Very High Resolution Radiometer, *Journal of Atmospheric and Oceanic Technology*, **16**: 656-681.

Thomas, R. F., Kingsford, R. T., Y, L. and Hunter, S. J., in press. Landsat mapping of annual inundation (1979-2006) of the Macquarie Marshes in semi-arid Australia, *International Journal of Remote Sensing*.

Thompson, J. R., Sorenson, H. R., Gavin, H. and Refsgaard, A., 2004. Application of the coupled MIKE SHE/MIKE 11 modelling system to a lowland wet grassland in southeast England, *Journal of Hydrology*, **293**: 151-179.

Thoms, M. C. and Sheldon, F., 2000. Lowland Rivers: An Australian introduction, *Regulated Rivers: Research & Management*, **16**: 375-383.

Thorp, J. H. and Delong, M. D., 1994. The riverine productivity model: an heuristic view of carbon sources and organic processing in large river ecosystems, *OIKOS*, **70**: 305-308.

Tockner, K., Malard, F. and Ward, J. V., 2000. An extension of the flood pulse concept, *Hydrological processes*, **14**: 2861-2883.

Toft, J. D., Simenstad, C. A., R, C. J. and Grimaldo, L. f., 2003. The effects of introduced Water Hyacinth on habitat structure, invertebrate assemblages, and fish diets, *Estuaries*, **26**: 746-758.

Tooth, S. and McCarthy, T. S., 2007. Wetlands in drylands: geomorphological and sedimentological characteristics, with emphasis on examples from southern Africa, *Progress in Physical Geography*, **31**: 3-41.

Trishchenko, A. P., Cihlar, J. and Li, Z., 2002. Effects of spectral response function on surface reflectance and NDVI measured with moderate resolution satellite sensors, *Remote Sensing of Environment*, 2002: 1-18.

Vannote, R., Minshall, G., Cummins, K., Sedell, J. and Cushing, C., 1980. The river continuum concept, *Canadian Journal of Fisheries and Aquatic. Sciences.*, **37**: 130-137.

Walker, K. F., Sheldon, F. and Puckridge, J. T., 1995. A perspective on dryland river ecosystems, *Regulated Rivers: Research and Management*, **11**: 85-104.

Ward, J. V., 1989. The four-dimensional nature of lotic ecosystems, *Journal of the North American Benthological Society,* **8**: 2-8.

Ward, J. V., 1998. Riverine landscapes: biodiversity patterns, disturbance regimes and aquatic conservation., *Biological Conservation,* **83**: 267-278.

Ward, J. V. and Stanford, J. A., 1983. The serial discontinuity concept of lotic ecosystems, In *Dynamics of Lotic Ecosystems* (Eds, Fontaine, T. and Bartell, S.) Ann Arbor Science, Ann Arbor, MI, pp. 347-356.

Ward, J. V. and Stanford, J. A., 1995. The serial discontinuity concept: extending the model to floodplain rivers, *Regulated Rivers: Research & Managemen*t, **10**: 159-168.

Warwick, N. W. M. and Brock, M. A., 2003. Plant reproduction in temporary wetlands: the effects of seasonal timing, depth, and duration of flooding, *Aquatic Botany*, **77**(2): 153-167.

Water Conservation and Irrigation Commission, 1972. *Report on Proposal for Distribution of Regulated Flow from Copeton Dam*, W.C. & I.C., Sydney.

Welsh, W. D., 2008. Water balance modelling in Bowen, Queensland, and the ten iterative steps in model development and evaluation, *Environmental Modelling & Software,* **23**: 195-205.

Whigham, P. A. and Young, W. J., 2001. Modelling river and floodplain interactions for ecological response, *Mathematical and Computer Modelling,* **33**(6-7): 635-647.

Wiens, J. A., 2002. Riverine landscapes: taking landscape ecology into the water, *Freshwater Biology,* **47**(4): 501-515.

Wilson, G., Bickel, T. O., J, B. P. and L, S. J., 2009. *Managing environmental flows in an agricultural landscape: the Lower Gwydir floodplain.* Final report to the Commonwealth Department of the Environment, Water, Heritage and Arts. University of New England, Armidale

Winemiller, K. O. (Ed.) 2005. Floodplain river food webs: Generalisations and implications for fisheries management. *Proceedings of the second international symposium on the management of large rivers for fisheries* (Volume II).

Wolski, P., Gumbricht, T. and McCarthy, T. S. (Eds.), 2002. Assessing future change in the Okavango Delta: the use of a regression model of the maximum annual flood in a Monte Carlo simulation *Conference on Environmental Monitoring of Tropical and Subtropical Wetlands*, 4-8 December 2002, Maun, Botswana.

Wolski, P. and Murray-Hudson, M., 2005. Flooding dynamics in a large low-gradient alluvial fan, the Okavango Delta, Botswana, from analysis and interpretation of a 30-year hydrometric record, *Hydrology and Earth System Sciences Discussions*, **2**: 1865-1892.

Wolski, P., Savenije, H., Murray-Hudson, M. and Gumbricht, T., 2006. Modelling of the flooding in the Okavango Delta, Botswana, using a hybrid reservoir-GIS model., *Journal of Hydrology*, **331**: 58-72.

Young, W. J., Cuddy, S. M., Marston, F. M. and Farley, T. F. N., 1999. *Environmental Flows Decision Support System. A prototype. Volume 1. Systems description,* CSIRO Land and Water, Technical Report 11/99.

Young, W. J., Lam, D. C. L., Ressel, V. and Wong, I. W., 2000. Development of an environmental flows decision support system, *Environmental Modelling and Software,* **15**(3): 257-265.

Young, W. J., Scott, A. C., Cuddy, S. M. and Rennie, B. A., 2003. *Murray flow assessment tool - a technical description*. Client Report, 2003., CSIRO Land and Water, Canberra.

Zhang, L. and Mitsch, W. J., 2005. Modelling hydrological processes in created freshwater wetlands: an integrated system approach, *Environmental Modelling & Software,* **20**(7): 935-946.

Zhang, X., Friedl, M., Schaaf, C., Strahler, A., Hodges, J., Gao, F., Reed, B. and Huete, A., 2003. Monitoring vegetation phenology using MODIS, *Remote Sensing of Environment,* **84**: 471-475.

Zhang, X., Hodges, J., Schaaf, C., Friedl, M., Strahler, A. and Gao, F. (Eds.), 2001. Global vegetation phenology from AVHRR and MODIS data *Proceedings of the IEEE International Geoscience and Remote Sensing Symposium,* Sydney, Australia.

Zoffoli, M. L., Kandus, P., Madanes, N. and Calvo, D. H., 2008. Seasonal and interannual analysis of wetlands in South America using the NOAA-AVHRR NDVI time series: the case of the Parana Delta Region, *Landscape Ecology*, **23**: 833-848.

Appendix 1: Landsat scenes

Table A1.1: Summary of Landsat scenes analysed for each event

Event start (Peak Q) (event size)	**< 1 month**	**1 -3months**	**3+ months**
3rd April, 1988 (moderately small)		7th June, 1988 23rd June, 1988	
7th July, 1988 (moderately small)		10th August, 1988	13th October, 1988
14th December, 1991 (small)	25th December, 1991 10th January, 1992	26th January, 1992	14th March, 1992 30th March, 1992
22nd January, 1995 (moderately small)		7th March, 1995	24th April, 1995 13th July, 1995
* 20th November, 1995 (moderately large)		20th December, 1995	
* 26th January, 1996 (moderately large)	6th February, 1996	9th March, 1996	10th April, 1996 12th May, 1996
* 31st January, 1997 (large)	8th February, 1997	12th March, 1997	13th April, 1997 31st May, 1997
4th March, 1999 (small)		19th April, 1999	9th August 1999 17th August, 1999
6th October, 1999 (moderate)	20th October, 1999	23rd November, 1999 29th November, 1999	25th February, 2000 28th March, 2000 29th April, 2000
16th November, 2000 (large)	23rd November, 2000 9th December, 2000		
29th January, 2001 (large)	11th February, 2001	15th March, 2001	31st March, 2001 16th April, 2001
27th November, 2001 (moderate)		28th December, 2001 13th January, 2002	29th January, 2002 2nd March, 2002 18th March, 2002 19th April, 2002
24th February, 2003* Including an ECA released December 2002. (moderate)	16th January, 2003 21st March, 2003	22nd April, 2003	
9th December, 2004 (moderately large)	12th December, 2004 28th December, 2004	13th January, 2005	14th February, 2005 19th April, 2005
1st July, 2005 (moderate)	24th July, 2005	9th August, 2005 25th August, 2005	26th September 2005

* validation events

Appendix 2: Flood assessments 1988-2005

April and July 1988

The two events in 1988 occurred in April and July. Both events were moderately small with a 40-day inflow of 38.2GL and peak inflow of 14.2GL in April and a 40-day inflow of 43.1GL and peak inflow of 18.1GL in July. Two Landsat scenes were analysed for the April event and two for the July event however it should be noted that further 42GL of inflows occurred in September-October 1988 which contributed to a total inflow for the July analysis of 85GL, or 144.1GL cumulative total from April to the last image analysis date on the 13th October. No AVHRR are available at 1km resolution for these events and Modis did not commence operations until 2001.

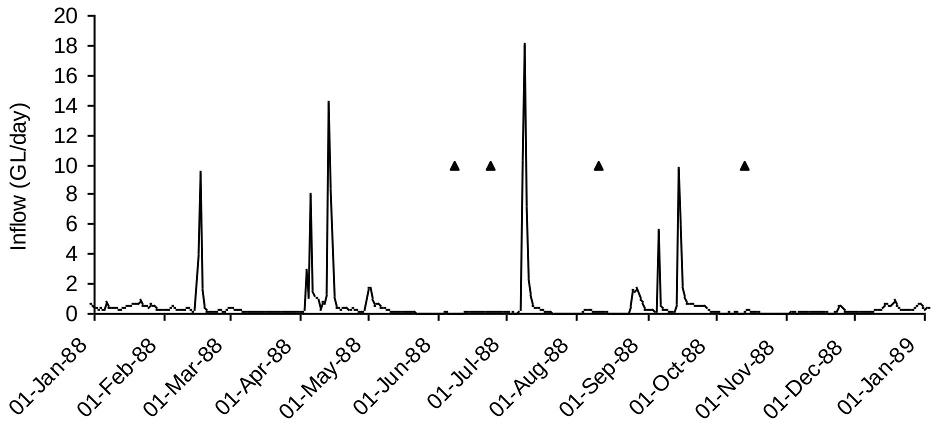

Figure A2.0.1: Gwydir River at Yarraman inflows 1988. Landsat scenes used in analysis ▲

Following the inflows in April areas of open water were detected but were predominantly associated with cleared cultivated land some distance from the channels and are more likely to be from localised rainfall saturating bare clay soil. The total area classified in April is 15 932ha (NDVI > 0.75). The results from the post-July analysis provides a better picture of the response from all inflows, with a total area of approximately 56 000ha classified as open water and highly responsive vegetation (NDVI > 0.75). The spatial pattern of response is consistent with mapped flood events of similar size.

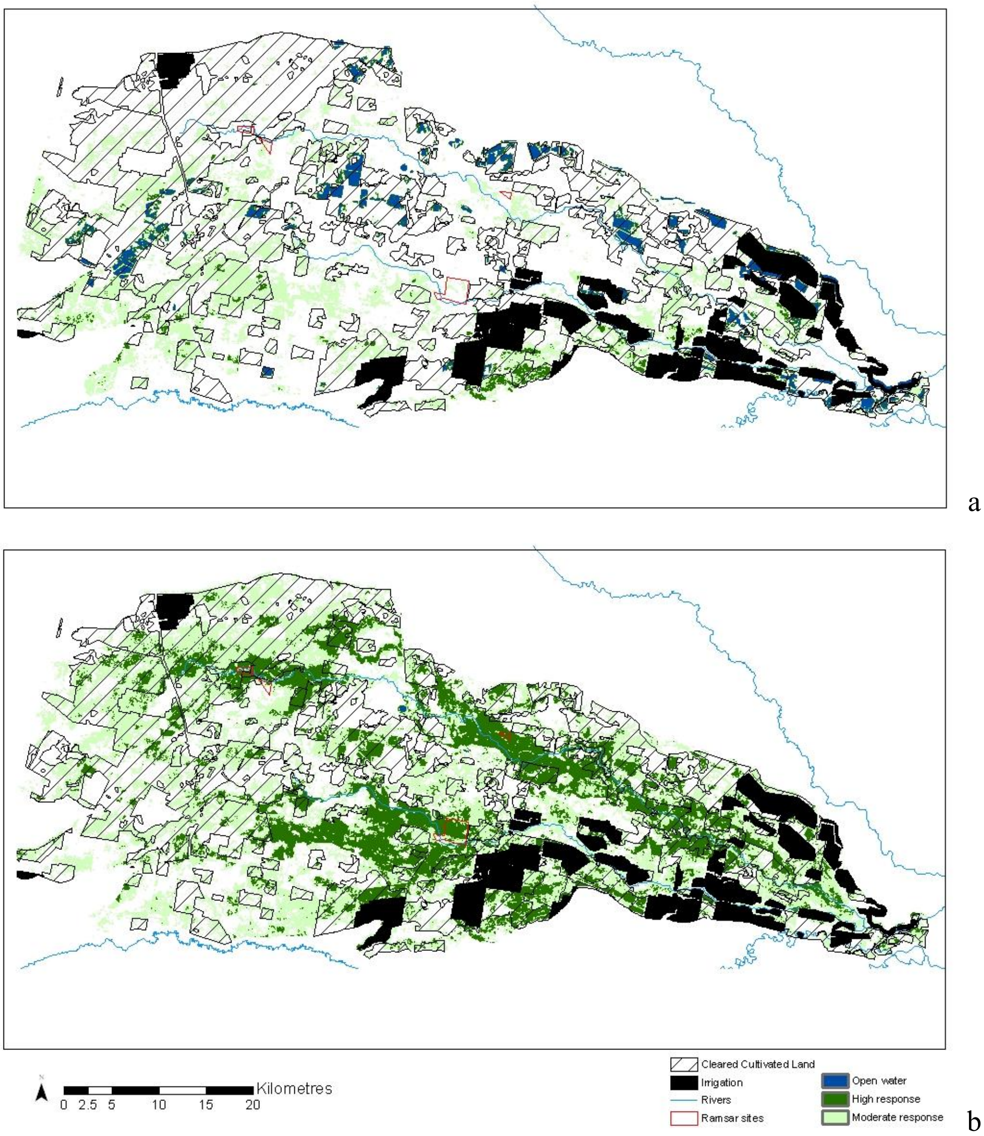

Figure A2.0.2: Areas classified as open water (NDVI < 0), high and moderate response (NDVI > 0.75 and 0.65) in 1988. a) post April peak and b) post July peak.

December 1991

In 1991 a very small peak of 4.2GL passed Yarraman gauge on the 14th December with a total volume of 22.3GL over 40 days. Although less than the 'event' trigger of 10GL generally discussed, it was useful to map this event as an indication for small ECA releases and also to test the NDVI threshold method sensitivity to large rainfall events, in this case 125mm fell over the study area on the 12th and 13th December. The event was also quite distinct temporally with low antecedent flows.

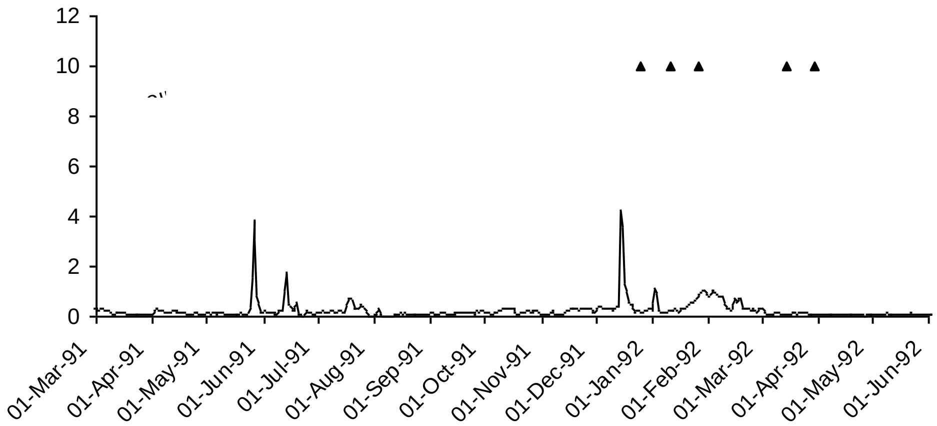

Figure A2.0.3: Gwydir River at Yarraman inflows 1991/2. Landsat scenes used in analysis ▲

The results of the Landsat analysis showed a very small area of response (2928 ha, NDVI > 0.75) in the core wetland areas immediately adjacent to Gingham Channel and the Lower Gwydir channel and did not detect large areas of open water flooding or response despite the high rainfall event. Neither Landsat nor Modis was available for this event.

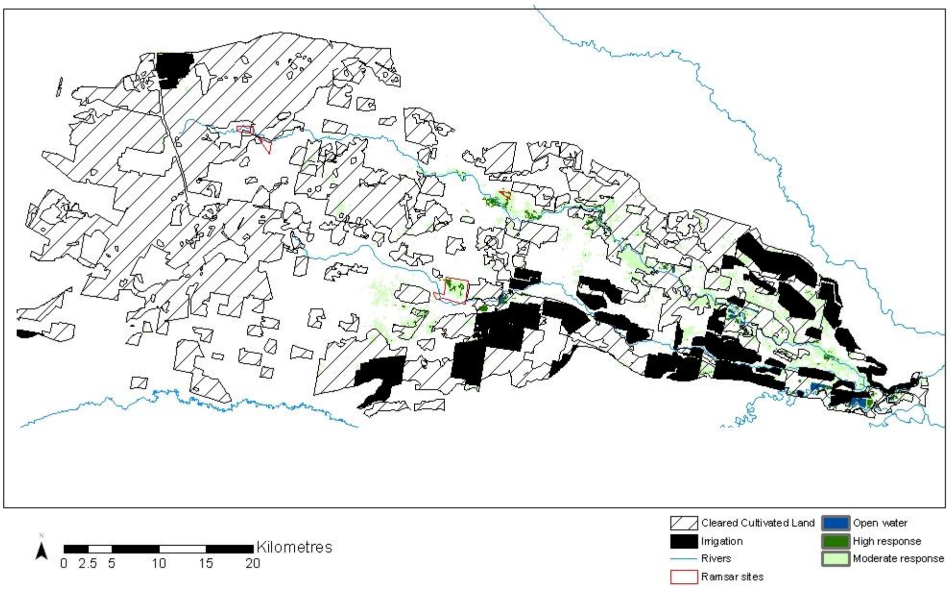

Figure A2.0.4: December 1991

January 1995

Following a prolonged dry period with no significant inflows for 1992, 1993 or 1994, a moderately small event with a peak inflow of 24.6GL and 40-day inflow of 46.8GL occurred in January 1995.

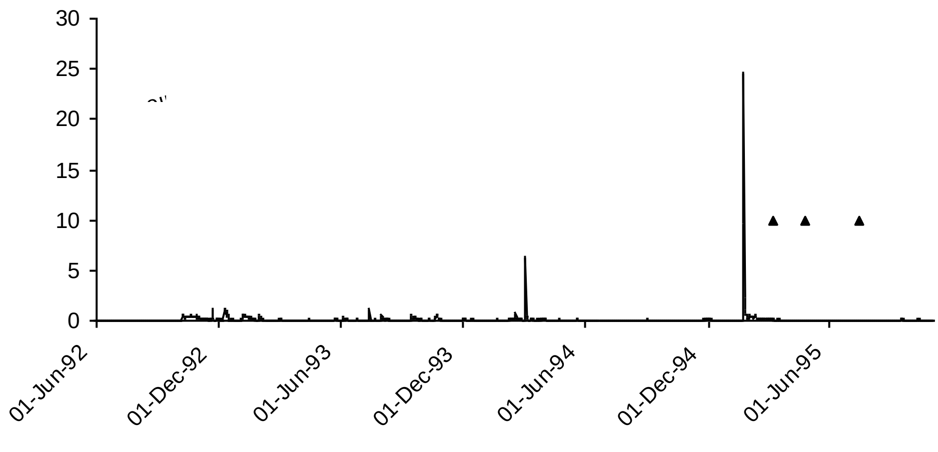

Figure A2.0.5 Gwydir River at Yarraman inflows 1994-5. Landsat scenes used in analysis ▲

Total area of response for the Landsat analysis (NDVI > 0.75) was 37 259ha and was confined primarily to the core wetland areas along the Gingham and Lower Gwydir Channels. The AVHRR analysis indicated a much larger area of 100 934ha wet or responding at a NDVI threshold of 0.52. The AVHRR result is very much an outlier in comparison to all the flood events analysed however it is not clear as to why this is the case.

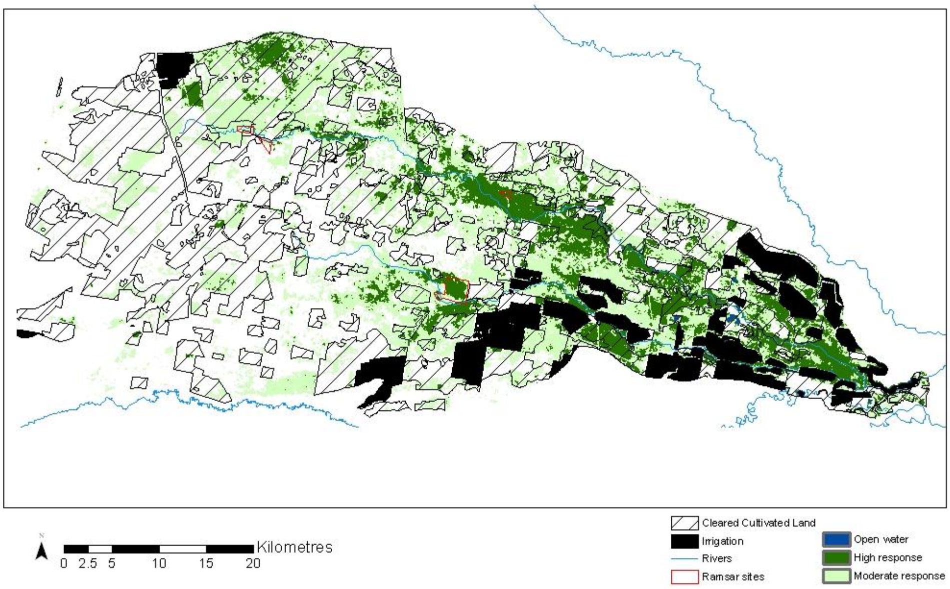

a

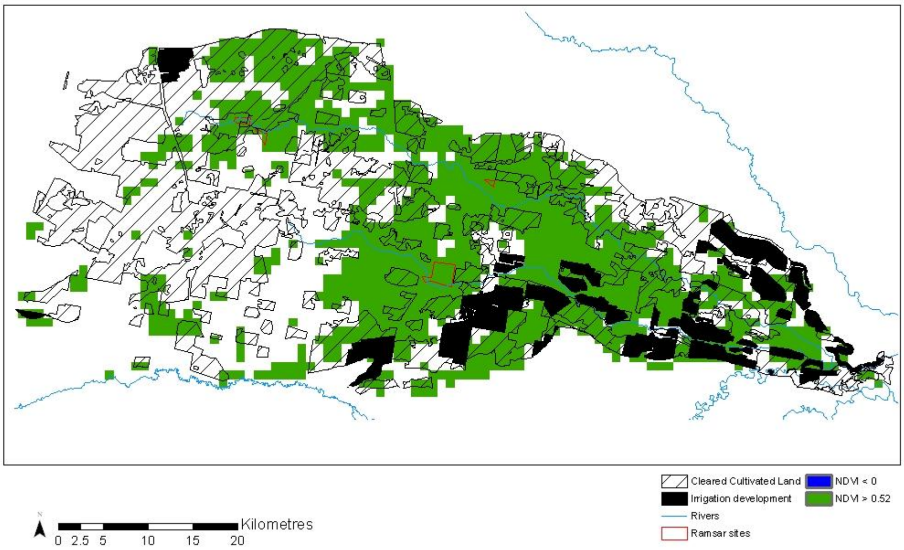

b

Figure A2.0.6: January 1995 a) Landsat and b) AVHRR

November 1995

The November 1995 event was a moderately large event with 40-day inflow of 144.6GL. The event peaked on the 24th November at 23.3GL/day and existing extent map showed almost 54 000ha flooded in the lower Gwydir and Gingham. Only a single Landsat image (20 December, 1995) was available post event, prior to the next large inflow. Similarly the AVHRR analysis was constrained to four MVC intervals while Modis was not available for this flood assessment.

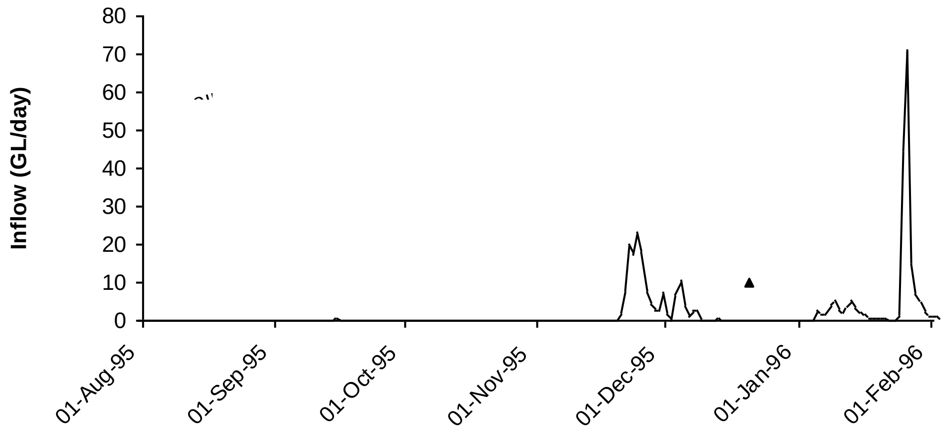

Figure A2.0.7: Gwydir River at Yarraman inflows 1995-6. Landsat scenes used in analysis ▲

Total area of response for the Landsat analysis (NDVI > 0.75) was 14 607ha. The AVHRR analysis indicated a much larger area of 51 000ha wet or responding at a NDVI threshold of 0.52, similar to the mapped extent area outlined in red.

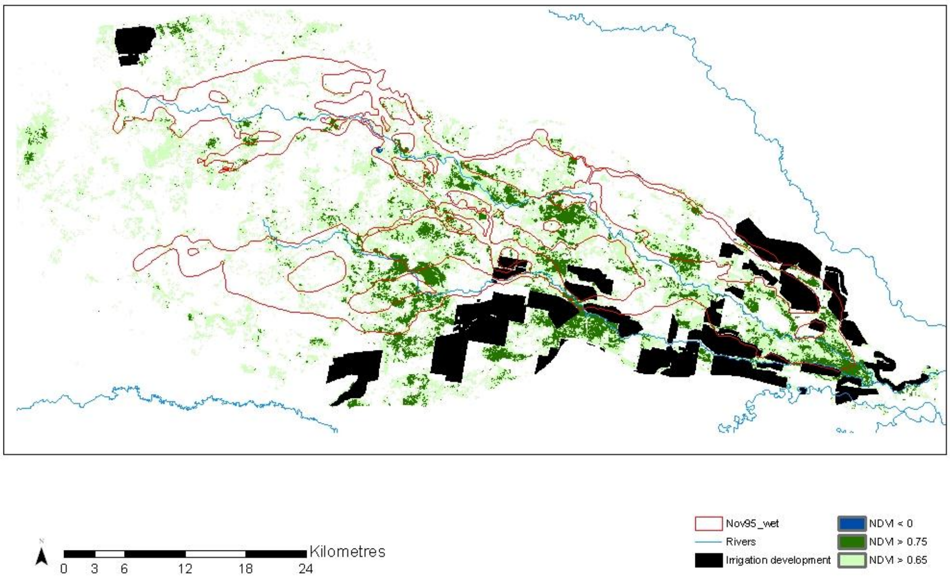

a

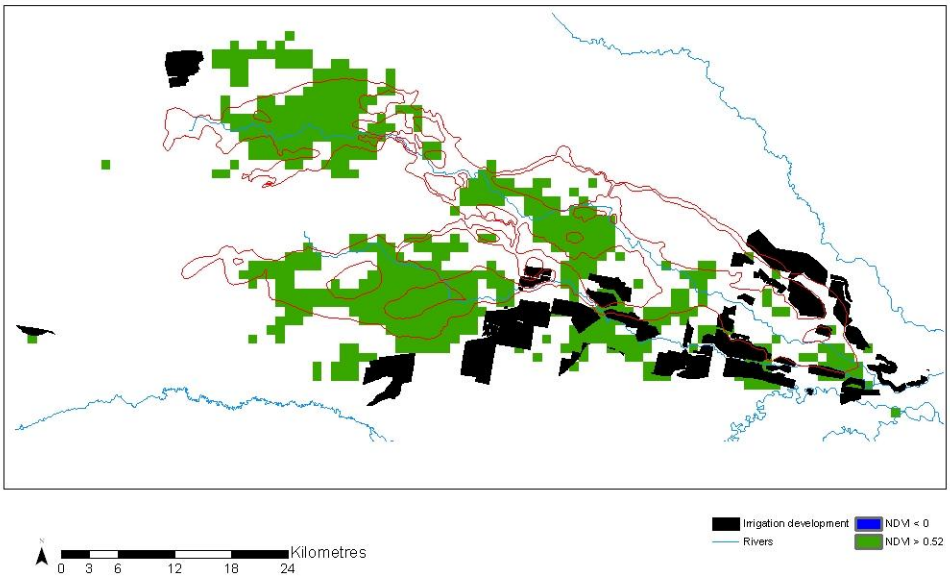

b

Figure A2.0.8: 1995 a) Landsat and b) AVHRR

January 1996

The January 1996 flood event had a similar 40-day inflow volume (167GL) to the previous event, however the peak was almost three times the size (70.8GL). Four Landsat scenes were available for the analysis covering a period of almost four months while the full six MVC periods were used to analyse the AVHRR data.

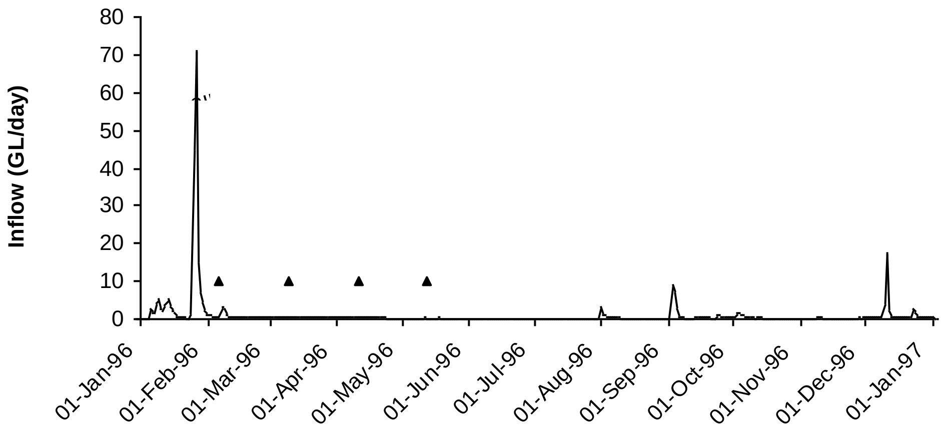

Figure A2.0.9: Gwydir River at Yarraman inflows 1996. Landsat scenes used in analysis ▲

Total area of response for the Landsat analysis (NDVI > 0.75) was 19 170ha. The AVHRR analysis indicated a much larger area of 52 783ha wet or responding at a NDVI threshold of 0.52, similar to the mapped extent area of 59 990ha outlined in red.

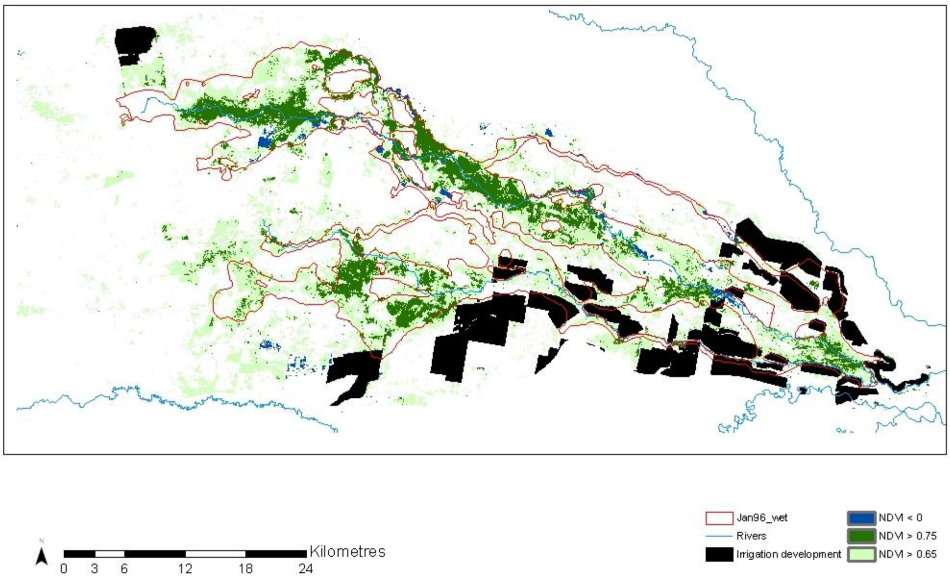

a

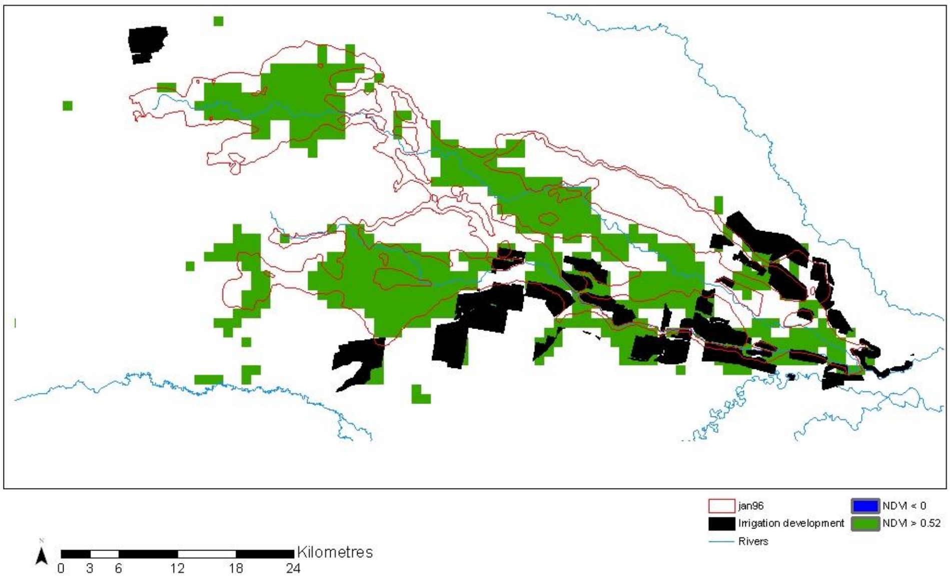

b

Figure A2.0.10: Jan 1996, a) Landsat and b) AVHRR

February 1997

A peak inflow 30 854GL occurred on the 2nd February, 1997 closely followed by a larger peak of 50.4GL on the 18th February, 1997 and over a 40 day period over 237GL flowed through Yarraman gauge resulting in a large event with mapped inundation area of over 100 000ha. Landsat imagery was available for four scenes post the initial flood peak and AVHRR imagery was analysed for the full 6 MVC periods.

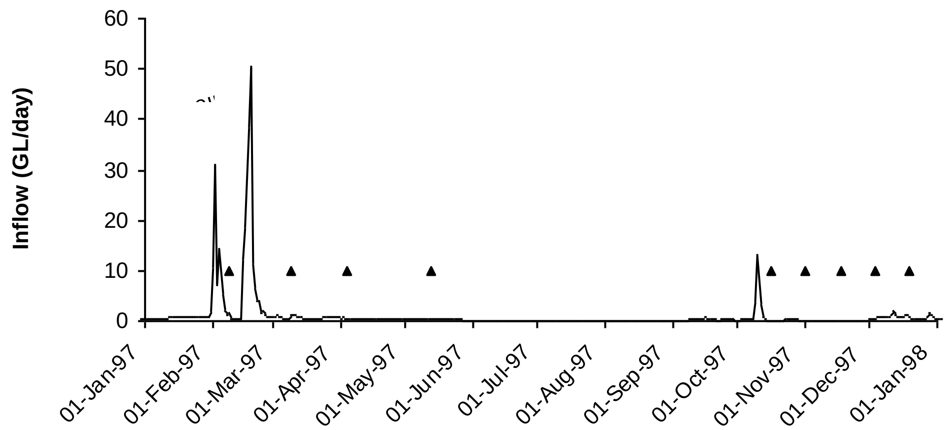

Figure A2.0.11: Gwydir River at Yarraman inflows 1997. Landsat scenes used in analysis ▲

The area of inundation and response from the Landsat analysis was 109 583ha and from the AVHRR analysis was 86 607ha. Both results compare relatively well to the mapped area of 101 915ha shown in red.

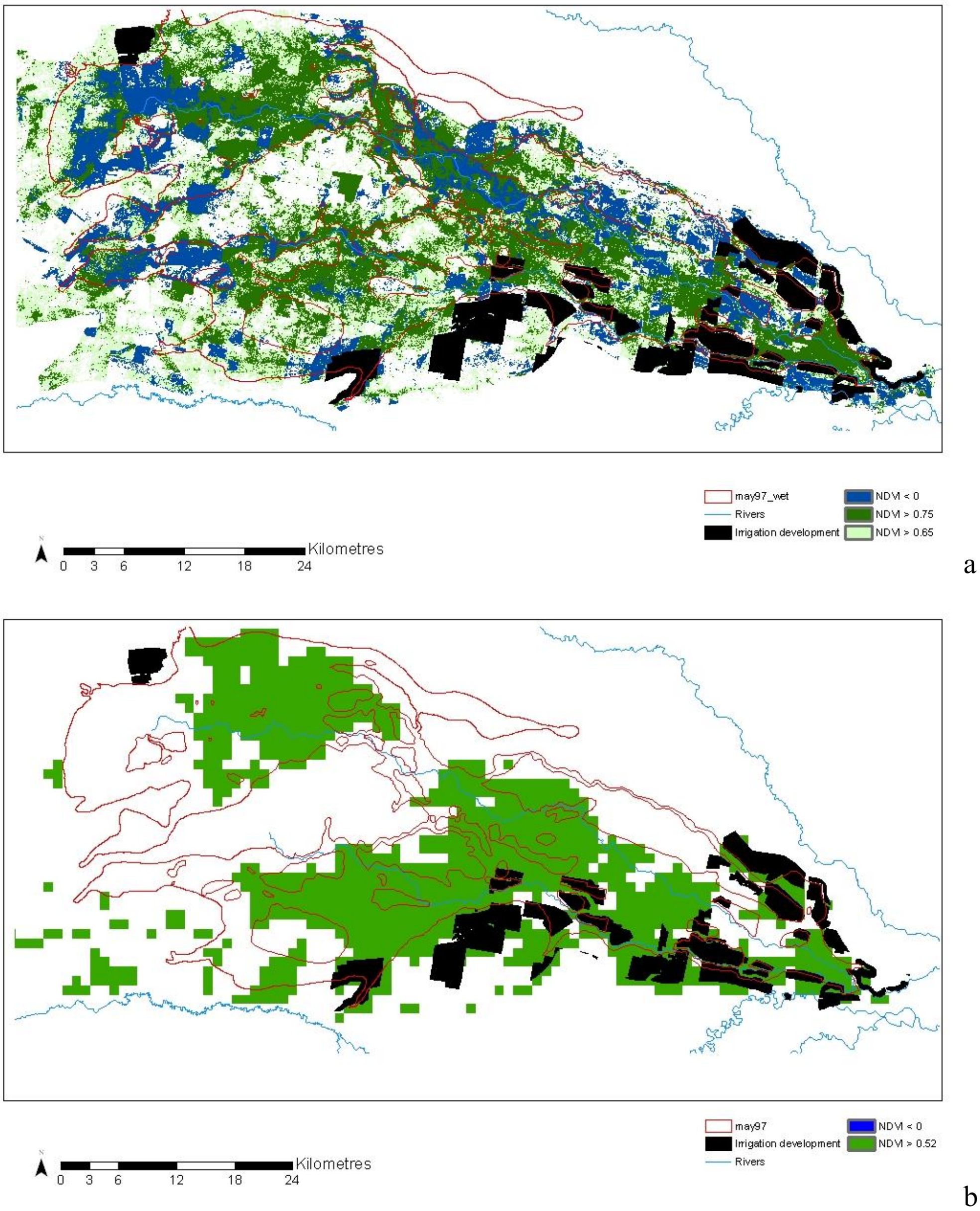

Figure A2.0.12: Jan1997, a) Landsat and b) AVHRR

October 1997

A small event peaked at 13.4GL on the 10th October, 1997 with a 40-day cumulative total of 27.4GL passing Yarraman gauge. No Landsat data was available and the analysis is limited to the 6-period AVHRR MVC dataset.

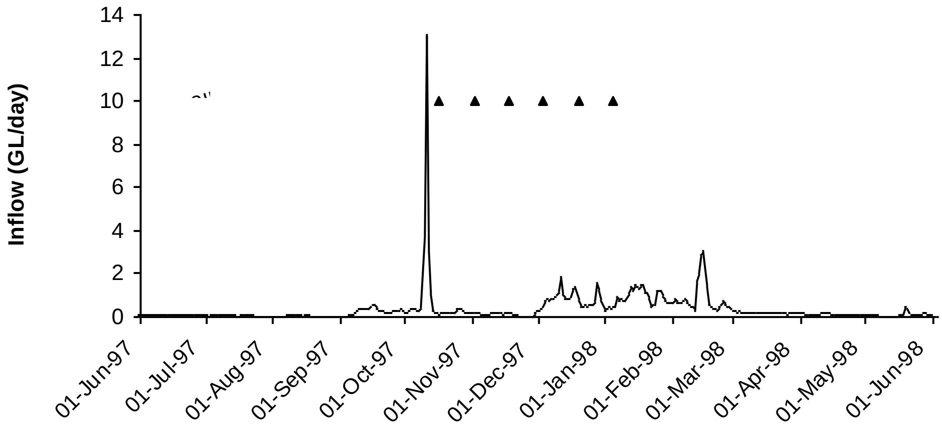

Figure A2.0.13: October 1997 flow and the AVHRR MVC periods (▲)

The AVHRR results indicate an area of 20 251ha responding to the flood in the core wetland areas.

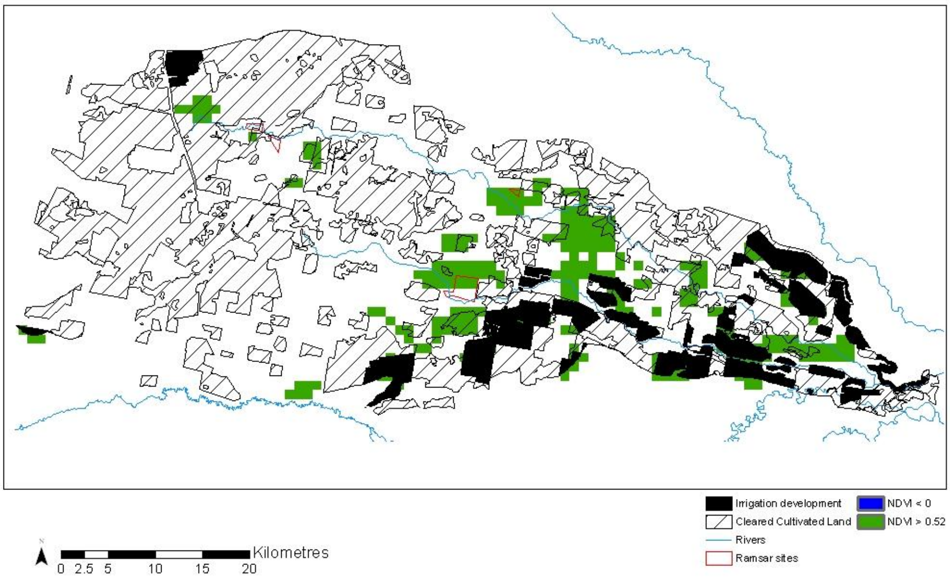

Figure A2.0.14: October 1997

July 1998

The July 1998 event was the largest event analysed and came after a relatively wet period from 1995 onwards. The 112.4GL peak occurred on the 30the July, 1998 with 366.6GL flowing past the gauge over the 40-day period. The event contained a number of peaks and continued for longer than the 40-day period that describes most flood events. The total inflow over the entire event was 823.2GL. Due to cloud cover their was no good quality Landsat images for analysis, however the AVHRR did contain sufficient good quality images to construct the 16-day MVCs for the period.

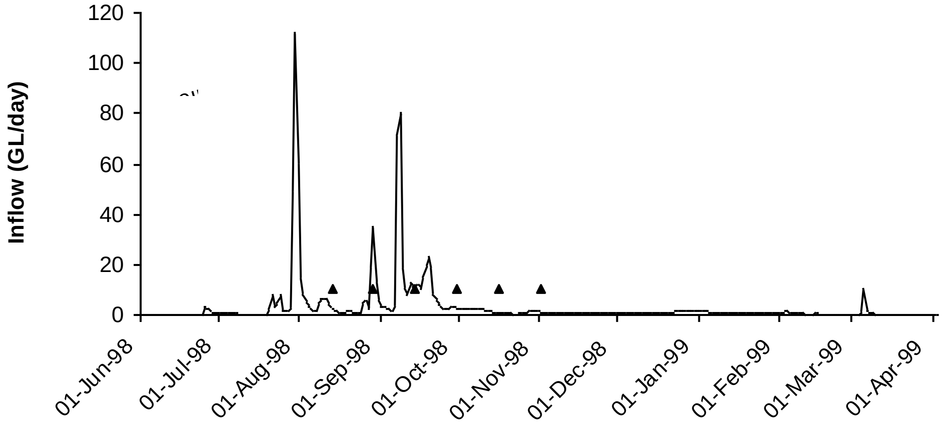

Figure A2.0.15: July 1998 event flow and the AVHRR MVC periods (▲)

The results showed most of the floodplains responding to this event, with over 165 000ha of response. Areas not responding were largely cleared cultivated areas.

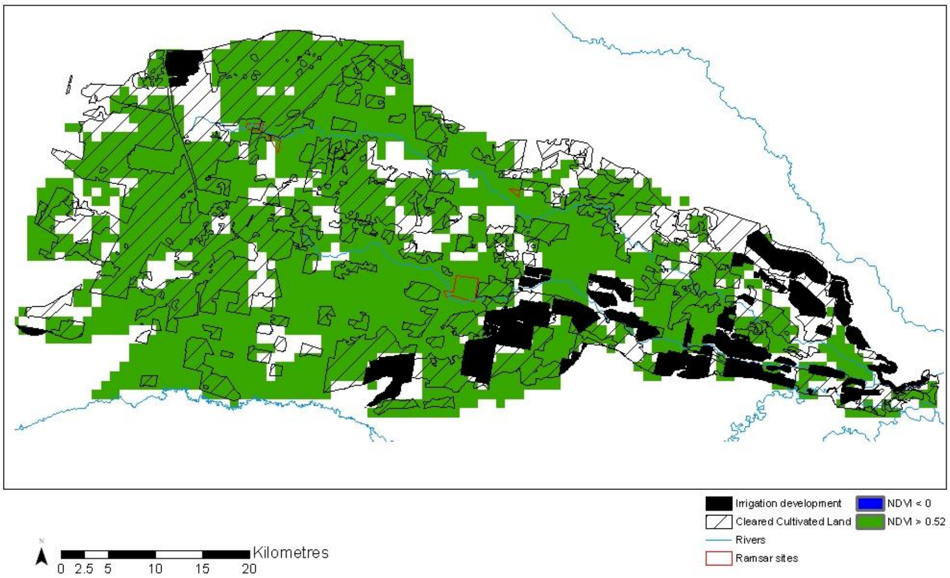

Figure A2.0.16: July 1998

March 1999

A small event peaked (10.2GL) on the 5th March, 1999 and had a 40-day volume of 21.4GL. Only a single Landsat image was available for this event along with the full 6-period AVHRR MVC.

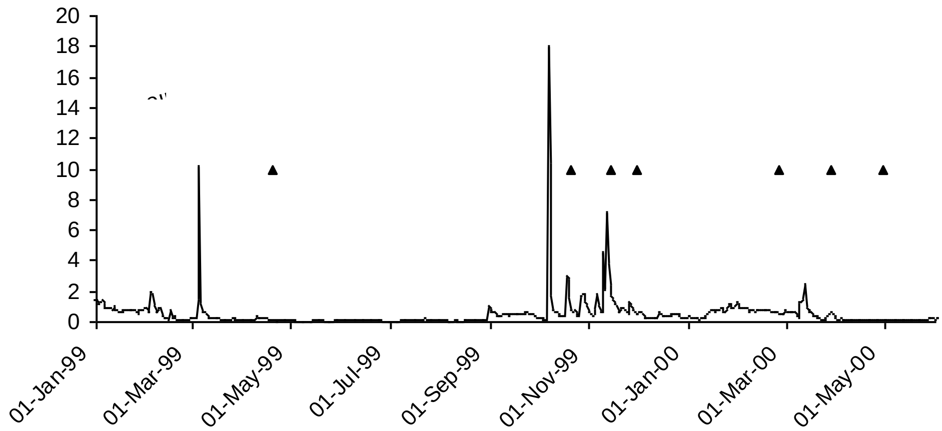

Figure A2.0.17: Gwydir River at Yarraman inflows 1999-2000. Landsat scenes used in analysis ▲

A total area of just 3 099ha was identified from the Landsat image with little evidence of response through core wetland areas. The AVHRR analysis classified a large area of cultivated land on the southern boundary of the study area classified as wet however further investigation indicated that this was some 6 weeks after the flood peak and unlikely to be associated with Gwydir flooding. There was no heavy rainfall nor inflows at this time to explain the area of low NDVI and the most likely possibility is cloud (unlikely as it was apparent over two subsequent MVC periods) or cultivation of soils with high soil moisture content. The main area of vegetation response was an area on the western extent of the Gingham Channel wetlands. The total area of response using the threshold method was 24 452ha (NDVI < 0 or NDVI > 0.52). Excluding the wet areas that overlapped cultivation gave an estimated response area of 16 589ha.

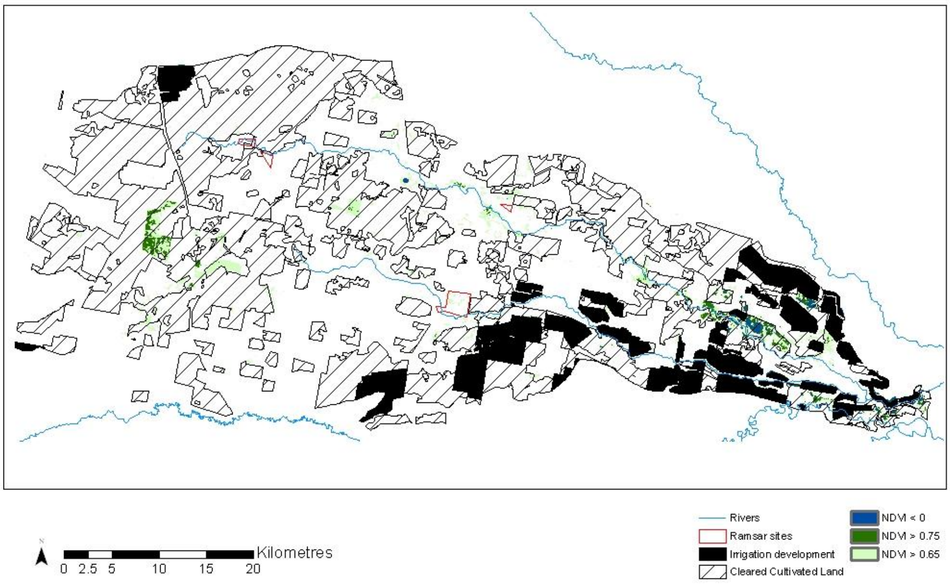

a

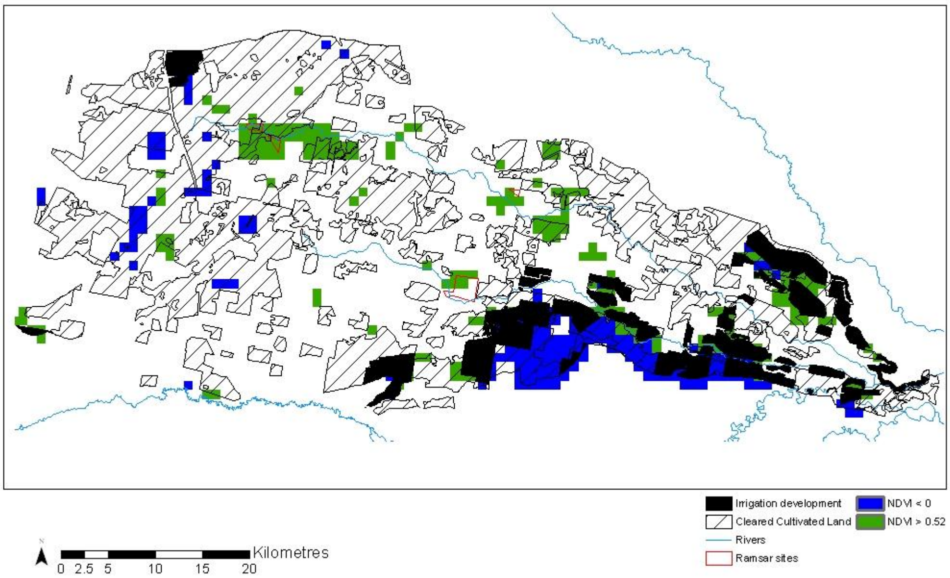

b

Figure A2.0.18: March 1999 a) Landsat and b) AVHRR

October 1999

On the 6th October, 1999 moderate event occurred with a peak of 18.1GL and a 40-day total 81.8GL. Landsat was available for six months post-peak while the full six MVC AVHRR periods were also analysed.

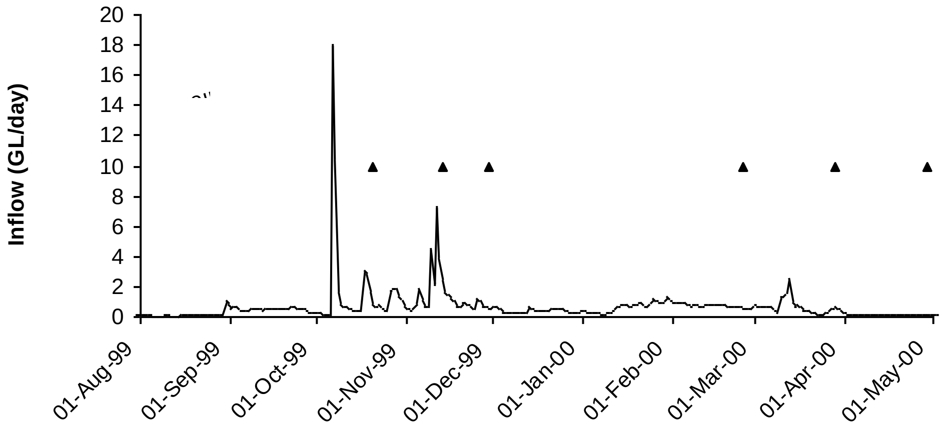

Figure A2.0.19: Gwydir River at Yarraman inflows 1999-2000. Landsat scenes used in analysis ▲

The results indicate a relatively large area of response for the Landsat analysis of 57 094ha. The area of response for AVHRR was much smaller at 19 174ha. In both cases an areas of cultivated land on the north-west extent of the study areas is found to be wet and may be associated with flooding from the Gil Gil Creek to the North. There was no subsequent vegetation response over this area. The AVHRR also detected wet areas in the western portions of the study area with no linkage to the channels. This is most likely an anomaly due to either localised heavy rainfall or cloud contamination not detected by the image acquisition and processing method.

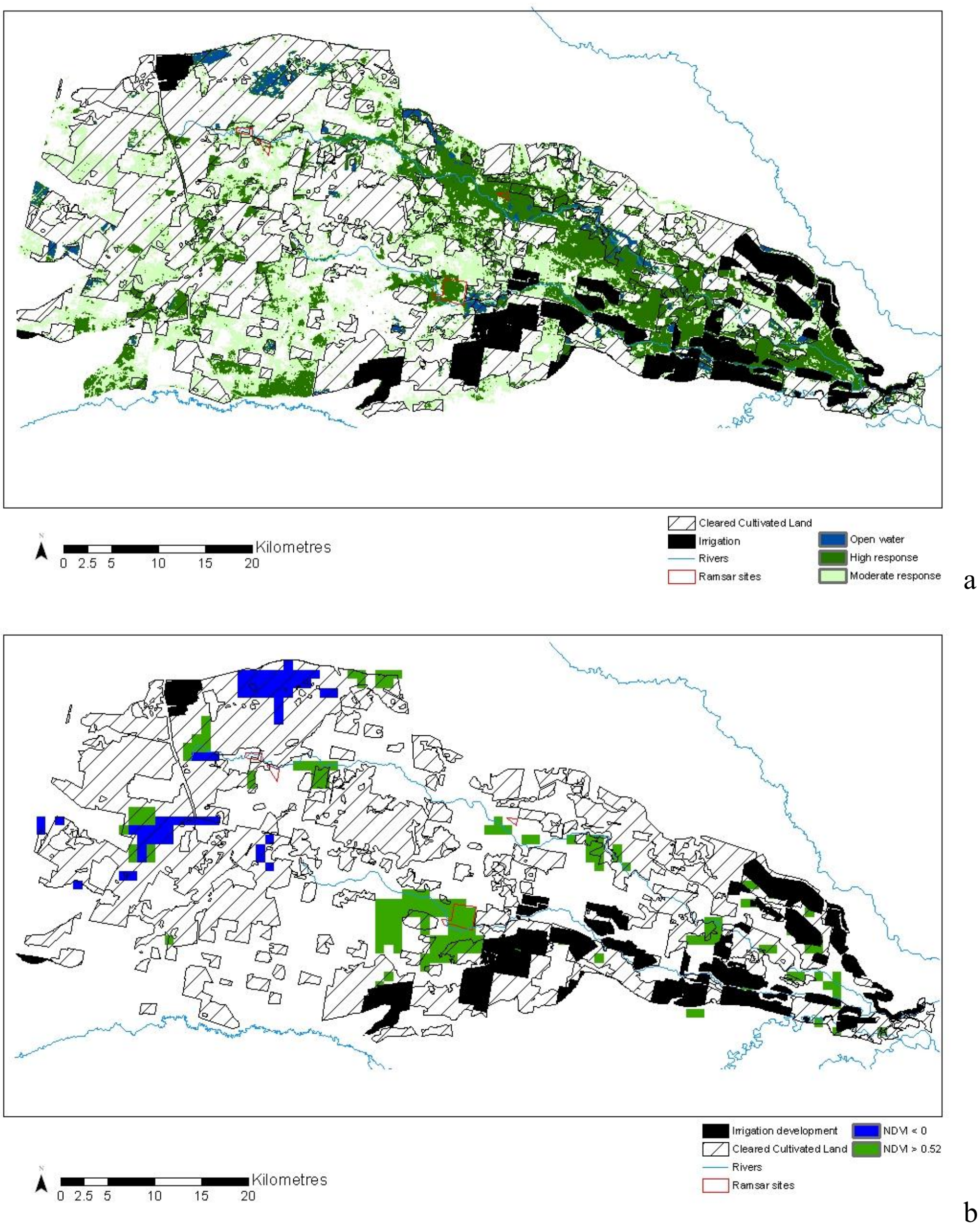

Figure A2.0.20: Oct 1999 a) Landsat and b) AVHRR

November 2000/ February 01

2000/2001 had two relatively large events, peaking at over 50GL (300GL over 40 days) on the 21st November 2000 followed by a peak of over 70GL (223GL over 40 days) on 3rd February 2001. The combined events had more than 570GL over 100 days.

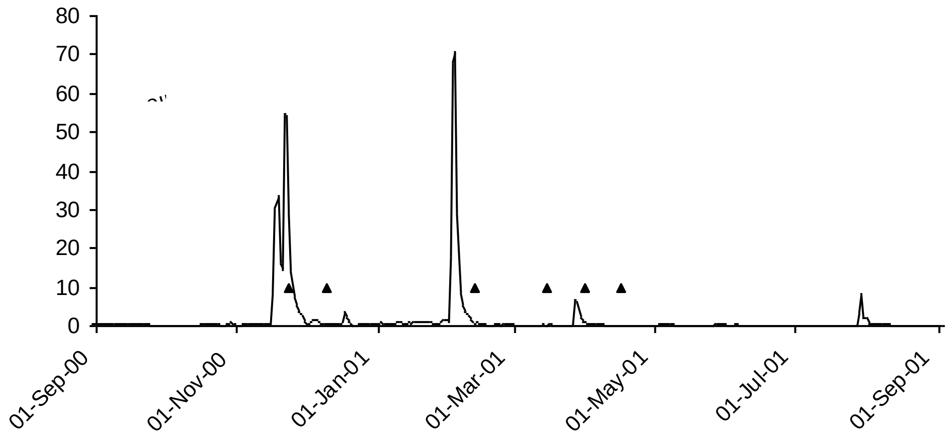

Figure A2.0.21: Gwydir River at Yarraman inflows 2000-2001. Landsat scenes used in analysis ▲

The November 2000 event had Landsat imagery available within a few days of the peak inflow providing an excellent opportunity to detect large expanses of open water flooding. The NDVI threshold of 0 clearly delineated areas of open water flooding with virtually no vegetation response found in the short time period to the next available Landsat scene in early December. The total area classified is 68 120ha. The analysis post February floods is dominated by vegetation response from the combined floods although a small area of open water is detected westward of the 2000 analysis. The total area is almost doubled at 134 854 ha.

Modis and AVHRR data were also available for these events. The November 2000 flood resulted in 107 422ha (Modis) and 66 032ha (AVHRR) classified with the majority of the area showing vegetation response and relatively large areas of open water flooding detected on the northern boundary of the study area coinciding with cultivated areas. The post February 2001 analysis gave a total response area of 89 074ha (Modis) and 67 109ha (AVHRR) with small areas of open water flooding persisting over some cultivated areas.

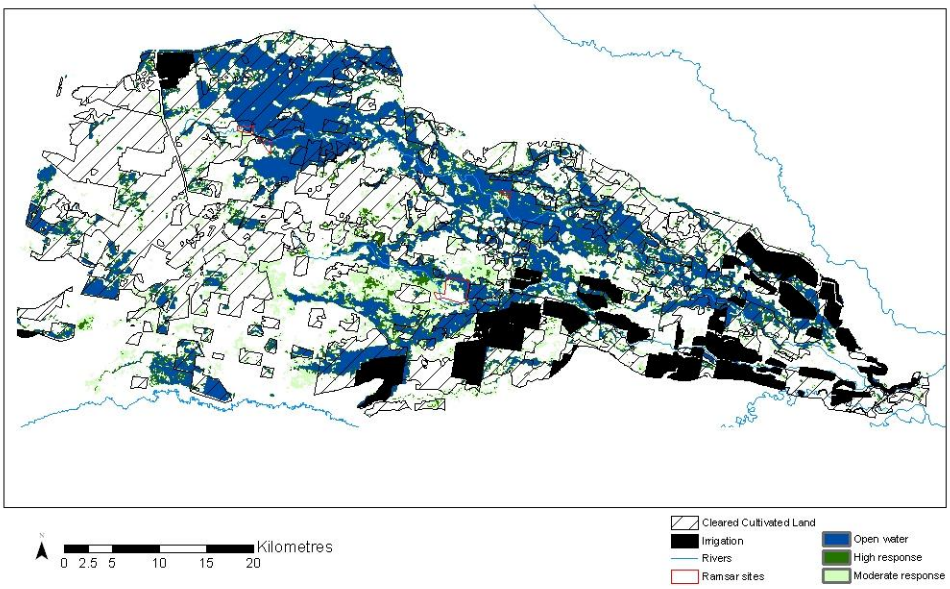
Cleared Cultivated Land
Irrigation
Rivers
Ramsar sites
Open water
High response
Moderate response
Kilometres
0 2.5 5 10 15 20

a

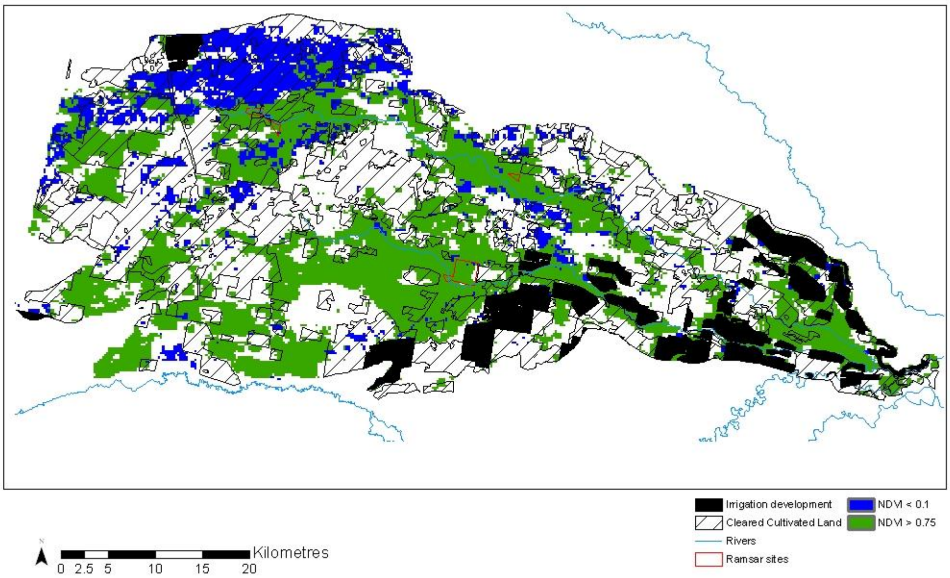
Irrigation development
Cleared Cultivated Land
Rivers
Ramsar sites
NDVI < 0.1
NDVI > 0.75
Kilometres
0 2.5 5 10 15 20

b

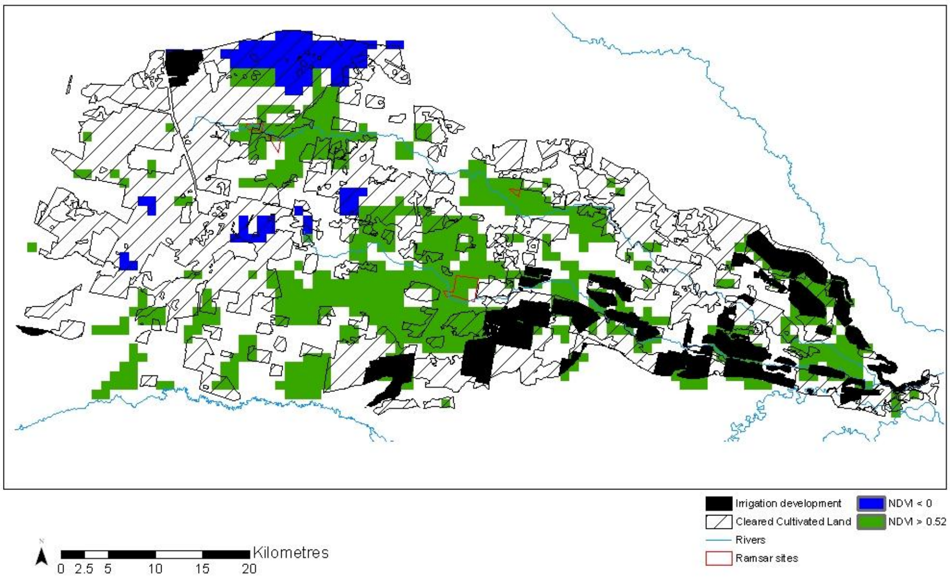

c

Figure A2.0.22: Nov 2000 a)Landsat, b) Modis and c) AVHRR

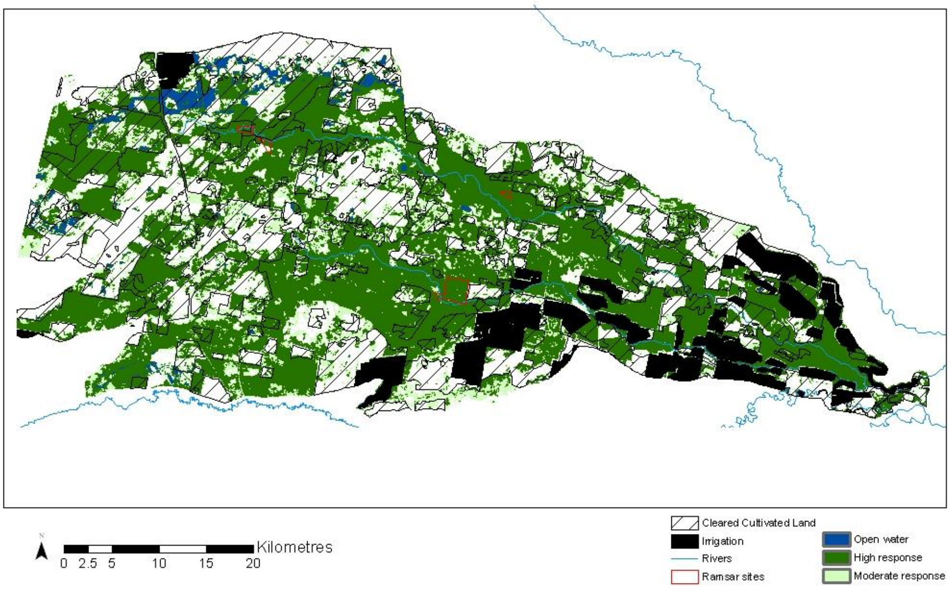
Cleared Cultivated Land
Irrigation
Rivers
Ramsar sites
Open water
High response
Moderate response
Kilometres
0 2.5 5 10 15 20

a

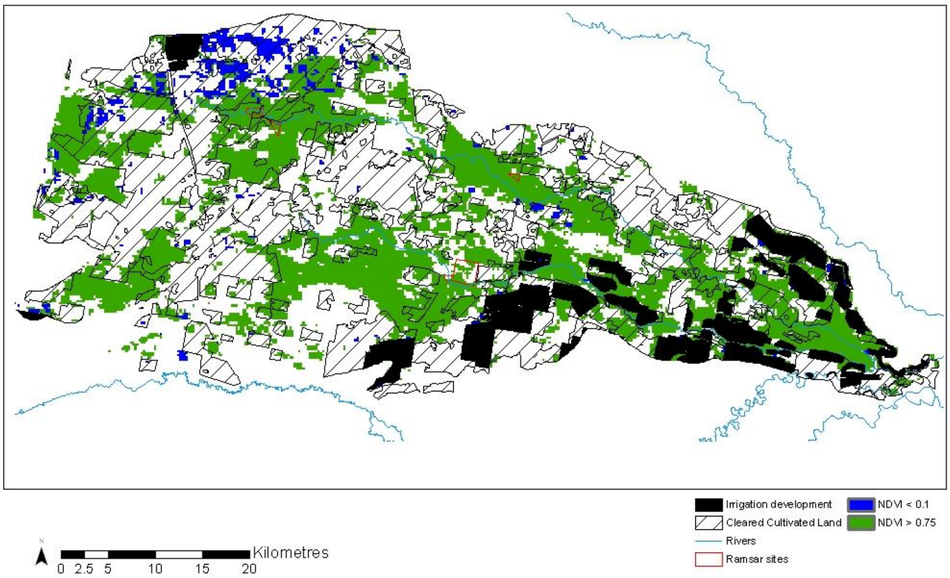
Irrigation development
Cleared Cultivated Land
Rivers
Ramsar sites
NDVI < 0.1
NDVI > 0.75
Kilometres
0 2.5 5 10 15 20

b

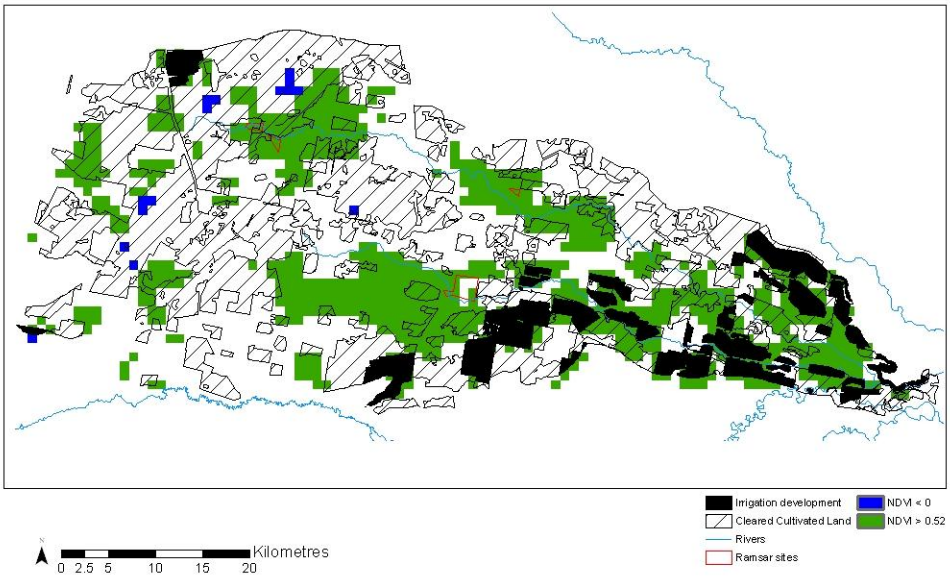

c

Figure A2.0.23: Feb2001 a) Landsat, b) Modis and c) AVHRR

November 2001

A peak of 26.8GL occurred on the 27th November, 2001 with a moderate 40-day cumulative inflow of 83.5GL. Six Landsat scenes were available for analysis as were six MVC Modis and AVHRR images.

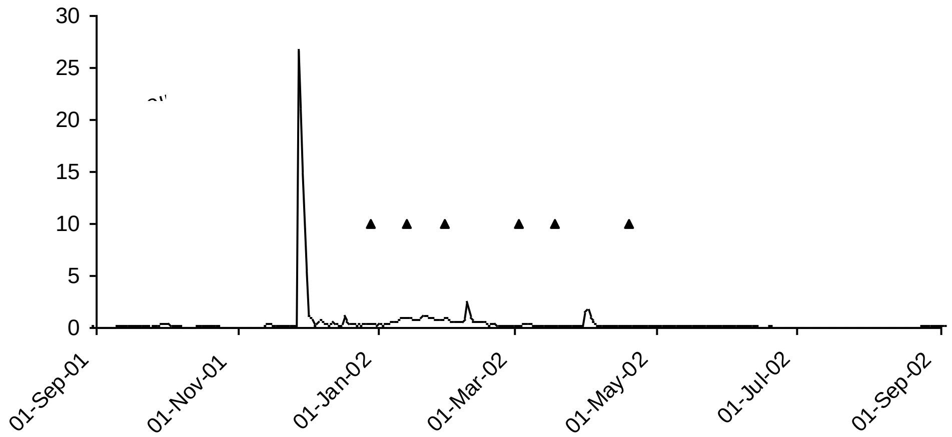

Figure A2.0.24: Gwydir River at Yarraman inflows 2001-2. Landsat scenes used in analysis ▲

A small area of response was detected using the Landsat analysis (10 648ha) that was in the vicinity of the Raft area and the Ramsar sites of Goddards Lease on the Gingham Channel and 'Old Dromana' on the Gwydir Channel. The Modis and AVHRR analysis had a similar spatial pattern of response however the areas were larger at 18 105ha and 20 682ha respectively.

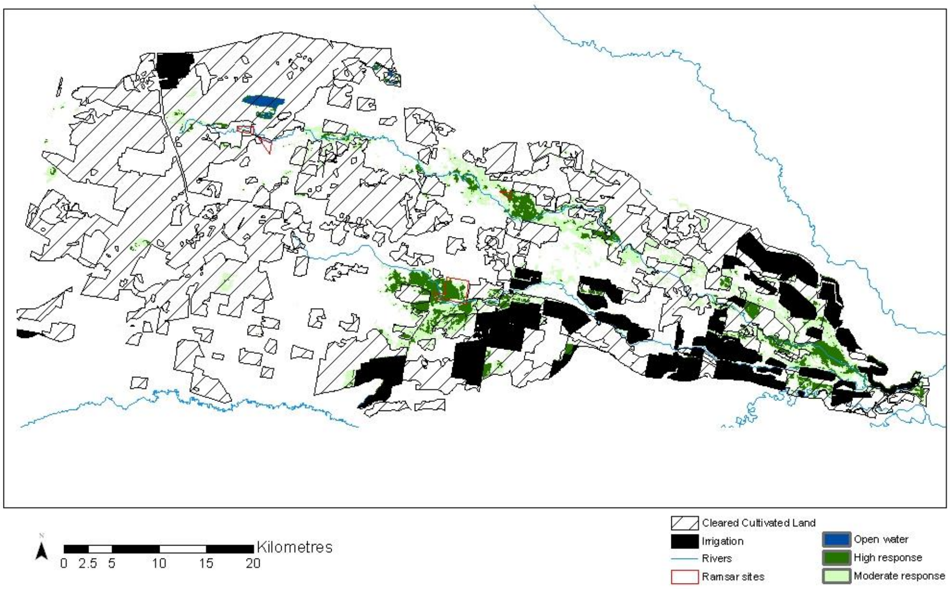
Cleared Cultivated Land
Irrigation
Rivers
Ramsar sites
Open water
High response
Moderate response
Kilometres
0 2.5 5 10 15 20

a

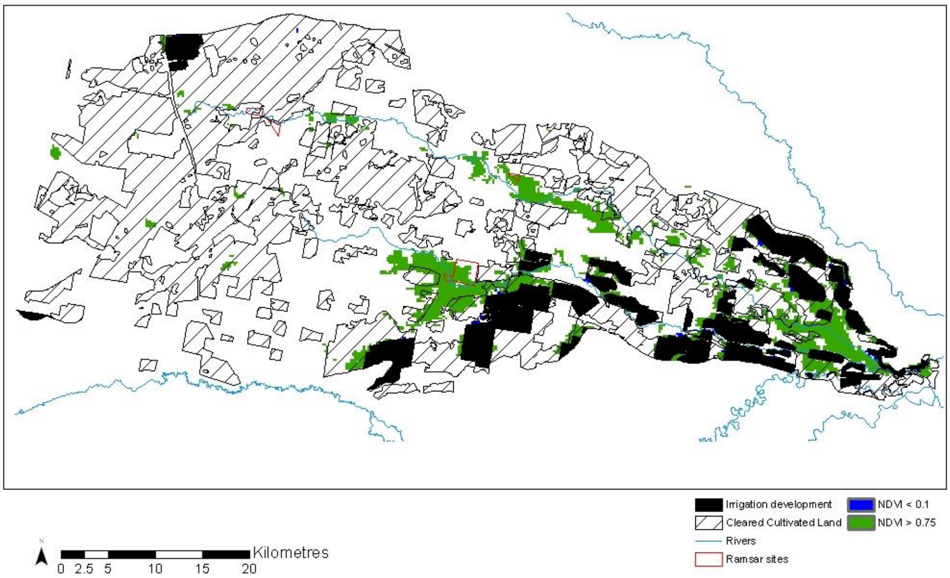
Irrigation development
Cleared Cultivated Land
Rivers
Ramsar sites
NDVI < 0.1
NDVI > 0.75
Kilometres
0 2.5 5 10 15 20

b

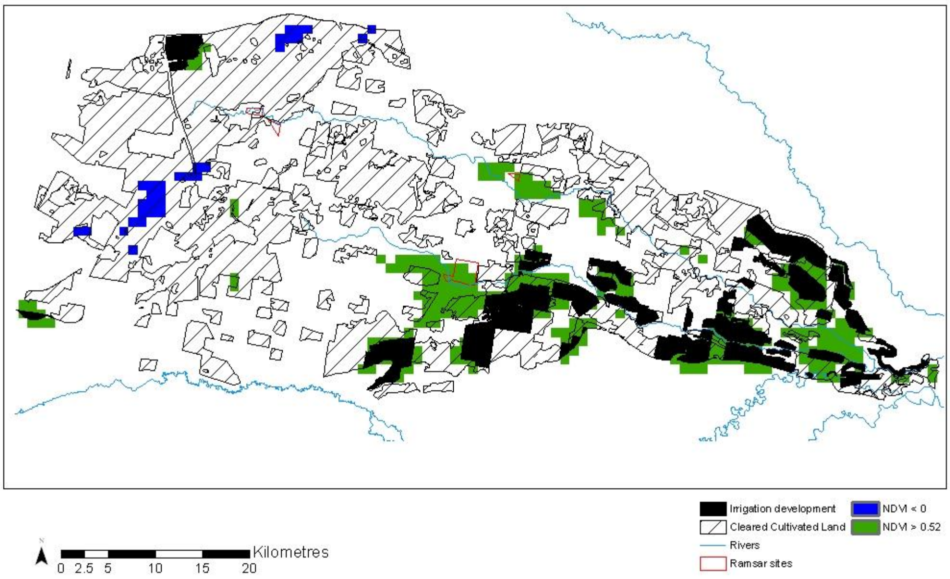

c

Figure A2.0.25: Nov2001. a) Landsat, b) Modis and c) AVHRR

December 2002/ February 2003

The December 2002 'event' was a planned ECA release from Copeton Dam of low peak volume (peak of just 1.4GL on 26th December 2002) over a short period with the aim of inundating small areas of core wetland. As the planned inflows were in the order of 0.5-1GL/day this event would not normally be detected as a significant inflow. Soon after the ECA release, a moderate natural event occurred with a peak of 29.8GL on the 25th February, 2003 and a 40-day inflow of 81.1GL. This analysis focuses on the entire period and includes three Landsat scenes as well as the analysis of 6 MVC periods for both Modis and AVHRR.

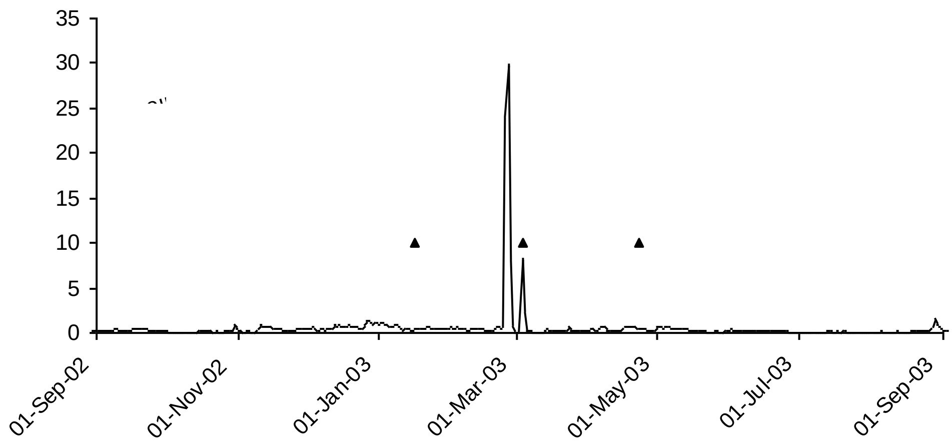

Figure A2.0.26: Gwydir River at Yarraman inflows 2002-3. Landsat scenes used in analysis ▲

The results of all analysis were very similar with 18 158ha indicated by Landsat, 17 885ha by Modis and 20 680 by AVHRR. The highly correlated results are most likely due to relatively dry landscape at the commencement of the event which results in much clearer distinction between areas responding to higher water availability and those of the surrounding landscape. AVHRR did again detect some areas as 'wet' in the western portion of the study area that were extremely unlikely to be flooded and were associated with cultivation. The wet threshold for AVHRR may give some false positives and needs to be checked on a case by case basis.

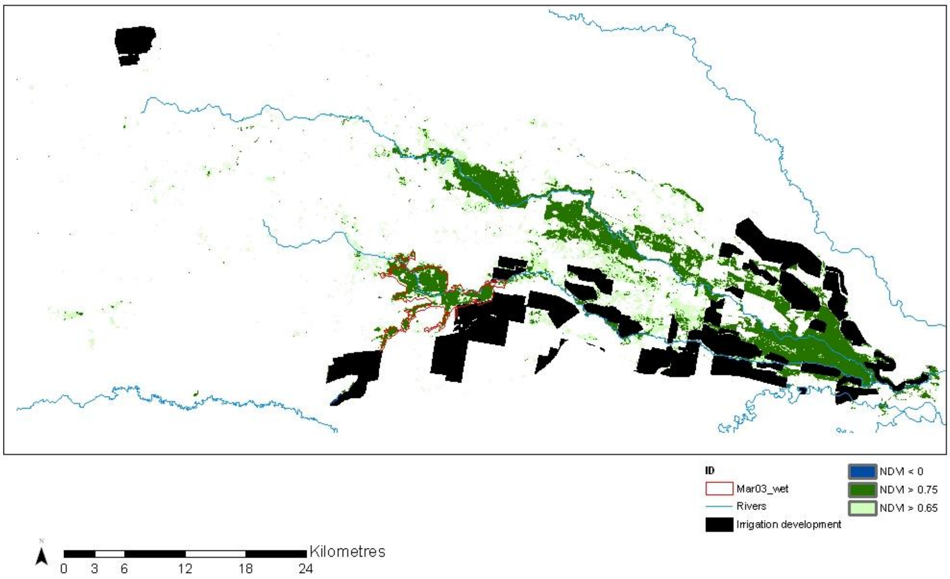
ID
Mar03_wet
Rivers
Irrigation development
NDVI < 0
NDVI > 0.75
NDVI > 0.65
Kilometres
0 3 6 12 18 24

a

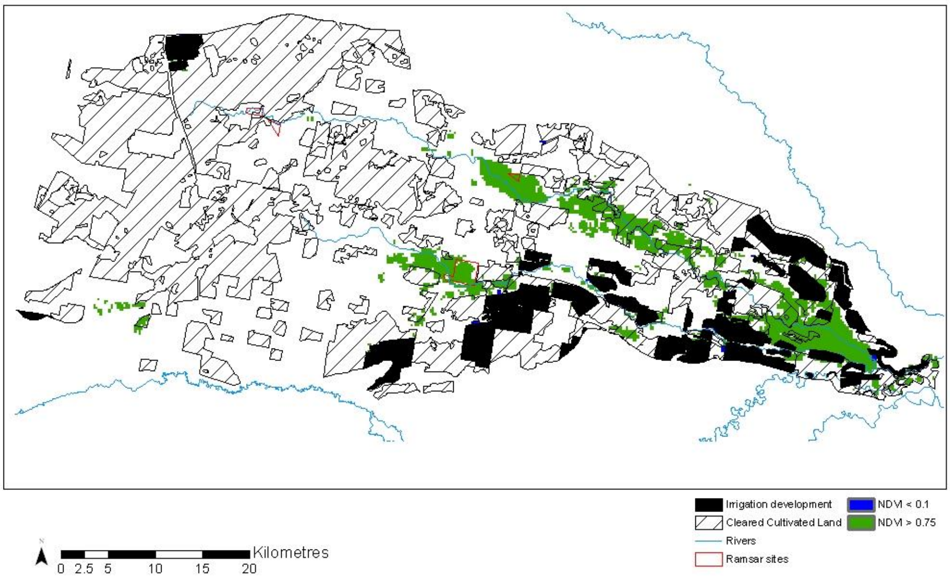
Irrigation development
Cleared Cultivated Land
Rivers
Ramsar sites
NDVI < 0.1
NDVI > 0.75
Kilometres
0 2.5 5 10 15 20

b

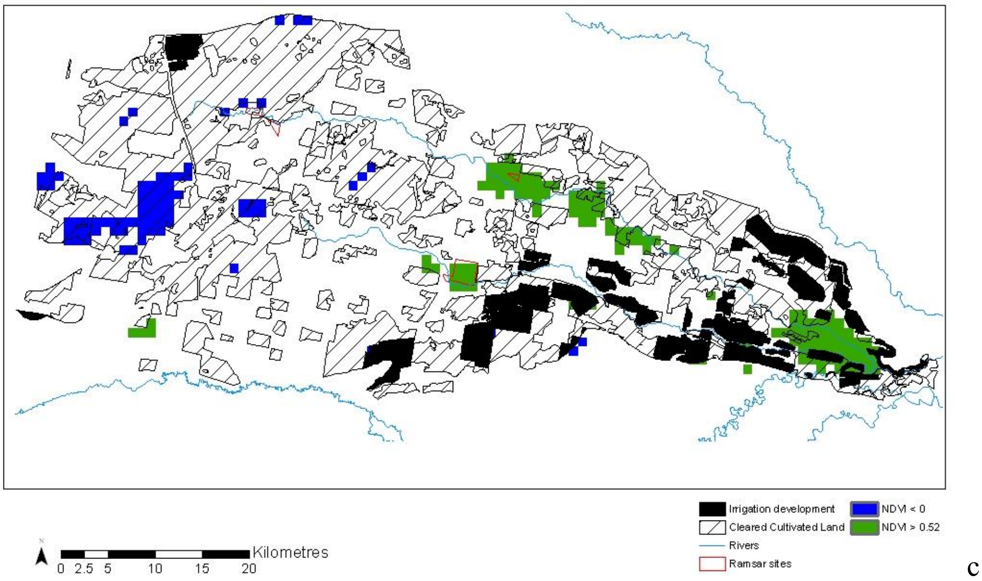

Figure A2.0.27: December 2002 – February 2003. a) Landsat, b) Modis and c) AVHRR.

December 2004

December 12th, 2004 event had several large flood peaks of 47.8GL (12th), 12.4GL (26th), 20.2 and 22.9GL (29th and 30th) with a 40-day volume of 204.9GL. Five Landsat images were available as well as both Modis and AVHRR MVC for six periods.

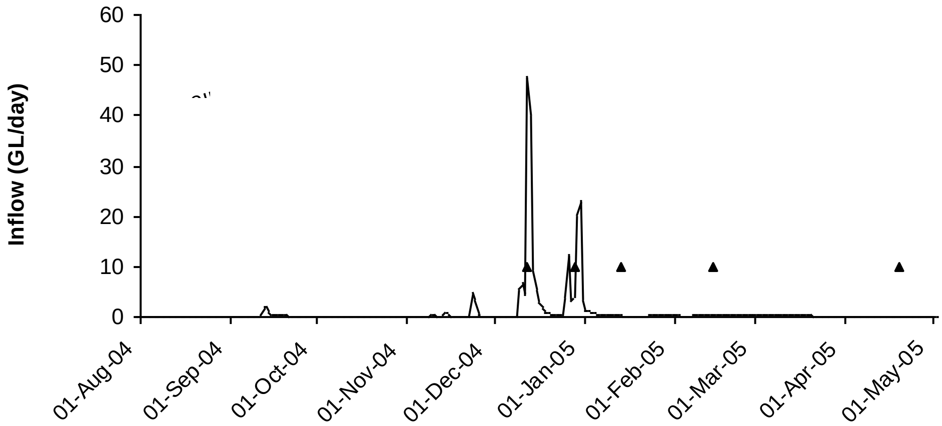

Figure A2.0.28: Gwydir River at Yarraman inflows 2004-5. Landsat scenes used in analysis ▲

Most of the study area was under open water at some point following the December 2004 event with Landsat images available soon after the flood peaks on the 12th December and again on the 29th December. The event also featured extremely heavy rainfall event (120mm) on the 10th December which resulted in localised flooding. The total area classified is 126 284ha and was predominantly classified as open water in the Landsat decision tree analysis.

With the MVC method of Modis and AVHRR tending towards response over wet areas, the only wet areas classified were in the western areas for the AVHRR where open water over cultivated land failed to elicit a rapid vegetation response. The difference in the area of open water for the two datasets is likely the product of the threshold used. The area of response for Modis is 36 554ha whilst for AVHRR it is 36 625 ha.

This analysis is interesting as the area of open water flooding does not necessarily result in vegetation response.

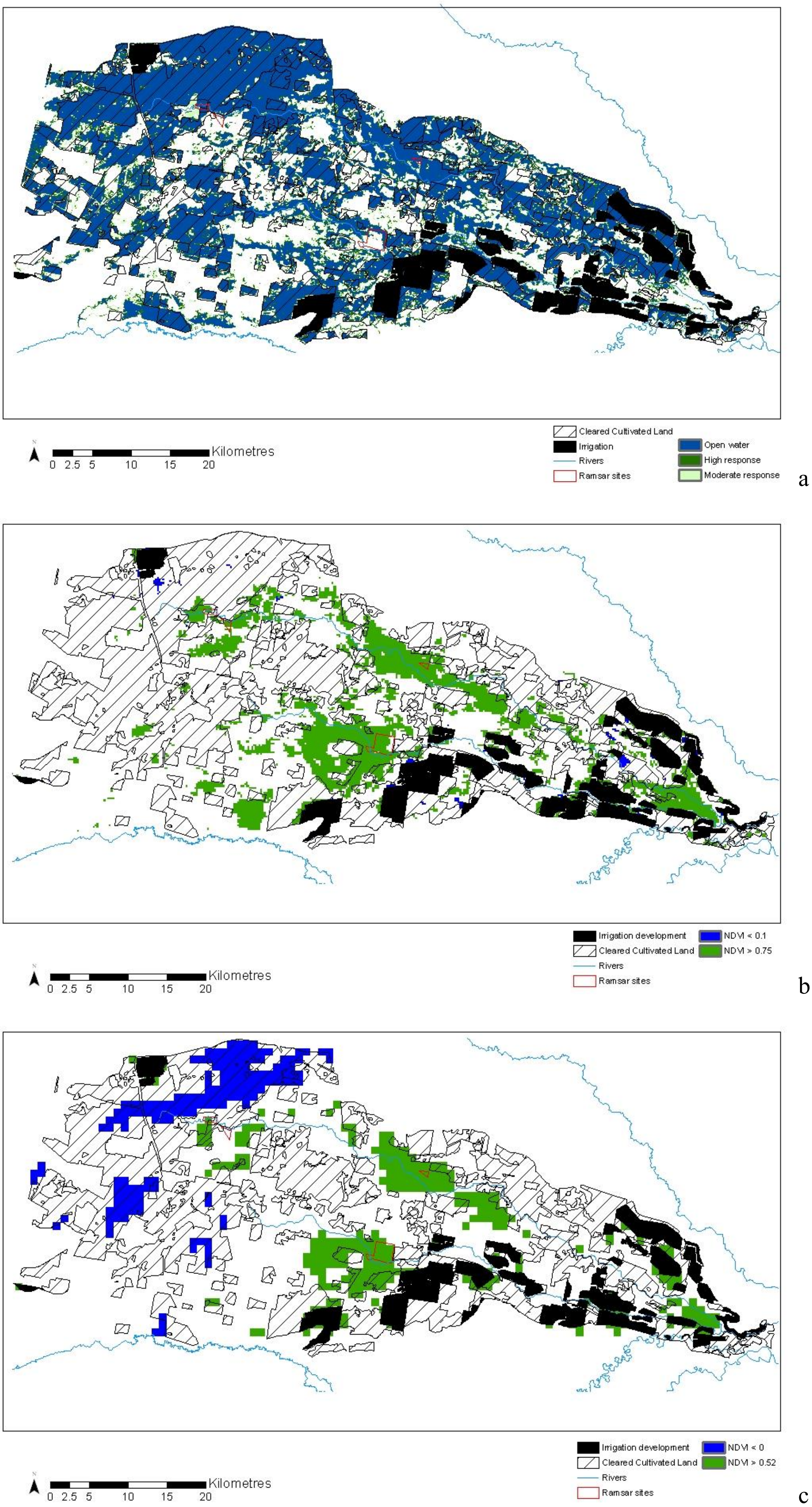
Cleared Cultivated Land
Irrigation
Rivers
Ramsar sites
Open water
High response
Moderate response
Kilometres
0 2.5 5 10 15 20
a
Irrigation development
Cleared Cultivated Land
Rivers
Ramsar sites
NDVI < 0.1
NDVI > 0.75
Kilometres
0 2.5 5 10 15 20
b
Irrigation development
Cleared Cultivated Land
Rivers
Ramsar sites
NDVI < 0
NDVI > 0.52
Kilometres
0 2.5 5 10 15 20
c

Figure A2.0.29: Dec 2004 a) Landsat, b) Modis and c) AVHRR

Appendix 3: Modelling ecosystem response to flooding: a remote sensing approach

Powell, S. J., Croke, B. F. W. and King, E. A. (Eds.), 2007. Modelling Ecosystem Response to Flooding: a Remote Sensing Approach. *MODSIM 2007 International Congress on Modelling and Simulation*. Modelling and Simulation Society of Australia and New Zealand, Christchurch, New Zealand.

Not included in PDF format. Please refer to attached link

http://mssanz.org.au/MODSIM07/papers/46_s60/ModelingEcosystems60_Powell_.pdf

Appendix 4: Modelling floodplain inundation for environmental flows: Gwydir wetlands, Australia

Powell, S. J., Letcher, R. A. and Croke, B. F. W., 2008. Modelling floodplain inundation for environmental flows: Gwydir wetlands, Australia, *Ecological Modelling*, **211**: 350-362.

Not included in PDF format. Please refer to attached link

http://www.sciencedirect.com/science/article/pii/S0304380007004784